

**Synthesis and Evaluation of Third-Order
Nonlinear Optical Properties of a few
1,3,4-Oxadiazole Based Push-Pull
Fluorophores**

*Thesis submitted to the
Cochin University of Science and Technology
In partial fulfilment of the requirements
for the degree of*

*Doctor of Philosophy
in
Chemistry*

*In the Faculty of Science
by*

SHANDEV P. P.

(Reg. No: 4360)

Under the supervision of

Dr. P. A. Unnikrishnan



**DEPARTMENT OF APPLIED CHEMISTRY
COCHIN UNIVERSITY OF SCIENCE AND TECHNOLOGY
KOCHI-682022, KERALA, INDIA**

December 2017

Dedicated

To my family and well-wishers.....

“You must never be fearful about what you are doing when it is right.”

Marie Curie

“He who can listen to the music in the midst of noise can achieve great things.”

Vikram Sarabhai

“When people throw stones at you, you turn them into milestones.”

Sachin Tendulkar



DEPARTMENT OF APPLIED CHEMISTRY
COCHIN UNIVERSITY OF SCIENCE AND TECHNOLOGY
KOCHI-682 022, KERALA, INDIA

Dr. P. A. Unnikrishnan
Assistant Professor
e-mail: paunni@gmail.com
Ph: 9846295151

CERTIFICATE

This is to certify that the thesis entitled “**Synthesis and evaluation of third-order nonlinear optical properties of a few 1,3,4-oxadiazole based push-pull fluorophores**” is a genuine record of research work carried out by **Mr. Shandev P. P.**, under my supervision, in partial fulfilment of the requirements for the degree of Doctor of Philosophy of Cochin University of Science and Technology, and further that no part thereof has been presented before for the award of any other degree. All the relevant corrections and modifications suggested by the audience and recommended by the doctoral committee of the candidate during the pre-synopsis seminar have been incorporated in the thesis.

*Kochi-22
December, 2017*

*P. A. Unnikrishnan
(Thesis Supervisor)*

DECLARATION

I hereby declare that the work presented in the thesis entitled **“Synthesis and evaluation of third-order nonlinear optical properties of a few 1,3,4-oxadiazole based push-pull fluorophores”** is the result of genuine research carried out by me under the supervision of **Dr. P. A. Unnikrishnan**, Assistant Professor of Organic Chemistry, Department of Applied Chemistry, Cochin University of Science and Technology, Kochi-22, and the same has not been submitted elsewhere for the award of any other degree.

*Kochi-22
December, 2017*

Shanley P. P.

Acknowledgements

Research work is like a symphony, I am very grateful to lots of people, who performed as musicians for the completion of my thesis. I would like to thank each and every one of them.

I express my deep sense of gratitude and profound respect to my supervisor Dr. P. A. Unnikrishnan, Assistant Professor, Department of Applied Chemistry, Cochin University of Science and Technology, who has helped, encouraged and given all freedom to my research work. It was a great honour to finish my work under his guidance.

I express my sincere thanks to Dr. S. Prathapan, Associate Professor, Department of Applied Chemistry, Cochin University of Science and Technology, for his valuable scientific guidance, constant encouragement and support throughout my research carrier, being my doctoral committee member.

I wish to thank Dr. K. Sreekumar, Head, Department of Applied Chemistry, CUSAT for all the support for my research.

I gratefully acknowledge the former Heads of the Department, Dr. K. Girishkumar, Dr. M. R. Prathapachandra Kurup and Dr. N. Manoj, for providing me with all the necessary facilities of the department for carrying out my research work. I would like to extend my sincere thanks to all the former and present members of the Faculty of the Department of Applied Chemistry. I thank the administrative staff of the Department and University office, CUSAT.

There have been lots of people who have been sitting beside me during the journey of last five years. They have directed me, placed facilities in front of me and showed the right paths. I wish to express my sincere thanks to Dr. Chandrasekharan K., Department of Physics, NIT Calicut for extending NLO facilities in their lab. I would also like to thank Dr. S. Jayalekshmi and Dr. M. K. Jayaraj, Department of Physics, CUSAT, Dr. Rajathy Sivalingam, School of Environmental studies, CUSAT for extending facilities in their department.

I take this opportunity to sincerely acknowledge Dr. Nirmala Rachel James, Department of Chemistry, IIST Thiruvananthapuram, Dr. K. George Thomas, Department of Chemistry, IISER Thiruvananthapuram and Dr. Sabu Thomas, MG University, Kottayam for extending their facilities in their department.

Special thanks to Dr. Jubi John, CSIR-NIIST for valuable advices and loving support.

A very special gratitude goes to CSIR, New Delhi for providing financial support for the work. I also thank SAIF, CUSAT for the analytical and spectral data.

I remember with respect and prayers all my teachers who encouraged me to go ahead with my career goals.

I am thankful to all my seniors Dr. Eason M. Mathew, Dr. Jomon P. Jacob, Dr. Reshma G., Dr. Sandhya R., Dr. Sajitha T. S., Dr. Nithya C., Dr. Kala K., Dr. Suma C. S., Cisy Abraham and Pravitha N. P. for the sincere support and warm friendship.

I thank my labmates for all the encouraging discussion and all the fun we had in our lab. I thank Aswathi, Amrutha chechi and saumya chechi, for their support and love; they made my journey happy and comfortable.

My heartfelt thanks to my juniour Remya for all the motivation and support that she gave me for conducting the experiments and completing my thesis writing.

A warm thanks to Jith, Nishad and Aswathy for their selfless support for carrying out the studies.

I remember the Cheerful days I have spent with my colleagues. I thank Mr. Tomson Devassia, Mr. Kiran James, Ms. Jesna A., Ms. Rani M., Ms. Vineetha P. K., Ms. Parvathy O. C., Ms. Seena Sebastian, Ms. Reshma and Ms. Haritha for the love and endless support they rendered to me.

I am so much grateful to my co-workers Shiju, Shijeesh, Rakesh for their friendship and support. I extend my thanks to Dr. Mahesh Kumar and Abhilash for their help.

During the course of my work, I had the pleasure of working with M. Phil and project students Jyothi, Aswathi, Sajeena, Fousia, Revathi, Lekshmi, Arya and Savitha. Their assistance during the presented work is gratefully acknowledged.

I remember Vishnu, my friend who passed away last year...

Special thanks to Rakeshettan, Avudi and Rahul for their loving friendship and support. I thank all my schoolmates, B. Sc., M. Sc. Classmates, friends from other labs of the department and my friends Bijoy, Murukan, Mani, Kunjappu, Perumal, Unni, Nidheesh, Akhilthe list is seemingly endless..... Thanks to one and all.

I am much indebted to Shanthi, she is my inspiration...I have no words to mention about my Pappa, Amma and my Sikha without them I am nothing. I remember my loving family members for their emotional backing and love. I remember Nisheeth, Hiroshettan, Amar.....too many to list here but you know who you are!...

Above all, I thank the Supreme Power I believe in, for giving me the strength and all the blessings showered on me.

SHANDEV P. P.

PREFACE

Organic π conjugated charge transfer chromophores are significantly used for third-order nonlinear applications owing to their high NLO susceptibility, short response time, excellent thermal stability and high structural flexibility. 1,3,4-Oxadiazoles are well known for high thermal and chemical stability, excellent photoluminescent quantum yield and electron deficient nature. A few reports on the synthesis and third order nonlinear optical properties of 1,3,4-oxadiazole based donor-acceptor (D-A) type polymers have appeared in the literature; nevertheless 1,3,4-oxadiazole based push-pull molecules for third order nonlinear optical properties are less explored. In this context, we designed and synthesized several phenothiazine, carbazole and pyrene appended 1,3,4-oxadiazoles with a view to evaluate their application in photonic devices. The major objectives of the present study are listed hereunder:

- Synthesis and characterization of a few 2,5-diaryl-1,3,4-oxadiazoles and 1,3,4-oxadiazole–thiophene hybrid molecules.
- Synthesis and evaluation of third-order nonlinear optical properties of a few 1,3,4-oxadiazole–phenothiazine push-pull fluorophores.
- Synthesis and evaluation of third-order nonlinear optical properties of a few 1,3,4-oxadiazole–carbazole push-pull fluorophores.
- Synthesis and evaluation of third-order nonlinear optical properties of a few 1,3,4-oxadiazole–pyrene push-pull fluorophores.

The thesis entitled “**Synthesis and evaluation of third-order nonlinear optical properties of a few 1,3,4-oxadiazole based push-pull fluorophores**” is divided into five chapters.

In **Chapter 1**, an introduction to push-pull fluorophores with special focus on 1,3,4-oxadiazole is presented. A brief discussion of applicability of 1,3,4-oxadiazole based materials in DSSCs, OLEDs and in third order non-linear optical applications and a brief history as well as experimental set-up of Z-scan technique are also presented. This chapter concludes with the outline of scope and objectives of the present research problem.

Chapter 2 of the thesis describes the synthesis and characterization of a few expandable 2,5-diaryl-1,3,4-oxadiazoles and 1,3,4-oxadiazole-thiophene hybrid molecules by employing relatively simple synthetic strategies. We have established facile protocols for expanding 1,3,4-oxadiazoles to highly conjugated linear architectures.

Synthesis of 1,3,4-oxadiazole-phenothiazine push-pull molecules by using iodine mediated oxidative cyclization of respective acyl hydrazones is detailed in **Chapter 3**. All the molecules were characterized by ^1H NMR, ^{13}C NMR and LC-MS analysis. The photophysical and electrochemical properties have been explored by UV-Vis absorption, fluorescence spectroscopy and cyclic voltammetry measurements. Density functional theory computations have been carried out for analyzing HOMO and LUMO. Thermal stability of these hybrids was analyzed by using TGA and DSC. The nonlinear optical properties and optical limiting threshold of the fluorophores were studied using Q switched Z scan technique with a 7 ns laser pulses at 532 nm.

Chapter 4 comprises the discussion on synthesis and characterization of a series of carbazole substituted 1,3,4-oxadiazole. The photophysical, electrochemical, theoretical and thermal properties have also been studied. Additionally nonlinear optical properties and optical limiting threshold of the fluorophores were studied using Q switched Z scan technique.

Chapter 5 focuses on the synthesis of a series of pyrene appended 1,3,4-oxadiazole derivatives. All the molecules were characterized by ^1H NMR, ^{13}C NMR and LC-MS analysis. The photophysical, electrochemical, theoretical, thermal and third order non-linear optical properties were also investigated.

The conclusions drawn from each part of the work done are presented in **Chapter 6**.

The structural formulae, schemes, tables and figures are numbered chapter-wise since each chapter of the thesis is organized as an independent unit. ^1H and ^{13}C NMR spectra of significant compounds reported in Chapters 2-5 are included as appendix to these chapters. Relevant references are included at the end of individual chapters. ^1H NMR and ^{13}C NMR spectra of significant compounds are presented as Appendix towards the end of relevant chapters.

List of Abbreviations

3PA	Three photon absorption
A	Acceptor
B3LYP	Becke, three parameter, Lee-Yang-Parr
D	Donor
DCM	Dichloromethane
DFG	Difference-frequency generation
DFT	Density functional theory
DFWM	Degenerate four-wave mixing
DMF	Dimethylformamide
DMSO	Dimethyl Sulfoxide
DSC	Differential scanning calorimetry
DSSC	Dye sensitized solar cell
HOMO	Highest occupied molecular orbital
HTM	Hole transporting material
ICT	Intramolecular charge transfer
LUMO	Lowest unoccupied molecular orbital
<i>m</i>	Meta
Nd-YAG	Neodymium-doped yttrium aluminium garnet
NLO	Nonlinear optics
<i>o</i>	Ortho
OA	Open aperture
OFET	Organic field effect transistor
OLED	Organic light emitting diode
OPVC	Organic photovoltaic cell
<i>p</i>	Para
PHOLED	Phosphorescent organic light emitting diode
RSA	Reverse saturable absorption
SFG	Sum-frequency generation
SHE	Standard hydrogen electrode
SHG	Second-harmonic generation
TCSPC	Time-correlated single photon counting
TGA	Thermogravimetric Analysis
TMS	Tetramethylsilane
XRD	X-ray diffraction

CONTENTS

	Page No.
CHAPTER 1	
1,3,4-Oxadiazole - an Overview	
1.1	Abstract 1
1.2	Introduction 1
1.3	1,3,4-Oxadiazole 4
1.3.1	1,3,4-Oxadiazole based D-A systems for OLEDs 8
1.3.2	1,3,4-Oxadiazole based D-A systems for DSSCs 14
1.4	Nonlinear Optics: An Outlook 19
1.4.1	Second-Harmonic Generation (SHG) 21
1.4.2	Sum-Frequency Generation (SFG) 23
1.4.3	Difference-Frequency Generation 24
1.4.4	Optical Parametric Oscillation 25
1.4.5	Third Harmonic Generation 25
1.4.6	Saturable Absorption (SA) 26
1.4.7	Two Photon Absorption (TPA) 26
1.4.8	Three Photon Absorption 26
1.4.9	Reverse Saturable Absorption (RSA) 27
1.4.10	Z-scan Technique 27
1.4.11	Open Aperture Z-scan 28
1.4.12	Closed Aperture Z-scan 29
1.4.13	Optical Power Limiting 31
1.4.14	1,3,4-Oxadiazole based D-A systems for NLO 33
1.4.15	1,3,4-Oxadiazole based polymers for third-order NLO applications 37
1.5	Objectives 45
1.6	References 45
CHAPTER 2	
Synthesis and characterization of a few unsymmetrical 2,5-diaryl- 1,3,4-oxadiazoles and 1,3,4-oxadiazole-thiophene hybrid molecules	
2.1	Abstract 53
2.2	Introduction 53
2.3	Results and discussion 54
2.3.1	Synthesis and characterization 59
2.3.2	Photophysical Properties 59
2.4	Conclusions 59
2.5	Experimental 61
2.5.1	Materials and methods 61
2.5.2	General procedure for the synthesis of N,N'-diacylhydrazines 3a-k 61
2.5.2.2	General procedure for the synthesis of 2,5-diaryl-1,3,4- oxadiazoles (4a-k) 62
2.5.2.3	General procedure for the synthesis of 1,3,4-oxadiazole- 62

	thiophene hybrid molecules (8a-j)	
2.5.3	Spectral and analytical data for significant compounds	62
2.6	General procedure for the synthesis of 1,3,4-oxadiazole-carbazole bipolar molecules (10a-c)	66
2.7	Synthesis of 4'-(5-(4-(5-(4-formylphenyl) thiophen-2-yl)phenyl)-1,3,4-oxadiazol-2-yl)biphenyl-4-carbaldehyde (12)	68
2.8	Synthesis of 4'-(5-(4-(9 <i>H</i> -carbazol-9-yl)phenyl)-1,3,4-oxadiazol-2-yl)biphenyl-4-carbaldehyde (13)	68
2.9	Synthesis of 4'-(5-(4-(9 <i>H</i> -carbazol-9-yl)phenyl)-1,3,4-oxadiazol-2-yl)- <i>N,N</i> -diphenyl-[1,1'-biphenyl]-4-amine (16)	69
2.10	References	70
2.11	Appendix	72

CHAPTER 3

Synthesis and evaluation of third-order nonlinear optical properties of a few 1,3,4-oxadiazole-phenothiazine push-pull fluorophores

3.1	Abstract	77
3.2	Introduction	77
3.3	Results and discussion	80
3.3.1	Synthesis and characterization	80
3.3.2	Photophysical properties	82
3.3.3	Electrochemical Properties	92
3.3.4	Theoretical studies	95
3.3.5	XRD characterization	97
3.3.6	Thermal properties	99
3.3.7	Nonlinear optical properties	102
3.4	Conclusions	106
3.5	Experimental sections	107
3.5.1	Reagents and instruments	107
3.5.2	Synthesis and characterization	108
3.6	References	114
3.7	Appendix	117

CHAPTER 4

Synthesis and evaluation of third-order nonlinear optical properties of a few 1,3,4-oxadiazole-carbazole push-pull fluorophores

4.1	Abstract	121
4.2	Introduction	122
4.3	Results and discussion	124
4.3.1	Synthesis and characterization	124
4.3.2	Photophysical properties	126
4.3.3	Electrochemical Properties	134
4.3.4	Theoretical studies	136
4.3.5	XRD characterization	139
4.3.6	Thermal properties	140
4.3.7	Nonlinear optical properties	142
4.4	Conclusions	146
4.5	Experimental sections	147
4.5.1	Reagents and instruments	147
4.5.2	Synthesis and characterization	148

4.6	References	152
4.7	Appendix	156

CHAPTER 5

Synthesis and evaluation of third-order nonlinear optical properties of a few 1,3,4-oxadiazole-pyrene push-pull fluorophores

5.1	Abstract	159
5.2	Introduction	159
5.3	Results and discussion	161
5.3.1	Synthesis of fluorophores	161
5.3.2	Photophysical properties	162
5.3.3	Electrochemical Properties	167
5.3.4	Theoretical studies	168
5.3.5	Thermal properties	170
5.3.6	Nonlinear optical properties	171
5.4	Conclusions	173
5.5	Experimental sections	174
5.5.1	Reagents and instruments	174
5.5.2	Synthesis and characterization	174
5.6	References	177
5.7	Appendix	179

CHAPTER 6

Summary and Conclusions	181
--------------------------------	-----

1,3,4-OXADIAZOLES - AN OVERVIEW

1.1. Abstract

1,3,4-Oxadiazoles are versatile heterocyclic compounds with interesting photophysical properties. A brief introduction to significant applications of 1,3,4-oxadiazole based materials in DSSCs, OLEDs and in third-order nonlinear optics is provided in this chapter. A brief history as well as experimental set-up of Z-scan technique is also presented in this chapter.

1.2. Introduction

Push-pull fluorophores are typical π conjugated systems that contain electron donors (D) and electron acceptors (A) coupled by a π bridge, possessing inherent intramolecular charge transfer (ICT) property (Fig. 1.1).^{1,2} These compounds play a crucial role in organic electronics, like organic field effect transistors (OFET),³ light-emitting diodes (OLED),⁴ photovoltaic cells (OPVC),⁵ nonlinear optical (NLO) materials,⁶⁻⁸ electro-optic materials,^{9,10} piezochromic materials,¹¹ photochromic^{12,13} and solvatochromic probes,¹⁴⁻¹⁶ etc. During ICT a cationic donor and an anionic acceptor are produced, which are stabilised by electrostatic attraction and this will create a new low energy molecular orbital. So the excitation energy from ground to excited state is in the visible region, which will produce charge transfer band and fluorophores become coloured. ICT also creates high asymmetric polarizability in the

entire molecular framework and this delocalization of electron density which in turn is responsible for their predominant nonlinear optical activity.¹⁷⁻¹⁹

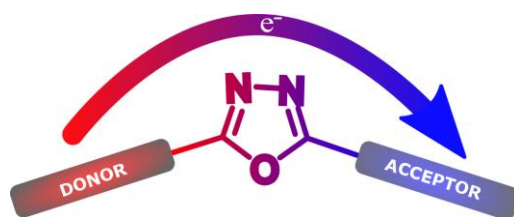


Fig. 1.1. Intramolecular charge transfer in D-A systems

For a push-pull system we can control the charge transfer by proper designing of donor, acceptor or π -bridge. ICT mainly depends on the electronegativity of the donor molecule and electron affinity of the acceptor molecule.²⁰ Molecules having functional groups with $+M$ effect as well as electron rich hetero aromatic or organometallic compounds can act as electron donors. Frequently used donors are phenothiazine,²¹ phenoxazine,^{22,23} triphenylamine,^{24,25} carbazole,^{26,27} ferrocene²⁸ etc. π -linker in D-A systems are often associated with a combination of multiple bonds like aromatic and heteroaromatic compounds such as phenyl,^{29,30} thiophene,³¹⁻³³ furan³⁴ etc. Molecules with $-M$ effects (NO_2 , CN, CHO etc.) and electron deficient heterocyclic compounds were commonly used as electron acceptors. The commonly used heterocyclic acceptors are oxadiazole,³⁵ triazine,³⁶ benzothiadiazole^{37,38,39} etc. A few selected examples for ICT compounds are shown in Fig. 1.2.

Several D-A systems incorporating oxadiazole core are reported in literature. Since the main focus of the present investigation is also on

oxadiazole based systems, a brief introduction to synthesis of oxadiazoles is included in this section.

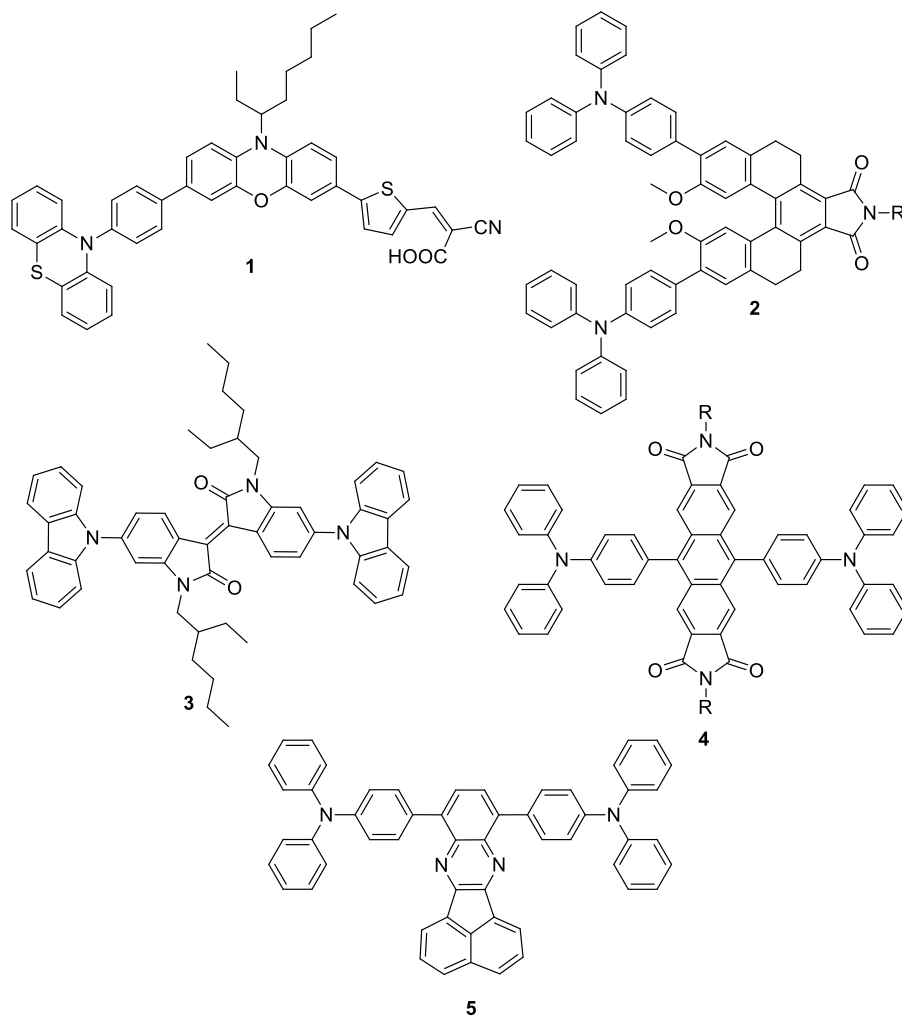


Fig. 1.2. Prototypical examples for compounds exhibiting ICT

1.3. 1,3,4-Oxadiazole

Oxadiazoles are a group of the electron deficient species in the family of heterocyclic compounds. Presence of one oxygen atom and two nitrogen atoms make oxadiazoles highly electron deficient.

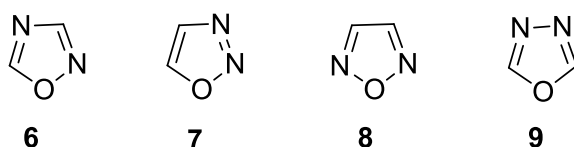
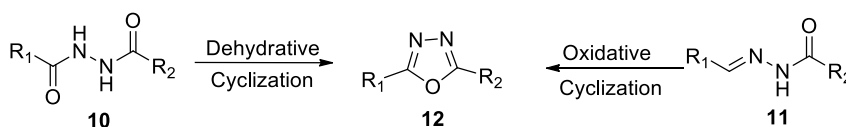


Fig. 1.3. Isomers of oxadiazole: 1,2,4-oxadiazole (**6**), 1,2,3-oxadiazole (**7**), 1,2,5-oxadiazole (**8**) and 1,3,4-oxadiazole (**9**)

There are four isomers known for oxadiazoles (**6-9**, Fig. 1.3). Among these, 1,2,4-oxadiazoles and 1,3,4-oxadiazoles are widely explored due to their potent applications in biological and organic electronics fields. 1,3,4-Oxadiazoles are in the spotlight since 1965 when the 1,3,4-oxadiazole core was successfully prepared by Ainsworth by employing thermolysis to ethyl formate.⁴⁰

For preparing 1,3,4-oxadiazole framework lots of methods have been developed.⁴¹⁻⁴⁴ Two important methodologies used for the synthesis of 1,3,4-oxadiazole core are dehydrative cyclization of diacylhydrazines and oxidative cyclization of acylhydrazones (Scheme 1.1). Commonly used reagents for dehydrative cyclization and oxidative cyclization are given in Table 1.1.

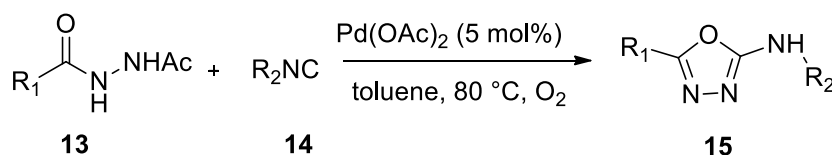


Scheme 1.1. Two important methodology for the preparation of 1,3,4-oxadiazole framework

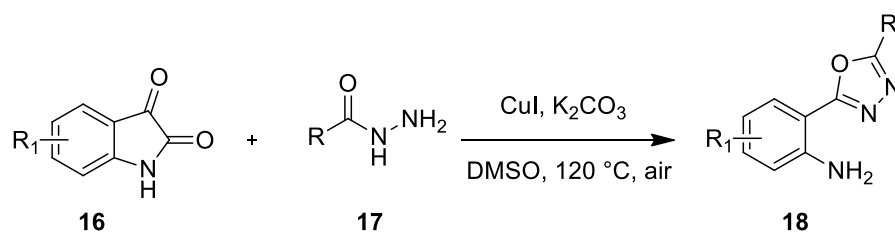
Table 1.1. Summary of reagents used for dehydrative cyclization and oxidative cyclization

Dehydrative Cyclization	Oxidative Cyclization
SOCl ₂	Hypervalent Iodine
PPA	Chloramine T
POCl ₃	CAN
H ₂ SO ₄	FeCl ₃
	PbO ₂
	Br ₂
	KMnO ₄
	HgO/I ₂

Recently, some other methodologies have also been developed for the synthesis of 1,3,4-oxadiazole framework. Xu and coworkers reported oxidative annulation reaction in presence of Pd catalyst where the reaction proceeds through isocyanide insertion to N-H and O-H bonds of hydrazides (Scheme 1.2).⁴⁵

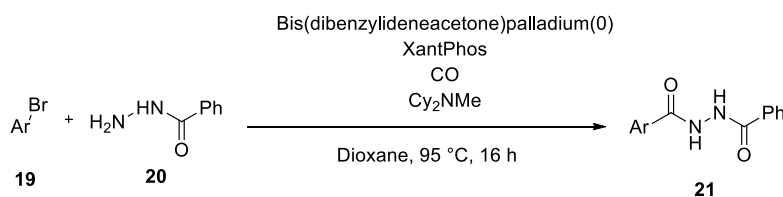
**Scheme 1.2.** Pd-mediated synthetic approach to 1,3,4-oxadiazoles

Wu and coworkers synthesized 2-(1,3,4-oxadiazol-yl)aniline derivatives from respective isatin and hydrazides. Here they used copper catalyzed decarboxylative coupling for making intramolecular C-O bond (Scheme 1.3). Formation of free NH₂ group by this reaction enables further transformations.



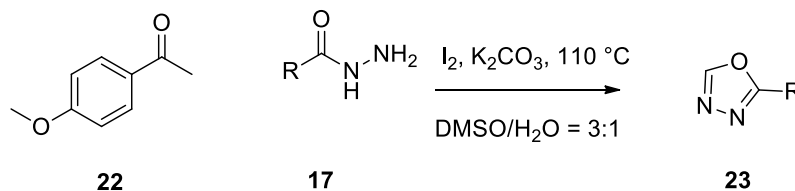
Scheme 1.3. Synthetic method to amine-appended 1,3,4-oxadiazoles

Skrydstrup and coworkers synthesized 1,3,4-oxadiazoles by palladium catalyzed carbonylative coupling. This coupling is employed for the transformation of aryl bromides to *N,N'*-diacylhydrazines by treating with acylhydrazines (Scheme 1.4).⁴⁶



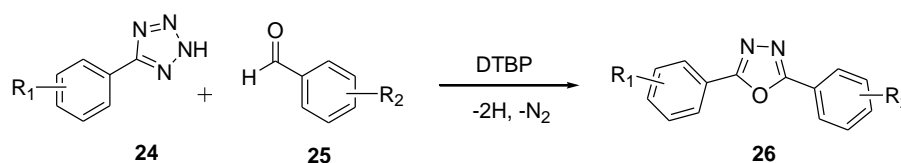
Scheme 1.4. Synthetic method for 1,3,4-oxadiazole precursors

Xu and coworkers in 2015 introduced a new synthetic strategy which involves direct annulation reaction between hydrazides and methyl ketones (Scheme 1.5). Main attraction of this strategy is the generality towards C (*sp*³)-H bonds.⁴⁷



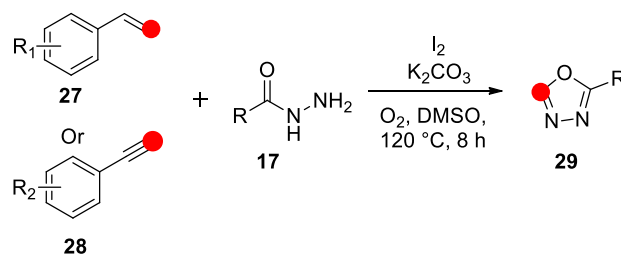
Scheme 1.5. Synthetic method to 1,3,4-oxadiazoles

A metal and base free protocol for 2,5-diaryl-1,3,4-oxadiazoles was developed by Wang in 2015.⁴⁸ It involves di-*tert*-butyl peroxide assisted cross-dehydrogenative coupling strategy. N-Acylation of aryltetrazoles using aryl aldehydes followed by thermal rearrangement leads to 1,3,4-oxadiazoles (Scheme 1.6).⁴⁸



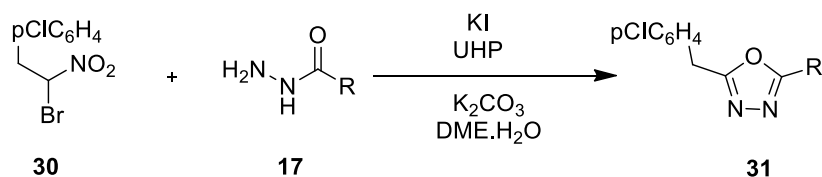
Scheme 1.6. Conversion of tetrazoles to 1,3,4-oxadiazoles

Guosheng and coworkers reported the iodine mediated one-pot synthesis of oxadiazole framework in 2016. This methodology involves oxidative cleavage of C(*sp*²)-H or C(*sp*)-H and subsequent cyclization and deacylation (Scheme 1.7).⁴⁹



Scheme 1.7. Guosheng's method for 1,3,4-oxadiazole synthesis

Alternatively, Tokumaru and coworkers synthesized 1,3,4-oxadiazoles from α -bromonitroalkanes and acylhydrazides under semi aqueous medium (Scheme 1.8).⁵⁰



Scheme 1.8. Synthesis of 1,3,4-oxadiazoles from α -bromonitroalkanes

1.3.1. 1,3,4-Oxadiazole based D-A systems for OLEDs

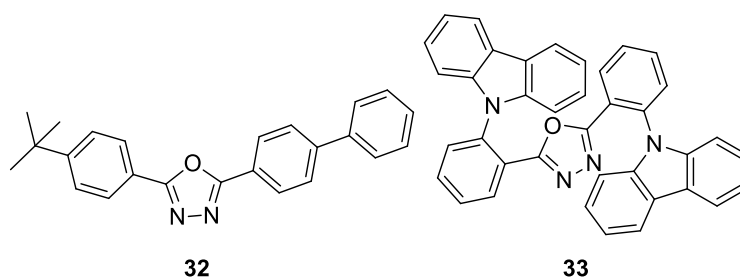
Organic light emitting diodes are widely used in flat panel displays and solid-state light emitting sources.^{51,52} OLEDs were introduced by Tang and Vanslyke in 1987.⁵³ Efficiency and lifetime are the two main factors which influence OLED. Recently, small bandgap organic molecules are extensively used for the production of OLEDs.⁵⁴

In OLEDs, electron-deficient species are used as electron-transport materials and the commonly used electron conductors are oxadiazole,⁵⁵ triazine,⁵⁶⁻⁵⁸ phenanthroline,^{59,60} quinoxaline,^{61,62} benzimidazole^{63,64} etc. Among these, oxadiazoles are attractive materials due to their excellent hole transporting capability, thermal stability and high fluorescence quantum yields.

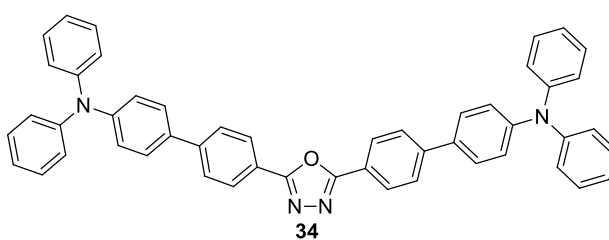
After the first report in which 2,5-disubstituted-1,3,4-oxadiazole **32** was used as an electron transport layer in OLED applications,⁶⁵ numerous small molecule and polymer based oxadiazole material have been designed and synthesized for LED applications.^{53,66}

Ma *et al.* in 2008 synthesized a simple carbazole-oxadiazole hybrid molecule **33**. They employed this bipolar host for green and red phosphorescent OLEDs. These molecules showed high thermal and

chemical stability and exhibited increased triplet energy level. Due to well-balanced injection and recombination of charge carriers, this bipolar host exhibits excellent quantum efficiency of 20.2% for green and 18.5% for deep red electrophosphorescence.⁶⁷

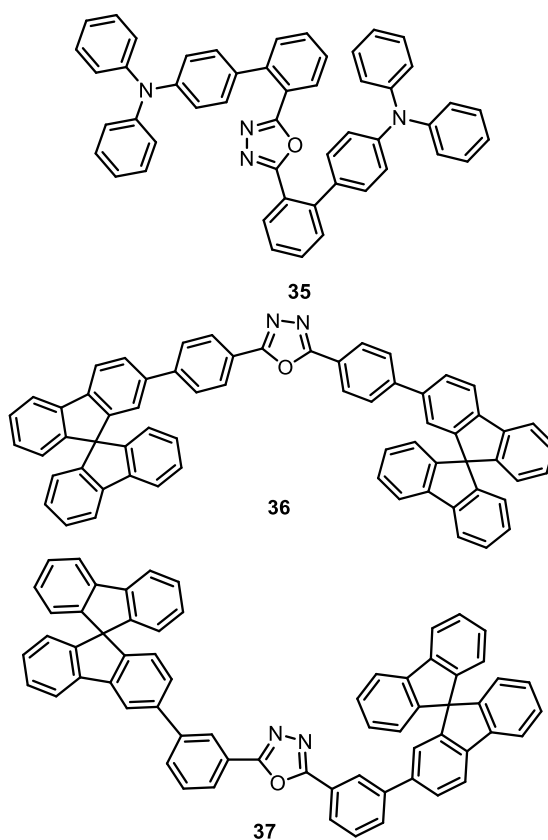


Two bipolar triphenylamine-oxadiazole hybrid molecules were synthesized by Zhigang Shuai and coworkers in 2009 (**34** & **35**). Both **34** and **35** showed intense blue shifted emission and were employed in red PHOLEDs and two colors based white OLEDs. The molecule containing triphenylamine linked at the ortho position (**35**) helps to retard the intramolecular charge transfer and also increases the triplet energy level in comparison with the para linked substrate **34**.⁶⁸

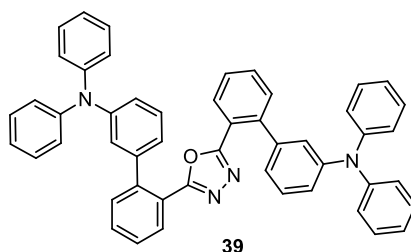
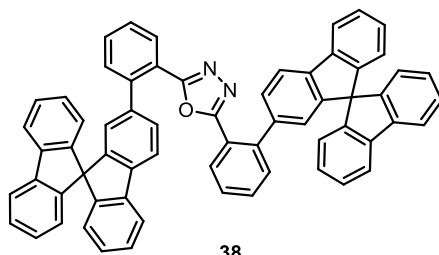


Ma *et al.* in 2010, synthesized highly thermally stable spirofluorene/oxadiazole hybrid molecules with different linkages between two components, which were used for green and red electrophosphorescence materials (**36-38**). The maximum diode

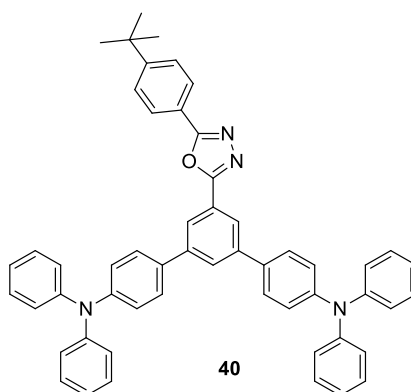
performance observed for the bipolar host is in the order $o > m > p$, which is due to the high triplet energy associated with the ortho linkage. They observed external quantum efficiency of 11.7% and 9.8% for green and red phosphorescence OLEDs, respectively.⁶⁹



In continuation, the same research group synthesized a triphenylamine/oxadiazole hybrid material which was used as a host and exciton blocking material (**39**). Using this hybrid material, they got 23.7% external quantum efficiency for PHOLEDs.⁷⁰

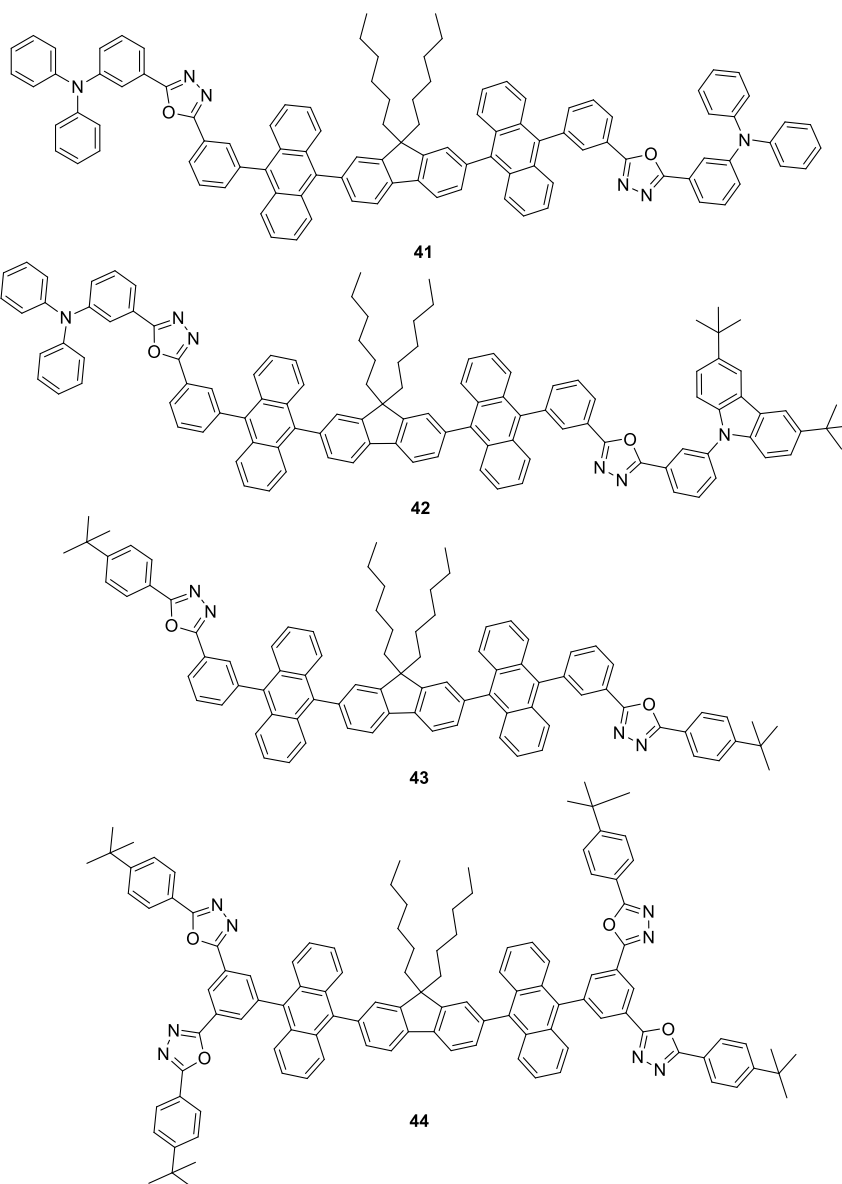


A *meta*-linked triphenylamine-oxadiazole based molecule for solution processed green and red electrophosphorescent devices was produced by Yang *et al.* (**40**). An efficiency of 13.3 cd A⁻¹ and 40.8 cd A⁻¹ for red POLED and green device, respectively were shown by the molecule.⁷¹

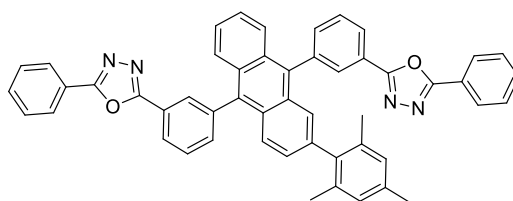


Yang *et al.* in 2011, synthesized four blue-light emitting fluorene cored anthracene derivatives along with electron deficient 1,3,4-

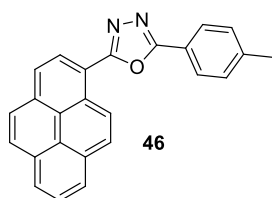
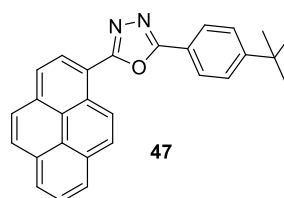
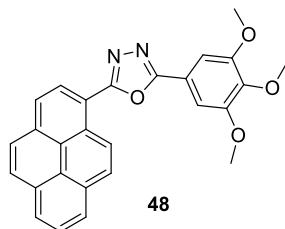
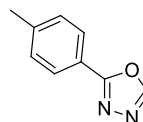
oxadiazole (**41-44**). They used these molecules for blue LEDs. Steric crowding created by the central fluorenyl bridge and anthracene moiety, hinders their aggregation in solid state.⁷¹



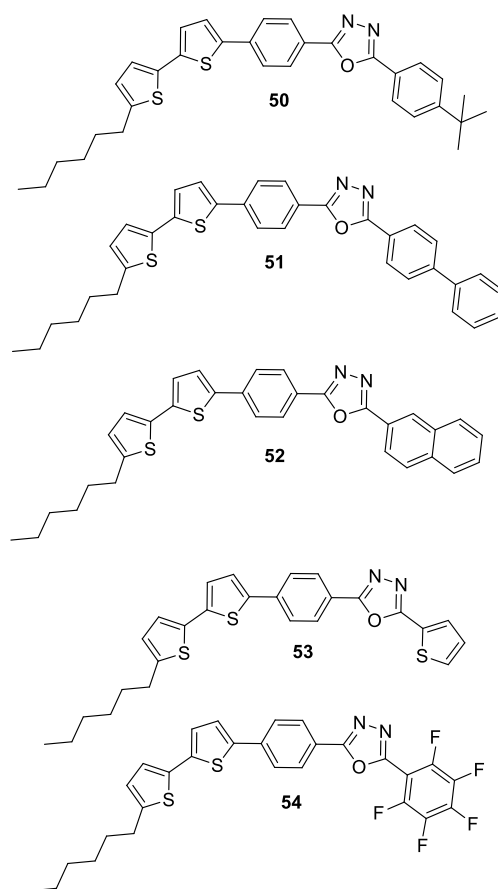
Su *et al.* in 2014 synthesized 9,10-diphenylanthracene and oxadiazole based blue light emitting fluorophore and employed it for OLED applications (**45**). Fluorophore **45** showed 4% external quantum efficiency and this is mainly due to its high charge transport nature.⁷²

**45**

Recently, Chidirala *et al.* synthesized pyrene-oxadiazole hybrid materials for OLEDs (**46-48** and **49**). The optical, thermal and electrochemical properties of these compounds were studied. In these molecules triplet to singlet energy transfer takes place due to the excited state charge transfer nature of these compounds and their emission is highly red shifted to green region.⁷³

**46****47****48****49**

Recently Deshapande *et al.* reported the synthesis of unsymmetrical bithiophene substituted 1,3,4-oxadiazoles by using palladium catalyzed Suzuki coupling reaction (**50-54**).⁷⁴ All the derivatives emitted deep blue fluorescence and exhibited good quantum yields.



1.3.2. 1,3,4-Oxadiazole based D-A systems for DSSCs

Dye sensitized solar cell (DSSC) introduced by Gratzel in 1991,⁷⁵ has fascinated a group of research community due to its low cost and environmentally benign nature. It constitutes a simple and efficient

photovoltaic device for the conversion of solar energy to electricity. Solar energy is one of the most abundant renewable sources of energy. In the commercial market DSSC became an efficient substitute for conventional inorganic solar cells due to its increased efficiency. In DSSC, sensitizer is one of the most crucial components which affect the cell performance: it produces excitons by absorbing sunlight, controls light harvesting and charge generation as well as charge separation. For a long period, ruthenium based complexes are widely used as sensitizer with the power conversion efficiency higher than 11%.⁷⁶⁻⁷⁸ The main disadvantage of Ru is its less abundancy. In comparison with inorganic materials, organic sensitizers can be prepared easily and recently organic dyes were reported with the conversion efficiency of 12.8% bettering that of Ru complexes.^{79,80}

The basic skeleton for organic sensitizer is donor- π spacer-acceptor geometry (Fig. 1.4).⁸¹ A good sensitizer should have electron acceptor part near to the semiconductor surface and donor part in the solution. Electronic communication between donor and acceptor creates long-lived charge separated state that is responsible for light harvesting character.

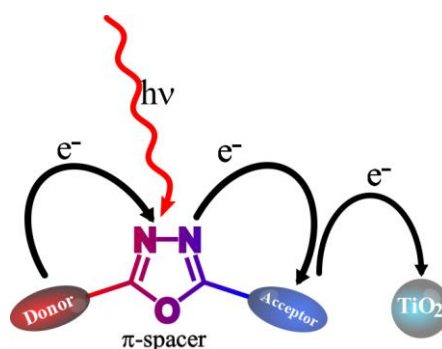
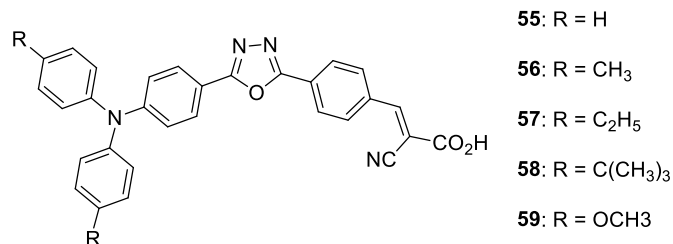


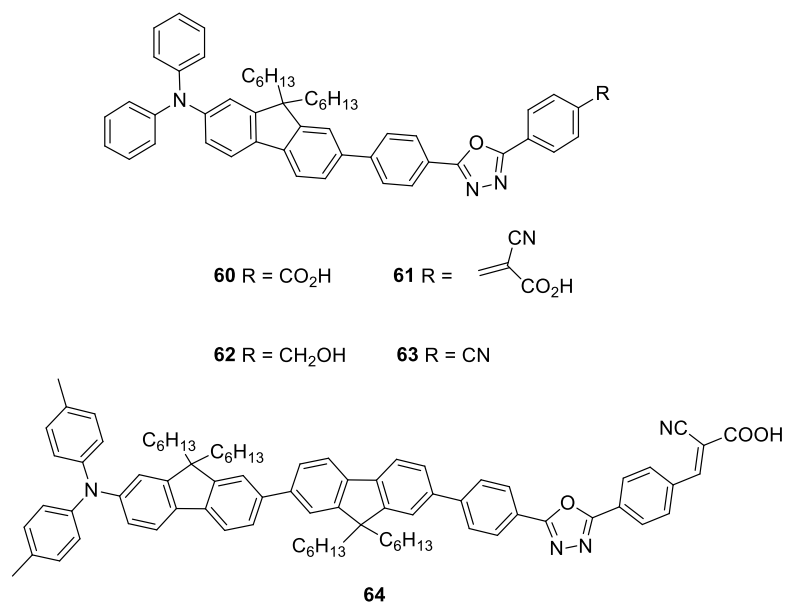
Fig. 1.4. Donor- π spacer-acceptor geometry for sensitizers

1,3,4-Oxadiazole was used as an effective π -spacer in sensitizers due to its high photoluminescence quantum yield, electron accepting property and excellent thermal stability.^{24,65,82}

Lin *et al.* in 2011, reported the synthesis of 1,3,4-oxadiazole based sensitizers for DSSCs. They introduced oxadiazole as π linker, triphenylamine as donor and cyanoacrylic acid as acceptor (**55-59**). Presence of triphenylamine makes the molecule nonplanar. This helps to interrupt the aggregation of sensitizers on the TiO₂ surface and thereby enhancing the efficiency of the devices. Compounds **55-59** showed photoconversion efficiency in the range of 2.79-3.21%.⁸³



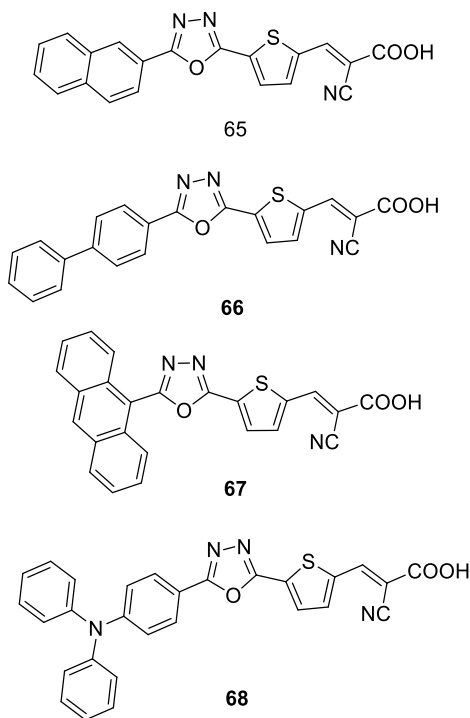
Moser *et al.* in 2014 reported the synthesis of a new 1,3,4-oxadiazole based dyes for solar light harvesting applications (**60-64**). These D- π -A sensitizers hold diphenylamine as a donor, fluorene-1,3,4-oxadiazole as π spacer and a series of acceptors (carboxylic acid, cyanoacrylic acid, alcohol and cyano group). They observed that the absorption properties of these dyes are in the UV region, which makes the dye sensitized TiO₂ transparent. The dye molecules **60** and **61** showed power conversion efficiencies of 1.28% and 2.19% respectively.⁸⁴



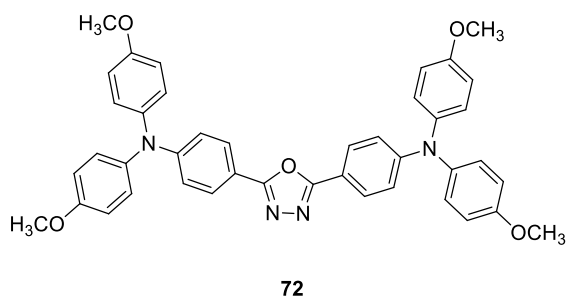
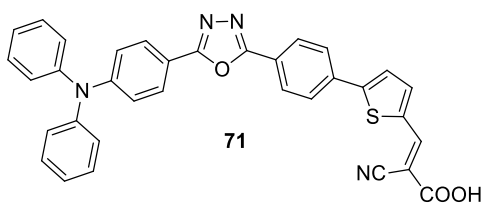
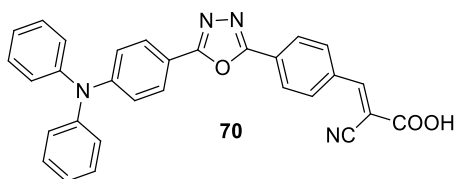
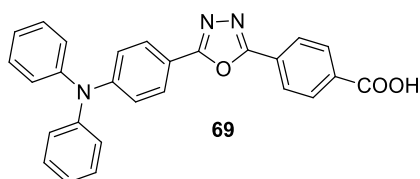
Umer Mehmood and coworkers in 2015, synthesized 1,3,4-oxadiazole based photosensitizers for DSSCs. In these dyes, they used biphenyl, anthracene and triphenylamine as the electron donating moiety, cyanoacrylic acid group as an electron acceptor and also as an anchoring group and oxadiazole as a π spacer (**65-68**). They observed that donor moiety influences the efficiency of DSSC. They got enhanced efficiency of 2.58% for anthracene attached dye **67**, in comparison with biphenyl, naphthalene and triphenyl amine incorporated dyes.⁸⁵

Hung *et al.* in 2015 reported the synthesis and photovoltaic applications of organic sensitizers having D-A- π -A framework. Here they used 1,3,4-oxadiazole as an auxiliary acceptor, triphenylamine as donor with varying π linkers and acceptors (**69-71**). They observed that conjugation length of the π -spacer has important role in photovoltaic

performance. Among the three dyes, **71** has shown increased efficiency of 2.72%.⁸⁶



Recently research community have huge interest in perovskite solar cells due to their high power conversion efficiency.^{87,88,89} In 2016, Carli *et al.* reported a new 1,3,4-oxadiazole based hole transport material (HTM) for efficient $\text{CH}_3\text{NH}_3\text{PbBr}_3$ perovskite solar cell (**72**). HTMs also play an important role in the stability of the perovskite layer and in its long term performance. Material based on **72** showed power conversion efficiency of 5.8%.⁹⁰



1.4. Nonlinear Optics: An Outlook

Interaction of light with light (photon with photon) in media is a sensation which is referred to as nonlinear optics. Invention of laser by Theodore H. Maiman in 1960, gave opportunity to the world to evaluate the interaction of high intensity light with media than previously viable. When interatomic field strength is interrupted by applied optical field,

optical nonlinearity works out. When Schwinger limit exceeds, even vacuum can be expected to show optical nonlinearity.

In linear dielectric media a linear relationship between induced polarization and the electric field strength holds as per Equation. 1.

$$\mathbf{P}(t) = \epsilon_0 \chi \mathbf{E}(t) \quad (1)$$

Where ϵ_0 is the permittivity of free space and χ represents the electric susceptibility of the medium.

When a laser beam is passed to a nonlinear dielectric media deviation occurs between induced polarization and electric field strength as shown in Fig. 1.20. Induced polarization can be explained by power series expansion (Eqn. 2),

$$\begin{aligned} \mathbf{P}(t) &= \epsilon_0 [\chi^{(1)} \tilde{\mathbf{E}}(t) + \chi^{(2)} \tilde{\mathbf{E}}^2(t) + \chi^{(3)} \tilde{\mathbf{E}}^3(t) + \dots] \quad (2) \\ &\equiv \tilde{\mathbf{P}}^{(1)}(t) + \tilde{\mathbf{P}}^{(2)}(t) + \tilde{\mathbf{P}}^{(3)}(t) + \dots \end{aligned}$$

Where $\chi^{(2)}$ and $\chi^{(3)}$ are second order and third order nonlinear optical susceptibilities respectively. Physical process that results from second order and third order polarization are totally different. The major difference between second and third order nonlinear optical interactions is that second order is absent in centrosymmetric systems, while third order polarization is shown by both centrosymmetric and noncentrosymmetric systems.⁹¹

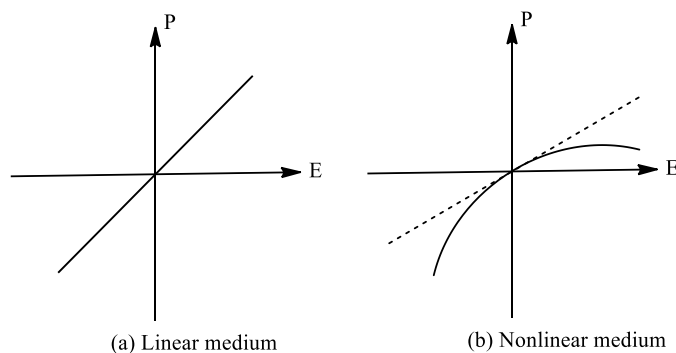


Fig. 1.5. P-E relation in linear and nonlinear media

1.4.1. Second-Harmonic Generation (SHG)

When a laser beam with definite field strength is incident upon a nonlinear medium, it induces second-order nonlinear susceptibility which is shown schematically in Fig. 1. 6.

$$\tilde{E}(t) = E e^{-i\omega t} + c. c.$$

The induced polarization is expressed as

$$\tilde{P}^{(2)}(t) = 2\epsilon_0^{(2)} E E^* + (\epsilon_0^{(2)} E^2 e^{-i2\omega t} + c.c.) \quad (3)$$

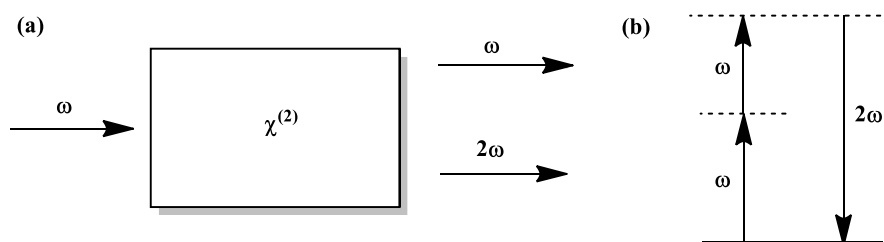


Fig. 1.6. (a) Geometry of second-harmonic generation, (b) Energy-level diagram defining second-harmonic generation.

The second term in the Equation 3 shows the contribution of frequency, 2ω and this creates radiation at the second harmonic frequency. In the first term the process of optical rectification (static electric field created across the nonlinear medium) occurs. We can tune the second-harmonic generation effectively for converting nearly all of the incident power of frequency ω to second-harmonic frequency 2ω . Main advantage of this process is that one can get a different frequency spectral region from a fixed frequency laser beam.⁹¹

Second harmonic waves are created by exchange of photons having different frequencies in the electric field. From the figure, two photons having frequency of ω are destroyed and a new photon having frequency 2ω is generated. In Fig. 1.6.b, solid line indicates ground state and dashed line specifies virtual level. The virtual level is not a real level of the system, which exists in the presence of the interacting field and in the presence of laser beam higher excitation occurs through this virtual level.⁹¹

When second order nonlinear optical medium consists of two different frequencies, *i.e*

$$\tilde{\mathbf{E}}(\mathbf{t}) = \mathbf{E}_1 e^{-i\omega_1 t} + \mathbf{E}_2 e^{-i\omega_2 t} + \text{c.c.} \quad (4)$$

Then the second order polarization is given by,

$$\begin{aligned} \tilde{\mathbf{P}}^{(2)}(\mathbf{t}) &= \epsilon_0^{(2)} \tilde{\mathbf{E}}(\mathbf{t})^2, \\ \tilde{\mathbf{P}}^{(2)}(\mathbf{t}) &= \epsilon_0^{(2)} [E_1^2 e^{-2i\omega_1 t} + E_2^2 e^{-2i\omega_2 t} + 2E_1 E_2 e^{-i(\omega_1 + \omega_2)t} + \\ & 2E_1 E_2^* e^{-i(\omega_1 - \omega_2)t} + \text{c.c.}] + 2\epsilon_0^{(2)} [E_1 E_1^* + E_2 E_2^*] \end{aligned}$$

$$\tilde{\mathbf{P}}^{(2)}(\mathbf{t}) = \sum_n \mathbf{P}(\omega_n) e^{-i\omega_n t}$$

The complex amplitudes of the various frequency components of nonlinear polarization are

$$\mathbf{P}(2\omega_1) = \varepsilon_0^{(2)} E_1^2 \text{ (SHG)}$$

$$\mathbf{P}(2\omega_2) = \varepsilon_0^{(2)} E_2^2 \text{ (SHG)}$$

$$\mathbf{P}(\omega_1 + \omega_2) = 2\varepsilon_0^{(2)} E_1 E_2 \text{ (SFG)}$$

$$\mathbf{P}(\omega_1 - \omega_2) = 2\varepsilon_0^{(2)} E_1 E_2^* \text{ (DFG)}$$

$$\mathbf{P}(0) = 2\varepsilon_0^{(2)} (E_1 E_1^* + E_2 E_2^*) \text{ (OR)}$$

Nonlinear polarization comprises of four different nonzero frequency components. Output signal is produced only when certain phase matching condition is satisfied, hence one of these frequency components are present in the radiation generated by the nonlinear interaction. By proper selection of polarization of the input radiation and orientation of the nonlinear medium, one can choose the irradiation of frequency components.⁹¹

1.4.2. Sum-Frequency Generation (SFG)

The nonlinear polarization expressed by the equation,

$$\mathbf{P}(\omega_1 + \omega_2) = 2\varepsilon_0^{(2)} E_1 E_2$$

This process is similar to that of second harmonic generation, except that in SFG the two phase matching input waves are at different frequencies. Schematic representation of SFG is shown in Fig. 1. 7.⁹¹

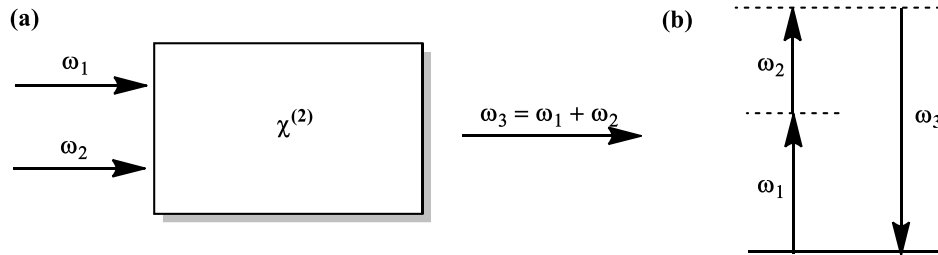


Fig. 1.7. SFG. (a) Geometry of the interaction, (b) Energy level description.

1.4.3. Difference-Frequency Generation (DFG)

The nonlinear polarization is given by the equation:

$$\mathbf{P}(\omega_1 - \omega_2) = 2\epsilon_0 \chi^{(2)} E_1 E_2^*$$

Here the frequency of the output wave is the difference of those of phase matched waves. In DFG, the high energy input wave (ω_1) is demolished and lower energy output wave (ω_3) is produced. DFG is shown schematically in Fig. 1.8.⁹¹

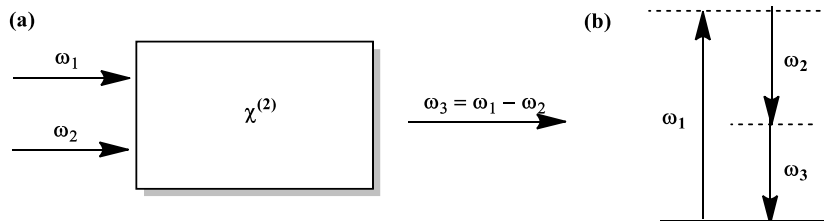


Fig. 1.8. DFG. (a) Generation of the interaction, (b) Energy level description.

1.4.4. Optical Parametric Oscillation

Here the orientation of nonlinear medium influences the output frequencies (Fig. 1.9).⁹¹

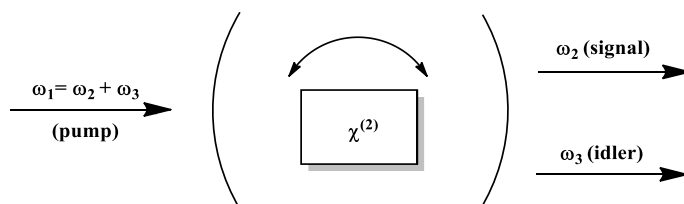


Fig. 1.9. Optical parametric oscillator

1.4.5. Third Harmonic Generation

Here output wave has frequency of 3ω and it is produced by an applied field of frequency ω , which is shown schematically in Fig. 1.10. In third harmonic generation three photons having frequency ω are destroyed and one photon having frequency 3ω is produced.

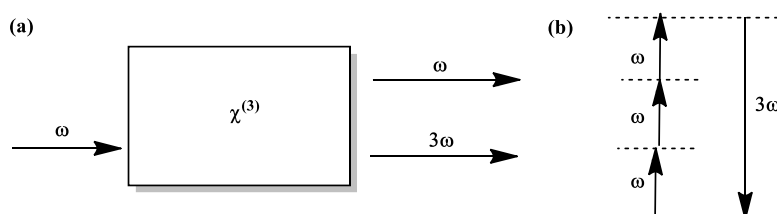


Fig. 1.10. Third-harmonic generation. (a) Geometry of the interaction, (b) Energy-level diagram.

Another term which is important in the case of third harmonic generation is nonparametric process, which involves population transfer from real level to another real level. When considering refractive index

of the medium, the real part is always associated with the parametric process and imaginary part associated with nonparametric process.⁹¹

1.4.6. Saturable Absorption (SA)

In SA, absorption of light by nonlinear medium decreases with increase in intensity of light. It is a nonparametric nonlinear process, where depletion in the ground state population occurred due to the strong absorption in the presence of high intense laser light. Thus absorption saturates and results in an increased transmittance of the system with increasing input intensity.⁹¹

1.4.7. Two Photon Absorption (2PA)

In 2PA, simultaneous absorption of two photons occurs and subsequently the atomic transition takes place from ground state to excited state (Fig. 1.11).⁹¹

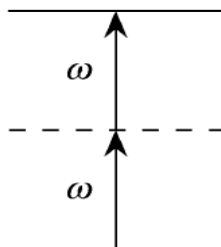


Fig. 1.11. Schematic representation of 2PA

1.4.8. Three Photon Absorption (3PA)

As the name implies here three photons are absorbed simultaneously for making transition from ground state to excited state,

which is schematically represented as in Fig. 1.12.⁹¹

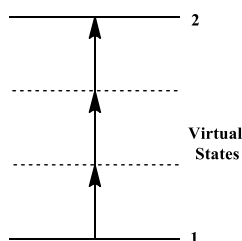


Fig. 1.12. Schematic representation of 3PA

1.4.9. Reverse Saturable Absorption (RSA)

It is a typical two-step process shown in Fig. 1.13. In RSA, when laser beam is passed through the nonlinear medium, ground state molecule gets excited to the next higher energy level. Again the excited state molecule absorbs a photon and get excited to the next higher energy level at sufficient intensity.⁹¹

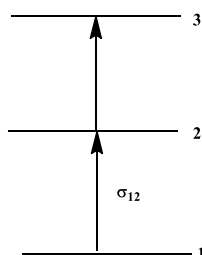


Fig. 1.13. Depiction of RSA

1.4.10. Z-Scan technique

Nonlinear optics community admires Sheik-Bahae,⁹² he introduced Z-scan technique to the world. Research groups are widely using Z-scan technique for analysing nonlinear refraction and absorption.

Main attraction of Z-scan technique is its simplicity in interpretation of results. Other techniques which are used for analysing third-order optical nonlinearities are degenerate four wave and three wave mixing, ellipse rotation, optical Kerr effect, two beam coupling etc. The main factors which influence optical nonlinearity are nonlinear absorption and nonlinear refraction. By using Z-scan technique we get information on the contribution of both nonlinear absorption and refraction.⁹²

In Z-scan, sample under study is moved towards the tightly focused Gaussian laser beam through Z direction (Fig. 1. 14). Depending on the position of the sample relative to focus, different intensities are passed through the sample. The parameter χ^3 mainly depends on coefficient of nonlinear refractive index n_2 and nonlinear absorptive coefficient β .

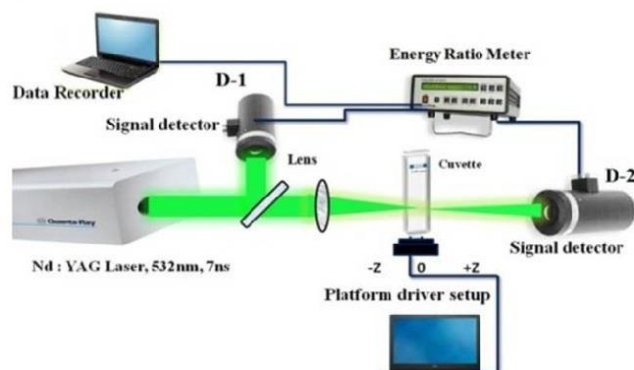


Fig. 1.14. Schematic representation of Z-scan experimental set up

1.4.11. Open aperture Z-scan

In open aperture Z-scan measurements, transmittance is measured without using an aperture in front of the far field detector. Nonlinear

absorption coefficient β is obtained by conducting open aperture Z-scan technique.

In this technique, sample experiences less intensity at the farfield so the medium exhibits linear behaviour. When the sample is at the focus the transmittance in the detector is totally changed which is shown by the appearance of an intense valley or peak at the focal point. When transmittance forms a peak at the focus, the process is called saturable absorption (SA) or negative absorption nonlinearity. Formation of a valley at the focus is responsible for the reverse saturable absorption (RSA) or positive absorption nonlinearity.⁹²

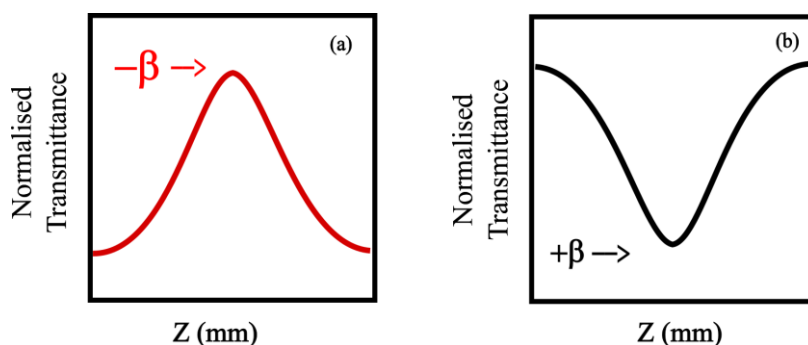


Fig. 1.15. Open aperture Z-scan traces (a) saturable absorption (b) reverse saturable absorption curves

1.4.12. Closed aperture Z-scan

As the term indicates, closed aperture Z-scan is the technique in which transmittance is measured in the presence of an aperture placed in front of the detector. Closed aperture Z-scan is used for the measurement of nonlinear index of refraction, n_2 . When high intensity laser beam is

passed through the medium, refractive index will change and this is referred to as nonlinear refraction.

In comparison to open aperture technique, here also when the sample is away from the focus, the intensity of refraction is very low due to low input intensity of laser beam. In other words, variation in the transmittance experienced by the detector is very low in the farfield. Material with a negative nonlinear refractive index is indicated by a transmittance maximum followed by a transmittance minimum. Further, a valley followed by a peak is the clear indication of positive nonlinear refractive index (Fig. 1.16).⁹²

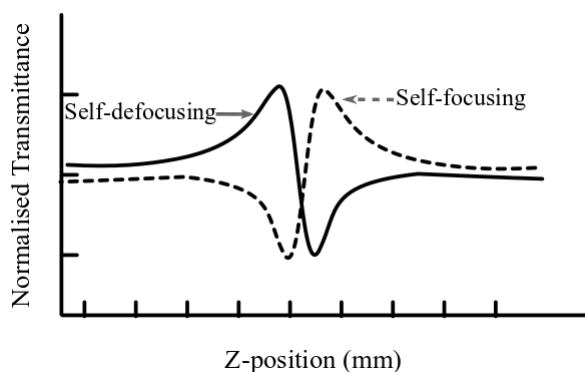


Fig. 1.16. Closed aperture Z-scan traces indicating self-focusing and defocusing nature

Using closed aperture Z-scan technique the information obtained regarding nonlinear refraction is highly complex due to the interference of nonlinear absorption. The graph itself gives information of absorbance interference, which is observed as an enhancement of peak. This is an indication of the involvement of saturable absorption. Similarly enhancement of valley gives information regarding interference of

reverse saturable absorption. Hence perfect nonlinear refraction parameter is obtained by comparing both open and closed aperture Z-scan data.⁹²

1.4.13. Optical Power Limiting

Protection of eyes and optical devices from high intensity laser light have received significant attention. Molecules with large non-linearity, broadband spectral response and fast response time are crucial for good optical limiting property. Lowering of optical threshold will enhance the optical response. Main factor which influence the optical power limiting is nonlinear absorption, hence open aperture Z-scan technique is used for measuring optical power limiting. A schematic representation of optical limiting material is given in Fig. 1.17.

The factors which influences the optical limiting properties are:

- Limiting threshold
- Stability
- Response time
- Linear transmittance
- Optical clarity

In organic materials like **74-79** proper tuning of electron delocalization by suitably substituting the donor and acceptor moieties will enhances the optical limiting property.⁸ In semiconductor materials lots of reports have appeared clarifying the influence of two photon absorption on optical limiting property.

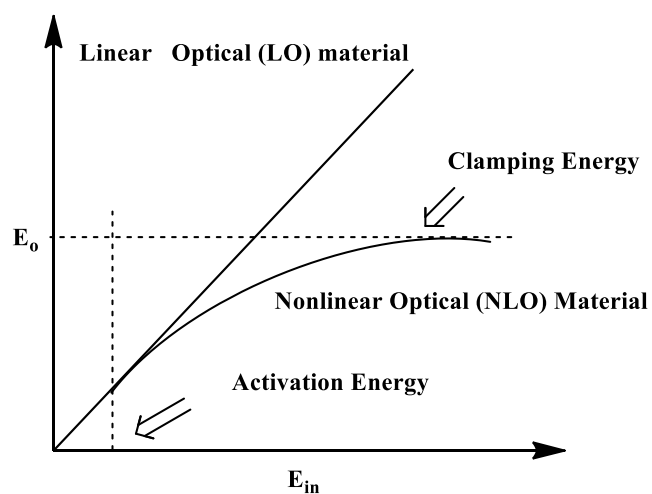
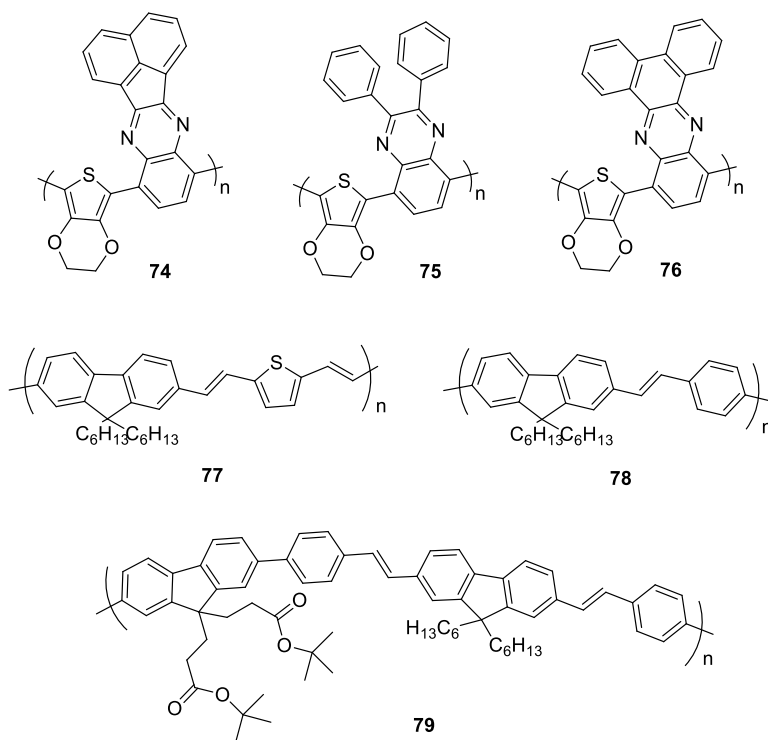


Fig. 1.17. Scheme depicting optical limiting material

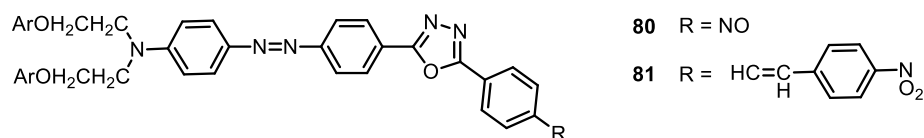


1.4.14. 1,3,4-Oxadiazole based D-A systems for NLO

Design and synthesis of push-pull organic molecules with desirable third order nonlinear properties are emerging as a trend setting area of research due to their enormous applications in the field of optical communication,^{93,94} information storage,^{95,96} two photon imaging,^{97,98} optical computing,^{99,100} optical power limiting and optical switching.¹⁰¹⁻¹⁰⁴ Organic π conjugated charge transfer chromophores are significantly used for these applications owing to their high NLO susceptibility,¹⁰⁵ short response time,¹⁰⁶ excellent thermal stability and high structural flexibility.¹⁰⁷

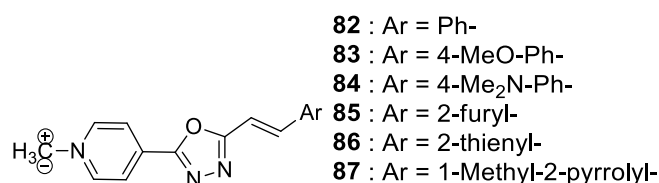
1,3,4-Oxadiazoles are well established molecules with high thermal and chemical stability, excellent photoluminescent quantum yield and electron deficient nature.¹⁰⁸⁻¹¹⁰ 1,3,4-Oxadiazole based push-pull molecules show excellent ICT character due to π electron delocalization producing high asymmetry in the molecule.¹¹¹

Roberto Centore in 2002 synthesized 1,3,4-oxadiazole chromophores **80** and **81**. They studied their second order nonlinear optical properties, the results showed that the synthesized compounds are NLO active.¹¹²



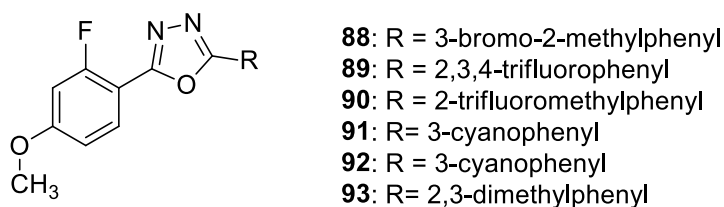
Mashraqui *et al.* in 2004 synthesized several oxadiazole based donor-acceptor molecules and studied their second order nonlinear

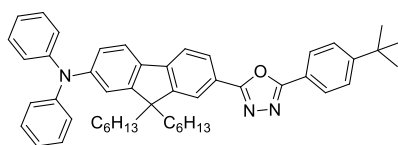
optical properties (**82-87**). In order to tune the polarizability of the molecules, they introduced various donors and acceptors onto the molecular system. Among various molecules synthesized, one having *p*-methoxyphenyl donor and the pyridinium acceptor (**83**) showed large second order nonlinearity.¹¹³



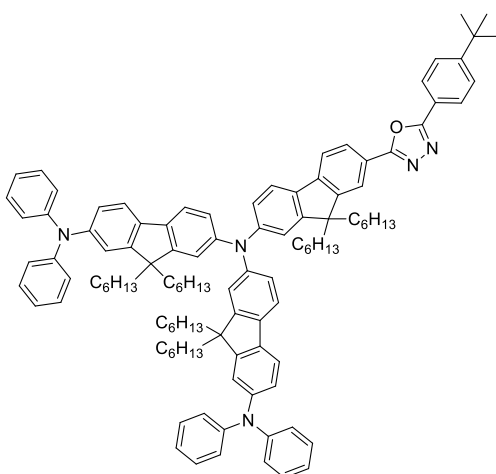
Isloor and coworkers in 2010 synthesized 2-fluoro-4-methoxy phenyl substituted 1,3,4-oxadiazoles and studied their third order nonlinear properties using open aperture *Z*-scan technique. Among these, bromo derivative **88** showed good optical limiting property.¹¹⁴

Lin *et al.* in 2012 reported the synthesis of small dendritic chromophores having fluorene and oxadiazoles as major building blocks (**94-96**). The fluorophores showed intense two photon absorption characteristics in the IR region. They observed that two photon absorption depends upon the electron donating branches in the D- π -A skeleton. Furthermore, the entire architecture also showed effective optical power limiting properties.¹¹⁵

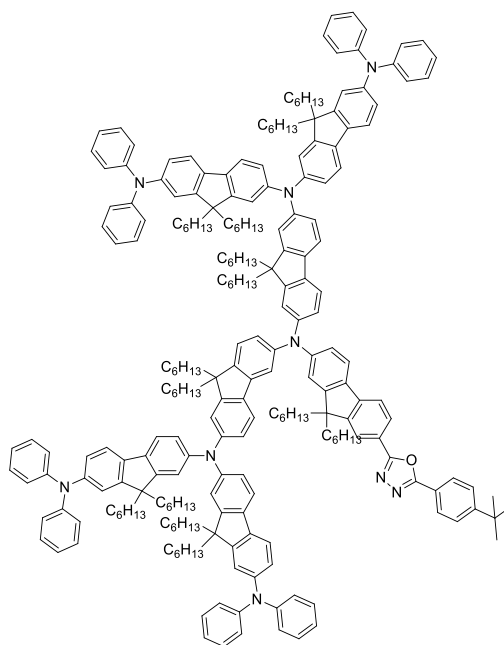




94



95



96

Recently in our laboratory, a few 1,3,4-oxadiazole and phenothiazine based conjugated donor-acceptor dyes were synthesized (**97**, **98**). Their third order nonlinear optical properties and optical limiting power were investigated using Nd-YAG laser with 7 ns laser pulses of 532 nm wavelength. The Z-scan results indicated that the compounds exhibited negative refractive index which was of the order 10^{-10} esu. The non-linear absorption coefficient (β , m/W) and third-order non-linear susceptibility ($\chi^{(3)}$, esu) of **97** and **98** are in the order of 10^{-10} and 10^{-11} (Table 1.2).

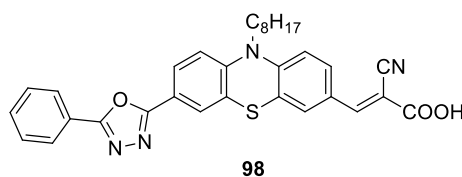
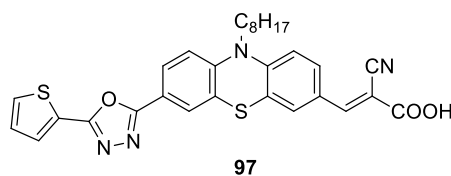


Table 1.2. NLO properties of **97** and **98**

Compound	Nonlinear absorption coefficient (β , m/W)	Nonlinear refractive index (n_2 , esu)	Imaginary part of nonlinear susceptibility ($\text{Im } \chi^{(3)}$, esu)	Real part of nonlinear susceptibility ($\text{Re } \chi^{(3)}$, esu)	Nonlinear susceptibility ($\chi^{(3)}$, esu)
97	15×10^{-10}	-2.36×10^{-10}	4.53×10^{-11}	2.35×10^{-12}	4.53×10^{-11}
98	12.9×10^{-10}	-2.47×10^{-10}	3.89×10^{-11}	2.46×10^{-12}	3.89×10^{-11}

1.4.15. 1,3,4-Oxadiazole based polymers for third-order NLO applications

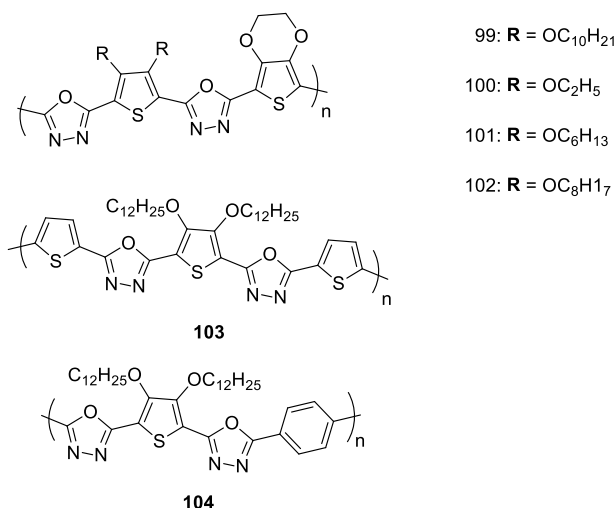
Donor-acceptor type conducting polymers are extensively used as NLO active materials.⁸ These types of polymers have large third order NLO susceptibility along the polymeric backbone. Similar to organic push-pull molecules, here also, polymers have high molecular hyperpolarizability (β) and dipole moment (μ), which are the essential properties for large third order nonlinear susceptibility.

Numerous reports have appeared in literature based on the NLO activity of D-A conjugated polymers.¹¹⁶ It is possible to tune the bandgaps of polymers by proper selection of donor and acceptor groups.¹¹⁷ Lowering bandgap further increases the conductivity and NLO activity of polymers. Steric repulsion between donor and acceptor also plays a vital role in electronic delocalization and charge asymmetry in the entire polymer system.

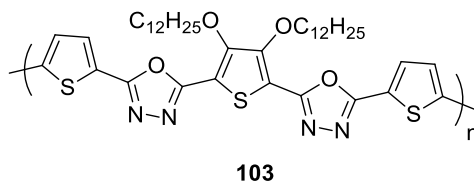
Polythiophenes based oligomers and polymers are widely employed in NLO purpose due to their attractive features like thermal stability, conductivity, film forming capability, solubility and easiness of preparation. In most of the reported works based on third order nonlinearity of 1,3,4-oxadiazole based conjugated polymers, electron donating groups are thiophene and electron accepters are oxadiazoles.

Adhikari and coworkers have extensively investigated thiophene - 1,3,4-oxadiazole D-A type polymers and their nonlinear optical properties. The third order NLO activity was studied using Z-scan

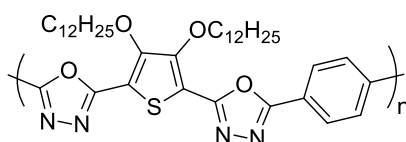
differential and four wave mixing (DFWM). Among these, polymer **99** exhibited best third order NLO activity and optical limiting property.¹¹⁸



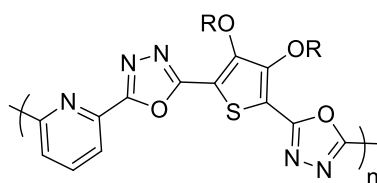
In continuation, Adhikari and coworkers reported the synthesis and nonlinear optical properties of poly {2,2'-(3,4-didodecyloxythiophene-2,5-diyl)bis[5-(2-thienyl)-1,3,4-oxadiazole]} (**103**). Two techniques namely single beam Z-scan (532 nm) and degenerate four-wave mixing (DFWM) using nanosecond laser pulses, were used for the investigation of NLO properties. A strong optical limiting property due to the three photon absorption (3PA) process was shown by the synthesized copolymer.¹¹⁹



Same group of researchers in 2010 synthesized a D-A conjugated polymer *viz.* poly(2-[3,4didodecyloxy-5-(1,3,4-oxadiazol-2-yl)thiophen-2-yl]-5-phenyl-1,3,4-oxadiazole) (**104**) and investigated their third order nonlinear activity by using Z-scan technique. Here 3,4-didodecyloxy thiophene and 1,3,4-oxadiazole components play the role of electron donating and electron accepting moieties respectively. In addition a nanocomposite of this polymer using nano TiO₂ was also prepared. The obtained β values (1×10^{-7} m/W and 2×10^{-7} m/W for polymer and nanocomposite films respectively) displayed good NLO properties. Both these compounds also exhibited excellent optical limiting properties.

**104**

In the same year, they synthesized D-A type polymers incorporated with alternate 3,4-dialkyloxythiophene and (1,3,4-oxadiazolyl)pyridines (**105-107**). The third order NLO properties of these polymers were studied using Z-scan technique using Nd: YAG laser at 532 nm and 7 ns laser pulses in solution phase. Among the three polymers, **107** has shown the best optical limiting property as well as nonlinear absorption. They observed that the alkoxy substituent at the 3rd and 4th carbon of the thiophene ring have marked effect on the optical limiting capacity. That is, here the electron donating capacity of the substituent enhances the optical limiting power.¹¹²



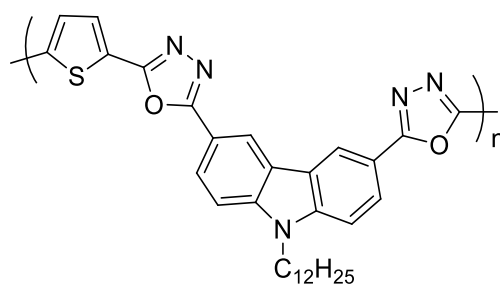
105: R = $n\text{-C}_3\text{H}_7$

106: R = $n\text{-C}_5\text{H}_{11}$

107: R = $n\text{-C}_7\text{H}_{15}$

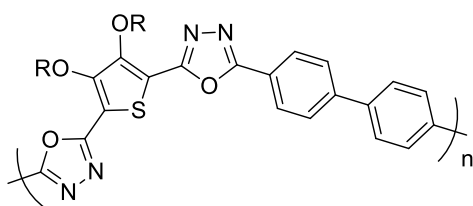
A polymer with same polymer backbone as that of polymers **105-107** with only change in the substituent R (i.e. R = $n\text{-C}_{14}\text{H}_{29}$) was synthesized and they also prepared composite of this polymer in solid poly(methylmethacrylate) matrix. From nanosecond Z-scan technique they observed that both solution as well as solid film exhibited good optical power limiting property in 7 ns laser pulses with 532 nm wavelength.¹²⁰

They also prepared D-A type polymer **108** which consists of 3,4-disubstituted thiophene and N-dodecylcarbazole as electron donors and 1,3,4-oxadiazole as electron withdrawing group. The polymer showed large third order nonlinear optical properties and optical limiting capabilities due to three photon absorption process.¹²¹



108

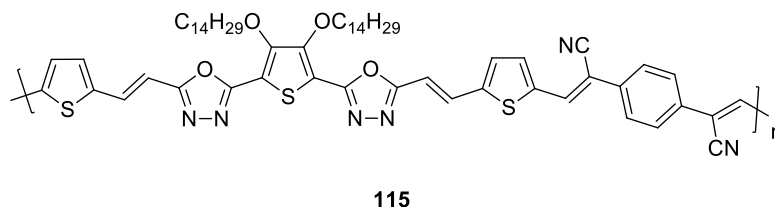
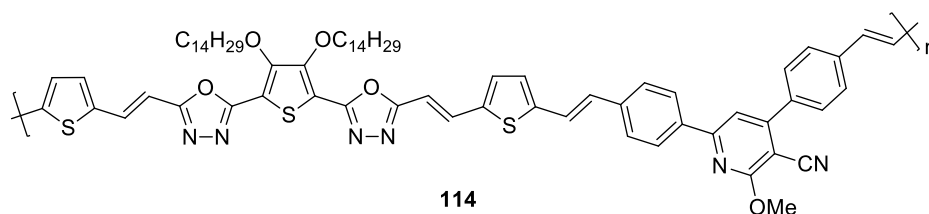
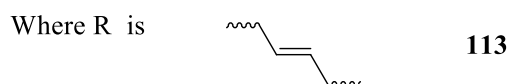
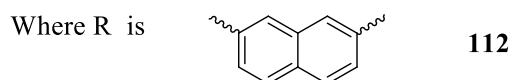
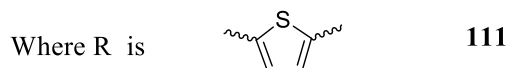
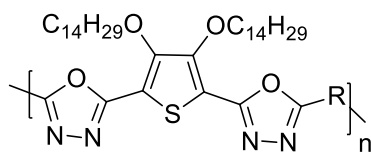
D-A type polymers having poly (3,4-dialkoxythiophene) and 1,3,4-oxadiazolyl-biphenyl moieties (**109** & **110**) also showed strong optical limiting property due to three photon absorption. The three photon absorption coefficient values of polymers **109** and **110** were found to be 9×10^{-24} and 17×10^{-24} respectively.¹²²



109: R = C₇H₁₅

110: R = C₁₄H₂₉

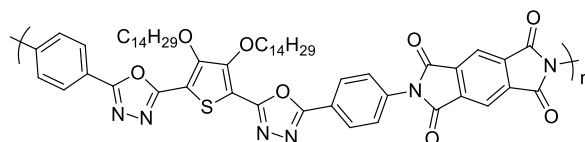
In 2012, they synthesized five D-A type conjugated polymers (**111-115**) having 1,3,4-oxadiazole core. These polymers are enriched with highly electron donating ditetradecyloxythiophene, naphthalene and vinylene units and strong electron withdrawing oxadiazole, cyanopyridine and cyanovinylene moieties. They observed that the important factors which influence the optical nonlinearity as well as optical limiting properties are conjugation length and structural tuning. Among the polymers, **114** showed increased optical limiting property with 2PA coefficient of 2.1×10^{-11} m/W.¹²³



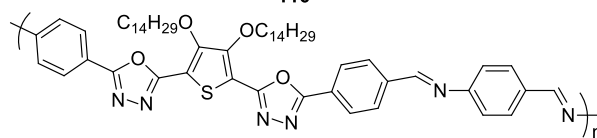
Thiophene and oxadiazole based polyamide and polyazomethine type polymers have been synthesized by the same group in 2013 (**116-119**). The polymers showed excellent optical limiting property with high two photon absorption coefficient (2PA).

Udaykumar *et al.* in 2014, synthesized polymers containing 1,3,4-oxadiazole, 3,4-didecyloxythiophene and triphenylamine units (**120** & **121**). Polymer **120** is linear while **121** is branched. They observed that

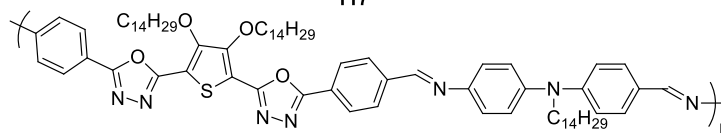
branching enhances the optical and thermal properties and also the device performance. Z-Scan technique gave clear indication of their high optical limiting property.¹²⁴



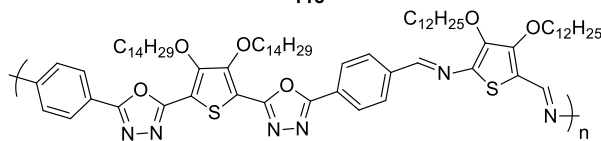
116



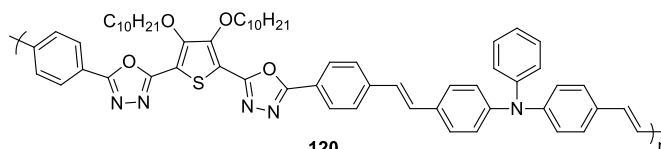
117



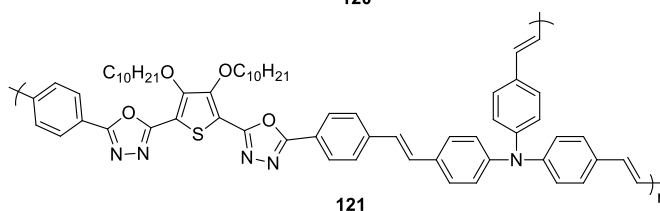
118



119



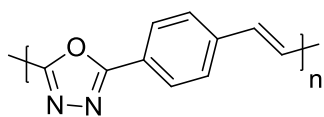
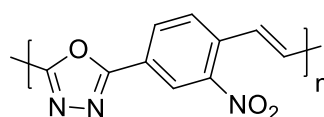
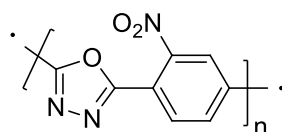
120



121

Very recently, Gopalakrishnan and coworkers reported the synthesis and investigation of third order nonlinear optical properties of

two conjugated polymers namely poly(*p*-phenylenevinylene-1,3,4-oxadiazole) (**122**) and poly(*p*-(nitro-phenylene)vinylene-1,3,4-oxadiazole) (**123**). They studied the third order NLO activity of these polymers by using Nd-YAG laser with 532 nm and 7 ns pulses.¹²⁵ In another report, the same group presented the nonlinear optical properties of poly(2-nitro-*p*-phenylene-1,3,4-oxadiazole) (**124**). It also showed good third order nonlinear optical property.¹²⁶

**122****123****124**

As evident from the above reports, 1,3,4-oxadiazole is a powerful acceptor and hence attaching electron rich molecules to oxadiazole enables strong intramolecular charge transfer and π electron delocalization over the whole system. This asymmetry of polarization will enhance third order nonlinear optical properties. Keeping this in mind, we have designed a few phenothiazine, carbazole and pyrene coupled 1,3,4-oxadiazole push-pull fluorophores. These fluorophores are potential candidates for third order NLO applications.

1.5. Objectives

- Synthesis and characterization of a few 2,5-diaryl-1,3,4-oxadiazoles and 1,3,4-oxadiazole–thiophene hybrid molecules.
- Synthesis and evaluation of third-order nonlinear optical properties of a few 1,3,4-oxadiazole–phenothiazine push-pull fluorophores.
- Synthesis and evaluation of third-order nonlinear optical properties of a few 1,3,4-oxadiazole–carbazole push-pull fluorophores.
- Synthesis and evaluation of third-order nonlinear optical properties of a few 1,3,4-oxadiazole–pyrene push-pull fluorophores.

1.6. References

- (1) Li, Y.; Liu, T.; Liu, H.; Tian, M. Z.; Li, Y. *Acc. Chem. Res.* **2014**, *47*, 1186.
- (2) Bureš, F. *RSC Adv.* **2014**, *4*, 58826.
- (3) Allard, S.; Forster, M.; Souhace, B.; Thiem, H.; Scherf, U. *Angew. Chem. Int. Ed.* **2008**, *47*, 4070.
- (4) Ohmori, Y. *Laser Photonics Rev.* **2010**, *4*, 300.
- (5) Hains, A. W.; Liang, Z.; Woodhouse, M. A.; Gregg, B. A. *Chem. Rev.* **2010**, *110*, 6689.
- (6) Burland, D. M.; Miller, R. D.; Walsh, C. A. *Chem. Rev.* **1994**, *94*, 31.
- (7) Marder, S. R. *Chem. Commun.* **2006**, *2*, 131.
- (8) Dini, D.; Calvete, M. J. F.; Hanack, M. *Chem. Rev.* **2016**, *116*, 13043.
- (9) Sullivan, P. A.; Dalton, L. R. *Chem. Rev.* **2010**, *110*, 25.
- (10) Luo, J.; Huang, S.; Shi, Z.; Polishak, B. M.; Zhou, X. H.; Jen, A. K. Y. *Chem. Mater.* **2011**, *23*, 544.

- (11) Chen, F.; Zhang, J.; Wan, X. *Chem. - A Eur. J.* **2012**, *18*, 4558.
- (12) Helmy, S.; Leibfarth, F. A.; Oh, S.; Poelma, J. E.; Hawker, C. J.; De Alaniz, J. R. *J. Am. Chem. Soc.* **2014**, *136*, 8169.
- (13) Lerch, M. M.; Wezenberg, S. J.; Szymanski, W.; Feringa, B. L. *J. Am. Chem. Soc.* **2016**, *138*, 6344.
- (14) Reichardt, C.; Welton, T. *Solvents and solvent effects in organic chemistry, Fourth edition Wiley-VCH Verlag GmbH & Co. KGaA* **2010**, 65.
- (15) Bureš, F.; Pytela, O.; Kivala, M.; Diederich, F. *J. Phys. Org. Chem.* **2011**, *24*, 274.
- (16) Bureš, F.; Pytela, O.; Diederich, F. *J. Phys. Org. Chem.* **2009**, *22*, 155.
- (17) Suponitsky, K. Y.; Liao, Y.; Masunov, A. E. *J. Phys. Chem. A* **2009**, *113*, 10994.
- (18) Kong, C.; Peng, M.; Shen, H.; Wang, Y.; Zhang, Q.; Wang, H.; Zhang, J.; Zhou, H.; Yang, J.; Wu, J.; Tian, Y. *Dye. Pigment.* **2015**, *120*, 328.
- (19) Sheng, N.; Liu, D.; Wu, J.; Gu, B.; Wang, Z.; Cui, Y. *Dye. Pigment.* **2015**, *119*, 116.
- (20) Lee, J. Y.; Kim, K. S.; Mhin, B. J. *J. Chem. Phys.* **2001**, *115*, 9484.
- (21) Huang, Z.-S.; Meier, H.; Cao, D. *J. Mater. Chem. C* **2016**, *4*, 2404.
- (22) Zhu, Y.; Babel, A.; Jenekhe, S. A. *Macromolecules* **2005**, *38*, 7983.
- (23) Tan, H.; Pan, C.; Wang, G.; Wu, Y.; Zhang, Y.; Zou, Y.; Yu, G.; Zhang, M. *Org. Electron. physics, Mater. Appl.* **2013**, *14*, 2795.
- (24) Dumur, F.; Goubard, F. *New J. Chem.* **2014**, *38*, 2204.
- (25) Mahmood, A. *Sol. Energy* **2016**, *123*, 127.
- (26) Venkateswararao, A.; Thomas, K. R. J.; Lee, C. P.; Li, C. T.; Ho, K. C. *ACS Appl. Mater. Interfaces* **2014**, *6*, 2528.
- (27) Sathiyam, G.; Sivakumar, E. K. T.; Ganesamoorthy, R.; Thangamuthu, R.; Sakthivel, P. *Tetrahedron Lett.* **2016**, *57*, 243.
- (28) Melomedov, J.; Ochsmann, J. R.; Meister, M.; Laquai, F.; Heinze, K. *Eur. J. Inorg. Chem.* **2014**, *18*, 2902.
- (29) Raju, T. B.; Vaghasiya, J. V.; Afroz, M. A.; Soni, S. S.; Iyer, P. K. *Org. Electron. physics, Mater. Appl.* **2016**, *39*, 371.
- (30) Giribabu, L.; Duvva, N.; Prasanthkumar, S.; Singh, S. P.; Han, L.; Bedja, I.; Gupta, R. K.; Islam, A. *Sustain. Energy Fuels* **2017**, *1*, 345.
- (31) Ren, X.; Jiang, S.; Cha, M.; Zhou, G.; Wang, Z. S. *Chem. Mater.* **2012**, *24*, 3493.
- (32) Samae, R.; Surawatanawong, P.; Eiamprasert, U.; Pramjit, S.; Saengdee, L.; Tangboriboonrat, P.; Kiatisevi, S. *European J. Org. Chem.* **2016**, *2016*, 3536.

- (33) Saritha, G.; Wu, J. J.; Anandan, S. *Org. Electron. physics, Mater. Appl.* **2016**, *37*, 326.
- (34) Lin, J. T.; Chen, P.; Yen, Y.; Hsu, Y.; Chou, H.; Yeh, M. P. *Org. Lett.* **2009**, *11*, 97.
- (35) Paun, A.; Hadade, N. D.; Paraschivescu, C. C.; Matache, M. *J. Mater. Chem. C* **2016**, *4*, 8596.
- (36) Ren, S.; Zeng, D.; Zhong, H.; Wang, Y.; Qian, S.; Fang, Q. *J. Phys. Chem. B* **2010**, *114*, 10374.
- (37) Sonar, P.; Singh, S. P.; Leclère, P.; Surin, M.; Lazzaroni, R.; Lin, T. T.; Dodabalapur, A.; Sellinger, A. *J. Mater. Chem.* **2009**, *19*, 3228.
- (38) Ledwon, P.; Zassowski, P.; Jarosz, T.; Lapkowski, M.; Wagner, P.; Cherpak, V.; Stakhira, P. *J. Mater. Chem. C* **2016**, *4*, 2219.
- (39) Ledwon, P.; Thomson, N.; Angioni, E.; Findlay, N. J.; Skabara, P. J.; Domagala, W. *RSC Adv.* **2015**, *5*, 77303.
- (40) Ainsworth, C. *J. Am. Chem. Soc.* **1965**, *87*, 5800.
- (41) Guin, S.; Ghosh, T.; Rout, S. K.; Banerjee, A.; Patel, B. K. *Org. Lett.* **2011**, *13*, 5976.
- (42) Sharma, S.; Sharma, P. K.; Kumar, N.; Dudhe, R. *Der Pharma Chem.* **2010**, *2*, 253.
- (43) Bhatia, S.; Gupta, M. *J. Chem. Pharm. Res.* **2011**, *3*, 137.
- (44) De Oliveira, C. S.; Lira, B. F.; Barbosa-Filho, J. M.; Lorenzo, J. G. F.; De Athayde-Filho, P. F. *Synthetic approaches and pharmacological activity of 1,3,4-oxadiazoles: A review of the literature from 2000-2012; Molecules* **2012**, *17*, 10192.
- (45) Fang, T.; Tan, Q.; Ding, Z.; Liu, B.; Xu, B. *Org. Lett.* **2014**, *16*, 2342.
- (46) Andersen, T. L.; Caneschi, W.; Ayoub, A.; Lindhardt, A. T.; Couri, M. R. C.; Skrydstrup, T. *Adv. Synth. Catal.* **2014**, *356*, 3074.
- (47) Gao, Q.; Liu, S.; Wu, X.; Zhang, J.; Wu, A. *Org. Lett.* **2015**, *17*, 2960.
- (48) Wang, L.; Cao, J.; Chen, Q.; He, M. *J. Org. Chem.* **2015**, *80*, 4743.
- (49) Fan, Y.; He, Y.; Liu, X.; Hu, T.; Yang, X.; Luo, X.; Huang, G. *J. Org. Chem.* **2016**, *81*, 6820.
- (50) Tokumaru, K.; Johnston, J. N. *Chem. Sci.* **2017**, *8*, 3187.
- (51) Burroughes, J. H.; Bradley, D. D. C.; Brown, A. R.; Marks, R. N.; Mackay, K.; Friend, R. H.; Burns, P. L.; Holmes, A. B. *Nature* **1990**, *347*, 539.
- (52) Baldo, M. A.; O'Brien, D. F.; You, Y.; Shoustikov, A.; Sibley, S.; Thompson, M. E.; Forrest, S. R. *Nature* **1998**, *395*, 151.
- (53) Tang, C. W.; Vanslyke, S. A. *Appl. Phys. Lett.* **1987**, *51*, 10.

- (54) Yook, K. S.; Lee, J. Y. *Chem. Rec.* **2016**, *16*, 159.
- (55) Tao, Y.; Yang, C.; Qin, J. *Chem. Soc. Rev.* **2011**, *40*, 2943.
- (56) Chen, H.-F.; Yang, S.-J.; Tsai, Z.-H.; Hung, W.-Y.; Wang, T.-C.; Wong, K.-T. *J. Mater. Chem.* **2009**, *19*, 8112.
- (57) Chen, D.; Su, S.-J.; Cao, Y. *J. Mater. Chem. C* **2014**, *2*, 9565.
- (58) Hu, M.; Liu, Y.; Chen, Y.; Song, W.; Gao, L.; Mu, H.; Huang, J.; Su, J. *RSC Adv.* **2017**, *7*, 7287.
- (59) Wu, K.; Zhang, T.; Zhan, L.; Zhong, C.; Gong, S.; Lu, Z. H.; Yang, C. *Adv. Opt. Mater.* **2016**, *4*, 1558.
- (60) Wei, X.-F.; Tan, W.-Y.; Zou, J.-H.; Guo, Q.-X.; Gao, D.-Y.; Ma, D.-G.; Peng, J.; Cao, Y.; Zhu, X.-H. *J. Mater. Chem. C* **2017**, *5*, 2329.
- (61) Thomas, K. R. J.; Lin, J. T.; Tao, Y. T.; Chuen, C. H. *Chem. Mater.* **2002**, *14*, 2796.
- (62) Chang, D. W.; Ko, S. J.; Kim, J. Y.; Dai, L.; Baek, J. B. *Synth. Met.* **2012**, *162*, 1169.
- (63) Hung, W.-Y.; Chi, L.-C.; Chen, W.-J.; Chen, Y.-M.; Chou, S.-H.; Wong, K.-T. *J. Mater. Chem.* **2010**, *20*, 10113.
- (64) Zhao, Y.; Wu, C.; Qiu, P.; Li, X.; Wang, Q.; Chen, J.; Ma, D. *ACS Appl. Mater. Interfaces* **2016**, *8*, 2635.
- (65) Adachi, C.; Tsutsui, T.; Saito, S. *Appl. Phys. Lett.* **1990**, *56*, 799.
- (66) Hughes, G.; Bryce, M. R. *J. Mater. Chem.* **2005**, *15*, 94.
- (67) Tao, Y.; Wang, Q.; Yang, C.; Wang, Q.; Zhang, Z.; Zou, T.; Qin, J.; Ma, D. *Angew. Chem. Int. Ed.* **2008**, *47*, 8104.
- (68) Tao, Y.; Wang, Q.; Shang, Y.; Yang, C.; Ao, L.; Qin, J.; Ma, D.; Shuai, Z. *Chem. Commun.* **2009**, No. 1, 77.
- (69) Tao, Y.; Ao, L.; Wang, Q.; Zhong, C.; Yang, C.; Qin, J.; Ma, D. *Chem. - An Asian J.* **2010**, *5*, 278.
- (70) Tao, Y.; Wang, Q.; Yang, C.; Zhong, C.; Qin, J.; Ma, D. *Adv. Funct. Mater.* **2010**, *20*, 2923.
- (71) Zhu, M.; Ye, T.; Li, C. G.; Cao, X.; Zhong, C.; Ma, D.; Qin, J.; Yang, C. *J. Phys. Chem. C* **2011**, *115*, 17965.
- (72) Wu, C.-L.; Chang, C.-H.; Chang, Y.-T.; Chen, C.-T.; Chen, C.-T.; Su, C.-J. *J. Mater. Chem. C* **2014**, *2*, 7188.
- (73) Chidirala, S.; Ulla, H.; Valaboju, A.; Kiran, M. R.; Mohanty, M. E.; Satyanarayan, M. N.; Umesh, G.; Bhanuprakash, K.; Rao, V. J. *J. Org. Chem.* **2016**, *81*, 603.

- (74) Deshapande, N.; Belavagi, N. S.; Sunagar, M. G.; Gaonkar, S.; Pujar, G. H.; Wari, M. N.; Inamdar, S. R.; Khazi, I. A. M. *RSC Adv.* **2015**, *5*, 86685.
- (75) O'Regan, B.; Gratzel, M. *Nature* **1991**, *353*, 737.
- (76) Nazeeruddin, M. K.; De Angelis, F.; Fantacci, S.; Selloni, A.; Viscardi, G.; Liska, P.; Ito, S.; Takeru, B.; Grätzel, M. *J. Am. Chem. Soc.* **2005**, *127*, 16835.
- (77) Gao, F.; Wang, Y.; Shi, D.; Zhang, J.; Wang, M.; Jing, X.; Humphry-baker, R.; Wang, P.; Zakeeruddin, S. M.; Gra, M. *J. Am. Chem. Soc.* **2008**, *130*, 10720.
- (78) Chen, C.; Wang, M.; Li, J.; Pootrakulchote, N.; Alibabaei, L.; Decoppet, J.; Tsai, J.; Gra, C.; Wu, C.; Zakeeruddin, S. M.; Gra, M. *ACS Nano*. **2009**, *3*, 3103.
- (79) Kakiage, K.; Aoyama, Y.; Yano, T.; Oya, K.; Kyomen, T.; Hanaya, M. *Chem. Commun.* **2015**, *51*, 6315.
- (80) Zhang, M.; Wang, Y.; Xu, M.; Ma, W.; Li, R.; Wang, P. *Energy Environ. Sci.* **2013**, *6*, 2944.
- (81) Clifford, J. N.; Martínez-Ferrero, E.; Viterisi, A.; Palomares, E. *Chem. Soc. Rev.* **2011**, *40*, 1635.
- (82) Adachi, C.; Tsutsui, T.; Saito, S. *Appl. Phys. Lett.* **1990**, *57*, 531.
- (83) Srinivas, K.; Sivakumar, G.; Ramesh Kumar, C.; Ananth Reddy, M.; Bhanuprakash, K.; Rao, V. J.; Chen, C. W.; Hsu, Y. C.; Lin, J. T. *Synth. Met.* **2011**, *161*, 1671.
- (84) Wielopolski, M.; Linton, K. E.; Marszałek, M.; Gulcur, M.; Bryce, M. R.; Moser, J. E. *Phys. Chem. Chem. Phys.* **2014**, *16*, 2090.
- (85) Umer Mehmood Ibnelwaleed A. Hussein, M. D. *Int. J. Photoenergy* **2015**, *2015*, 8.
- (86) Mane, S. B.; Cheng, C. F.; Sutanto, A. A.; Datta, A.; Dutta, A.; Hung, C. H. *Tetrahedron* **2015**, *71*, 7977.
- (87) Mitzi, D. B.; Feild, C. A.; Harrison, W. T. A.; Guloy, A. M. *Nature* **1994**, *369*, 467.
- (88) Bi, D.; Tress, W.; Dar, M. I.; Gao, P.; Luo, J.; Renevier, C.; Schenk, K.; Abate, A.; Giordano, F.; Correa Baena, J.-P.; Decoppet, J.-D.; Zakeeruddin, S. M.; Nazeeruddin, M. K.; Grätzel, M.; Hagfeldt, A. *Sci. Adv.* **2016**, *2*, e1501170.
- (89) Rand, B. P.; Genoe, J.; Heremans, P.; Poortmans, J. *Prog. Photovolt Res. Appl.* **2007**, *15*, 659.
- (90) Carli, S.; Baena, J. P. C.; Marianetti, G.; Marchetti, N.; Lessi, M.; Abate, A.; Caramori, S.; Grätzel, M.; Bellina, F.; Bignozzi, C. A.; Hagfeldt, A. *ChemSusChem* **2016**, *9*, 657.

- (91) (a) *Nonlinear Optics (Third Edition)* Robert W. Boyd, ISBN- 968-0-12-369470-6.
(b) *Handbook of Nonlinear Optics*, R. Li. Sutherland, Second Edition, Marcel Dekker, New York (2003).
(c) *Physics of Nonlinear Optics*, Gungs. He and Song H. Liu, *World Scientific*, Singapore (1999).
- (92) (a) Sheik-Bahae, M.; Said, A. A.; Wei, T.-H.; Hagan, D. J.; Van Stryland, E. W. *Quantum Electron. IEEE J.* **1990**, *26*, 760.
(b) Sheik-Bahae, M.; Said, A. A.; Stryland, W. E. *Opt. Lett.* **1989**, *14*, 955.
- (93) Garmire, E. *Opt. Express* **2013**, *21*, 30532.
- (94) Tang, C.; Zheng, Q.; Zhu, H.; Wang, L.; Chen, S.-C.; Ma, E.; Chen, X. *J. Mater. Chem. C* **2013**, *1*, 1771.
- (95) Tao, H.; Levine, B. G.; Martínez, T. J. *J. Phys. Chem. A* **2009**, *113*, 13656.
- (96) Gindre, D.; Iliopoulos, K.; Krupka, O.; Champigny, E.; Morille, Y.; Sallé, M. *Opt. Lett.* **2013**, *38*, 4636.
- (97) Albota, M. *Science* **1998**, *281*, 1653.
- (98) Pawlicki, M.; Collins, H. A.; Denning, R. G.; Anderson, H. L. *Angew. Chem. Int. Ed.* **2009**, *48*, 3244.
- (99) Ando, M.; Kadono, K.; Haruta, M.; Sakaguchi, T. *Nature* **1995**, 625.
- (100) Fainman, Y.; Ma, J.; Lee, S. H. *Mater. Sci. Reports* **1993**, *9*, 53.
- (101) Hales, J. M.; Cozzuol, M.; Screen, T. E. O.; Anderson, H. L.; Perry, J. W. *Opt. Express* **2009**, *17*, 18478.
- (102) He, G. S.; Tan, L. S.; Zheng, Q.; Prasad, P. N. *Chem. Rev.* **2008**, *108*, 1245.
- (103) Gieseking, R. L.; Mukhopadhyay, S.; Risko, C.; Marder, S. R.; Brédas, J. L. *Adv. Mater.* **2014**, *26*, 68.
- (104) Ohkoshi, S.; Takano, S.; Imoto, K.; Yoshikiyo, M.; Namai, A.; Tokoro, H. *Nat. Photonics* **2013**, *8*, 65.
- (105) Changshui, H.; Li, Y.; Song, Y.; Li, Y.; Liu, H.; Zhu, D. *Adv. Mater.* **2010**, *22*, 3532.
- (106) Li, W.; Zhou, X.; Tian, W. Q.; Sun, X. *Phys. Chem. Chem. Phys.* **2013**, *15*, 1810.
- (107) Xu, J.; Semin, S.; Niedzialek, D.; Kouwer, P. H. J.; Fron, E.; Coutino, E.; Savoini, M.; Li, Y.; Hofkens, J.; Uji-I, H.; Beljonne, D.; Rasing, T.; Rowan, A. E. *Adv. Mater.* **2013**, *25*, 2084.
- (108) Wang, C.; Jung, G.-Y.; Batsanov, A. S.; Bryce, M. R.; Petty, M. C. *J. Mater. Chem.* **2002**, *12*, 173.

- (109) Cha, S. W.; Choi, S. H.; Kim, K.; Jin, J. I. *J. Mater. Chem.* **2003**, *13*, 1900.
- (110) Schulz, B.; Bruma, M.; Brehmer, L. *Adv. Mater.* **1997**, *9*, 601.
- (111) Wong, M. Y.; Leung, L. M. *Dye. Pigment.* **2017**, *145*, 542.
- (112) Carella, A.; Castaldo, A.; Centore, R.; Fort, A.; Tuzi, A. *J. Chem. Soc., Perkin Trans. 2* **2002**, 1791.
- (113) Mashraqui, S. H.; Bhattacharya, M.; Das, P. K. *Opt. Mater.* **2004**, *27*, 257.
- (114) Chandrakantha, B.; Isloor, A. M.; Philip, R.; Mohesh, M.; Shetty, P.; Vijesh, A. M. **2011**, *34*, 887.
- (115) Lin, T. C.; Lee, Y. H.; Huang, B. R.; Hu, C. L.; Li, Y. K. *Tetrahedron* **2012**, *68*, 4935.
- (116) Cassano, T.; Tommasi, R.; Babudri, F.; Cardone, a; Farinola, G. M.; Naso, F. *Opt. Lett.* **2002**, *27*, 2176.
- (117) Narayanan, S.; Raghunathan, S. P.; Poulouse, A. C.; Mathew, S.; Sreekumar, K.; Sudha Kartha, C.; Joseph, R. *New J. Chem.* **2015**, *39*, 2795.
- (118) Kiran, A. J.; Udayakumar, D.; Chandrasekharan, K.; Adhikari, A. V.; Shashikala, H. D. *J. Phys. B At. Mol. Opt. Phys.* **2006**, *39*, 3747.
- (119) Hegde, P. K.; Adhikari, A. V.; Manjunatha, M. G.; Suchand Sandeep, C. S.; Philip, R. *Synth. Met.* **2009**, *159*, 1099.
- (120) Poornesh, P.; Hegde, P. K.; Umesh, G.; Manjunatha, M. G.; Manjunatha, K. B.; Adhikari, A. V. *Opt. Laser Technol.* **2010**, *42*, 230.
- (121) Manjunatha, M. G.; Adhikari, A. V.; Hegde, P. K.; Suchand Sandeep, C. S.; Philip, R. *J. Electron. Mater.* **2010**, *39*, 2711.
- (122) Hegde, P. K.; Vasudeva Adhikari, A.; Manjunatha, M. G.; Suchand Sandeep, C. S.; Philip, R. *Polym. Int.* **2011**, *60*, 112.
- (123) Vishnumurthy, K. A.; Sunitha, M. S.; Adhikari, A. V. *Eur. Polym. J.* **2012**, *48*, 1575.
- (124) Prashanth Kumar, K. R.; Murali, M. G.; Udayakumar, D. *Des. Monomers Polym.* **2014**, *17*, 7.
- (125) Kaippamangalath, N.; Gopalakrishnapanicker, U. *Polym. Int.* **2016**, *65*, 1221.
- (126) Kaippamangalath, N.; Chandrasekharan, E. S. K. *J. Mater. Sci.* **2016**, *51*, 4748.

SYNTHESIS AND CHARACTERIZATION OF A FEW UNSYMMETRICAL 2,5-DIARYL-1,3,4-OXADIAZOLES AND 1,3,4-OXADIAZOLE-THIOPHENE HYBRID MOLECULES

2.1. Abstract

Incorporation of both 1,3,4-oxadiazole and thiophene units in an ordered fashion into a single polymer chain is one of our primary goals. To this end, we synthesized several symmetrical and unsymmetrical expandable 2,5-diaryl-1,3,4-oxadiazoles and oxadiazole-thiophene hybrid molecules by both pre and postfunctionalization strategies. Synthesis and characterization of target molecules are described in this chapter.

2.2. Introduction

2,5-Diaryl-1,3,4-oxadiazoles are privileged scaffolds due to their wide range of applications in pharmacology and organic electronics. In the biological field, they are widely employed as antimicrobial, anti-inflammatory, anticonvulsant and antiviral agents.^{1,2} Furthermore their attractive photophysical properties make them potential candidates for optoelectronic devices.

Oxadiazole based small molecules and polymers are widely investigated by virtue of their high thermal and chemical stability, high photoluminescent quantum yield and electron deficient nature.³⁻⁵ Synthesis of 1,3,4-oxadiazoles can be achieved easily by several methods using cheap starting materials.^{6,7} On top of this, it is easy to incorporate

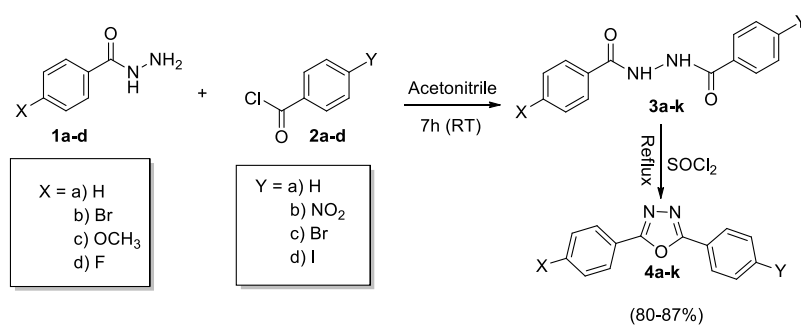
functional groups to 2,5-diaryl-1,3,4-oxadiazoles by judicious selection of starting materials (prefunctionalization) and further manipulation of the attached functional groups (postfunctionalization) is also possible.

Combination of electron deficient 1,3,4-oxadiazole with electron rich thiophene in a single molecular architecture will create a simple push-pull system. This type of small molecules and D-A type polymers are widely employed in organic electronics.⁸⁻¹¹ In this context, we explored the synthesis of 2,5-disubstituted 1,3,4-oxadiazoles and 1,3,4-oxadiazole-thiophene hybrid molecules. Our target 1,3,4-oxadiazoles are prefunctionalized with groups compatible for further manipulation. Electron deficient nature of 1,3,4-oxadiazoles ensures facile nucleophilic substitution at the 4'-position of 2- and 5-aryl substituents present on oxadiazole core. Exploiting this possibility, it should be feasible to attach carbazole units on to oxadiazole-thiophene hybrids. Due to inherent excellent electron donating capacity and thermal stability, carbazole is an attractive ingredient in materials for organic electronics.¹³⁻¹⁶

2.3. Results and Discussion

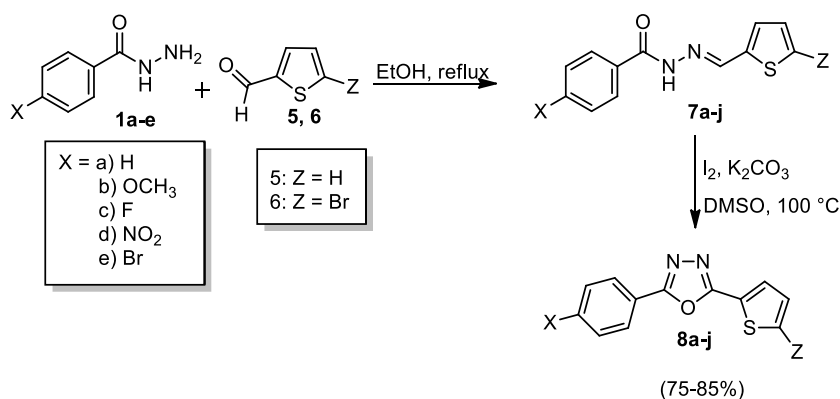
We successfully synthesized several symmetrical and unsymmetrical 2,5-diaryl-1,3,4-oxadiazoles and 1,3,4-oxadiazole-thiophene hybrid molecules employing simple metal-free reaction pathways. Depending on the availability of required starting materials, two distinct procedures were adapted for the synthesis of oxadiazoles. Thionyl chloride mediated dehydrative cyclization of diacylhydrazines was used for the synthesis of several 2,5-diaryl-1,3,4-oxadiazoles. Diacylhydrazines, in turn, were synthesized by the reaction between

acylhydrazines and acid chlorides. This method is compatible with the synthesis of both symmetrical and unsymmetrical diacylhydrazines. General reaction scheme for the synthesis of diaryloxadiazoles from the corresponding diacylhydrazines is presented in Scheme 2.1.



Scheme 2.1. Synthesis of 2,5-diaryl-1,3,4-oxadiazoles

For incorporating thiophene substituents onto oxadiazole core, we adopted iodine-mediated oxidative cyclization reaction of the



Scheme 2.2.

corresponding acyl hydrazones **7a-j**. Required acyl hydrazones were generated by the reaction between acylhydrazines **1a-e** and thiophene carboxaldehydes **5** and **6** (Scheme 2.2).¹² By adapting this method, we

could prepare several thiophene incorporated oxadiazoles **8a-j** in good yields.

Structures of synthesized 2,5-diaryl-1,3,4-oxadiazoles and 1,3,4-oxadiazole-thiophene hybrid molecules are given in Chart 2.1 and Chart 2.2 respectively.

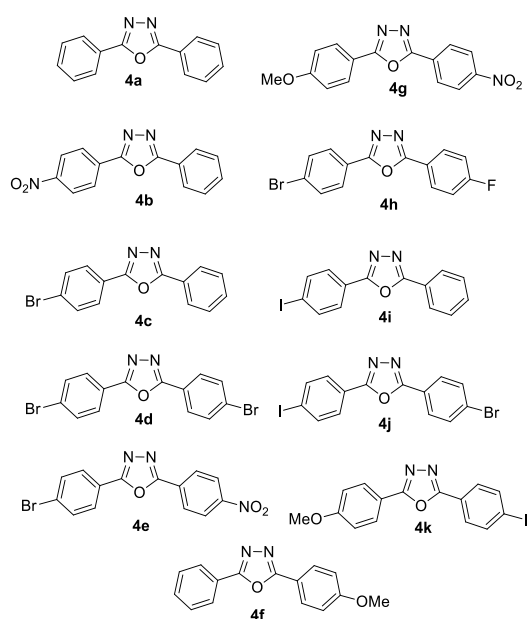


Chart 2.1. Structure of 2,5-diaryl-1,3,4-oxadiazoles **4a-k**

It may be noted that several compounds listed in Charts 2.1 and 2.2 are amenable for selective postfunctionalization. Compounds **4h** and **8h**, for example have two substituents that can be selectively replaced by other substituents. Nucleophilic displacement of 4-fluoro substituent on diaryloxadiazoles **4h**, **8e** and **8h** is facilitated by strong cooperative electron withdrawing ability of oxadiazole ring and the fluoro substituent reminiscent of facile nucleophilic substitution on Sanger's reagent.¹⁷ Indeed, the fluoro substituent could be readily replaced on treatment with

a suitable nucleophile such as carbazole to yield expanded oxadiazoles **10a-c** (Scheme 2.3).

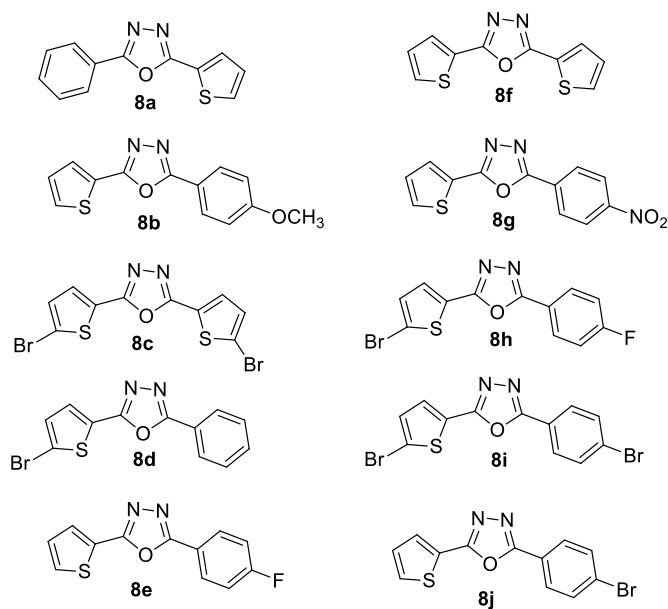
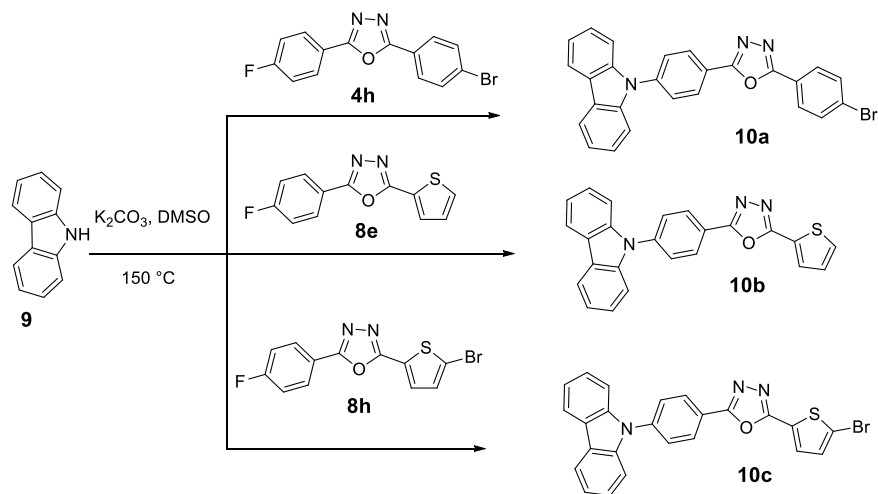
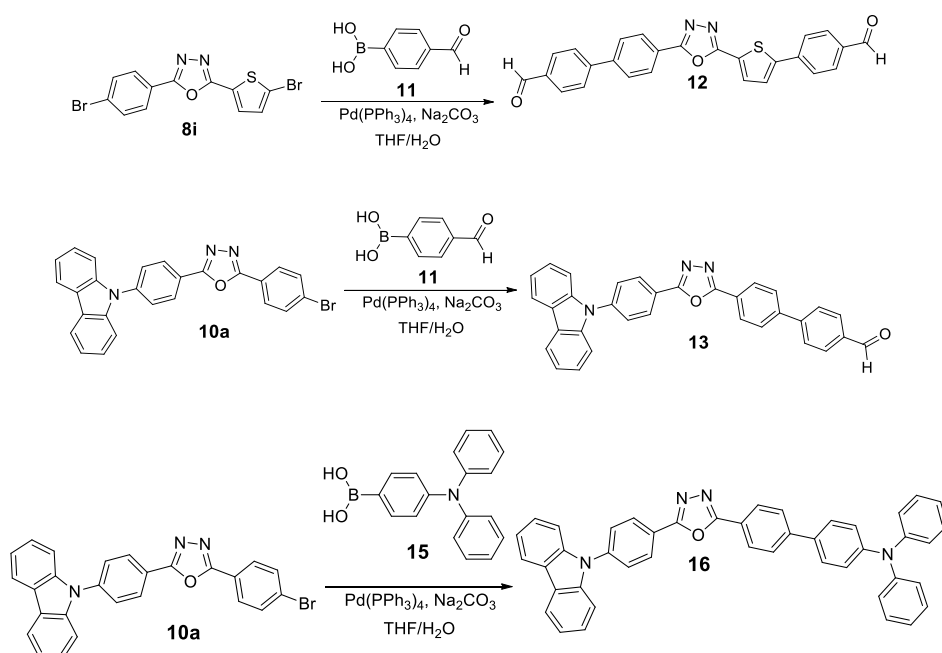


Chart 2.2. Structure of 1,3,4-oxadiazoles-thiophene hybrids **8a-j**



Scheme 2.3. Synthesis of **10a-c**

Bromo substituents present in several oxadiazoles synthesized by us enable facile Pd-mediated coupling reactions. Suzuki coupling reaction provided a robust method to functionalize compounds such as **8i** and **10a** to give expanded oxadiazoles such as **12**, **13** and **16** respectively (Scheme 2.4). It may be noted that the formyl groups present in **12** and **13** open a plethora of opportunities for further functionalization.



Scheme 2.4. Synthesis of **12**, **13** and **16**

Thus, we exploited diverse reactivity of suitably substituted oxadiazoles for their selective postfunctionalization to yield several expanded oxadiazoles. Our postfunctionalization strategy is both robust and flexible ensuring highly conjugated molecular arrays. The downside, however, is that increase in number of aromatic rings in a linear chain resulted in concomitant decrease in their solubility in common organic solvents.

2.3.1. Synthesis and Characterization

In the present study, thionyl chloride mediated dehydrative cyclisation of N,N'-diacylhydrazines was adopted for the synthesis of 2,5-diaryl-1,3,4-oxadiazoles **4a-k** (Scheme 2.1).¹⁸

For attaching the thiophene moiety to an oxadiazole ring we adopted a transition metal free method, which involve iodine mediated oxidative cyclization of acyl hydrazones (Scheme 2.2).¹²

2.3.2. Photophysical Properties

2.3.2.1. UV-Vis Absorption and Photoluminescence (PL) spectra

The UV-Vis absorbance and emission spectra of expanded molecules **10b**, **12**, **13** and **16** in CHCl₃ are shown in Fig. 2.1 and data are listed in Table 2.1. The bands observed at shorter wavelengths corresponds to π - π^* transitions of electron donor moieties whereas the less intense absorption band at longer wavelength (340-371 nm) can be assigned to intramolecular charge transfer transitions (ICT). In the molecules maximum absorption (371 nm) and emission (440 nm) wavelengths are shown by **16**, which is a typical bipolar compound having D-A-D architecture in which carbazole and triphenylamine as donors and 1,3,4-oxadiazole as acceptor.

2.4. Conclusions

This chapter is dedicated towards development of robust strategies towards 1,3,4-oxadiazole based push-pull molecules. We have synthesized a series of symmetrical and unsymmetrical 2,5-diaryl-1,3,4-

oxadiazoles and 1,3,4-oxadiazole-thiophene hybrid molecules *via* simple synthetic pathways. Methods adopted are compatible with a variety of functional groups including nitro, bromo, iodo, fluoro and methoxy attached to the peripheral aryl group. Furthermore, we expanded a few selected molecules to elaborate hybrid materials by employing nucleophilic aromatic substitution and Suzuki coupling reactions. Preliminary photophysical investigations showed that the expanded molecules exhibit good absorption and emission properties. All new compounds were identified on the basis of various analytical and spectroscopic techniques. Work reported in this chapter acts as a primer for synthetic strategies adopted in following chapters.

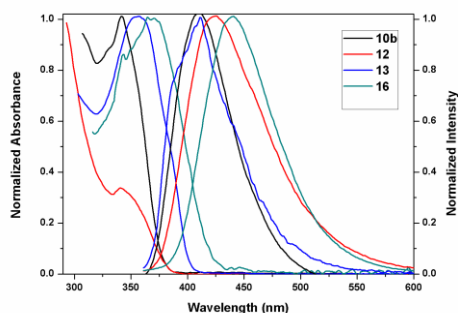


Fig. 2.1. Normalized absorption and emission spectra of compounds **10b**, **12**, **13** and **16**

Table 2.1. Summary of absorption and emission profiles of the compounds **10b**, **12**, **13** and **16**

Compound	Absorption (λ_{max}^{abs}) (nm)	Emission (λ_{max}^{em}) (nm)
10b	342	410
12	341	426
13	357	411
16	371	440

2.5. Experimental

2.5.1. Materials and Methods

All reactions were carried out in oven dried glassware. Solvents chosen for the experiments were distilled and dried by utilising standard protocols. Starting materials were purchased from either *Sigma-Aldrich*, *Spectrochem Chemicals* or from *Alfa Aesar* and were used without further purification. The products were purified by recrystallization from proper solvent systems. Melting points were determined on a *Neolab* melting point apparatus and are uncorrected. Infrared spectra were recorded on *Jasco 4100* and *ABB Bomem (MB Series)* FT-IR spectrometers. The ^1H and ^{13}C NMR spectra were recorded on a 400 MHz *Bruker Avance III* FT-NMR spectrometer with tetramethylsilane (TMS) as internal standard. Chemical shifts (δ) are reported in parts per million (ppm) downfield of TMS. Elemental analysis was performed using *ElementarSysteme (Vario EL III)*. Molecular mass was determined by electron impact (EI) method using GC-MS (*Agilent GC-7890A, Mass-5975C*). Absorption spectra were recorded using *Evolution 201 UV-Vis* spectrophotometer. Emission spectra were recorded using *Shimadzu-RF-5301PC* spectrofluorophotometer.

2.5.2. General procedure for the synthesis of N,N'-diacylhydrazines (3a-k)

Acid chloride (**2a-d**, 1.1 mmol) was added to a suspension of acid hydrazide (**1a-d**, 1 mmol) in dry acetonitrile (10 mL). The reaction mixture was stirred for 7 h (RT) and the solid product obtained was filtered and purified by recrystallization from ethanol.

2.5.2.2. General procedure for the synthesis of 2,5-diaryl-1,3,4-oxadiazoles (4a-k)

Diacylhydrazine (**3a-k**, 2 mmol) was mixed with thionyl chloride (10 mL) and the mixture was refluxed for 2 h. The resulting mixture was poured onto crushed ice and stirred vigorously. The solid product obtained was collected by gravity filtration, washed with water and recrystallized from ethanol.

2.5.2.3. General procedure for the synthesis of 1,3,4-oxadiazole-thiophene hybrid molecules (8a-j)

In a general procedure, a solution of thiophenecarboxaldehyde (**5a,b**, 1 mmol) and acylhydrazine (**1a-e**, 1 mmol) in ethanol (10 mL) was refluxed until the condensation was complete (monitored by TLC) and the solvent was evaporated under reduced pressure. The resulting residue was redissolved in DMSO (5 mL), followed by addition of potassium carbonate (3 mmol) and iodine (1.2 mmol) in sequence. The reaction mixture was stirred at 100 °C until the conversion was complete (monitored by TLC). After cooling to room temperature, it was treated with 5% sodium thiosulfate (20 mL) and extracted with ethyl acetate. The combined organic layer was washed with brine, dried over anhydrous sodium sulfate and solvent was removed under reduced pressure. Residue obtained was purified by silica gel column chromatography using a mixture of ethyl acetate and hexane as eluent.

2.5.3. Spectral and analytical data for significant compounds

2.5.3.1. 2,5-Diphenyl-1,3,4-oxadiazole (4a)

(Yield: 85%, mp: 137-140 °C).^{12,18}

2.5.3.2. 2-(4-Nitrophenyl)-5-phenyl-1,3,4-oxadiazole (4b)

(Yield: 87%, mp: 220-225 °C).^{12,18}

2.5.3.3. 2-(4-Bromophenyl)-5-phenyl-1,3,4-oxadiazole (4c)

(Yield: 86%, mp: 167-170 °C).^{18,19}

2.5.3.4. 2,5-bis(4-Bromophenyl)-1,3,4-oxadiazole (4d)

(Yield: 80%, mp: 255-260 °C).^{18,20}

2.5.3.5. 2-(4-Bromophenyl)-5-(4-nitrophenyl)-1,3,4-oxadiazole (4e)

(Yield: 83%, mp: 190-194 °C).¹⁸

2.5.3.6. 2-(4-Methoxyphenyl)-5-phenyl-1,3,4-oxadiazole (4f)

(Yield: 83%, mp: 147-152 °C).^{12,18}

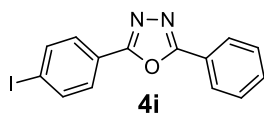
2.5.3.7. 2-(4-Methoxyphenyl)-5-(4-nitrophenyl)-1,3,4-oxadiazole (4g)

(Yield: 81%, mp: 193-198 °C).¹⁸

2.5.3.8. 2-(4-Bromophenyl)-5-(4-fluorophenyl)-1,3,4-oxadiazole (4h)

(Yield: 85%, mp: 205-210 °C).²¹

2.5.3.9. 2-(4-Iodophenyl)-5-phenyl-1,3,4-oxadiazole (4i)



Yield: 82%, mp: 155-160 °C; IR (KBr): 2975, 1433, 1216, 1050, 510 cm^{-1} ; ^1H NMR (500 MHz, CDCl_3): δ (ppm) 8.15 (d, $J = 7.5$ Hz, 2H), 7.93-7.87 (m, 4H), 7.58-7.55 (m, 3H); MS: m/z 348 (M^+), 349 ($M+1$); Elemental analysis calculated for $\text{C}_{14}\text{H}_9\text{IN}_2\text{O}$: C: 48.30, H: 2.61, N: 8.05; Found C: 48.28, H: 2.60, N: 8.03.

2.5.3.10. 2-(4-Bromophenyl)-5-(4-iodophenyl)-1,3,4-oxadiazole (4j)

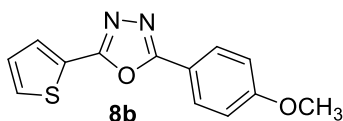
(Yield: 82%, mp: 240-244 °C).^{18,22}

2.5.3.11. 2-(4-Iodophenyl)-5-(4-methoxyphenyl)-1,3,4-oxadiazole (4k)

(Yield: 83%, mp: 160-165 °C).²³

2.5.3.12. 2-Phenyl-5-(thiophen-2-yl)-1,3,4-oxadiazole (8a)

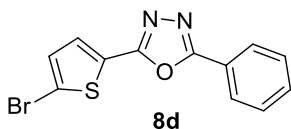
(Yield: 82%, mp: 115-120 °C).^{12,24}

2.5.3.13. 2-(4-Methoxyphenyl)-5-(thiophen-2-yl)-1,3,4-oxadiazole (8b)²⁵

Yield: 78%, mp: 135-140 °C; IR (KBr): 2876, 1560, 1235, 1048, 536 cm^{-1} ; $^1\text{H NMR}$ (500 MHz, CDCl_3): δ (ppm) 7.97 (d, $J = 9$ Hz, 2H), 7.73-7.47 (m, 2H), 7.19-6.93 (m, 3H), 3.82 (s, 3H); MS: m/z 258 (M^+), 259 ($M+1$); Elemental analysis calculated for $\text{C}_{13}\text{H}_{10}\text{N}_2\text{O}_2\text{S}$: C: 60.45, H: 3.90, N: 10.85, S: 12.41; Found C: 60.43, H: 3.91, N: 10.86, S: 12.40.

2.5.3.14. 2, 5-bis(5-Bromothiophen-2-yl)-1,3,4-oxadiazole (8c)

(Yield: 79%, mp: 132-137 °C).²⁶

2.5.3.15. 2-(5-Bromothiophen-2-yl)-5-phenyl-1,3,4-oxadiazole (8d)

Yield: 75%, mp: 115-120 °C; IR (KBr): 2900, 1428, 1214, 1078, 610 cm^{-1} ; $^1\text{H NMR}$ (500 MHz, CDCl_3): δ (ppm) 8.10-8.09 (m, 2H), 7.58-7.51 (m, 4H), 7.26-7.15 (m, 1H); MS: m/z 308 (M^+), 309 ($M+1$); Elemental analysis calculated for $\text{C}_{12}\text{H}_7\text{BrN}_2\text{OS}$: C: 46.92, H: 2.30, N: 9.12, S: 10.44; Found C: 46.91, H: 2.31, N: 9.13, S: 10.42.

2.5.3.16. 2-(4-Fluorophenyl)-5-(thiophen-2-yl)-1,3,4-oxadiazole (8e)

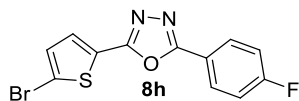
(Yield: 83%, mp: 125-130 °C).

2.5.3.17. 2,5-di(Thiophen-2-yl)-1,3,4-oxadiazole (8f)

Yield: 82%, mp: 120 °C; IR (KBr): 2982, 1425, 1212, 1082, 650 cm^{-1} ; ^1H NMR (500 MHz, CDCl_3): δ (ppm) 7.74-7.73 (m, 2H), 7.49-7.48 (m, 2H), 7.19-7.09 (m, 2H); ^{13}C NMR (125 MHz, CDCl_3): δ (ppm) 159.3, 129.2, 128.8, 127.2, 13.9; MS: m/z 233 (M^+), 234 ($M+1$); Elemental analysis calculated for $\text{C}_{18}\text{H}_6\text{N}_2\text{OS}_2$: C: 51.26, H: 2.58, N: 11.96, S: 27.37; Found C: 51.24, H: 2.57, N: 11.95, S: 27.38.

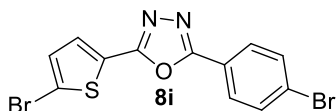
2.5.3.16. 2-(4-Nitrophenyl)-5-(thiophen-2-yl)-1,3,4-oxadiazole (8g)

Yield: 85%, mp: 195-200 °C; IR (KBr): 2976, 1538, 1465, 1113, 650, 568; ^1H NMR (500 MHz, CDCl_3): δ (ppm) 8.34 (d, $J = 9$ Hz, 2H), 8.24 (d, $J = 9$ Hz, 2H), 7.83 (d, $J = 3$ Hz, 1H), 7.17 (t, $J = 4.5$ Hz, 1H); MS: m/z 273 (M^+), 274 ($M+1$); Elemental analysis calculated for $\text{C}_{12}\text{H}_7\text{N}_3\text{O}_3\text{S}$: C: 52.74, H: 2.58, N: 15.38, S: 11.73; Found C: 52.73, H: 2.57, N: 15.37, S: 11.74.

2.5.3.17. 2-(5-Bromothiophen-2-yl)-5-(4-fluorophenyl)-1,3,4-oxadiazole (8h)

Yield: 81%, mp: 125-130 °C; IR (KBr): 2972, 1495, 1233, 1077, 560 cm^{-1} ; ^1H NMR (500 MHz, CDCl_3): δ (ppm) 8.05-8.02 (m, 2H), 7.50-7.49 (m, 1H), 7.19-7.09 (m, 3H); ^{13}C -NMR (125 MHz, CDCl_3): δ (ppm) 164.8, 162.8, 162.2, 158.7, 130.1, 128.9, 128.2, 125.4, 118.7, 115.5, 115.4; MS: m/z 325 (M^+), 326 ($M+1$); Elemental analysis calculated for $\text{C}_{12}\text{H}_6\text{BrFN}_2\text{OS}$: C: 44.33, H: 1.86, N: 8; Found C: 44.31, H: 1.70.

2.5.3.18. 2-(4-bromophenyl)-5-(5-bromothiophen-2-yl)-1,3,4-oxadiazole (8i)



Yield: 78%, mp: 135-140 °C; ^1H NMR (500 MHz, CDCl_3): δ (ppm) 7.97-7.95 (m, 2H), 7.68-7.57 (m, 3H), 7.27-7.16 (m, 1H); ^{13}C -NMR (125 MHz, CDCl_3): δ (ppm) 163.4, 159.3, 132.5, 131.2, 130.1, 128.3, 126.7, 126.3, 122.4, 118.4; MS: m/z 386 (M^+), 387 ($M+1$); Elemental analysis calculated for $\text{C}_{12}\text{H}_6\text{Br}_2\text{N}_2\text{OS}$: C: 37.33, H: 1.57, N: 7.26, S: 8.31; Found C: 37.31, H: 1.56, N: 7.25, S: 8.30.

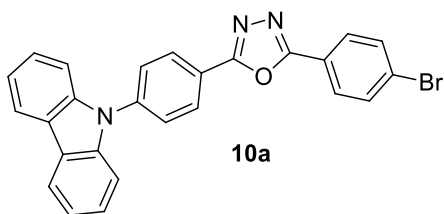
2.5.3.18. 2-(4-bromophenyl)-5-(thiophen-2-yl)-1,3,4-oxadiazole (8j)



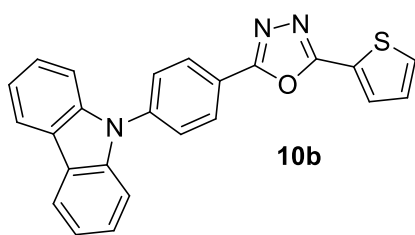
Yield: 83%, mp: 125-130 °C; IR (KBr): 2988, 1480, 1245, 1097, 660 cm^{-1} ; ^1H NMR (500 MHz, CDCl_3): δ (ppm) 7.99-7.19 (m, 7H); MS: m/z 307 (M^+), 308 ($M+1$); Elemental analysis calculated for $\text{C}_{12}\text{H}_7\text{BrN}_2\text{OS}$: C: 46.92, H: 2.30, N: 9.12, S: 10.44; Found C: 46.91, H: 2.28, N: 9.10, S: 10.43.

2.6. General procedure for the synthesis of 1,3,4-oxadiazole-carbazole bipolar molecules (10a-c)

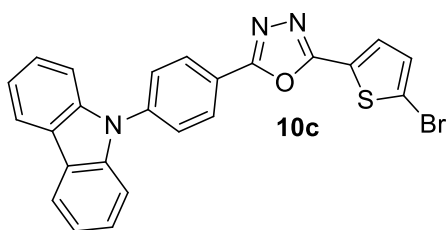
A mixture of carbazole (**9**, 1 mmol), respective fluoroarene (**4h**, **8e** and **8h**, 1 mmol) and K_2CO_3 (3 mmol) in 1.5 mL of DMSO was stirred at 150 °C for 12 h under nitrogen atmosphere until the reaction was complete (monitored by TLC). After cooling to room temperature, the mixture was poured into water, filtered and then purified through silica gel column chromatography using a mixture of ethyl acetate and hexane as eluent.



Yield: 41%, mp: 195-200 °C; IR (KBr): 2956, 1480, 1212, 1090, 560 cm^{-1} ; ^1H NMR (500 MHz, CDCl_3): δ (ppm) 8.39-7.25 (m, 8H); ^{13}C -NMR (125 MHz, CDCl_3): δ (ppm) 164.8, 162.9, 139.1, 131.4, 128.2, 127.6, 127.2, 126.2, 125.5, 125.2, 122.8, 121.6, 119.6, 119.4, 115.5, 115.4, 108.6; MS: m/z 465 (M^+), 466 ($M+1$); Elemental analysis calculated for $\text{C}_{26}\text{H}_{16}\text{BrN}_3\text{O}$: C: 66.97, H: 3.46, N: 9.01; Found C: 66.95, H: 3.43, N: 9.02.



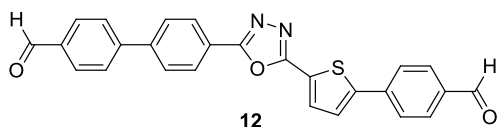
Yield: 38%, mp: 210-215 °C; IR (KBr): 2985, 1439, 1245, 1087, 601 cm^{-1} ; ^1H NMR (500 MHz, CDCl_3): δ (ppm) 8.37-7.22 (m, 15H); ^{13}C -NMR (125 MHz, CDCl_3): δ (ppm) 164.7, 162.7, 162.4, 162.1, 160.0, 159.8, 139.9, 139.2, 129.3, 129.2, 128.9, 128.8, 128.2, 128.1, 127.5, 127.2, 126.1, 125.2, 124.0, 122.7, 121.1, 119.6, 119.4, 115.5, 115.3, 108.7. MS: m/z 393 (M^+), 394 ($M+1$); Elemental analysis calculated for $\text{C}_{24}\text{H}_{15}\text{N}_3\text{OS}$: C: 73.26, H: 3.84, N: 10.68, S: 8.15; Found C: 73.24, H: 3.83, N: 10.64, S: 8.16.



Yield: 35%, mp: 192-197 °C; IR (KBr): 2965, 1498, 1225, 1100, 575 cm^{-1} ; ^1H NMR (500 MHz, CDCl_3): δ (ppm) 8.30-5.22 (m, 13H); MS: m/z 473 (M^+), 474 ($M+1$); Elemental analysis calculated for $\text{C}_{24}\text{H}_{14}\text{BrN}_3\text{OS}$: C: 61.03, H: 2.99, N: 8.90, S: 6.79; Found C: 61.01, H: 2.96, N: 8.87, S: 6.78.

2.7. Synthesis of 4'-(5-(4-(5-(4-formylphenyl) thiophen-2-yl)phenyl)-1,3,4-oxadiazol-2-yl)biphenyl-4-carbaldehyde (**12**)

A mixture of 4-formylphenylboronic acid (**11**, 0.52 mmol), 2-(4-bromophenyl)-5-(5-bromothiophen-2-yl)-1,3,4-oxadiazole (**8i**, 0.26 mmol), Pd(PPh₃)₄ (5% mmol) and Na₂CO₃ (2.6 mmol) in 15 mL of THF and 1.5 mL of distilled water was stirred at 80 °C for 24 h under nitrogen atmosphere. After completion of reaction (monitored by TLC), the resulting mixture was cooled to room temperature and then poured into water and extracted with ethyl acetate. The organic extracts were collected and dehydrated with sodium sulfate. After removal of solvent, the crude product was purified by column chromatography using ethyl acetate and hexane as eluent.



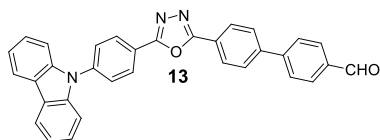
12

Yield: 35%, mp: 135-140 °C; IR (KBr): 2972, 1696, 1450, 1210, 1189, 670 cm⁻¹; ¹H NMR (500 MHz, CDCl₃): δ (ppm) 10.02 (s, 1H), 9.98 (s, 1H), 7.94-7.19 (m, 10H); MS: *m/z* 436 (*M*⁺), 437 (*M*+1); C₂₆H₁₆N₂O₃S: C: 71.54, H: 3.69, N: 6.42, S: 7.35; Found C: 71.52, H: 3.67, N: 6.41, S: 7.36.

2.8. Synthesis of 4'-(5-(4-(9*H*-carbazol-9-yl)phenyl)-1,3,4-oxadiazol-2-yl)biphenyl-4-carbaldehyde (**13**)

A mixture of 4-formylphenylboronic acid (**11**, 0.21 mmol), 2-(4-(9*H*-carbazol-9-yl)phenyl)-5-(4-bromophenyl)-1,3,4-oxadiazole (**10a**, 0.21 mmol), Pd(PPh₃)₄ (5% mmol) and Na₂CO₃ (1.05 mmol) in 3.2 mL of THF and 0.3 mL of distilled water was stirred at 80 °C for 24 h under nitrogen atmosphere. After completion of reaction (monitored by TLC),

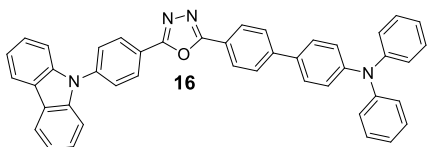
the resulting mixture was cooled to room temperature and then poured into water and extracted with ethyl acetate. The organic extracts were collected and dried with sodium sulfate. After removal of solvent, the crude product was purified by chromatograph using ethyl acetate and hexane as eluent.



Yield: 60%, mp: 190-195 °C. IR (KBr): 2980, 1698, 1477, 1220, 1100, 575 cm^{-1} ; ^1H NMR (500 MHz, CDCl_3): δ (ppm) 10.09 (s, 1H), 8.42-7.26 (m, 20H); ^{13}C -NMR (125 MHz, CDCl_3): δ (ppm) 191.1, 163.5, 163.3, 144.6, 142.2, 140.3, 139.2, 134.8, 129.5, 127.7, 127.2, 126.8, 126.6, 126.3, 125.27, 122.8, 119.7, 119.5, 108.7; MS: m/z 491 (M^+), 492 ($M+1$); Elemental analysis calculated for $\text{C}_{33}\text{H}_{21}\text{N}_3\text{O}_2$: C: 80.64, H: 4.31, N: 8.55; Found C: 80.61, H: 4.30, N: 8.53.

2.9. Synthesis of 4'-(5-(4-(9H-carbazol-9-yl)phenyl)-1,3,4-oxadiazol-2-yl)-N,N-diphenyl-[1,1'-biphenyl]-4-amine (16)

This compound was prepared by a procedure similar to that of **12** except that (4-(diphenylamino)phenyl)boronic acid (**15**, 0.21mmol) was used as the reactant instead of 4-formylphenylboronic acid (**11**).



Yield: 40%, mp: 210-215 °C; IR (KBr): 2976, 1444, 1295, 1047, 650 cm^{-1} ; ^1H NMR (500 MHz, CDCl_3): δ (ppm) 8.33-8.31 (m, 2H), 8.14-8.13 (m, 2H), 8.06 (d, $J = 7.5$ Hz, 2H), 7.73-7.71 (m, 2H), 7.68-7.66 (m, 2H), 7.46-7.41 (m, 4H), 7.37-7.34 (m, 2H), 7.25-7.18 (m, 7H), 7.09-7.06 (m, 6H), 6.99-6.96 (m, 2H); ^{13}C -NMR (125 MHz, CDCl_3): δ (ppm) 163.6, 162.7, 147.1, 146.3, 143.0, 139.8, 132.0, 128.3, 127.4, 126.7, 126.4, 126.2, 125.9,

125.1, 123.7, 122.8, 122.3, 121.5, 120.9, 119.5, 119.4, 108.6, 95.1; MS: m/z 630 (M^+), 631 ($M+1$); $C_{44}H_{30}N_4O$: C: 83.79, H: 4.79, N: 8.88; Found C: 83.77, H: 4.78, N: 8.86.

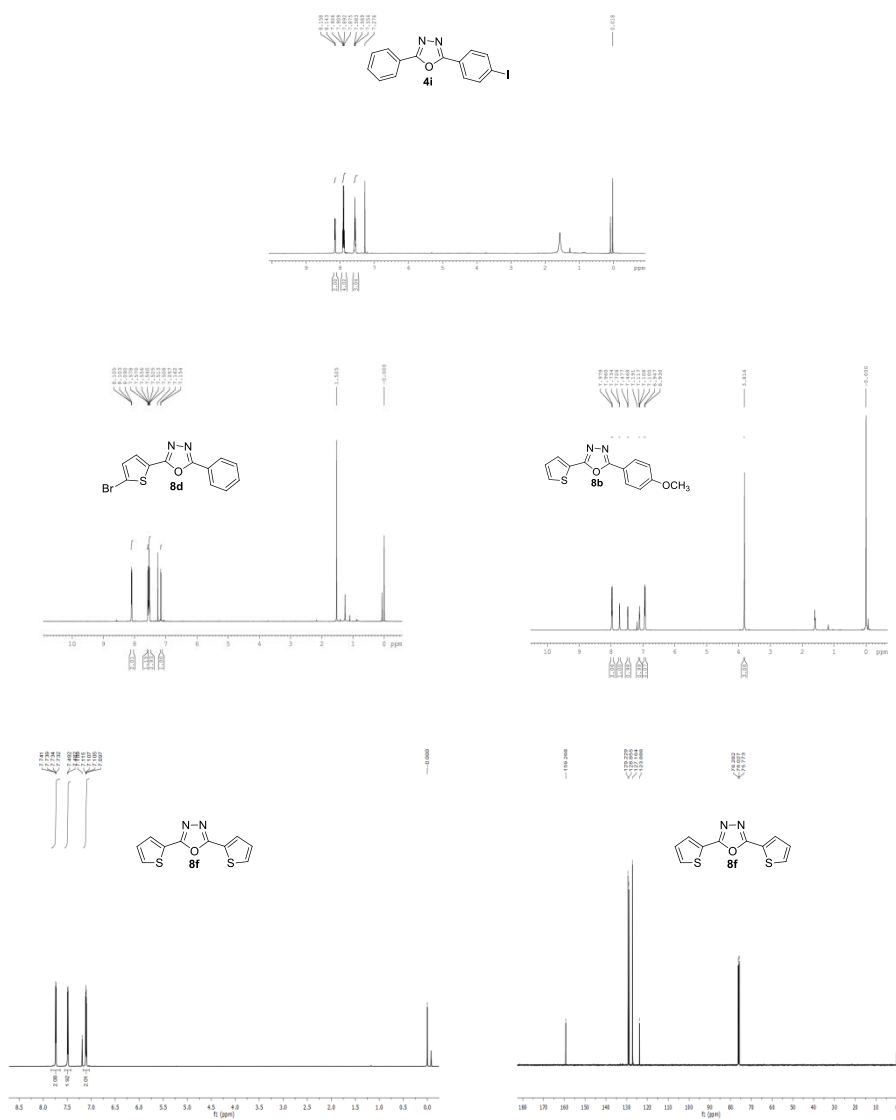
2.10. References

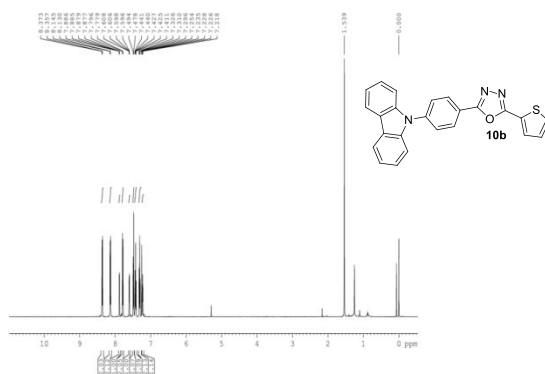
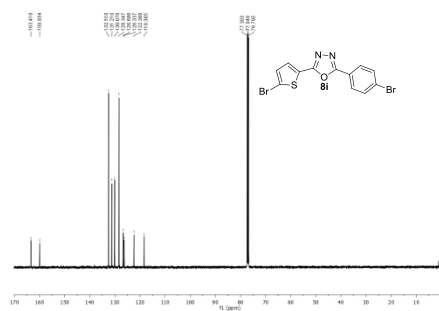
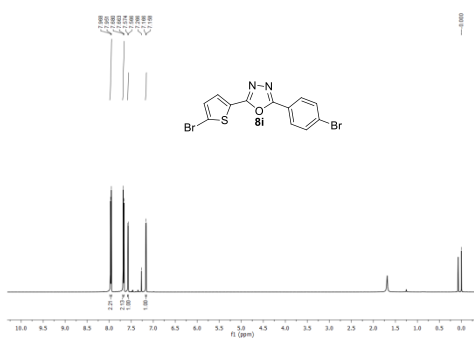
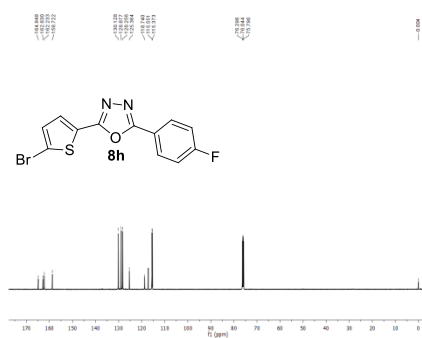
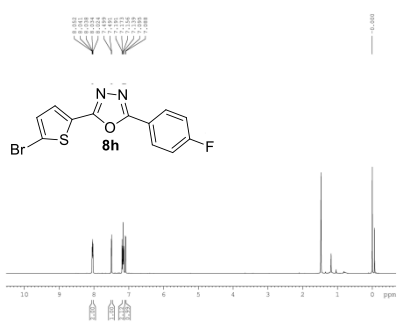
- (1) Omar, F. .; Mahfouz, N. M.; Rahman, M. . *Eur. J. Med. Chem.* **1996**, *31*, 819.
- (2) Somani, R.; Shirodkar, P. *Der. Pharma. Chem.* **2009**, *1*, 130.
- (3) Mitschke, U.; Bäuerle, P. *J. Mater. Chem.* **2000**, *10*, 1471.
- (4) Rehmann, N.; Ulbricht, C.; Köhnen, A.; Zacharias, P.; Gather, M. C.; Hertel, D.; Holder, E.; Meerholz, K.; Schubert, U. S. *Adv. Mater.* **2008**, *20*, 129.
- (5) He, G. S.; Tan, L. S.; Zheng, Q.; Prasad, P. N. *Chem. Rev.* **2008**, *108*, 1245.
- (6) Guin, S.; Ghosh, T.; Rout, S. K.; Banerjee, A.; Patel, B. K. *Org. Lett.* **2011**, *13*, 5976.
- (7) Sharma, S.; Sharma, P. K.; Kumar, N.; Dudhe, R. *Der Pharma Chem.* **2010**, *2*, 253.
- (8) Deshapande, N.; Belavagi, N. S.; Sunagar, M. G.; Gaonkar, S.; Pujar, G. H.; Wari, M. N.; Inamdar, S. R.; Khazi, I. A. M. *RSC Adv.* **2015**, *5*, 86685.
- (9) Higashihara, T.; Wu, H. C.; Mizobe, T.; Lu, C.; Ueda, M.; Chen, W. C. *Macromolecules* **2012**, *45*, 9046.
- (10) Carella, A.; Castaldo, A.; Centore, R.; Fort, A.; Tuzi, A. *J. Chem. Soc., Perkin Trans. 2* **2002**, 1791.
- (11) Zhao, B.; Liu, D.; Peng, L.; Li, H.; Shen, P.; Xiang, N.; Liu, Y.; Tan, S. *Eur. Polym. J.* **2009**, *45*, 2079.
- (12) Yu, W.; Huang, G.; Zhang, Y.; Liu, H.; Dong, L.; Yu, X.; Li, Y.; Chang, J. *J. Org. Chem.* **2013**, *78*, 10337.
- (13) Kotchapradist, P.; Prachumrak, N.; Tarsang, R.; Jungstittiwong, S.; Keawin, T.; Sudyoadsuk, T.; Promarak, V. *J. Mater. Chem. C* **2013**, *1*, 4916.
- (14) Venkateswararao, A.; Thomas, K. R. J.; Lee, C. P.; Li, C. T.; Ho, K. C. *ACS Appl. Mater. Interfaces* **2014**, *6*, 2528.
- (15) Ooyama, Y.; Inoue, S.; Nagano, T.; Kushimoto, K.; Ohshita, J.; Imae, I.; Komaguchi, K.; Harima, Y. *Angew. Chem. Int. Ed.* **2011**, *50*, 7429.

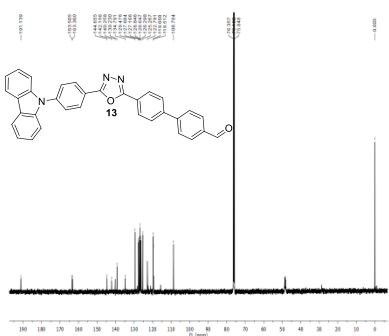
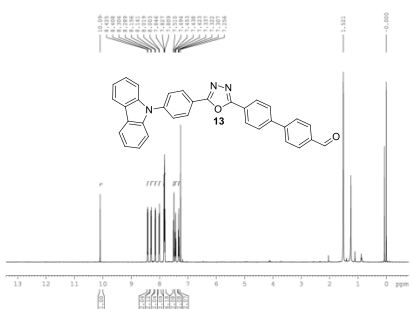
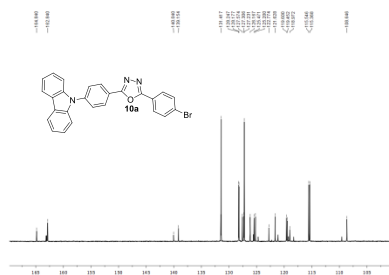
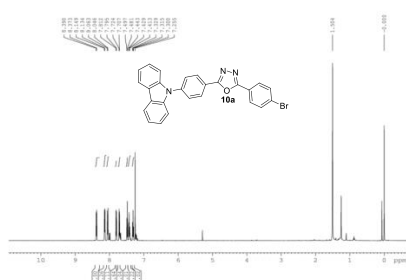
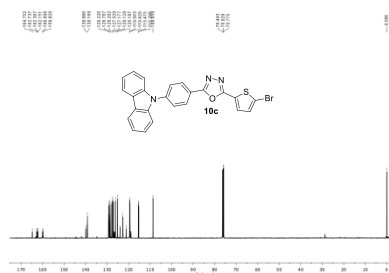
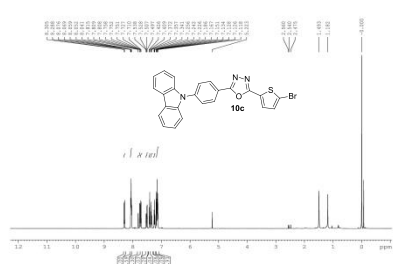
- (16) Sathiyar, G.; Sivakumar, E. K. T.; Ganesamoorthy, R.; Thangamuthu, R.; Sakthivel, P. *Tetrahedron Lett.* **2016**, *57*, 243.
- (17) Sanger, F. *The Biochemical Journal* **1945**, *39*, 507.
- (18) Iqbal, R.; Zareef, M.; Ahmed, S.; Khan, K. M. *Jour. Chem. Soc. Pak.* **2006**, *28*, 165.
- (19) Wang, L.; Cao, J.; Chen, Q.; He, M. *J. Org. Chem.* **2015**, *80*, 8743.
- (20) Kudelko, A.; Wroblowska, M.; Jarosz, T.; Laba, K.; Lapowski, M. *Arkivoc*, **2015**, *5*, 287.
- (21) Shang, Z. *Synth. Commun.* **2006**, *36*, 2927.
- (22) Cheng, Y. J.; Luh, T. Y. *Chem. - A Eur. J.* **2004**, *10*, 5361.
- (23) Watanabe, H.; Ono, M.; Ikeoka, R.; Nakayama, M. *Biorg. Med. Chem.* **2009**, *17*, 6402.
- (24) Jasiak, K.; Kudelko, A.; Zielinski, W.; Kuznik, N. *Arkivoc* **2017**, (ii), 87.
- (25) Majji, G.; Rout, S. K.; Guin, S.; Gogoi, A.; Patel, B. K. *RSC Adv.* **2014**, *4*, 5357.
- (26) Namratha, B.; Nitinkumar, S.; D'Souza Janice, N.; Gaonkar Santosh, L. *Res. J. Chem. Sci.* **2013**, *3*, 51.

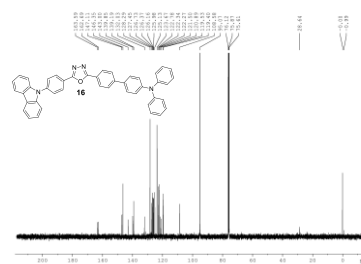
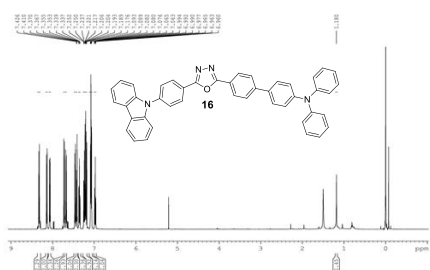
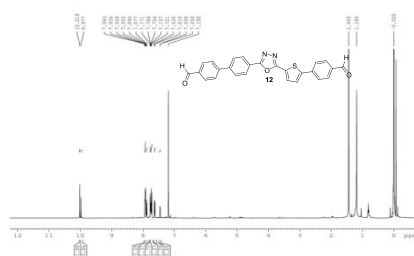
2.11. Appendix

^1H NMR and ^{13}C NMR spectra of significant compounds









**SYNTHESIS AND EVALUATION OF THIRD-ORDER
NONLINEAR OPTICAL PROPERTIES OF A FEW
1,3,4-OXADIAZOLE-PHENOTHIAZINE
PUSH-PULL FLUOROPHORES**

3.1. Abstract

In pursuit of donor-acceptor systems for potential photonic application, a series of 1,3,4-oxadiazole-phenothiazine push-pull molecules were designed and synthesized using simple iodine mediated oxidative cyclization of respective acyl hydrazone precursors. Structure of all new compounds were confirmed by ^1H NMR, ^{13}C NMR and LC-MS analysis. Their photophysical and electrochemical properties were explored by UV-Vis absorption spectroscopy, fluorescence spectroscopy and cyclic voltammetry measurements. Density functional theory (DFT) computations were carried out for analyzing HOMO and LUMO, computed values correlated well with the experimental results. Thermal studies revealed thermal stability of these compounds. Powder XRD patterns confirmed crystalline nature of the compounds. Nonlinear optical properties of the D-A molecules were also studied using Q switched Z-scan technique with 7 ns laser pulses at 532 nm. The molecules exhibited good third-order nonlinear absorption and optical power limiting property at 532 nm.

3.2. Introduction

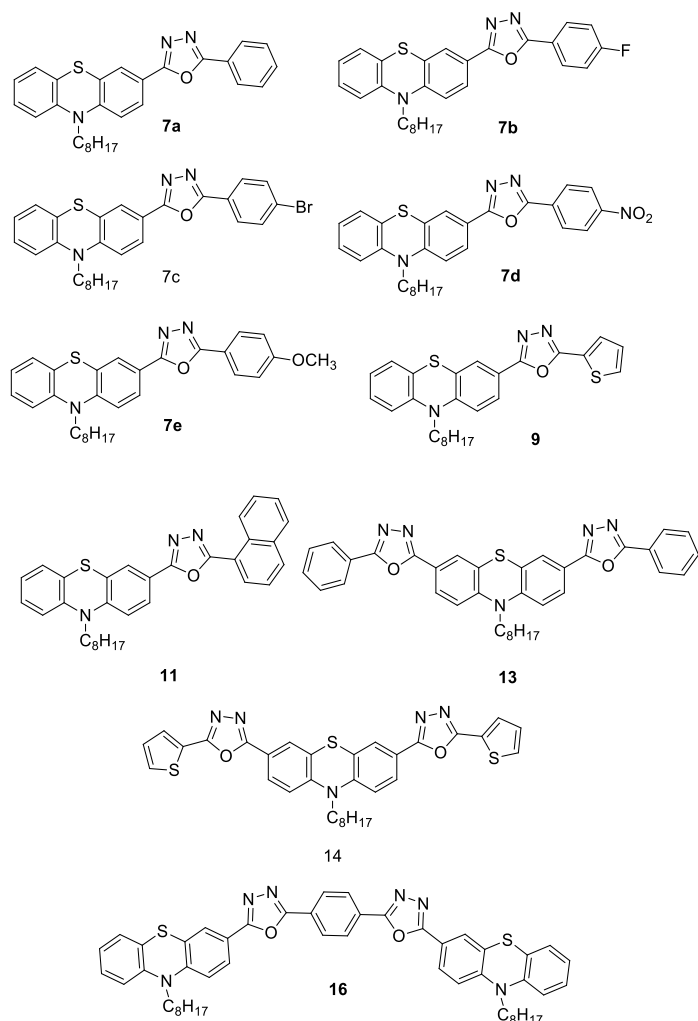
Design and synthesis of push-pull organic molecules with desirable third order nonlinear properties are emerging as a trend setting area of research due to their enormous applications in the field of optical communication,^{1,2} information storage,^{3,4} two photon imaging,⁵⁻⁷ optical computing,^{8,9} optical power limiting and optical switching.¹⁰⁻¹³ Organic π

conjugated charge transfer chromophores are widely used for these applications owing to their high NLO susceptibility,¹⁴ short response time,¹⁵ excellent thermal stability and high structural flexibility.¹⁵ Polarization of the push-pull chromophore and generation of a molecular dipole by intramolecular charge transfer (ICT) is responsible for large third order nonlinearity.¹⁶

1,3,4-Oxadiazoles are well established molecules with high thermal and chemical stability, excellent photoluminescent quantum yield and electron deficient nature.¹⁷⁻¹⁹ 1,3,4-Oxadiazole based push-pull molecules show excellent ICT character due to π electron delocalization producing high asymmetry in the molecule.²⁰

Phenothiazine is an active ingredient in many optoelectronic devices because of their striking electron rich character. “Butterfly conformation” of the phenothiazine ring enhances the ICT property by suppressing the excimer formation.²¹⁻²⁴ Recently, Leung and coworkers reported that 1,3,4-oxadiazole-phenothiazine push-pull fluorophores show good quantum efficiency, electrochemical stability and facilitate facile functionalization.²⁰

By virtue of being a powerful acceptor, 1,3,4-oxadiazole may be expected to offer high nonlinearity when linked to different donors. Keeping this in mind, we have designed and synthesized a few 1,3,4-oxadiazole and phenothiazine based push-pull fluorophores in which phenothiazine act as electron donor and 1,3,4-oxadiazole as electron acceptor (Chart 3.1).

**Chart 3.1.** Selected targets

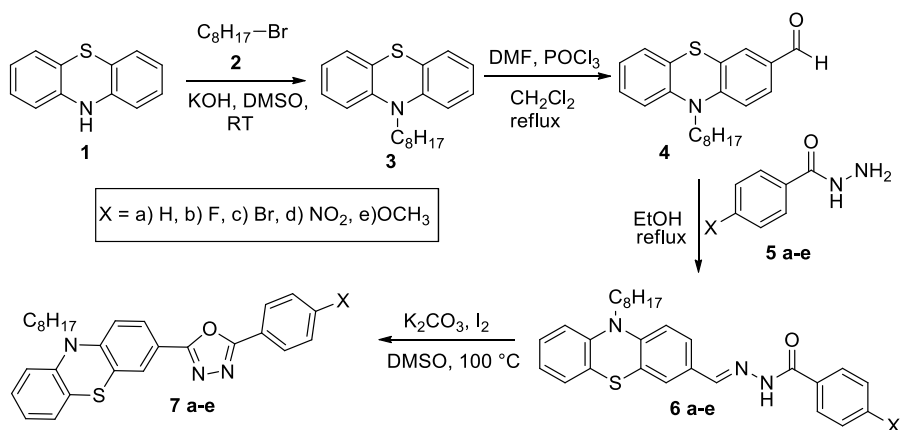
Optoelectronic properties of these push-pull systems can potentially be tuned by changing substituents attached to the 1,3,4-oxadiazole core. Compounds **7a-d**, **9** and **11** are simple push-pull systems whereas **13**, **14** and **16** possess expanded chromophoric building blocks. Their structural, photophysical, electrochemical, theoretical and thermal properties were investigated. Further the nonlinear optical

properties of these molecules were monitored by Q-switched Z-scan technique. All the synthesized molecules are NLO active exhibiting good optical limiting property.

3.3. Results and Discussion

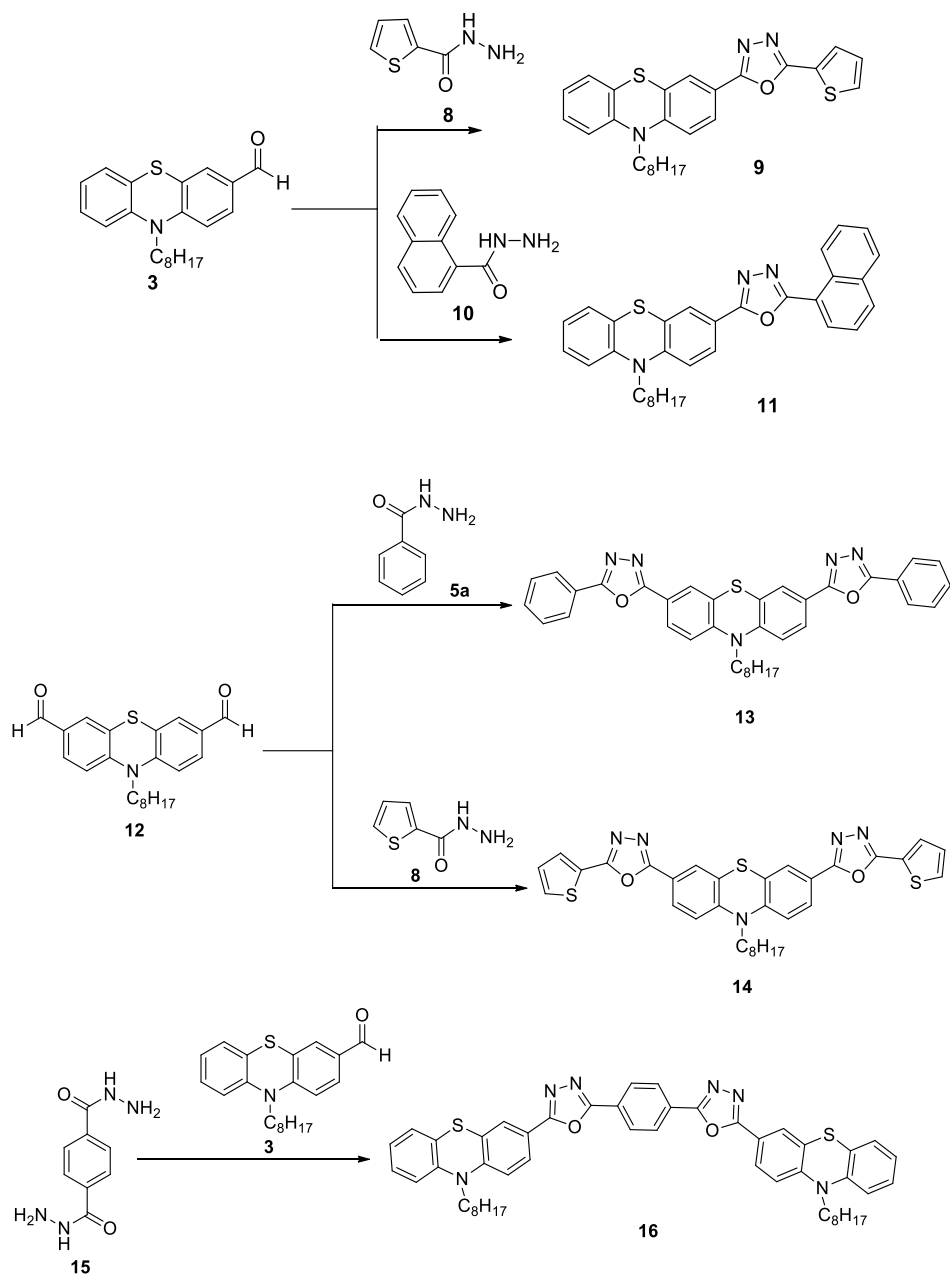
3.3.1. Synthesis and Characterization

A relatively simple and efficient transition metal free iodine mediated oxidative cyclization was used for the synthesis of final compounds as shown in Scheme 3.1 for **7a-e**.²⁵



Scheme 3.1. Synthesis of **7a-e**

Adapting the procedure outlined in Scheme 3.1, compounds **9**, **11**, **13**, **14** and **16** were prepared by changing the aryl aldehyde and aroyl hydrazine precursors as outlined in Scheme 3.2.

Scheme 3.2. Synthesis of **9**, **11**, **13**, **14** and **16**

Compounds **7a-e** are simple bipolar molecules having phenothiazine-(5-aryl)oxadiazole framework. We have introduced both electron withdrawing and electron releasing para substituents on to the 5-aryl substituent on oxadiazole core. Compounds **9** and **11** possess D- π -D type architecture having electron rich thiophene and naphthalene rings respectively in place of phenyl group. Fluorophores **13** and **14** are expanded molecules with D-A-D-A-D type building blocks and **16** is having D-A- π -A-D type framework.

3.3.2. Photophysical Properties

3.3.2.1. UV-Vis Absorption and Photoluminescence (PL) spectra

All the molecules are soluble in common organic solvents such as toluene, dichloromethane, dimethylformamide and dimethyl sulfoxide. Normalized UV-Vis absorption spectra of the fluorophores in CHCl₃ (HPLC grade) are collected in Fig. 3.1. Absorption maxima (λ_{max}) for compounds **7a**, **7d**, **9**, **11**, **13**, **14** and **16** are 367, 405, 370, 371, 389, 390 and 394 nm respectively. The bands observed at shorter wavelengths corresponds to π - π^* transitions of electron donor moieties whereas the less intense absorption band at longer wavelength (300-400 nm) can be assigned to ICT in each fluorophores (*vide infra*). ICT absorption maxima redshifts depend on the conjugation lengths and the electronic effects of the attached molecule. In the series, the fluorophore **7a** showed lowest λ_{max} of 367 nm and **7d** displayed highest λ_{max} of 405 nm (Table 3.1). **7d** is a typical D- π -A framework having strongly electron withdrawing nitro group.

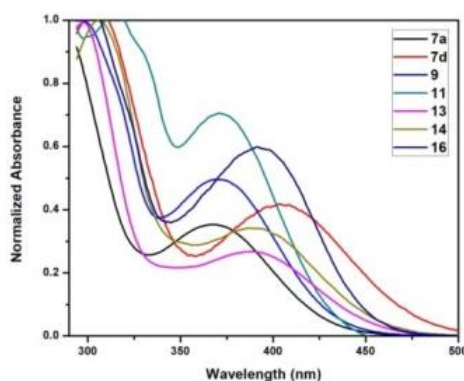


Fig. 3.1. Normalized UV-Vis absorption spectra of compounds **7a**, **7d**, **9**, **11**, **13**, **14** and **16** in CHCl_3 at room temperature

Normalized emission spectra of all the compounds in chloroform recorded at room temperature are collected in Fig. 3.2. The emission maxima of **7a**, **7d**, **9**, **11**, **13**, **14** and **16** are 488, 538, 494, 497, 500, 502 and 504 nm respectively. In the series, maximum and minimum emission wavelengths are shown by derivatives **7d** and **7a** respectively. The Stokes shift value of compounds is in the range of $5707\text{--}6833\text{ cm}^{-1}$ (Table 3.1). These large Stokes shift values indicate charge transfer nature of the emissive excited state.

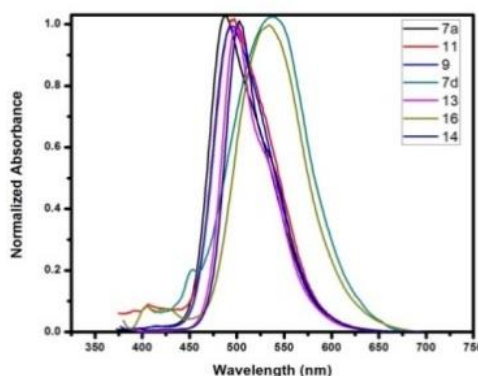


Fig. 3.2. Normalized emission spectra of compounds **7a**, **7d**, **9**, **11**, **13**, **14** and **16** in CHCl_3 at room temperature

3.3.2.2. Quantum Yield (ϕ) measurements

Fluorescence quantum yield is the ratio of photons absorbed to photons emitted through fluorescence; in other words it describes the efficiency of the conversion of absorbed light to emitted light. Fluorescence quantum yield (ϕ) of all fluorophores were measured in chloroform at room temperature by comparison with quinine sulfate (**7a**, **9** and **11**) and 9,10-diphenylanthracene (**7d**, **13**, **14** and **16**) of known quantum yield (ϕ) using Equation 3.1.²⁶ The known fluorescence quantum yield (ϕ_F) of quinine sulfate in 0.1 M H₂SO₄ and 9,10-diphenylanthracene in cyclohexane are 0.54 and 1.00 respectively.

$$\phi = \phi_R \frac{I \frac{n_{\text{solvent}}^2}{A} \frac{A_R}{n_R^2} \frac{I_R}{I_R}}{I} \quad (3.1)$$

Where I is the integrated intensity, A is the optical density, n is the refractive index and R stands for reference dye with known quantum yield. The calculated quantum yields of all the fluorophores are in the range of 0.36 to 0.76 (Table 3.1).

3.3.2.3. Optical Bandgap

Optical bandgap (E_g^{opt}) values were estimated from the onset of the low energy side of the absorption spectra (λ_{onset} , solution) to the baseline according to Equation 3.2 and are summarized in Table 3.2. Optical bandgap of the molecules are in the range of 2.16 - 2.88 eV. It was noticed that nitro substituted **7d** has the lowest optical bandgap of 2.16 eV.

$$E_g^{opt} = 1240/\lambda_{onset} \quad (3.2)$$

Table 3.1. Summary of absorption and emission profiles of the oxadiazole-phenothiazine fluorophores

Compounds	Absorption $\lambda_{\max}^{\text{abs}}$ (nm)	Emission $\lambda_{\max}^{\text{em}}$ (nm)	Stokes Shift (cm^{-1})	Quantum Yield
7a	367 (4.32)	488	6682	0.76
7d	405 (3.40)	538	6104	0.36
9	370 (4.17)	494	6784	0.55
11	371 (4.46)	497	6833	0.61
13	389 (3.98)	500	5707	0.63
14	390 (4.39)	502	5721	0.57
16	394 (4.23)	534	6654	0.58

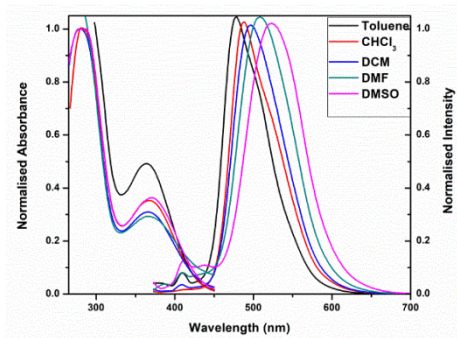
Table 3.2. Summary of optical bandgap of fluorophores

Compound	E_g^{opt} (eV)
7a	2.85 (435)
7d	2.16 (573)
9	2.88 (430)
11	2.86 (433)
13	2.74 (453)
14	2.69 (461)
16	2.77 (447)

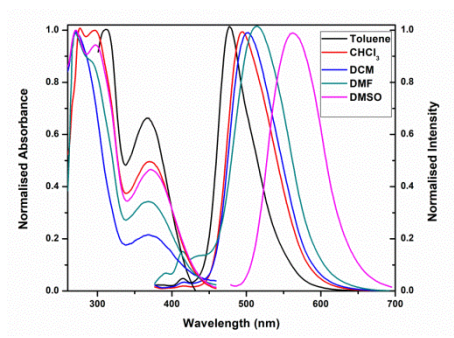
3.3.2.4. Solvatochromic Behavior

To understand the nature of intramolecular charge transfer characteristics (ICT) of the fluorophores, solvatochromic studies have been carried out as summarized in Table 3.3 and Fig. 3.3. Solvent effects were monitored using general solvents like toluene, chloroform, dichloromethane, dimethylformamide and dimethyl sulfoxide. With increasing solvent polarity, ICT bands exhibit redshift in absorption maxima whereas $n-\pi^*$ transitions exhibit the opposite trend. We observed

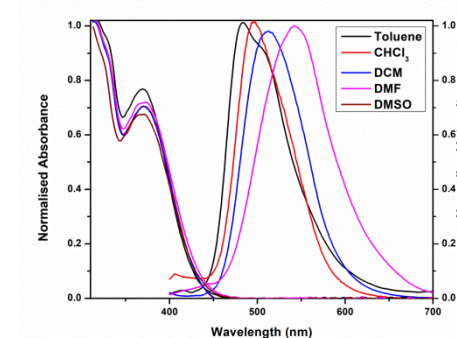
a slight redshift (<10 nm) in the absorption maximum with respect to increasing solvent polarity on moving from toluene to DMF. Redshift in emission maxima with respect to increasing solvent polarity was more pronounced suggesting polar nature of the excited state in comparison with the ground state. However, there are exceptions to the general trend described above. We observed that 1) shift in both absorption and emission maxima in DMSO bucked the general trend, and 2) compound **11** containing a naphthyl substituent behaved anomalously.



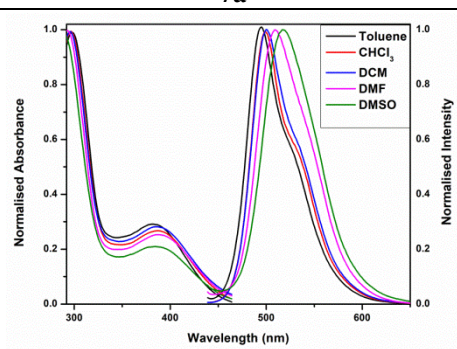
7a



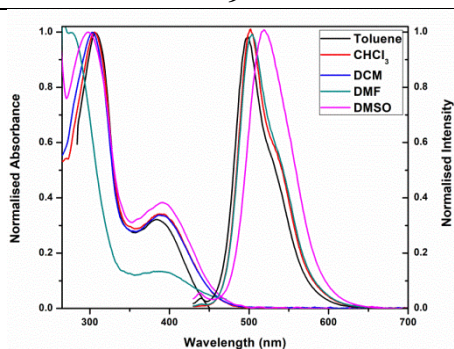
9



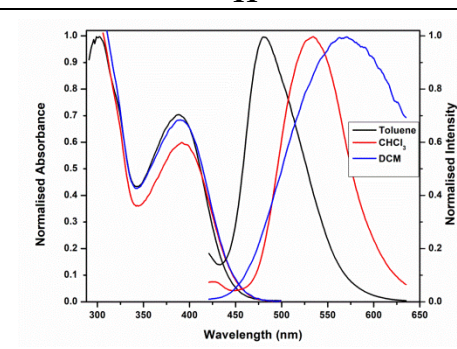
11



13



14



16

Fig. 3.3. Normalized absorption and emission spectra of compounds in general solvents

Table 3.3. Summary of optical properties of fluorophores

		7a			9		
Solvents	Dielectric Constant	Absorption λ_{max}^{abs} (nm) (log ϵ)	Emission λ_{max}^{em} (nm)	Stokes Shift (cm⁻¹)	Absorption λ_{max}^{abs} (nm) (log ϵ)	Emission λ_{max}^{em} (nm)	Stokes Shift (cm⁻¹)
Ph-CH ₃	2.38	364 (4.10)	478	6552	367 (3.90)	478	6327
CHCl ₃	4.81	367 (4.32)	488	6756	370 (4.17)	494	6784
DCM	9.08	367 (4.37)	497	7127	371 (4.19)	501	6994
DMF	38.25	368 (4.03)	508	7489	392 (4.11)	513	6017
DMSO	47.00	373 (3.80)	523	7689	373 (3.95)	564	9079

		11			13		
Solvents	Dielectric Constant	Absorption λ_{max}^{abs} (nm) (log ϵ)	Emission λ_{max}^{em} (nm)	Stokes Shift (cm⁻¹)	Absorption λ_{max}^{abs} (nm) (log ϵ)	Emission λ_{max}^{em} (nm)	Stokes Shift (cm⁻¹)
Ph-CH ₃	2.38	369 (4.11)	505	7298	384 (3.69)	495	5839
CHCl ₃	4.81	371 (4.42)	497	6833	389 (3.98)	500	5707
DCM	9.08	371 (4.33)	513	7461	390 (4.73)	501	5681
DMF	38.25	370 (3.89)	543	8611	390 (4.25)	509	5995
DMSO	47.00	370 (3.68)	Non-emissive	--	389 (3.52)	517	6364

Table 3.3. Summary of optical properties of fluorophores (continued...)

Solvents	Dielectric Constant	14			16		
		Absorption λ_{max}^{abs} (nm) (log ϵ)	Emission λ_{max}^{em} (nm)	Stokes Shift (cm ⁻¹)	Absorption λ_{max}^{abs} (nm)	Emission λ_{max}^{em} (nm)	Stokes Shift (cm ⁻¹)
Ph-CH ₃	2.38	385 (3.82)	499	5934	388	452	5026
CHCl ₃	4.81	390 (4.39)	502	5721	394	534	6654
DCM	9.08	390 (4.52)	504	5799	391	571	8062
DMF	38.25	390 (3.35)	505	5839			
DMSO	47.00	391 (3.22)	518	6270			

3.3.2.5. Time Resolved Fluorescence Decay

Fluorescence decay of various compounds were monitored in toluene and DMF. Characteristic time resolved fluorescence decay profiles of selected compounds are shown in Fig. 3.4(a,b,c) and their fluorescence life times are summarized in Table 3.4. The decay experiments were executed at an excitation wavelength of 340 nm and the decays were examined at respective emission maxima. The fluorescence lifetimes are observed to be in nanosecond time scales. The decays are fitted monoexponentially except for compounds **7a** in toluene and **11** in DMF. These two decays are fitted triexponentially; such multiexponential emission decay behavior are reported in literature.²⁷

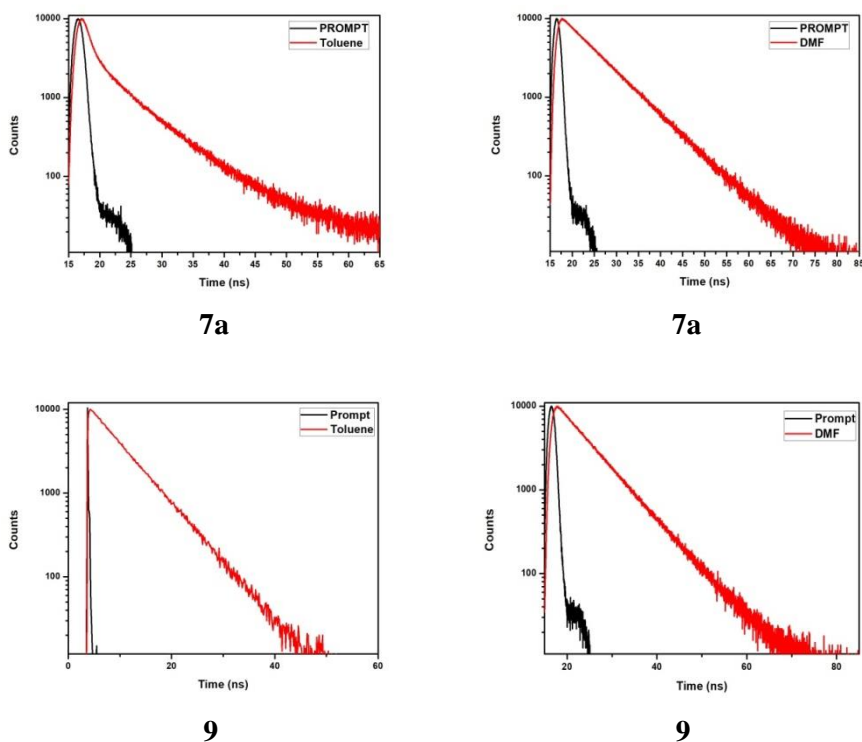


Fig. 3.4a. Fluorescence decay curves of fluorophores **7a**, **9** in toluene and DMF

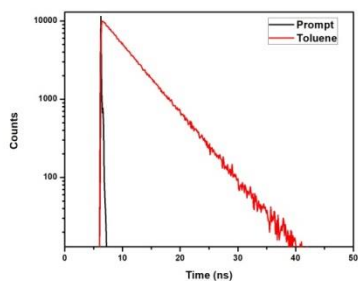
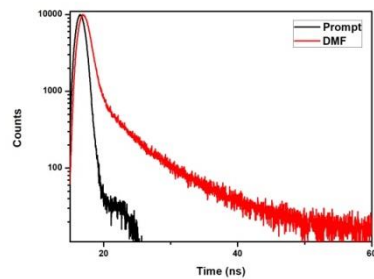
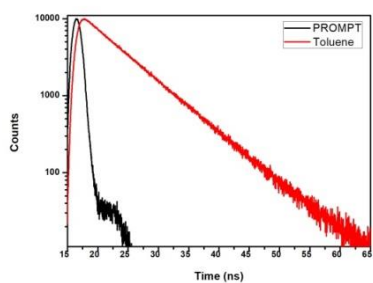
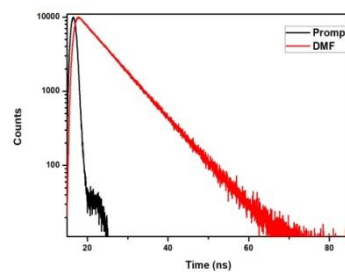
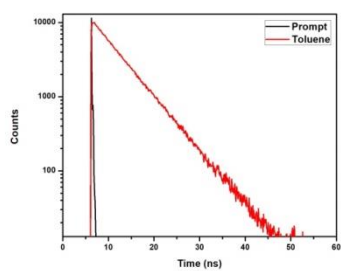
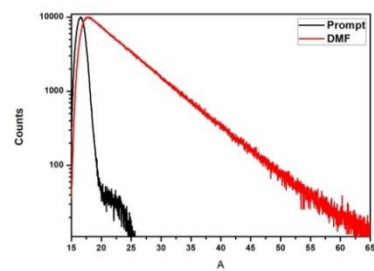
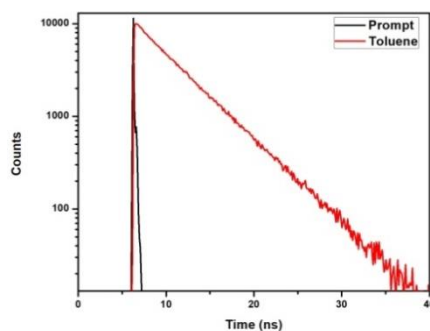
**11****11****13****13****14****14**

Fig. 3.4b. Fluorescence decay curves of fluorophores **11**, **13** and **14** in toluene and DMF

**16****Fig. 3.4c.** Fluorescence decay curves of fluorophores **16** in toluene**Table 3.4.** Summary of fluorescence lifetime in toluene and DMF

Compound	Toluene (ns)	DMF (ns)
	τ	τ
7a	τ_1 - 1.98 (20.81%) τ_2 - 7.07 (52.06%) τ_3 - 0.54 (27.12%)	7.87
9	6.09	7.04
11	4.97	τ_1 - 2.48 (11.06%) τ_2 - 7.32 (15.84%) τ_3 - 0.51 (73.10%)
13	6.57	6.96
14	5.81	6.61
16	4.73	Non emissive

3.3.3. Electrochemical Properties

Electrochemical properties of these fluorophores were studied by cyclic voltammetry at room temperature in degassed dichloromethane. CV was done in a three-electrode cell with Pt disc as working electrode, Ag/AgCl as reference electrode and Pt wire as auxiliary electrode with a scan rate of 100 mV/s using 0.1 M $n\text{Bu}_4\text{NPF}_6$ as supporting electrolyte and ferrocene as internal standard in dry dichloromethane. The corrected

values are reported against standard hydrogen electrode (SHE) (0.22 V). Using cyclic voltammetry, HOMO-LUMO energy levels of these D-A molecules were calculated. Cyclic voltammogram of the compounds are shown in Fig. 3.5(a,b) HOMO and LUMO energy levels were calculated using Equations 3.3 and 3.4 respectively (Table 3.5).²⁸

$$\text{HOMO} = - [E_{ox}^{onset} + 4.44] \text{ (eV)} \quad (3.3)$$

$$\text{LUMO} = - [\text{HOMO} + E_g^{opt}] \text{ (eV)} \quad (3.4)$$

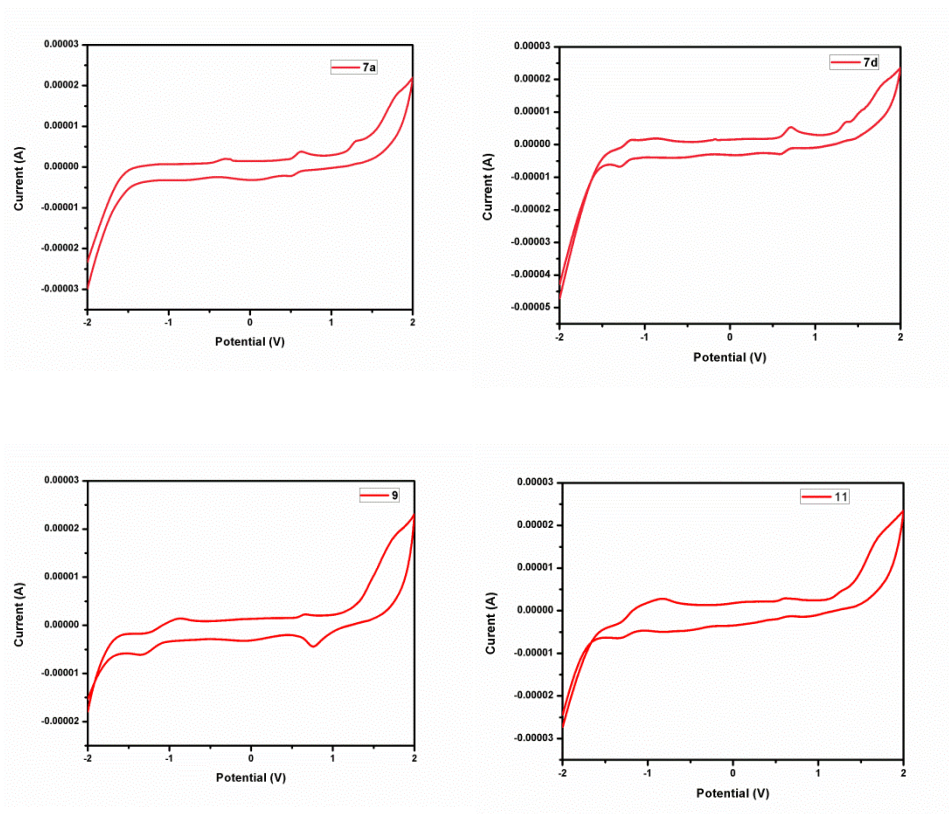


Fig. 3.5a. Cyclic voltammograms of fluorophores **7a**, **7d**, **9**, **11**

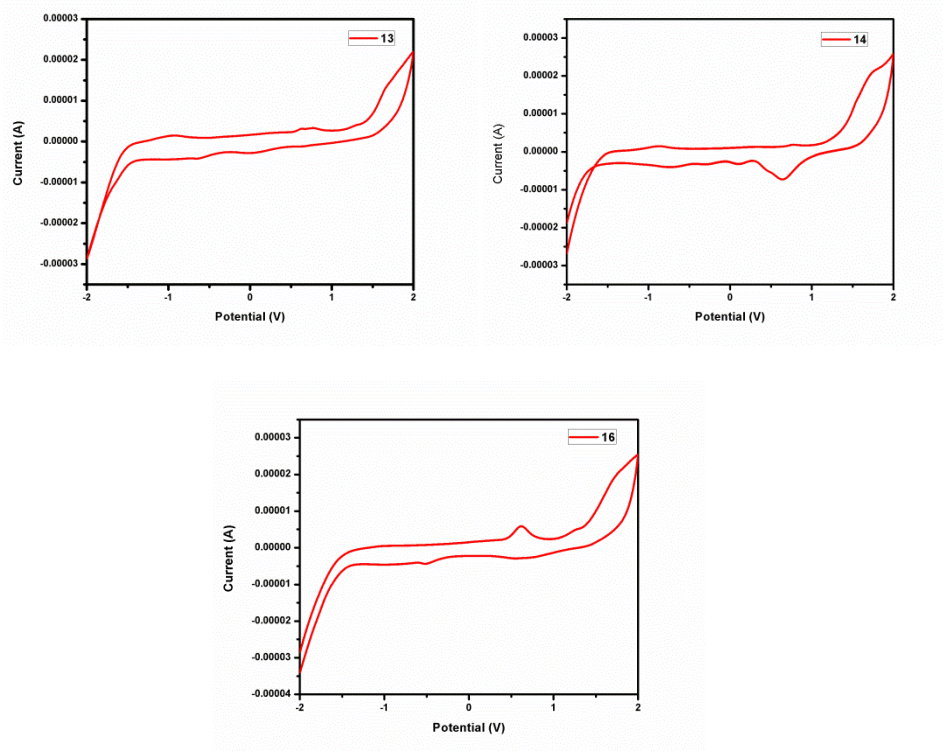


Fig. 3.5b. Cyclic voltammograms of fluorophores **13**, **14** and **16**

Table 3.5. Electrochemical properties of the fluorophores

Compound	E_{onset}^{ox} (V)	E_{onset}^{ox} vs E_{FOC} / V	HOMO (eV)	LUMO (eV)	E_g^{EC} (eV)
7a	0.62	0.84	-5.28	-2.43	2.85
7d	0.59	0.81	-5.25	-3.09	2.16
9	0.55	0.77	-5.21	-2.33	2.88
11	0.51	0.73	-5.17	-2.31	2.86
13	0.53	0.75	-5.19	-2.45	2.74
14	0.68	0.90	-5.34	-2.65	2.69
16	0.44	0.66	-5.10	-2.33	2.77

$E_{FOC} = 0.22$ V vs Ag/ AgCl.

3.3.4. Theoretical Studies

To evaluate the geometry and HOMO-LUMO energy levels of the D-A molecules, density functional theory (DFT) calculations were executed using GAUSSIAN 09 quantum chemistry package and B3LYP exchange-correlation functional.²⁹ Optimized ground state geometry and electron density distribution in HOMO and LUMO are shown in Fig. 3.6(a,b).

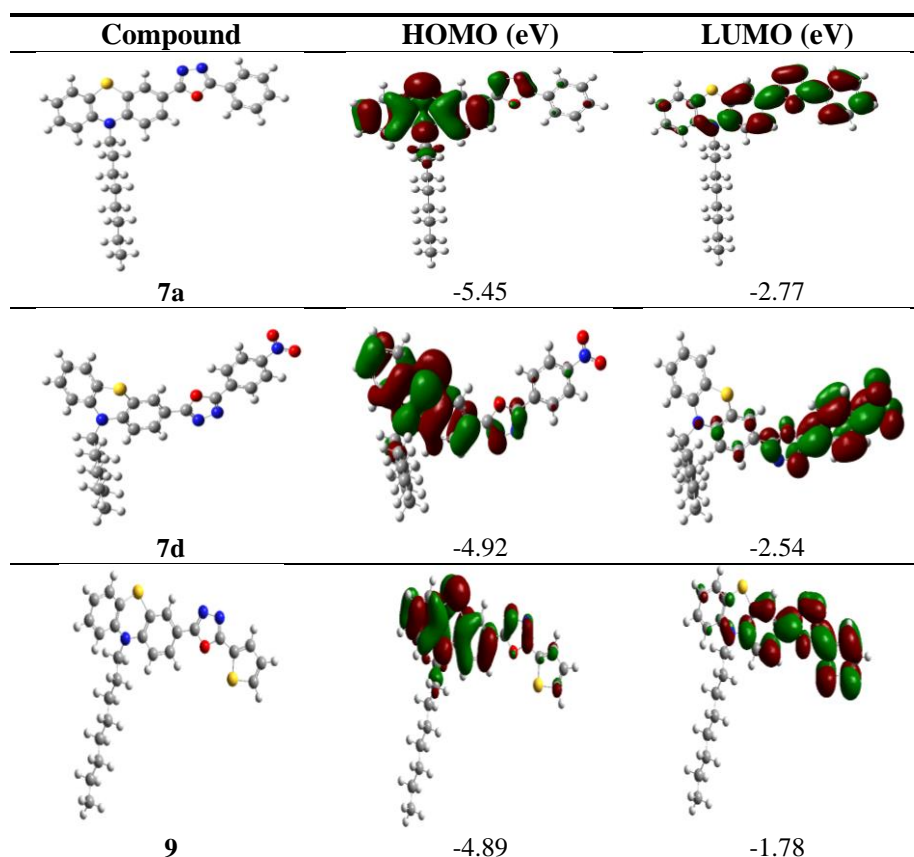


Fig. 3.6a. HOMO and LUMO levels and optimized molecular structures of fluorophores **7a**, **7d** and **9**

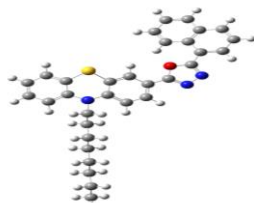
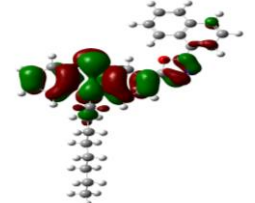
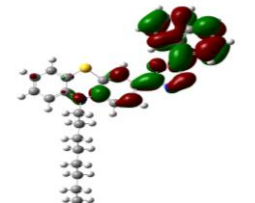
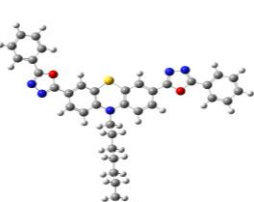
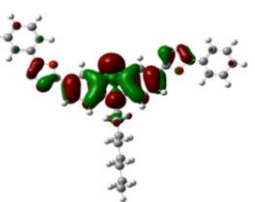
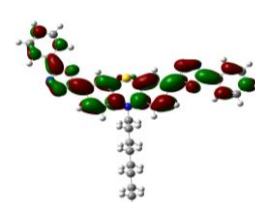
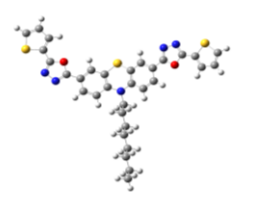
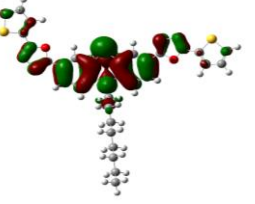

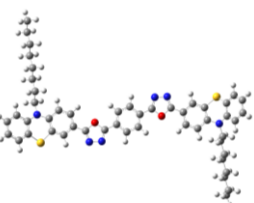
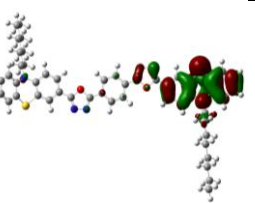
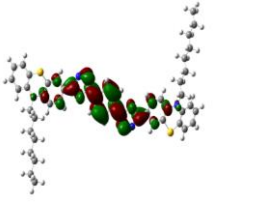
Compound	HOMO (eV)	LUMO (eV)
 11	 -4.68	 -1.51
 13	 -5.04	 -2.77
 14	 -5.30	 -1.94
 16	 -5.33	 -2.06

Fig. 3.6b. HOMO and LUMO levels and optimized molecular structures of fluorophores **11**, **13**, **14** and **16**

From the figure, it is clear that the electron density in HOMO is predominantly located on phenothiazine fragment, which is in

accordance with the strong electron donating ability of phenothiazine ring. Moreover electron density in LUMO is concentrated on oxadiazole framework, which suggests the strong electron accepting power of oxadiazoles. HOMO and LUMO mapping clearly depicts the charge separation in the entire molecular systems suggesting strong intramolecular charge transfer property. The theoretically calculated HOMO and LUMO values are in the range of (-5.45 to -4.68 eV) and (-2.77 to -1.51 eV) respectively. Due to the presence of nitro group, LUMO level is lowered which resulted in lowest bandgap in **7d** (2.38 eV) and which further leads to the substantial bathochromic shift in absorption spectrum. Energy level diagrams of frontier orbitals for different compounds under investigation are shown in Fig. 3.7.

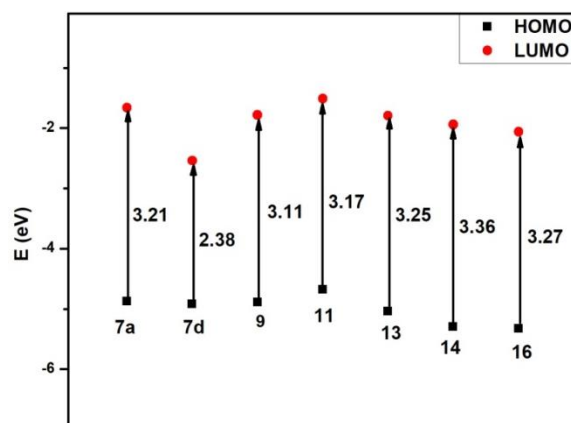


Fig. 3.7. Energy diagram of the frontier orbitals for **7a-16** calculated from DFT

3.3.5. XRD Characterization

Powder XRD pattern of the compounds showed both sharp and broad peaks indicating their semi-crystalline nature with the exception of **14** which is amorphous. As shown in Fig 3.8(a,b), in each fluorophore a

diffraction peak at 2θ values 4-5 degree was observed, which indicates that the long alkyl chain effectively disrupt the approach of conjugated backbone. Broader and less intense diffraction peaks around 2θ values 20-25 degree are attributed to second order reflection.³⁰

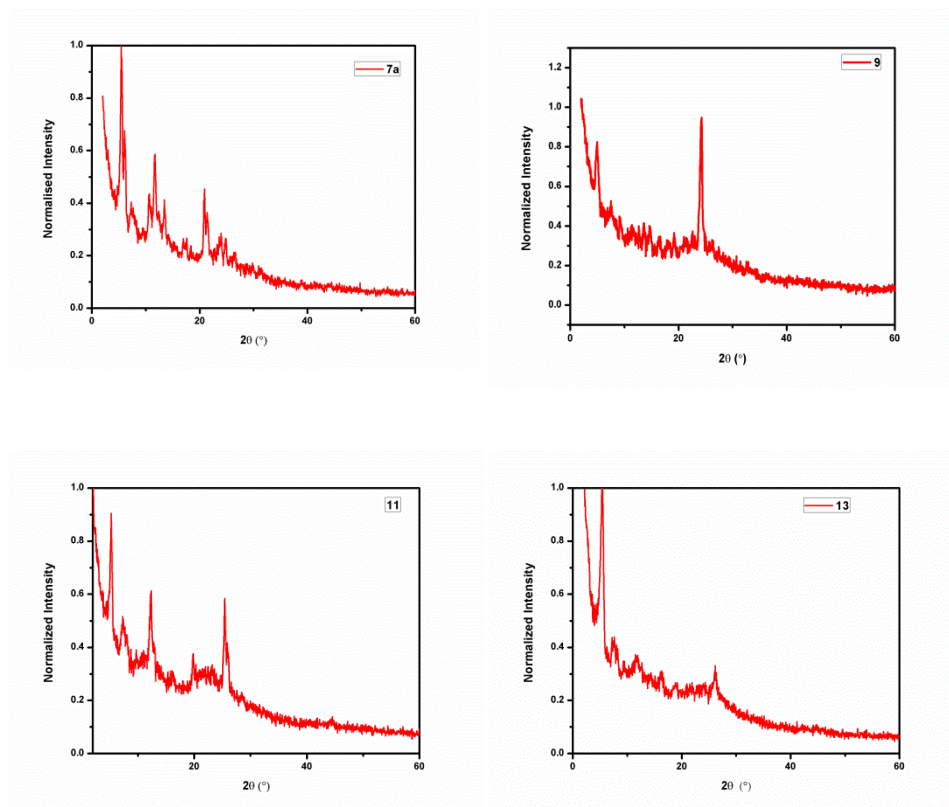


Fig. 3.8a. Powder XRD patterns of the fluorophores **7a**, **9**, **11** and **13**

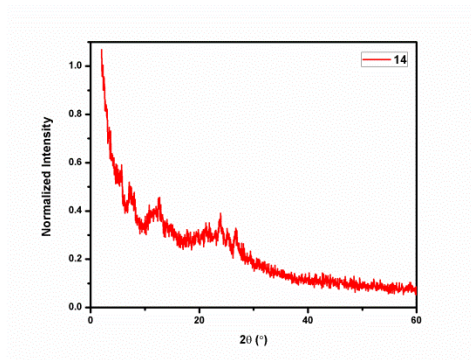


Fig. 3.8b. Powder XRD patterns of the fluorophore **14**

3.3.6. Thermal Properties

Thermal and morphological stabilities were monitored by differential scanning calorimetry (DSC) and thermogravimetric analysis (TGA). The results are shown in Fig. 3.9(a,b) and Fig. 3.10(a,b) and their thermal properties are summarized in Table 3.6. Phase transition characteristics of these compounds were investigated using DSC and it discloses that compounds **13** and **16** are semi-crystalline and their DSC curves showed glass transition temperature T_g at 105 and 84 °C respectively. Compounds showed melting points in the range of 82-205 °C. Crystallization temperature is observed only for compound **14**, which is at 158 °C. The TGA results showed that molecules are thermally stable with 5% weight loss in the range of 303-379 °C.

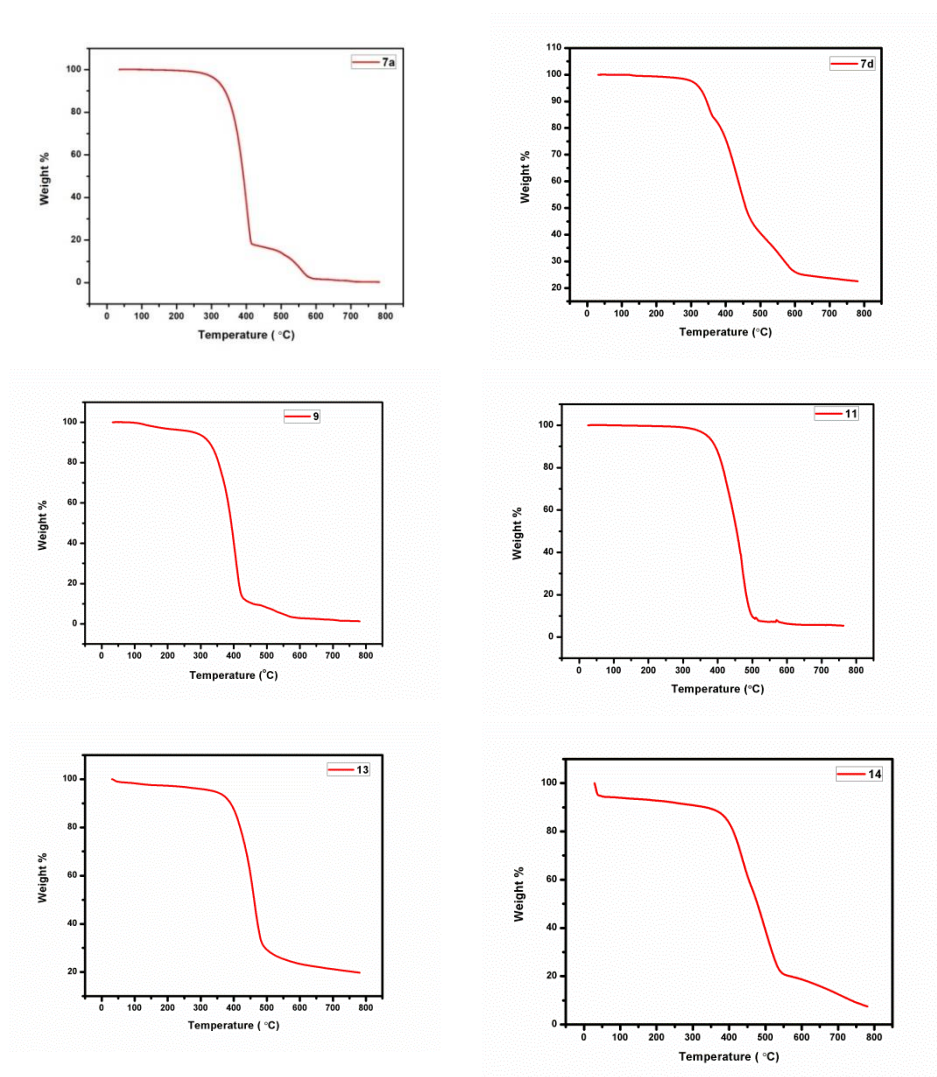


Fig. 3.9a. Thermogram traces of fluorophores **7a**, **7d**, **9**, **11**, **13** and **14**

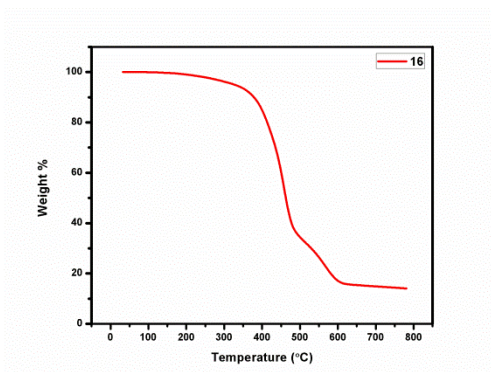


Fig. 3.9b. Thermogram traces of fluorophore 16

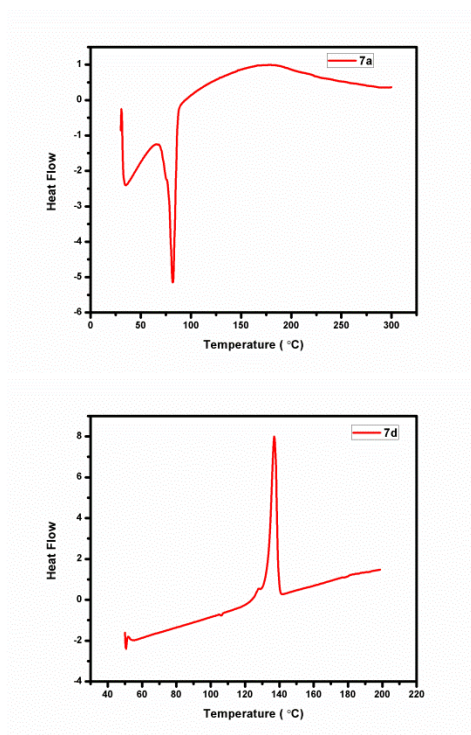


Fig. 3.10a. DSC traces of fluorophores 7a, 7d

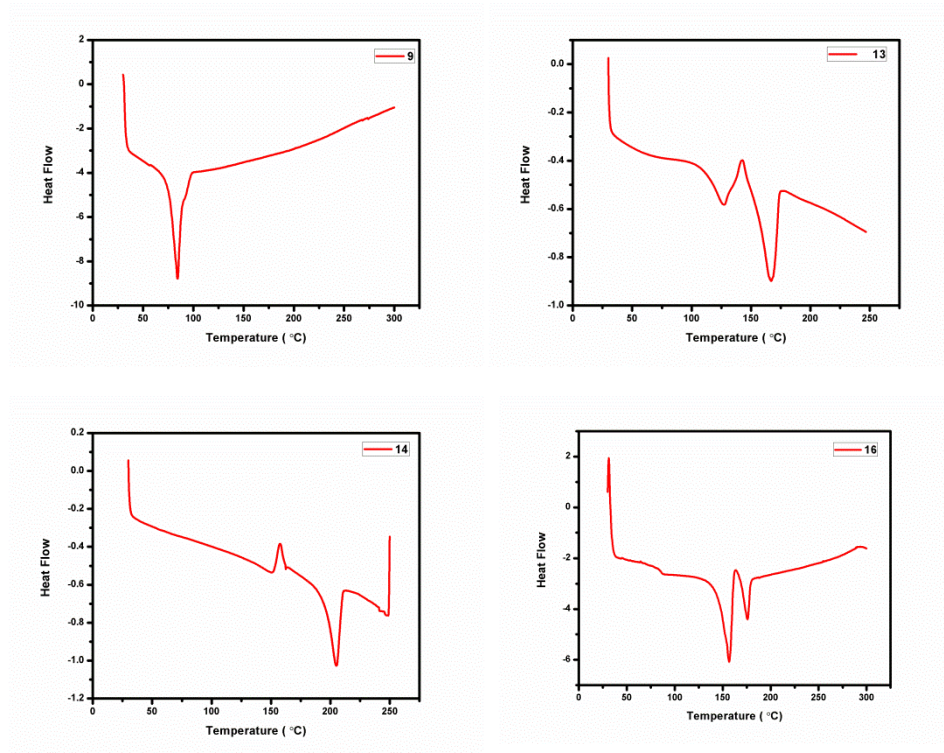


Fig. 3.10b. DSC traces of fluorophores **9**, **13**, **14** and **16**

Table 3.6. Thermal properties of the fluorophores

Compound	Glass transition temperature, T_g (°C)	Melting point, T_m (°C)	Crystallization temperature, T_c (°C)	Decomposition temperature (°C)
7a	-	82	-	354
7d	-	137	-	325
9	-	84	-	333
11	-	-	-	379
13	105	167	-	303
14	-	205	158	-
16	84	157	-	326

3.3.7. Nonlinear Optical Properties

The third order nonlinear optical properties of D-A molecules were investigated using Z-scan technique.³¹ Open aperture (OA) Z-scan

traces of molecules in dilute CHCl_3 are shown in Fig. 3.11. The solid curves in the Fig. 3.11 are theoretical fit to the experimental data, which is fitted with two photon absorption (TPA) mechanism which suggest that TPA is involved in the exhibition of NLO property.

Using open aperture Z-scan configuration, the NLO absorption coefficients of all the targeted molecules were calculated using Equation 3.5.³² All the compounds displayed reverse saturable absorption (RSA) with a positive absorption coefficient.

$$T(z) = \frac{c}{q_0\sqrt{\pi}} \int_{-\infty}^{\infty} \ln(1 + q_0 e^{-t^2}) dt \quad (3.5)$$

Where $q_0(z, r, t) = \beta I_0(t) L_{\text{eff}}$ and $L_{\text{eff}} = (1 - e^{-\alpha z})/\alpha$ are the effective thickness with the linear absorption coefficient, α and I_0 is the irradiance at focus. The imaginary part of the third-order susceptibility, $\text{Im } \chi^{(3)} = \frac{n_0^2 c^2 \beta}{240 \omega \pi^2}$ where n_0 is the linear refractive index of compounds, c is the velocity of light under vacuum and ω is the angular frequency of radiation used.

The nonlinear absorption coefficient β and imaginary part of nonlinear susceptibility ($\text{Im } \chi^{(3)}$) are calculated and summarized in Table 3.7. Results obtained in NLO revealed that fluorophores exhibited good nonlinear optical characteristics, which indicates the π electron delocalization and polarizability in the molecules. Among the molecules **16** showed highest nonlinear responses with a β value of 9.85×10^{-10} m/W and $\text{Im } \chi^{(3)}$ is 3.33×10^{-11} . Compound **16** is a highly expanded molecule with D-A- π -A-D architecture, large electronic delocalization occurs from

the terminal phenothiazine moiety to oxadiazole ring which further enhances the polarizability of the molecule.

3.3.7.1. Optical Power Limiting

Protection of eyes and optical devices from high intensity laser light has received significant attention. Large non-linearity, broadband spectral response and fast response time are crucial for good optical limiting property. Lowering of optical threshold will enhance the optical response. A graph is drawn between the input fluence and output fluence for the sample irradiated at 532 nm using 7 ns laser pulses. Input fluence corresponding to half of normalized transmittance gives the optical limiting threshold and the curves for various compounds under investigation are given in Fig. 3.11(a,b,c).

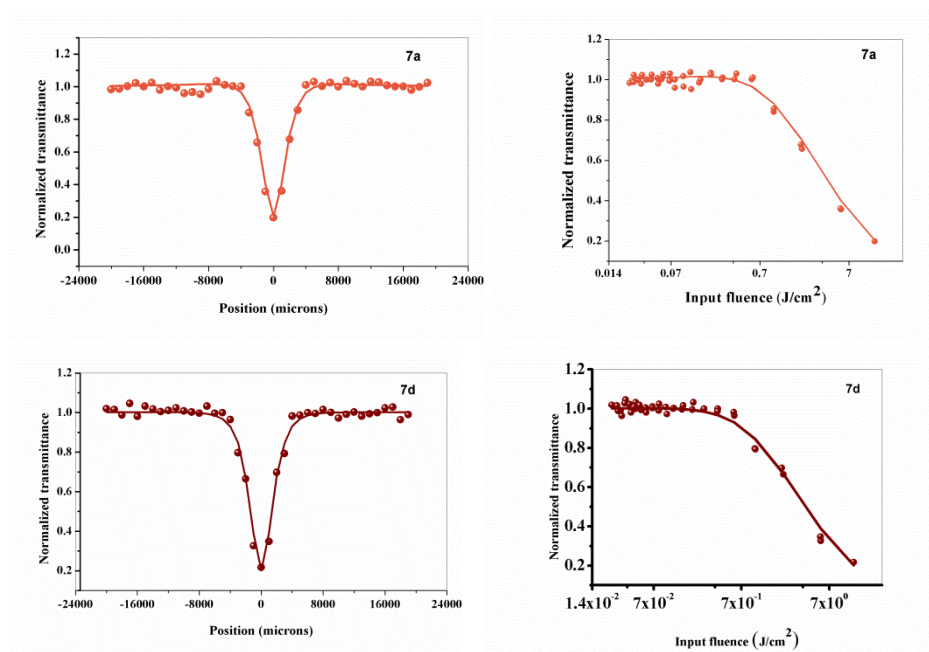


Fig. 3.11a. Normalised open aperture and optical limiting curves of **7a** and **7d**

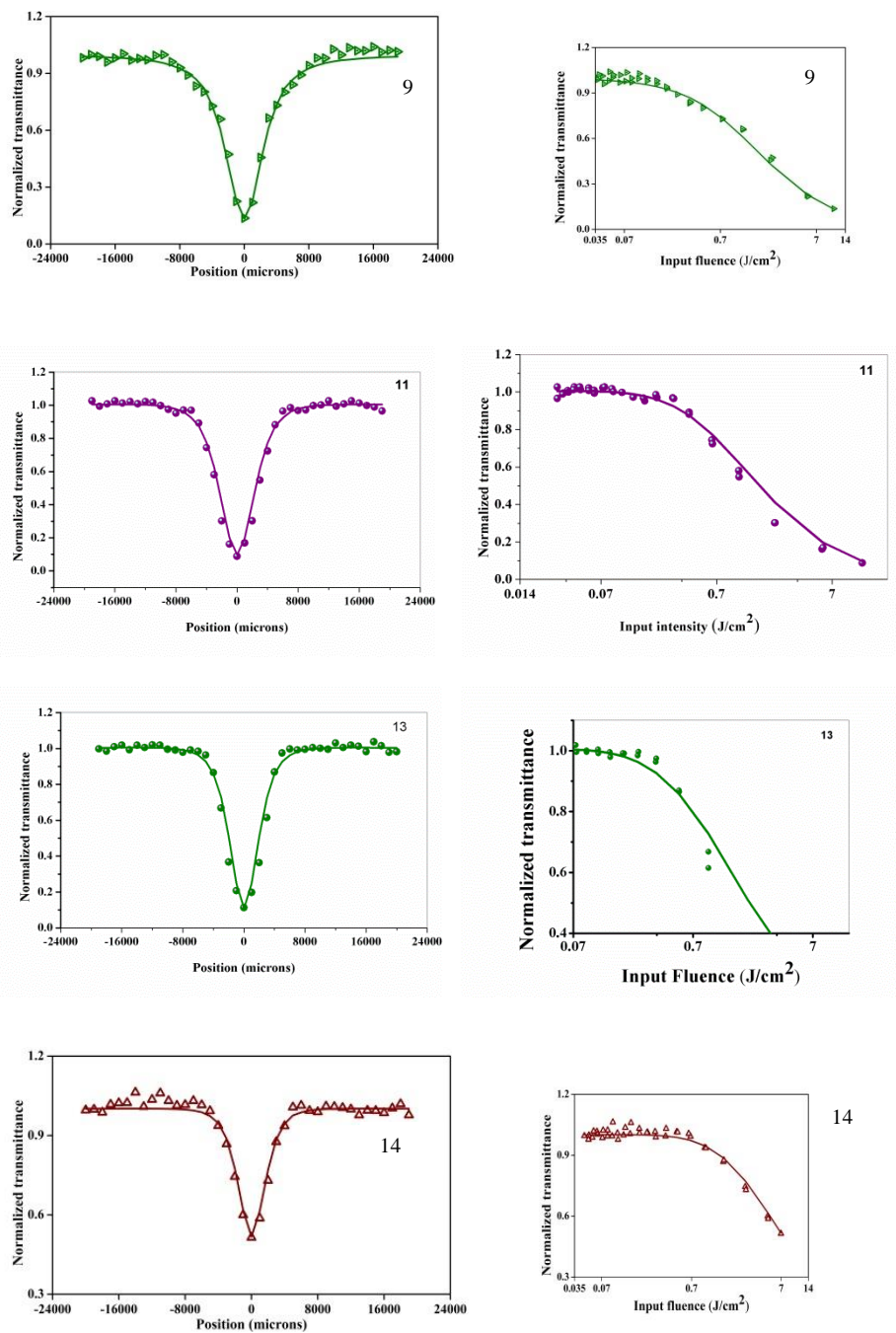


Fig. 3.11b. Normalised open aperture and optical limiting curves of 9, 11, 13 and 14

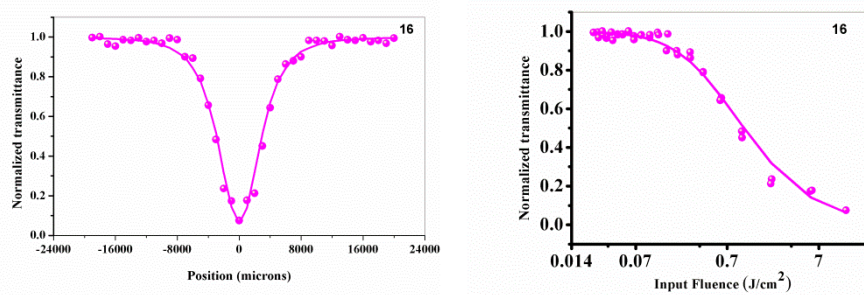


Fig. 3.11c. Normalised open aperture and optical limiting curves of **16**

Table 3.7. NLO properties of the compounds

Molecule	Nonlinear absorption coefficient (β , m/W)	Imaginary part of nonlinear susceptibility ($\text{Im } \chi^{(3)}$, esu)	Optical Limiting Threshold (J/cm^2)
7a	2.89×10^{-10}	9.77×10^{-12}	3.84
7d	2.80×10^{-10}	9.47×10^{-12}	2.37
9	5.52×10^{-10}	18.59×10^{-12}	2.37
11	7.31×10^{-10}	2.48×10^{-11}	1.70
13	5.15×10^{-10}	1.74×10^{-11}	2.04
14	1.50×10^{-10}	4.95×10^{-12}	7.12
16	9.85×10^{-10}	3.33×10^{-11}	1.02

3.4. Conclusions

We have synthesized a few 1,3,4-oxadiazole-phenothiazine push-pull fluorophores. These fluorophores are found to be highly emissive with high quantum yields. All the fluorophores showed positive solvatochromic behavior particularly in the emission spectra which indicates the more polar nature of excited state compared to the ground state. Due to high electron donating ability of phenothiazine, we observed strong π electron delocalization in the entire molecular framework. Ground state optimized geometry of the molecules also confirms the π electron delocalization. Due to this asymmetric

polarizability, these molecules showed high third order nonlinear optical property which is confirmed by relatively good nonlinear absorption coefficient (β) value. We also observed that these molecules exhibit potential optical limiting property. Hence these fluorophores are promising candidates for further photonic applications.

3.5. Experimental Section

3.5.1. Reagents and instruments

All commercially available chemical reagents were procured from Alfa Aesar and Sigma Aldrich and were used without further purification. The required starting materials 10-octyl-10*H*-phenothiazine-3-carbaldehyde (**3**) and 10-octyl-10*H*-phenothiazine-3,7-dicarbaldehyde (**12**) were prepared according to the reported procedures.^{33,34} ^1H and ^{13}C NMR spectra were recorded on Bruker Avance III, 400 MHz and Bruker AMX 500 spectrometers with tetramethylsilane (TMS) as internal standard; chemical shifts (δ) are given in ppm relative to TMS.

Absorption spectra were recorded using Evolution 201 UV-Vis spectrophotometer. Emission spectra were recorded using Shimadzu-RF-5301PC spectrofluorophotometer. All electrochemical experiments were performed in dry dichloromethane using *n*-Bu₄NPF₆ as the supporting electrolyte and platinum as the working electrode in a CH instrument with a scan rate of 100 mV/s. DFT calculations were performed using the software package Gaussian 09 for Windows. The basis set for the optimization of the structure is B3LYP/6-31G(d,p). The input files were prepared and submitted to the Gaussian 09 software and the results were

displayed using the graphic software Gauss view 5. Powder X-ray diffraction (XRD) patterns were obtained using a Rigaku X-ray diffractometer with Cu K α radiation (1.542 Å).

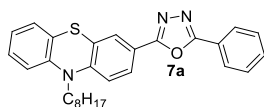
A Q-switched Nd:YAG laser with a pulse width of 7 ns at 532 nm was used as a source of light in the Z-scan experiments. Fluorescence lifetime was measured using a Horiba Fluorolog-3 Time-correlated single photon counting system (TCSPC). Fluorescence lifetime values were determined by deconvolution of the data with exponential decay using DAS6 decay analysis software. Thermogravimetric measurements were performed on a TA instrument Q 50 Thermogravimetric analyzer under nitrogen with a heating rates of 10 °C/min. Differential scanning calorimetry (DSC) was carried out on Mettler Toledo DSC 822e with a continuous Nitrogen flow and a heating rate of 10 °C/min.

3.5.2. Synthesis and Characterization

3.5.2.1. Synthesis of 2-(10-octyl-10H-phenothiazin-3-yl)-5-phenyl-1,3,4-oxadiazole (7a)

A solution of 10-octyl-10H-phenothiazine-3-carbaldehyde (**4**, 340 mg, 1mmol,) and benzohydrazide (**5a**, 137 mg, 1 mmol) in ethanol was heated to 80 °C for 8 h and the resulting residue was dissolved in DMSO (3 mL) followed by the addition of K₂CO₃ (414 mg, 3 mmol) and I₂ (304 mg, 1.2 mmol) in sequence. The reaction mixture was again stirred at 100 °C until the complete consumption of the starting materials. The reaction mixture was cooled to room temperature and treated with 5 % Na₂S₂O₃ (20 mL) and then extracted with ethyl acetate. The organic layer was washed successively with brine and the combined organic layer was

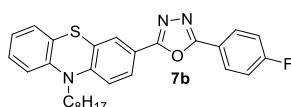
dried over anhydrous Na_2SO_4 and concentrated under reduced pressure and the residue purified by silica gel column chromatography (hexane-ethyl acetate, 9:1) yielded the product as a yellow solid.



Yield: 62%, mp: 80-85 °C; UV-Vis (CHCl_3): 367 nm (λ_{max}); IR (KBr): 2923, 1460, 1258, 1028, 618 cm^{-1} ; ^1H NMR (500 MHz, CDCl_3): δ (ppm) 7.99-6.87 (m, 12H), 3.88 (t, $J = 7$ Hz, 2H), 1.84 – 0.85 (m, 15H); ^{13}C -NMR (125 MHz, CDCl_3): δ (ppm) 164.7, 162.7, 162.2, 128.1, 128.0, 126.5, 119.2, 115.4, 115.3, 114.7, 95.1, 30.7, 28.1, 25.6, 21.6, 13.0; MS: m/z 455 (M^+), 456 ($M+1$); Elemental analysis calculated for $\text{C}_{28}\text{H}_{29}\text{N}_3\text{OS}$: C: 73.81, H: 6.42, N: 9.22, S: 7.04; Found C: 73.80, H: 6.40, N: 9.21, S: 7.03.

3.5.2.2. Synthesis of 2-(4-fluorophenyl)-5-(10-octyl-10H-phenothiazin-3-yl)-1,3,4-oxadiazole (7b)

The reaction was performed according to the procedure 3.5.2.1. with 10-octyl-10H-phenothiazine-3-carbaldehyde (340 mg, 1 mmol) and 4-fluorobenzohydrazide (154 mg, 1 mmol). Yellow solid.

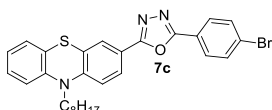


Yield: 75%, mp: 82-87 °C; IR (KBr): 2855, 1510, 1455, 1035, 682 cm^{-1} ; ^1H NMR (500 MHz, CDCl_3): δ (ppm) 8.13-6.86 (m, 11H), 3.88 (t, $J = 7$ Hz, 2H), 1.88-1.79 (m, 2H), 1.47-1.41 (m, 2H), 1.34-1.25 (m, 8H), 0.87 (t, 3H); ^{13}C -NMR (125 MHz, CDCl_3): δ (ppm) 164.7, 162.7, 162.3, 128.1, 126.5, 125.4, 124.4, 119.2, 116.4, 116.3, 114.7, 114.2, 30.7, 28.1, 25.8, 21.6, 13; MS: m/z 473 (M^+), 474 ($M+1$); Elemental analysis calculated for $\text{C}_{28}\text{H}_{28}\text{FN}_3\text{OS}$: C: 71.01, H: 5.96, N: 8.87, S: 6.77; Found C: 71.03, H: 5.95, N: 8.56, S: 6.76.

3.5.2.3. Synthesis of 2-(4-bromophenyl)-5-(10-octyl-10H-phenothiazin-3-yl)-1,3,4-oxadiazole (7c)

The reaction was performed according to the procedure 3.5.2.1.

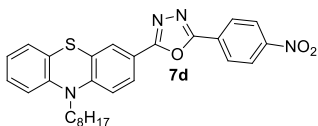
with 10-octyl-10*H*-phenothiazine-3-carbaldehyde (339 mg, 1 mmol) and 4-bromobenzohydrazide (215 mg, 1 mmol). Yellow solid.



Yield: 73%, mp: 100-105 °C; IR (KBr): 2920, 1580, 1435, 1084, 689, 550; ¹H NMR (500 MHz, CDCl₃): δ (ppm) 7.99-6.87 (m, 11H), 3.90 (t, 2H), 1.83 (m, 2H), 1.46-1.42 (m, 2H), 1.33-1.25 (m, 8H), 0.86 (t, 3H).; ¹³C-NMR (125 MHz, CDCl₃): δ (ppm) δ 131.2, 130.3, 127.2, 126.9, 125.3, 116.3, 113.5, 99.0, 30.7, 28.1, 30.6, 28.1, 24.1, 21.6, 13.1; MS: *m/z* 535 (*M*⁺), 536 (*M*+1); Elemental analysis calculated for C₂₈H₂₈BrN₃OS: C: 62.92, H: 5.28, N: 7.86, S: 6.00; Found C: 62.91, H: 5.26, N: 7.84, S: 5.98.

3.5.2.4. Synthesis of 2-(4-nitrophenyl)-5-(10-octyl-10*H*-phenothiazin-3-yl)-1,3,4-oxadiazole (7d)

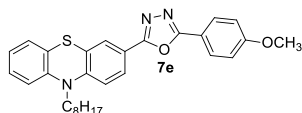
The reaction was performed according to the procedure 3.5.2.1. with 10-octyl-10*H*-phenothiazine-3-carbaldehyde (339 mg, 1 mmol), 4-nitrobenzohydrazide (181 mg, 1 mmol), K₂CO₃ (414 mg, 3 mmol) and I₂ (304 mg, 1.2 mmol). Red solid.



Yield: 65%, mp: 135-140 °C; UV-Vis (CHCl₃) λ_{max} 405 nm; IR (KBr): 2980, 1540, 1470, 1125, 650, 568; ¹H NMR (500 MHz, CDCl₃): δ (ppm) 8.31-8.29 (m, 2H), 8.22 (d, *J* = 8.5 Hz, 1H), 7.74 (s, 1H), 7.10 (t, *J* = 8 Hz, 1H), 7.05 (d, *J* = 7.5 Hz, 1H), 6.91-6.80 (m, 3H), 3.81 (t, *J* = 7 Hz, 2H), 1.75 (t, *J* = 7.5 Hz, 2H), 1.40-1.18 (m, 10H), 0.79 (t, *J* = 7 Hz, 3H).; ¹³C-NMR (125 MHz, CDCl₃): δ (ppm) δ 164.0, 161.4, 148.4, 147.8, 142.8, 128.5, 126.6, 126.5, 125.6, 124.7, 124.6, 123.4, 122.3, 115.9, 114.8, 114.3, 46.8, 30.7, 2.1, 25.8, 25.7, 21.6, 13.0; MS: *m/z* 500 (*M*⁺), 501 (*M*+1); Elemental analysis calculated for C₂₈H₂₈N₄O₃S: C: 67.18, H: 5.64, N: 11.19, S: 6.41; Found C: 67.17, H: 5.63, N: 11.18, S: 6.40.

3.5.2.5. Synthesis of 2-(4-methoxyphenyl)-5-(10-octyl-10H-phenothiazin-3-yl)-1,3,4-oxadiazole (7e)

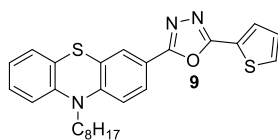
The reaction was performed according to the procedure 3.5.2.1. with 10-octyl-10H-phenothiazine-3-carbaldehyde (339 mg, 1 mmol), 4-methoxybenzohydrazide (168 mg, 1 mmol), K₂CO₃ (414 mg, 3 mmol) and I₂ (304 mg, 1.2 mmol). Yellow solid.



Yield: 80%, mp: 122-127 °C; IR (KBr): 2820, 1590, 1480, 1012, 690 cm⁻¹; ¹H NMR (500 MHz, CDCl₃): δ (ppm) 7.98-7.96 (m, 2H), 7.83-7.81 (m, 1H), 7.74 (m, 1H), 7.11-6.80 (m, 7H), 3.81-3.80 (m, 5H), 1.77-1.71 (m, 2H), 1.39-1.34 (m, 2H), 1.24-1.18 (m, 11H), 0.80-0.77 (m, 3H); ¹³C NMR (125 MHz, CDCl₃): δ (ppm) 163.1, 162.6, 161.2, 147.1, 143.0, 127.6, 126.5, 125.2, 124.4, 124.3, 122.8, 122.1, 116.8, 115.5, 114.7, 114.2, 113.4, 54.4, 46.7, 30.7, 28.1, 25.8, 21.6, 13.1; MS: *m/z* 485 (*M*⁺), 486 (*M+I*); Elemental analysis calculated for C₂₉H₃₁N₃O₂S: C: 71.72, H: 6.43, N: 8.65, S: 6.60; Found C: 71.70, H: 6.41, N: 8.64, S: 6.61.

3.5.2.6. Synthesis of 2-(10-octyl-10H-phenothiazin-3-yl)-5-(thiophen-2-yl)-1,3,4-oxadiazole (9)

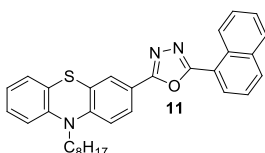
The title compound was prepared by a procedure similar to that of 7a except that thiophene-2-carbohydrazide (142 mg, 1mmol) was used as the reactant instead of benzohydrazide. Yellow solid.



Yield: 80%, mp: 82-87 °C; UV-Vis (CHCl₃) λ_{max} 370 nm; IR (KBr): 3071, 1578, 1461, 1404, 1258, 1098, 1029, 803; ¹H NMR (500 MHz, CDCl₃): δ (ppm) 7.82 (dd, *J* = 8.4, 2.0 Hz, 1H), 7.48 (dd, *J* = 4.8, 1.2 Hz, 1H), 7.12-7.05 (m, 3H), 6.90-6.80 (m, 3H), 3.81 (t, 2H), 1.79-0.78 (m, 15H); ¹³C-NMR (125 MHz, CDCl₃): δ (ppm) 162.5, 159.4, 147.3, 143.0, 128.9, 128.5, 127.1, 126.5, 126.5, 125.3, 124.5, 124.4, 124.3, 122.8, 122.1, 116.4, 114.7, 114.3, 46.8, 30.7, 28.2, 28.1, 25.8, 25.8, 21.6, 13.0; MS: *m/z* 461 (*M*⁺), 462 (*M+I*); Elemental analysis calculated for C₂₆H₂₇N₃OS₂: C: 67.65, H: 5.90, N: 9.10, S: 13.89; Found C: 67.64, H: 5.89, N: 9.11, S: 13.88.

3.5.2.7. Synthesis of 2-(naphthalen-1-yl)-5-(10-octyl-10H-phenothiazin-3-yl)-1,3,4-oxadiazole (11)

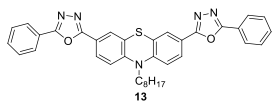
This compound was prepared by a procedure similar to that of **7a** except that 1-naphthohydrazide (160 mg, 1 mmol) was used as the reactant instead of benzohydrazide. Yellow solid.



Yield: 80%, mp: 82-87 °C; UV-Vis (CHCl₃) λ_{max} 371 nm; IR (KBr): 3050, 1560, 1430, 1380, 1240, 1050, 855; ¹H NMR (500 MHz, CDCl₃): δ (ppm) 9.18 (d, *J* = 8.8 Hz, 1H), 8.09-8.07 (m, 1H), 7.88-7.78 (m, 4H), 7.58-7.54 (m, 1H), 7.46-7.42 (m, 2H), 7.07-7.00 (m, 2H), 6.85-6.77 (m, 3H), 3.73 (t, *J* = 7.2 Hz, 2H), 1.71-1.67 (m, 2.15), 1.34-1.14 (m, 11H), 0.78-0.75 (m, 3H); ¹³C-NMR (125 MHz, CDCl₃): δ (ppm) 163.1, 162.5, 147.2, 142.9, 132.8, 131.3, 129.0, 127.6, 127.1, 127.0, 126.5, 126.4, 125.6, 125.4, 125.3, 125.2, 124.5, 124.3, 123.8, 122.7, 122.1, 119.5, 116.6, 114.7, 114.2, 46.7, 30.7, 28.2, 28.1, 25.8, 25.7, 21.6, 13.0; MS: *m/z* 505 (*M*⁺), 506 (*M*+1); Elemental analysis calculated for C₃₂H₃₁N₃OS: C: 76.01, H: 6.18, N: 8.31, S: 6.34; Found C: 76.00, H: 6.17, N: 8.30, S: 6.33.

3.5.2.8. Synthesis of 5,5'-(10-octyl-10H-phenothiazine-3,7-diyl)bis(2-phenyl-1,3,4-oxadiazole) (13)

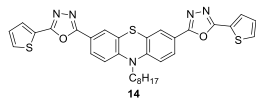
This compound was prepared by a procedure similar to that of **7a**, except that 10-octyl-10H-phenothiazine-3,7-dicarbaldehyde (367 mg, 1 mmol) was used as the reactant instead of 10-octyl-10H-phenothiazine-3-carbaldehyde and two equivalence of benzohydrazide (272 mg, 2 mmol) is added. Cyclization occurs in both sides to yield the product as orange solid.



Yield: 68%, mp: 165-170 °C; UV-Vis (CHCl₃) λ_{max} 389 nm; IR (KBr): 3050, 2945, 1550, 1460, 1436, 1200; ¹H NMR (500 MHz, CDCl₃): δ (ppm) 8.06-8.05 (m, 4H), 7.89-7.77 (m, 4H), 7.47-7.46 (m, 6H), 6.89 (d, *J* = 8.5 Hz, 2H), 3.86 (t, *J* = 7.5 Hz, 2H), 1.81-1.75 (m, 2H), 1.43-1.19 (m, 10 H), 0.79 (t, *J* = 7 Hz, 3H); ¹³C-NMR (125 MHz, CDCl₃): δ (ppm) 163.3, 162.8, 145.9, 130.7, 128.1, 125.9, 125.6, 124.6, 123.6, 122.9, 117.6, 114.7, 47.1, 30.7, 28.2, 28.1, 25.7, 25.6, 21.6, 13.0; MS: *m/z* 599 (*M*⁺), 600 (*M*+1); Elemental analysis calculated for C₃₆H₃₃N₅O₂S: C: 72.09, H: 5.55, N: 11.68, S: 5.35; Found C: 72.07, H: 5.53, N: 11.66, S: 5.34.

3.5.2.9. Synthesis of 5,5'-(10-octyl-10H-phenothiazine-3,7-diyl)bis(2-(thiophen-2-yl)-1,3,4-oxadiazole) (14)

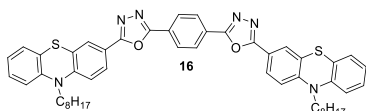
This compound was prepared by a procedure similar to that of **13**, except that two equivalence of thiophene-2-carbohydrazide (284 mg, 2 mmol) is used in place of benzohydrazide. Orange solid.



Yield: 74%, mp: 203-208 °C; UV-Vis (CHCl₃) λ_{max} 390 nm; IR (KBr): 3097, 2963, 1586, 1464, 1404, 1262; ¹H NMR (500 MHz, CDCl₃): δ (ppm) 7.85 (dd, *J* = 8.5, 2.0 Hz, 2H), 7.77-7.76 (m, 4H), 7.50 (d, *J* = 5 Hz, 2H), 7.14-7.12 (m, 2H), 6.90 (d, 2H), 3.87 (t, *J* = 7.5 Hz, 2H), 1.42-1.18 (m, 12H), 0.80 (t, *J* = 6.5 Hz, 3H); ¹³C-NMR (125 MHz, CDCl₃): δ (ppm) 188.9, 162.1, 159.6, 148.5, 145.4, 130.7, 129.2, 129.1, 128.7, 127.4, 127.2, 125.6, 124.6, 124.1, 123.7, 123.2, 117.7, 114.9, 114.3, 47.3, 30.7, 28.17, 25.7, 21.6, 13.0; MS: *m/z* 611 (*M*⁺), 612 (*M*+1); Elemental analysis calculated for C₃₂H₂₉N₅O₂S₃: C: 62.82, H: 4.78, N: 11.45; S: 15.72; Found C: 62.80, H: 4.76, N: 11.44, S: 15.71

3.5.2.10. Synthesis of 1,4-bis(5-(10-octyl-10H-phenothiazin-3-yl)-1,3,4-oxadiazol-2-yl)benzene (16)

This compound was prepared by a procedure similar to that of **7a**, except that terephthalohydrazide (194 mg, 1 mmol) is used in place of benzohydrazide and two equivalence of 10-octyl-10H-phenothiazine-3-carbaldehyde (678 mg, 2 mmol) is added then cyclization occurs on both sides to yield the product as orange solid.



Yield: 66%, mp: 155-160 °C; UV-Vis (CHCl₃) λ_{max} 394 nm; IR (KBr): 3045, 2893, 1555, 1412, 1380, 1212; ¹H NMR (500 MHz, CDCl₃): δ (ppm) 8.19 (s, 4H), 7.85 (d, $J = 8.5$ Hz, 2H), 7.76 (s, 2H), 7.11-7.05 (m, 4H), 6.90-6.80 (m, 6H), 3.81 (t, $J = 8.5$ Hz, 4H), 1.78-1.72 (m, 5H), 1.39-1.18 (m, 23H), 0.81-0.78 (m, 3H); ¹³C-NMR (125 MHz, CDCl₃): δ (ppm) 163.5, 162.3, 147.5, 142.9, 126.5, 126.3, 125.5, 124.6, 124.4, 122.7, 122.2, 116.3, 114.7, 114.2, 46.8, 30.7, 28.2, 25.8, 25.7, 21.6, 13.1; MS: m/z 832 (M^+), 833 ($M+1$); Elemental analysis calculated for C₅₀H₅₂N₆O₂S₂: C: 72.08, H: 6.29, N: 10.09, S: 7.70; Found C: 72.07, H: 6.27, N: 10.08, S: 7.69.

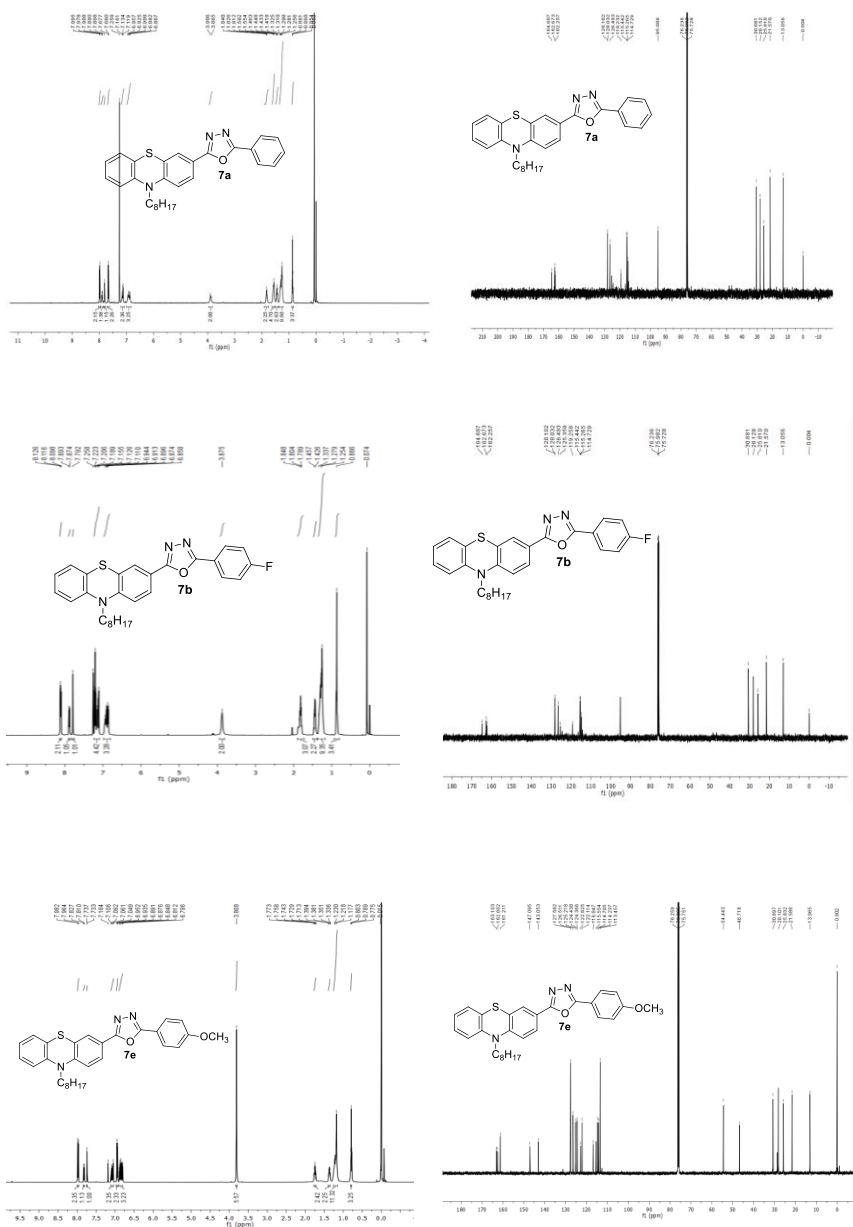
3.6. References

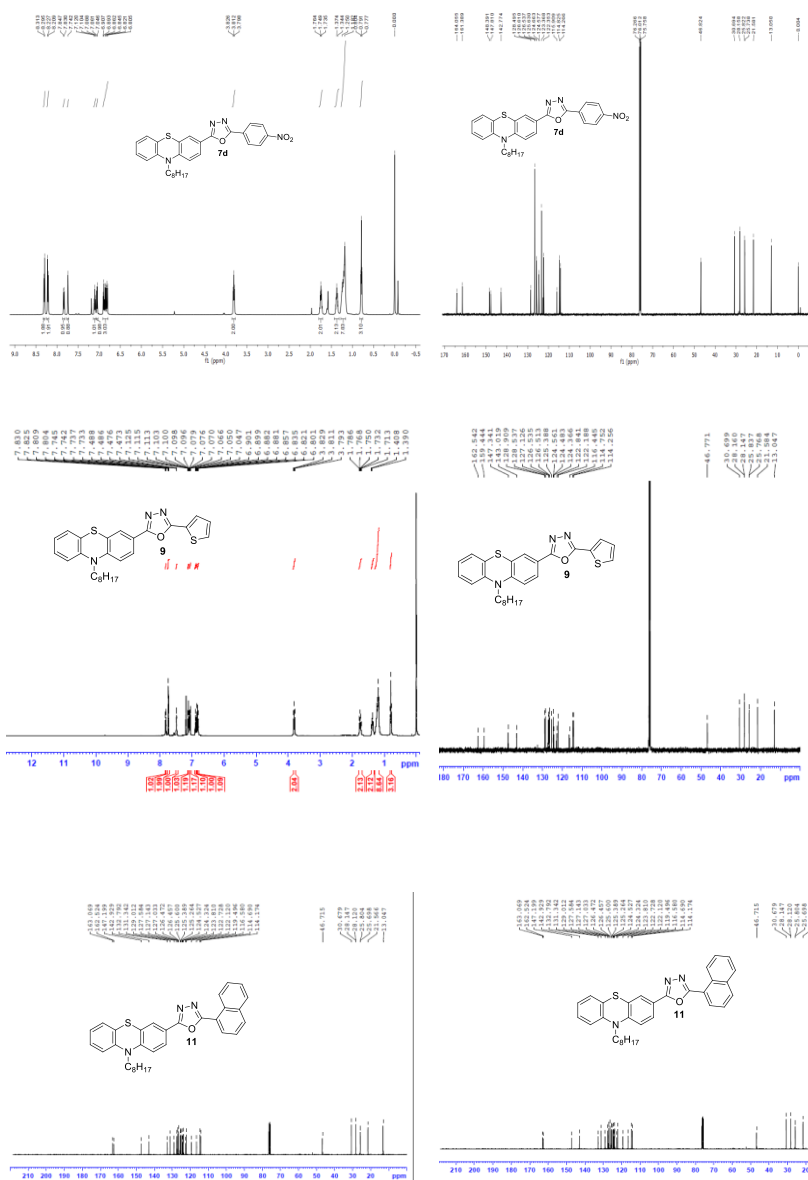
- (1) Garmire, E. *Opt. Express* **2013**, *21*, 30532.
- (2) Tang, C.; Zheng, Q.; Zhu, H.; Wang, L.; Chen, S.-C.; Ma, E.; Chen, X. *J. Mater. Chem. C* **2013**, *1*, 1771.
- (3) Dvornikov, A. S.; Walker, E.P.; Rentzepis, P. M. *J. Phys. Chem. A* **2009**, *113*, 13633.
- (4) Gindre, D.; Iliopoulos, K.; Krupka, O.; Champigny, E.; Morille, Y.; Sallé, M. *Opt. Lett.* **2013**, *38*, 4636.
- (5) Albota, M. *Science* **1998**, *281*, 1653.
- (6) Pawlicki, M.; Collins, H. A.; Denning, R. G.; Anderson, H. L. *Angew. Chem. Int. Ed.* **2009**, *48*, 3244.
- (7) Yang, C.; Zheng, M.; Li, Y. P.; Zhang, B. L.; Li, J. F.; Bu, L. Y.; Liu, W.; Sun, M. X.; Zhang, H. C.; Tao, Y.; Xue, S. F.; Yang, W. J. *J. Mater. Chem. A* **2013**, *1*, 5172.
- (8) Ando, M.; Kadono, K.; Haruta, M.; Sakaguchi, T. *Nature* **1995**, *374*, 625.
- (9) Fainman, Y.; Ma, J.; Lee, S. H. *Mater. Sci. Reports* **1993**, *9*, 53.
- (10) Hales, J. M.; Cozzuol, M.; Screen, T. E. O.; Anderson, H. L.; Perry, J. W. *Opt. Express* **2009**, *17*, 18478.
- (11) He, G. S.; Tan, L. S.; Zheng, Q.; Prasad, P. N. *Chem. Rev.* **2008**, *108*, 1245.

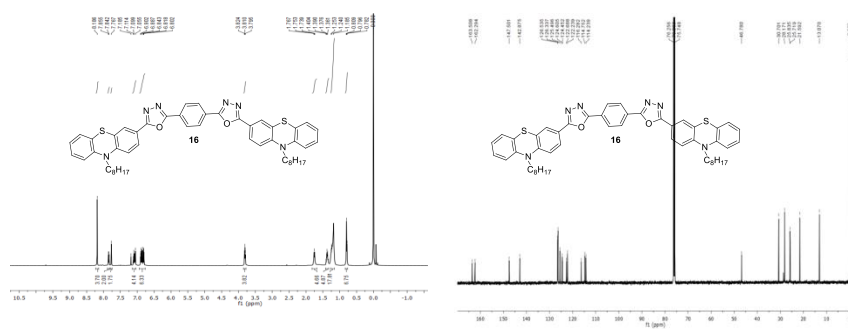
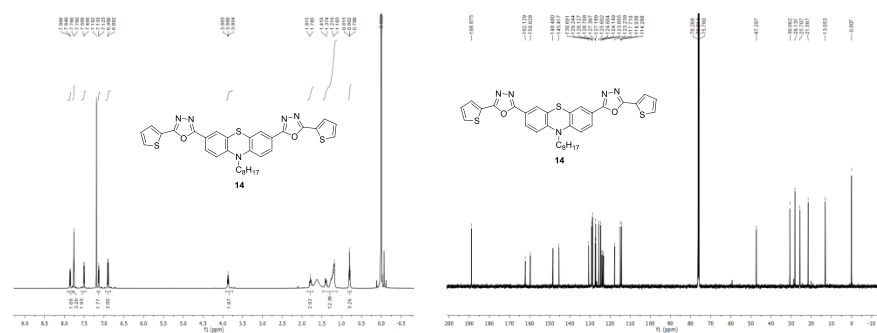
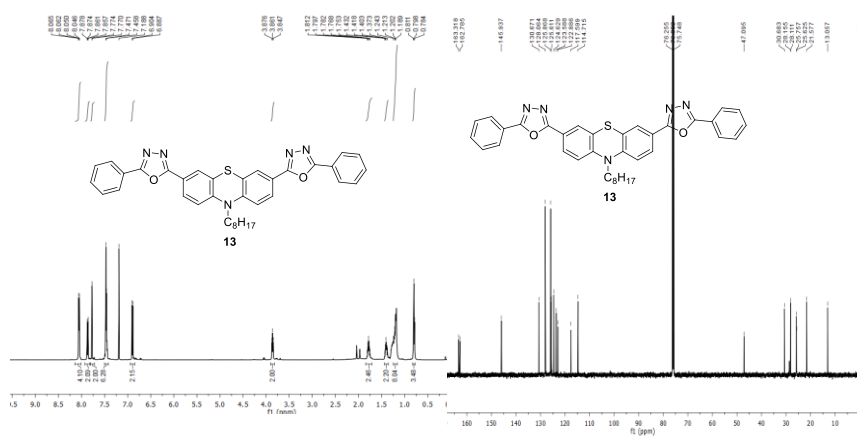
- (12) Gieseking, R. L.; Mukhopadhyay, S.; Risko, C.; Marder, S. R.; Brédas, J. L. *Adv. Mater.* **2014**, *26*, 68.
- (13) Ohkoshi, S.; Takano, S.; Imoto, K.; Yoshikiyo, M.; Namai, A.; Tokoro, H. *Nat. Photonics* **2013**, *8*, 65.
- (14) Changshui, H.; Li, Y.; Song, Y.; Li, Y.; Liu, H.; Zhu, D. *Adv. Mater.* **2010**, *22*, 3532.
- (15) Li, W.; Zhou, X.; Tian, W. Q.; Sun, X. *Phys. Chem. Chem. Phys.* **2013**, *15*, 1810.
- (16) Jiang, D.; Chen, S.; Xue, Z.; Li, Y.; Liu, H.; Yang, W.; Li, Y. *Dye. Pigment.* **2016**, *125*, 100.
- (17) Wang, C.; Jung, G.-Y.; Batsanov, A. S.; Bryce, M. R.; Petty, M. C. *J. Mater. Chem.* **2002**, *12*, 173.
- (18) Cha, S. W.; Choi, S. H.; Kim, K.; Jin, J. I. *J. Mater. Chem.* **2003**, *13*, 1900.
- (19) Schulz, B.; Bruma, M.; Brehmer, L. *Adv. Mater.* **1997**, *9*, 601.
- (20) Wong, M. Y.; Leung, L. M. *Dye. Pigment.* **2017**, *145*, 542.
- (21) Luo, J.-S.; Wan, Z.-Q.; Jia, C.-Y. *Chinese Chem. Lett.* **2016**, *27*, 1304.
- (22) Liu, F.; Wang, H.; Yang, Y.; Xu, H.; Yang, D.; Bo, S.; Liu, J.; Zhen, Z.; Liu, X.; Qiu, L. *Dye. Pigment.* **2015**, *114*, 196.
- (23) Aizawa, N.; Tsou, C. J.; Park, I. S.; Yasuda, T. *Polym. J.* **2017**, *49*, 197.
- (24) El-Shishtawy, R. M.; Al-Zahrani, F. A. M.; Afzal, S. M.; Razvi, M. A. N.; Al-amshany, Z. M.; Bakry, A. H.; Asiri, A. M. *RSC Adv.* **2016**, *6*, 91546.
- (25) Yu, W.; Huang, G.; Zhang, Y.; Liu, H.; Dong, L.; Yu, X.; Li, Y.; Chang, J. *J. Org. Chem.* **2013**, *78*, 10337.
- (26) Allen, M. W. *Measurement of Fluorescence Quantum Yields*. Technical note 52019, Thermo Fisher Scientific, Madison, WI, USA
- (27) Deshapande, N.; Pujar, G. H.; Sunagar, M. G.; Khazi, I. A. M. *Chemistryselect.* **2017**, *2*, 1793.
- (28) Deshapande, N.; Belavagi, N. S.; Sunagar, M. G.; Khazi, I. A. M. *RSC Adv.* **2015**, *5*, 86685.
- (29) Gaussian 09, Revision D.01, M. J. Frisch, G. W. Trucks, H. B. Schlegel, G. E. Scuseria, M. A. Robb, J. R. Cheeseman, G. Scalmani, V. Barone, B. Mennucci, G. A. Peterson, H. Nakatsuji, M. Caricato, X. Li, H. P. Hratchian, A. F. Izmaylov, J. Bloino, G. Zheng, J. L. Sonnenberg, M. Hada, M. Ehra, K. Toyota, R. Fukuda, J. Hasegawa, M. Ishida, T. Nakajima, Y. Honda, O. Kitao, H. Nakai, T. Vreven, J. A. Montgomery, Jr., J. E. Peralta, F. Ogliaro, M. Bearpark, J. J. Heyd, E. Brothers, K. N. Kudin, V. N. Staroverov, T. Keith, R. Kobayashi, J. Normand, K. Raghavachari, A. Rendell, J. C. Burant, S. S. Iyengar, J. Tomasi, M. Cossi, N. Raga, J. M. Millam, M. Klene, J. E. Knox, J. B. Cross, V. Bakken, C. Adamo, J. Jaramillo, R. Gomperts, R. E. Stratmann,

- O. Yazyev, A. J. Austin, R. Cammi, C. Pomelli, J. W. Ochterski, R. L. Martin, K. Morokuma, V. G. Zakrzewski, G. A. Voth, P. Salvador, J. J. Dannenberg, S. Dapprich, A. D. Daniels, O. Farkas, J. B. Foresman, J. V. Ortiz, J. Cioslowski, and D. J. Fox, *Gaussian, Inc.*, Wallingford CT, **2013**.
- (30) Fan, L.; Cui, R.; Jiang, L.; Zou, Y.; Li, Y.; Qian, D. *Dye. Pigment.* **2015**, *13*, 458.
- (31) Sheik-Bahae, M.; Said, A. A.; Wei, T. H.; Hagan, D. J.; Stryland, E. W. *IEEE J. Quantum Electron.* **1990**, *26*, 760.
- (32) Zhang, C.; Song, Y.; Xu, Y.; Fun, H.; Fang, G.; Wang, Y. *J. Chem. Soc. Dalton Trans.* **2000**, *16*, 2823.
- (33) El-Shishtawy, R. M.; Al-Zahrani, F. A. M.; Al-amshany, Z. M.; Asiri, A. M. *Sensors Actuators, B Chem.* **2017**, *240*, 288.
- (34) Zhang, J.; Xu, B.; Chen, J.; Wang, L.; Tian, W. *J. Phys. Chem. C* **2013**, *117*, 23117.

3.7. Appendix

¹H NMR and ¹³C NMR spectra of significant compounds





**SYNTHESIS AND EVALUATION OF
THIRD-ORDER NONLINEAR OPTICAL PROPERTIES
OF A FEW 1,3,4-OXADIAZOLE-CARBAZOLE
PUSH-PULL FLUOROPHORES**

4.1. Abstract

In continuation of our pursuit for ideal donor-acceptor systems for photonic applications, we designed and synthesized a second series of push-pull fluorophores with carbazole and 1,3,4-oxadiazole as donor and acceptor components respectively using simple iodine mediated oxidative cyclization of respective acyl hydrazones. Structural authenticity of all the compounds was confirmed by ^1H NMR, ^{13}C NMR and LC-MS analysis. These chromophores contain carbazole groups as electron donor (D) and electron deficient 1,3,4-oxadiazole as acceptor (A). Their photophysical properties were investigated by UV-Vis absorption, fluorescence spectroscopy and time resolved fluorescence measurements. Further, steady-state absorption and fluorescence measurements were carried out in solvents having different polarities to assess intramolecular charge-transfer nature of these fluorophores. These compounds exhibited large Stokes shifts indicating charge transfer nature of their excited states. The collective cyclic voltammetry and theoretical calculations were executed to demonstrate the structure-property relationship and ICT features of these fluorophores. Theoretical values are found to be well-matched with experimental results. Their thermal and morphological stabilities were checked by differential scanning calorimetry (DSC) and thermogravimetric analysis (TGA). Thermal studies revealed that all the molecules are thermally stable. The nonlinear optical properties of the D-A molecules were also studied using Q switched Z-scan technique with a 7 ns laser pulses at 532 nm. The molecules exhibited good third-order nonlinear absorption and optical power limiting property at this wavelength. The results confirmed that the fluorophores could play an important role in organic electronics and photonics applications.

4.2. Introduction

Third-order nonlinear optical materials have received remarkable attention by the research community due to their wide range of optoelectronic and photonic applications.¹⁻¹³ Among these, organic push-pull molecules have strong π electron delocalisation which in turn intensifies their third-order nonlinear optical properties.

In pursuit of new NLO materials, we used the 1,3,4-oxadiazole based push-pull system for our study. 1,3,4-Oxadiazoles are attractive framework in the area of organic electronics due to the excellent photophysical properties and electron deficient nature.¹⁴⁻¹⁷ In comparison with NLO activity studies on 1,3,4-oxadiazole based D-A type polymers the push-pull molecules are less explored.

Among the heterocyclic systems, carbazole is one of the effective electron donors due to the presence of central pyrrole ring. In addition, functionalization of carbazole at different positions is easy for further tuning of the system.^{18,19} Owing to the electron transporting ability of carbazole, it is widely employed in DSSCs, OLEDs and in third-order nonlinear optical materials.²⁰⁻²⁸ Only very few reports are available on molecules and polymers incorporating both 1,3,4-oxadiazole and carbazole for various applications in the field of organic electronics.²⁹⁻³⁶

We have designed and synthesized a library of 1,3,4-oxadiazole-carbazole push-pull fluorophores in which carbazole act as electron donating moiety and 1,3,4-oxadiazole core as accepting template (Chart 4.1). Here substituents attached to oxadiazole core were responsible for

the modification of photophysical, electrochemical, thermal and third-order nonlinear optical properties of the systems.

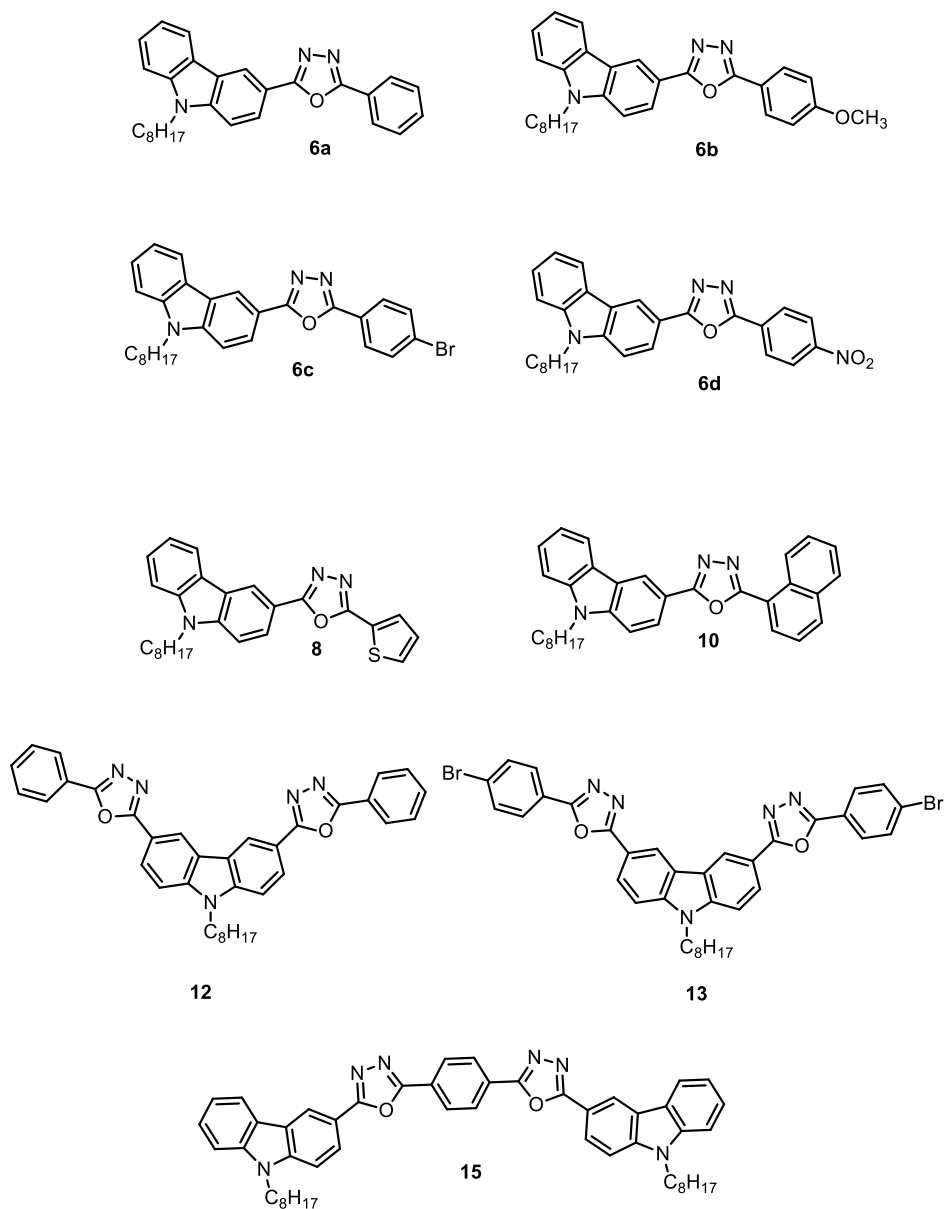
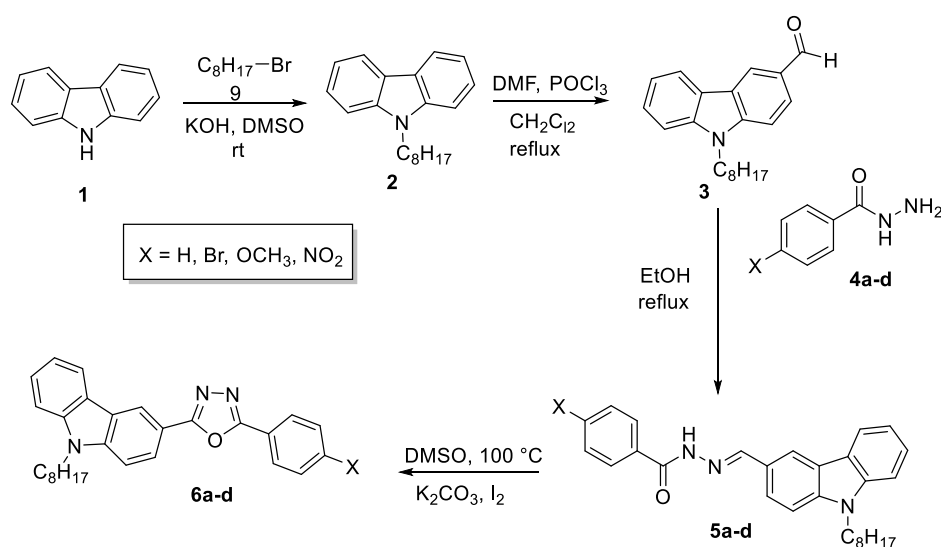


Chart. 4.1. Selected push-pull targets

4.3. Results and Discussion

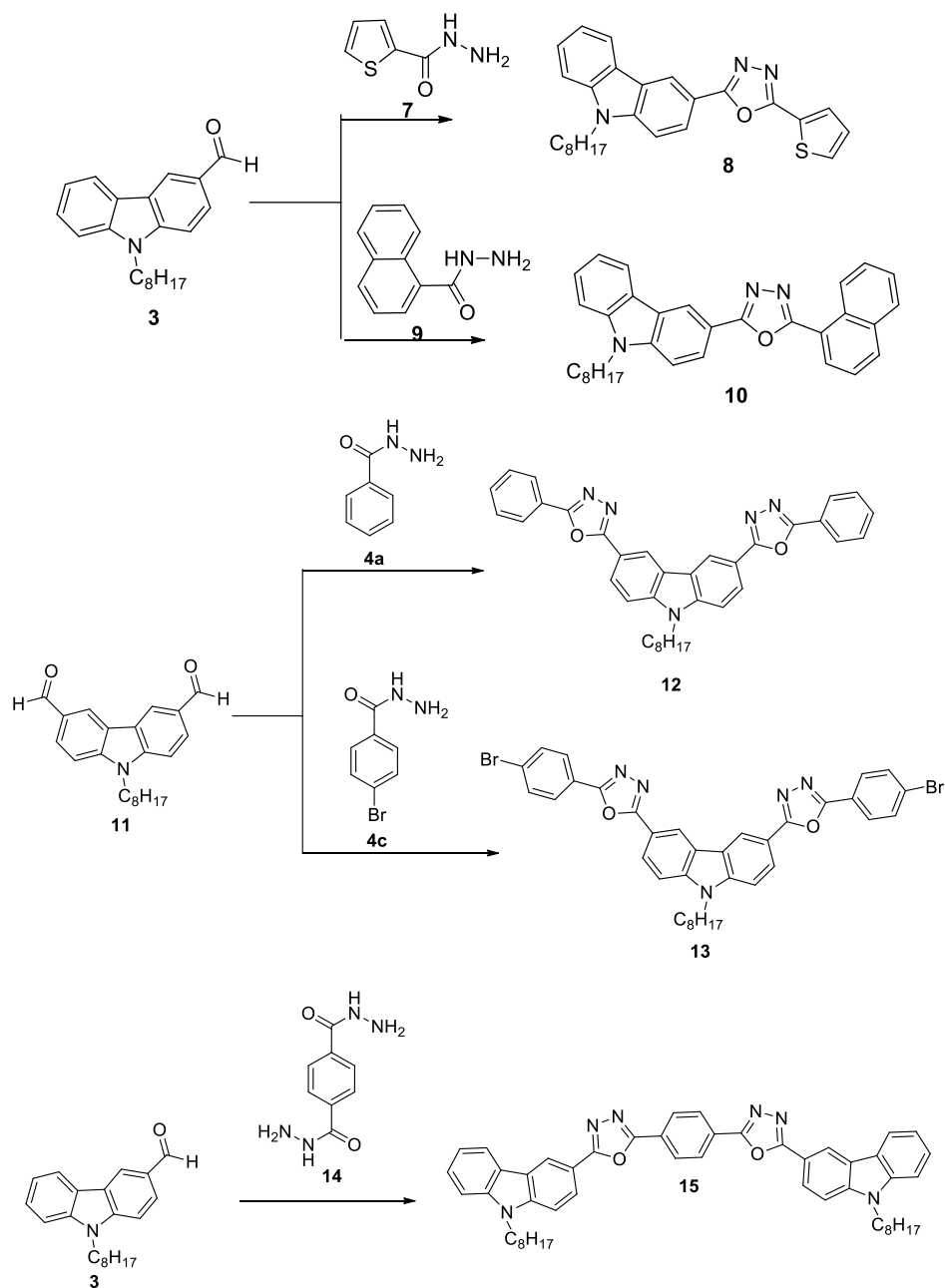
4.3.1. Synthesis and characterization

Iodine mediated oxidative cyclization was employed for the synthesis of final compounds as shown in Scheme 4.1 for **6a-d**.³⁷ These compounds were characterized by ¹H NMR, ¹³C NMR, IR spectroscopy and mass spectrometry.



Scheme 4.1. Synthesis of **6a-d**

Exploiting the procedure outlined in Scheme 4.1, compounds **8**, **10**, **12**, **13** and **15** were prepared by changing the aryl aldehyde and aroylhydrazine substrates as shown in Scheme 4.2.



Scheme 4.2. Synthesis of **8**, **10**, **12**, **13** and **15**

Compounds **6a-d** are simple bipolar molecules having carbazole-(5-aryl)oxadiazole framework. We have synthesized fluorophores with

both electron donor and electron acceptor groups as para substituents on the 5-aryl substituent on oxadiazole core. Compounds **8** and **10** have D- π -D type construction having electron rich thiophene and naphthalene rings respectively in place of phenyl group. Fluorophores **12** is an expanded molecule with D-A-D-A-D type building blocks and **15** is having a D-A- π -A-D type framework. Compound **13** is a potential monomer suitable for further manipulation.

4.3.2. Photophysical Properties

4.3.2.1. UV-Vis Absorption and Photoluminescence (PL) spectra

All the molecules are soluble in common organic solvents such as toluene, dichloromethane, dimethylformamide and dimethyl sulfoxide. Fig. 4.1 shows the normalized UV-Vis absorption spectra of the fluorophores in CHCl₃ (HPLC grade). The maximum absorption wavelengths (λ_{max}) of compounds **6a**, **6d**, **8**, **10**, **12**, and **15** are 328, 371, 331, 340, 348 and 348 nm respectively. The bands observed at shorter wavelengths relates to π - π^* transitions of electron donor moieties whereas the less intense absorption band at longer wavelengths (320-371 nm) can be assigned to intramolecular charge transfer transitions (ICT) in each fluorophores. Depending on the conjugation lengths and the electronic effects of the attached molecule, distinct redshift was observed for ICT absorption maxima. In the sequence, fluorophore **6a** showed lowest λ_{max} of 328 nm and **6d** exhibited highest λ_{max} of 371 nm (Table 4.1). **6d** is a distinctive D- π -A framework having strongly electron withdrawing nitro group.

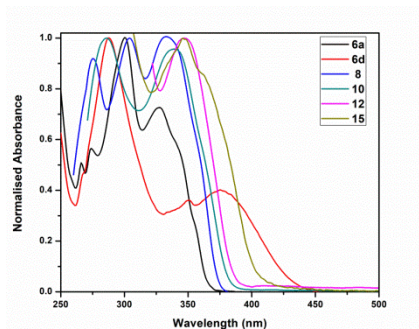


Fig. 4.1. Normalized UV-Vis absorption spectra of compounds in CHCl_3 at room temperature

Normalized emission spectra of all the compounds in chloroform at room temperature are shown in Fig. 4.2. The emission maxima of **6a**, **6d**, **8**, **10**, **12** and **15** were 383, 440, 397, 414, 387 and 434 nm respectively. In the series, maximum and minimum emission wavelengths are shown by derivatives **6d** and **6a** respectively. The Stokes shift value of compounds is in the range of $2896\text{--}5694\text{ cm}^{-1}$ (Table 4.1). Charge transfer nature of the emissive excited state was confirmed by these high Stokes shift values.

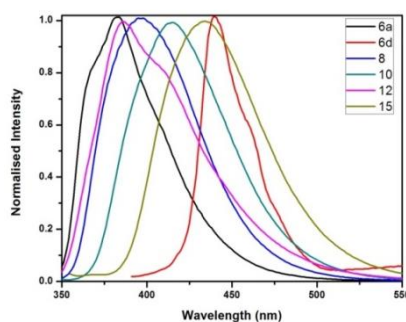


Fig. 4.2. Normalized emission spectra of compounds in CHCl_3 at room temperature

4.3.2.2. Quantum Yield (ϕ) measurements

Fluorescence quantum yields (ϕ) of all fluorophores were measured in chloroform at room temperature by comparison with quinine sulfate of known quantum yield (ϕ) using Equation 4.1.³⁸

$$\Phi = \phi_R \frac{I}{A} \frac{n_{\text{solvent}}^2}{n_R^2} \frac{A_R}{I_R} \quad (4.1)$$

Where I is the integrated intensity, A is the optical density, n is the refractive index and R stands for reference dye with known quantum yield. The calculated quantum yields of all the fluorophores are in the range of 0.32 to 0.61 (Table 4.1).

Table 4.1. Summary of absorption and emission profiles of the oxadiazole-carbazole fluorophores

Compound	Absorption $\lambda_{\text{max}}^{\text{abs}}$ (log ϵ) (nm)	Emission $\lambda_{\text{max}}^{\text{emi}}$ (nm)	Stokes Shift (cm^{-1})	Quantum Yield
6a	328 (3.95)	383	4378	0.42
6d	371 (3.75)	440	4299	0.35
8	331 (4.08)	397	5023	0.53
10	340 (4.32)	414	5257	0.61
12	348 (3.30)	387	2896	0.32
15	348 (4.20)	434	5694	0.60

4.3.2.3. Optical bandgap calculations

Optical bandgap (E_g^{opt}) values were estimated from the onset of the low energy side of the absorption spectra (λ_{onset} , solution) to the baseline according to Equation 4.2 and are summarized in Table 4.2. Optical bandgap of the molecules is in the range of 2.30-3.40 eV.

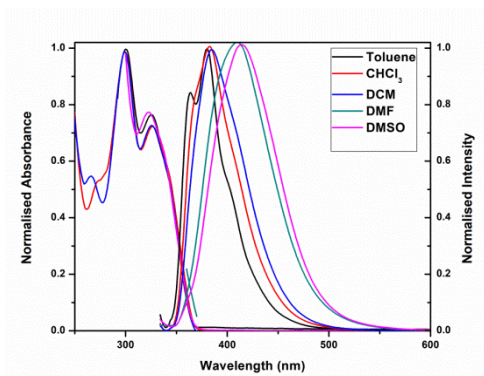
$$E_g^{opt} = 1240/\lambda_{onset} \quad (4.2)$$

Table 4.2. Optical bandgaps of fluorophores

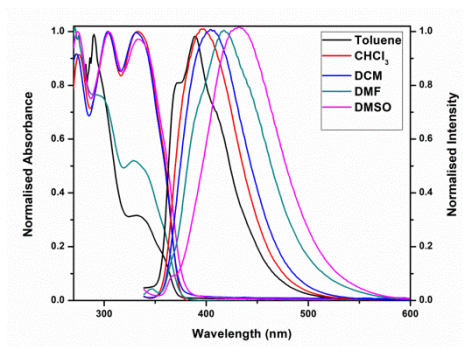
Compound	E_g^{opt} (eV)
6a	3.40 (364)
6d	2.86 (434)
8	3.30 (376)
10	2.30 (376)
15	3.10 (400)

4.3.2.4. Solvatochromic behaviour

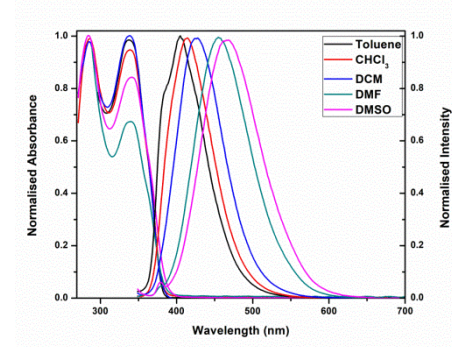
To understand the nature of intramolecular charge transfer characteristics (ICT) of the fluorophores, solvatochromic studies were carried out and the results are summarized in Table 4.3 and Fig. 4.3. Solvent effects were monitored using common solvents like toluene, chloroform, dichloromethane, dimethylformamide and dimethyl sulfoxide. Depending upon solvent polarity, the absorption and emission profiles of the compounds are shifted due to interaction of fluorophores with solvents. Results showed that all the molecules exhibited a slight redshift of the absorption maximum on moving from toluene to DMF but a slight variation for the absorption maxima in DMSO is observed. Redshift in emission maxima with respect to increasing solvent polarity was more pronounced suggesting polar nature of the excited state in comparison with the ground state. Compound **6a** and **15** behaved anomalously.



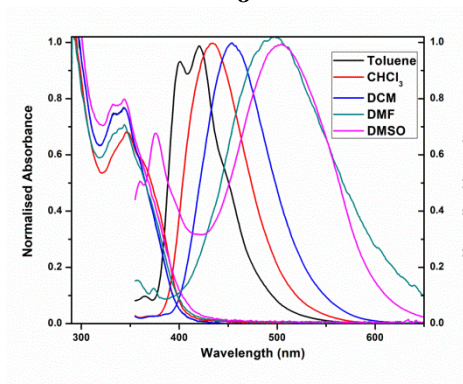
6a



8



10



15

Fig. 4.3. Normalized absorption and emission spectra of compounds in general solvents

Table 4.3. Summary of optical properties of fluorophores

		6a			8		
Solvents	Dielectric Constant	Absorption λ_{max}^{abs} (nm) (log ϵ)	Emission λ_{max}^{em} (nm)	Stokes Shift (cm^{-1})	Absorption λ_{max}^{abs} (nm) (log ϵ)	Emission λ_{max}^{em} (nm)	Stokes Shift (cm^{-1})
Ph-CH ₃	2.38	326 (3.85)	380	4359	334 (3.85)	390	4299
CHCl ₃	4.81	328 (3.95)	383	4378	331 (4.08)	397	5022
DCM	9.08	328 (4.37)	384	4446	332 (4.62)	406	5489
DMF	38.25	329 (3.83)	410	6005	333 (3.90)	418	6107
DMSO	47.00	323 (3.50)	415	6863	334 (4.03)	432	6792

		10			15		
Solvents	Dielectric Constant	Absorption λ_{max}^{abs} (nm) (log ϵ)	Emission λ_{max}^{em} (nm)	Stokes Shift (cm^{-1})	Absorption λ_{max}^{abs} (nm) (log ϵ)	Emission λ_{max}^{em} (nm)	Stokes Shift (cm^{-1})
Ph-CH ₃	2.38	338 (4.29)	405	4894	344 (3.91)	420	5260
CHCl ₃	4.81	340 (4.32)	414	5257	348 (4.20)	434	5694
DCM	9.08	340 (4.35)	426	5938	347 (4.33)	454	6792
DMF	38.25	340 (4.40)	456	7481	345 (3.80)	497	8864
DMSO	47.00	341 (4.10)	467	7912	345 (3.55)	504	9144

4.3.2.5. Time Resolved Fluorescence Decay

The fluorescence decay nature of selected fluorophores was monitored in toluene and DMF. Fig. 4.4(a,b) shows the time resolved fluorescence decay profiles of fluorophores. The decay experiments were carried out at an excitation wavelength of 340 nm and the decays were scrutinized with respect to corresponding emission maxima. The fluorescence lifetimes are observed to be in nanosecond time scales. Compared to 1,3,4-oxadiazole-phenothiazine fluorophores described in Chapter 3, 1,3,4-oxadiazole-carbazole fluorophores showed complex decay behaviour. Such multiexponential emission decays are reported in literature.³⁹ The lifetime values are summarized in Table 4.5.

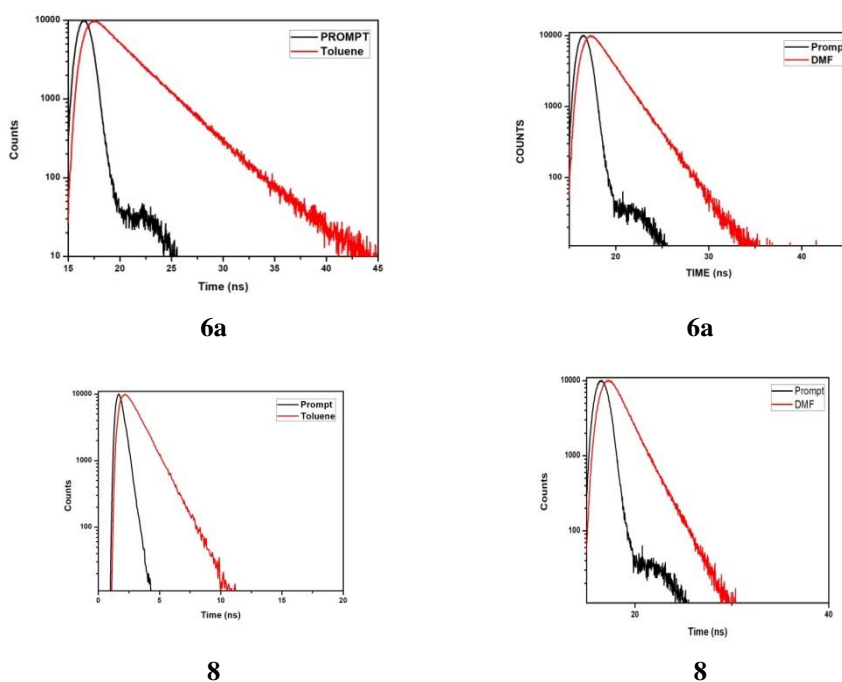


Fig. 4.4a. Fluorescence lifetime decay curves of fluorophores **6a, 8** in toluene and DMF

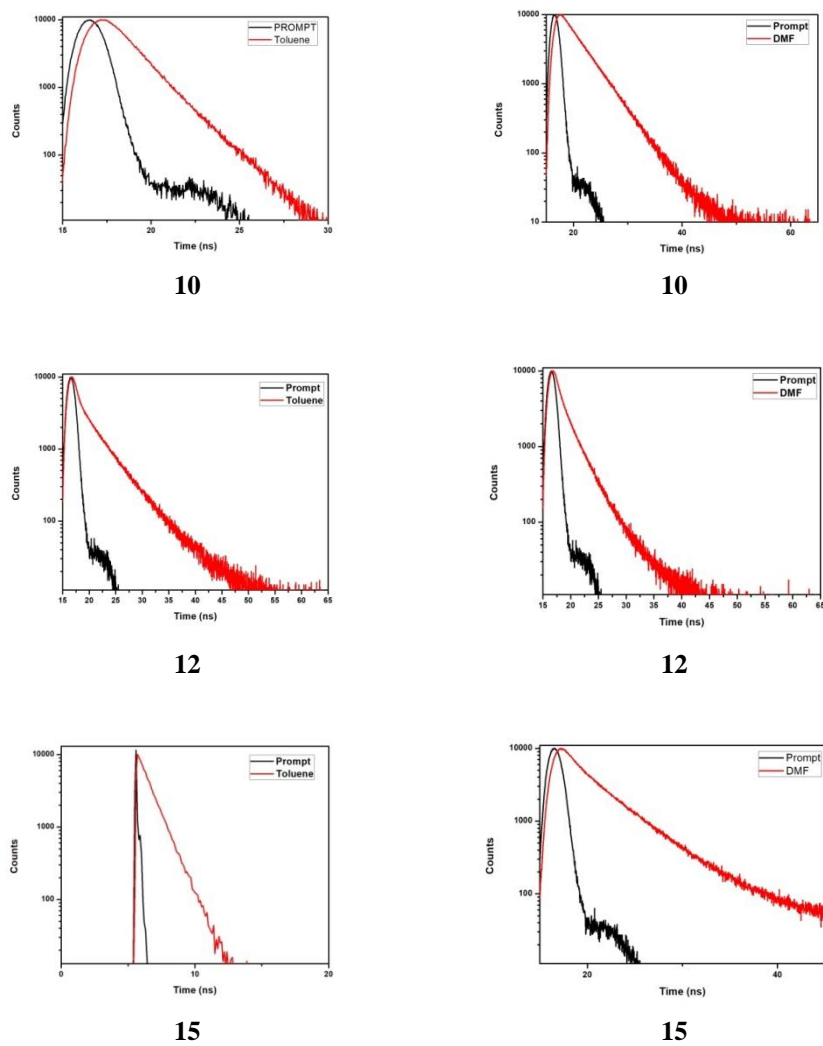


Fig. 4.4b. Fluorescence lifetime decay curves of fluorophores **10**, **12**, **15** in toluene and DMF

Table 4.5. Fluorescence lifetime of fluorophores

Compound	Toluene (ns) τ	DMF (ns) τ
6a	τ_1 - 2.35 (26.21%)	2.30
	τ_2 - 3.76 (73.79%)	
8	1.19	1.38
10	τ_1 - 1.20 (53.02%)	3.81
	τ_2 - 1.79 (46.98%)	
12	τ_1 - 2.29 (22.98%)	τ_1 - 2.01 (48.43%)
	τ_2 - 5.13 (42.25%)	τ_2 - 4.86 (14.34%)
	τ_3 - 0.08 (34.77%)	τ_3 - 0.07 (37.23%)
15	1.04	τ_1 - 2.21 (24.64%)
		τ_2 - 4.66 (64.64%)
		τ_3 - 0.51 (10.73%)

4.3.3. Electrochemical Properties

Using cyclic voltammetry (CV), we have calculated HOMO-LUMO energy levels of these D-A molecules. CV was done in a three-electrode cell with Pt disc as working electrode, Ag/AgCl as reference electrode and Pt wire as auxiliary electrode with a scan rate of 100 mV/s using 0.1 M *n*Bu₄NPF₆ as supporting electrolyte and ferrocene as the internal standard in dry dichloromethane. Cyclic voltammogram of the compounds are shown in Fig. 4.5. HOMO and LUMO energy levels were calculated according to the Equations 4.3 and 4.4 respectively and summarized in Table 4.6.⁴⁰

$$\text{HOMO} = - [E_{ox}^{onset} + 4.44] \text{ (eV)} \quad (4.3)$$

$$\text{LUMO} = - [\text{HOMO} + E_g^{opt}] \text{ (eV)} \quad (4.4)$$

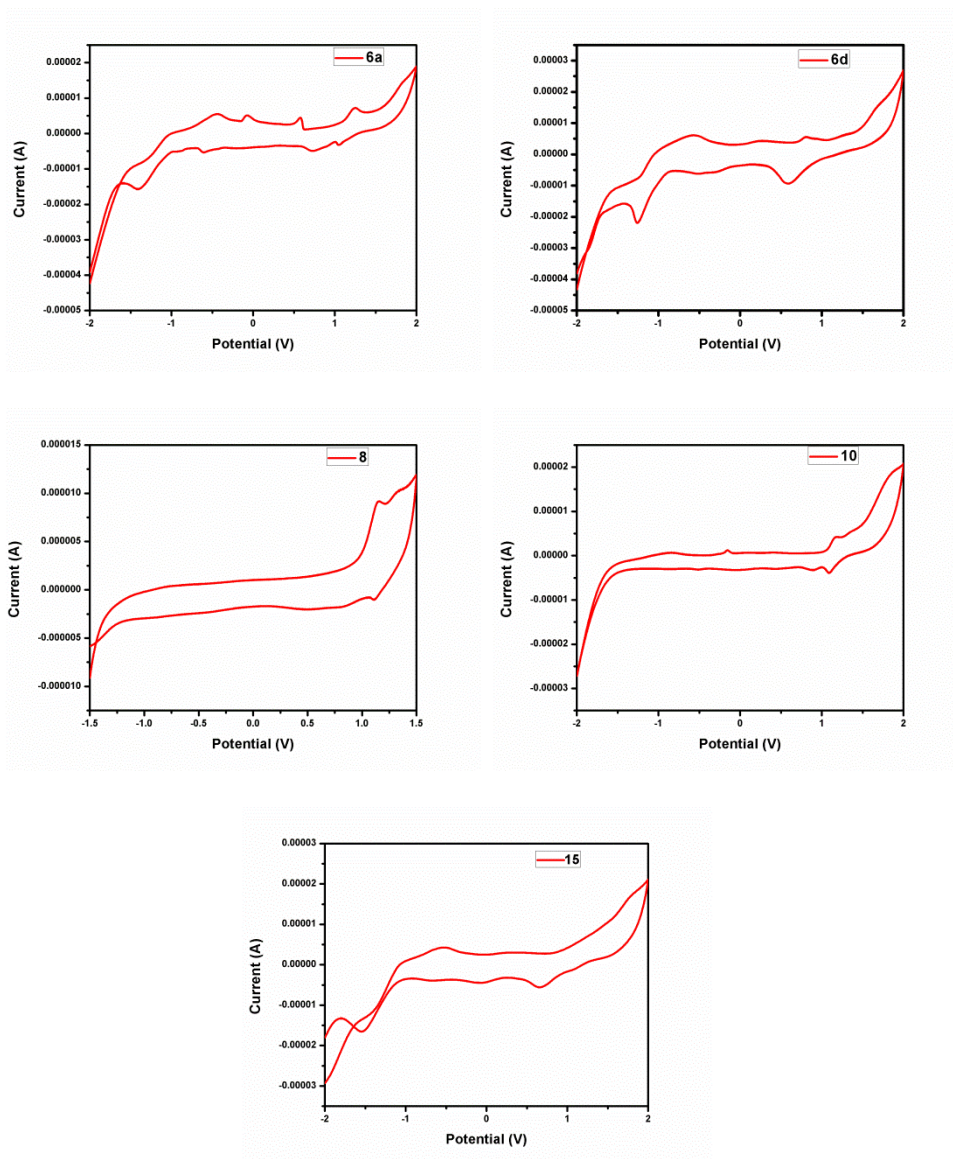


Fig. 4.5. Cyclic voltammogram of compounds **6a**, **6d**, **8**, **10** and **15**

Table 4.6. Electrochemical properties of compounds

Compound	E_{onset}^{ox} (V)	E_{onset}^{ox} vs E_{Foc}/V	HOMO (eV)	LUMO (eV)	E_g^{EC} (eV)
6a	0.53	0.75	-5.19	-1.79	3.40
6d	0.69	0.91	-5.35	-2.49	2.86
8	0.98	1.20	-5.64	-2.34	3.30
10	1.06	1.28	-5.72	-3.00	2.72
15	0.53	0.60	-5.04	-1.94	3.10

$E_{FOC} = 0.22$ V vs Ag/ AgCl.

4.3.4. Theoretical studies

To determine the geometry and HOMO-LUMO energy levels of the fluorophores, DFT calculations were implemented using GAUSSIAN 09 quantum chemistry package and B3LYP exchange-correlation functional.⁴¹ The ground state optimized geometry, HOMO and LUMO are shown in Fig. 4.6(a,b) From the figure, it is clear that the electron clouds of HOMO energy levels are mainly placed on carbazole fragment, and this is due to the strong electron donating capability of carbazole moiety. Moreover LUMO levels are concentrated on oxadiazole framework, which suggest the strong the electron accepting potential of oxadiazoles. HOMO and LUMO mapping clearly portrays the charge separation in the fluorophores signifying strong intramolecular charge transfer property. The theoretically calculated HOMO and LUMO values are in the range of (-5.22 to -6.30 eV) and (-1.56 to -2.88 eV) respectively. As in the case of 1,3,4-oxadiazole-phenothiazine fluorophores, here also nitro derivative (**6d**) exhibited lowest bandgap (3.33 eV) and which further leads to the substantial bathochromic shift in absorption spectrum. The energy level diagram of the frontier orbitals are shown in Fig. 4.7.

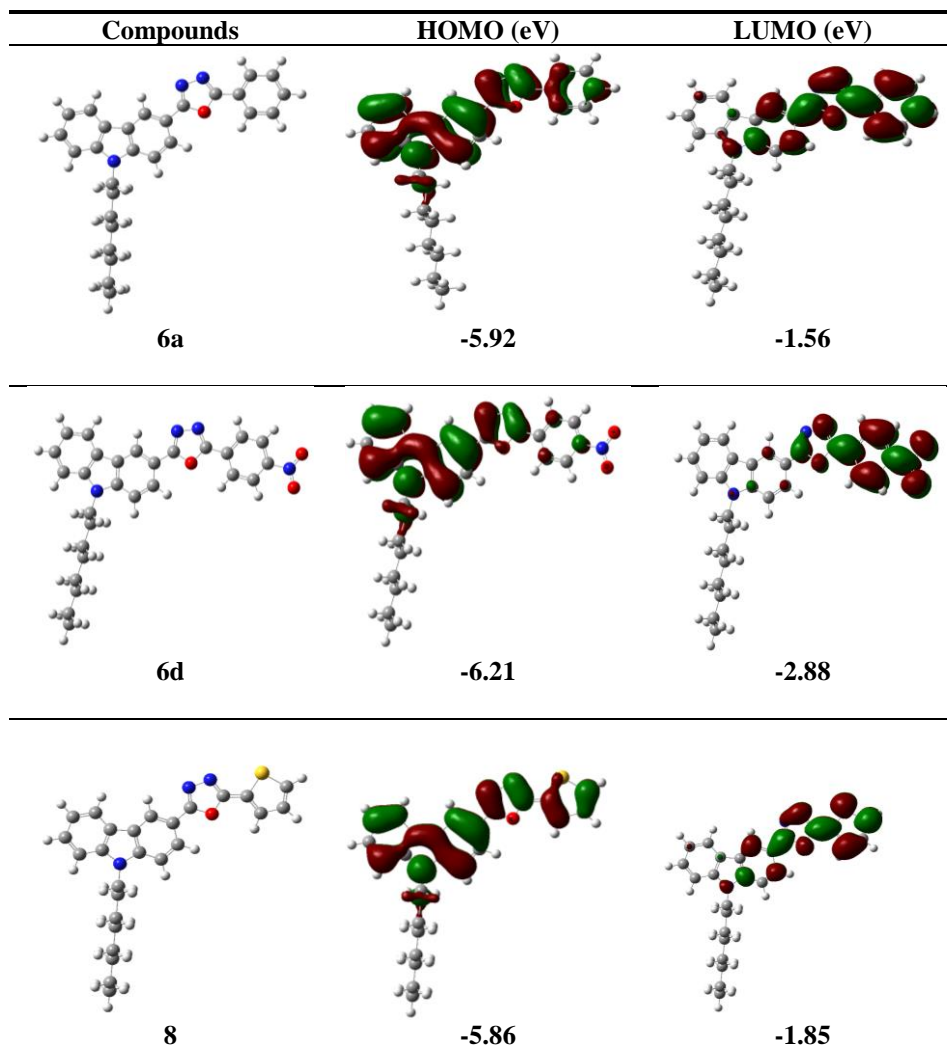


Fig. 4.6a. HOMO and LUMO levels and optimized molecular structures of fluorophores **6a**, **6d**, **8**

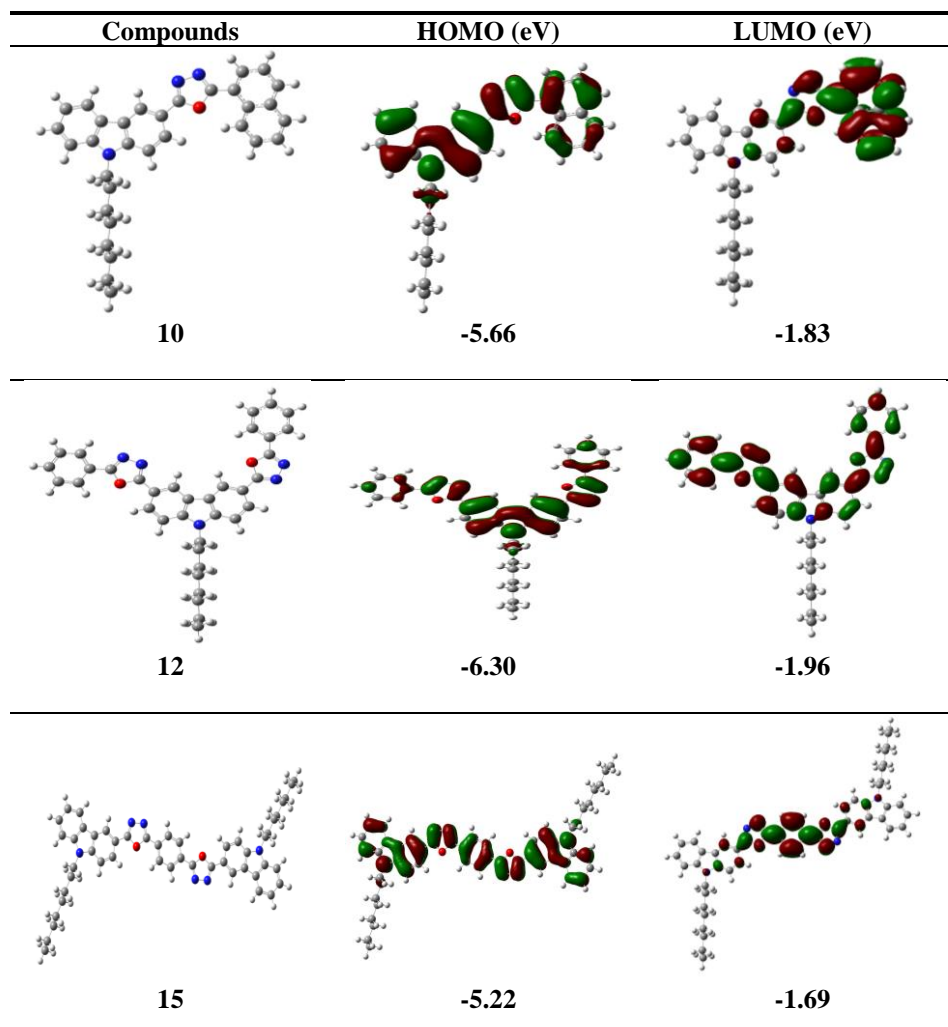


Fig. 4.6b. HOMO and LUMO levels and optimized molecular structures of fluorophores 10, 12, 15

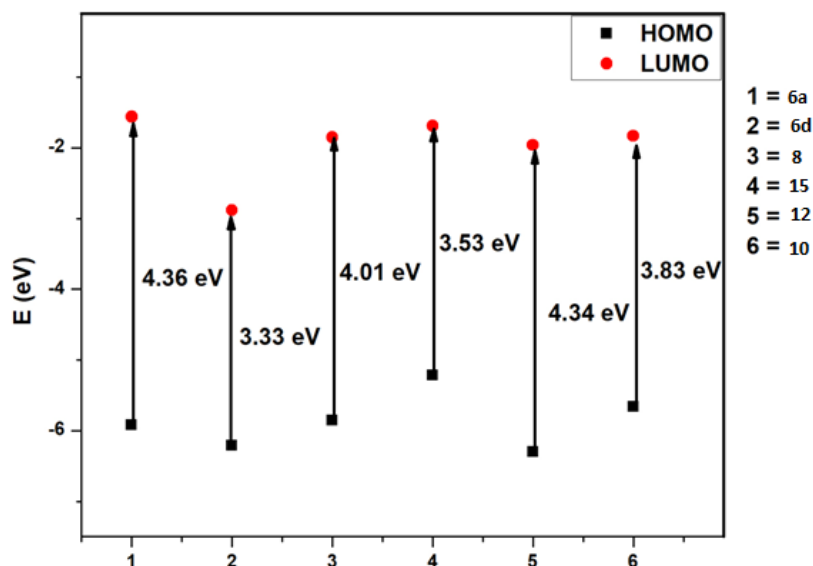


Fig. 4.7. Energy diagram of the frontier orbitals for **6a-15** calculated from DFT

4.3.5. XRD Characterization

Powder XRD pattern of the representative compounds showed both sharp and broad peaks signifying their semi-crystalline nature. As shown in Fig 4.8, in each fluorophores a diffraction peak at 2θ values 4-5 were observed, which indicate that the long alkyl chain effectively disrupt the approach of conjugated backbone. Broader and less intense diffraction peaks around 2θ values 20-25 is attributed to the second order reflection.⁴² This orderly pattern is favourable for the effective charge transportation in the entire molecular framework.

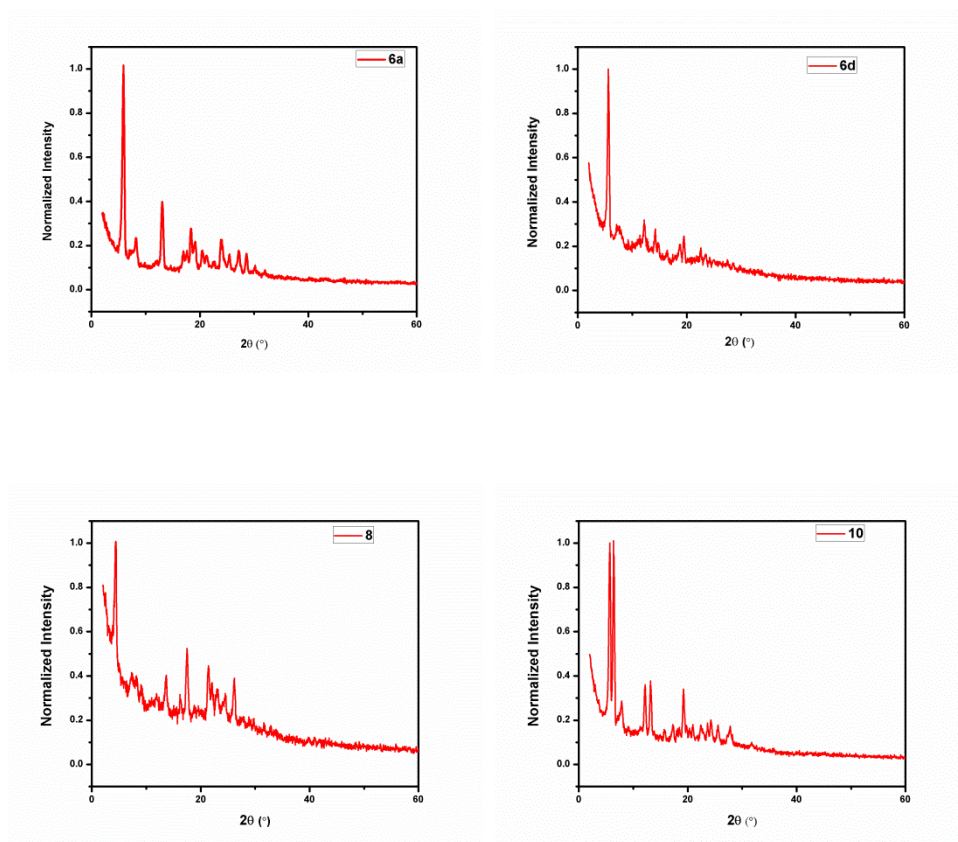


Fig. 4.8. Powder XRD patterns of the fluorophores **6a**, **6d**, **8** and **10**

4.3.6. Thermal Properties

The thermal properties of the representative compounds were monitored by differential scanning calorimetry (DSC) and thermal gravimetric analysis (TGA). The results are shown in Fig. 4.9 and 4.10 and are listed in Table 4.7. The phase transition characteristics of the compounds **6a**, **6d**, **8** and **10** were examined using DSC and it revealed that the compounds are crystalline and its crystallisation temperatures were observed at 108, 184 and 163 °C for **6a**, **6d** and **8** respectively. DSC

curve also showed melting points in the range of 119-155 °C. The TGA results confirmed that the fluorophores **6a**, **6d** and **8** are thermally stable with 5% weight loss in the range of 303-323 °C.

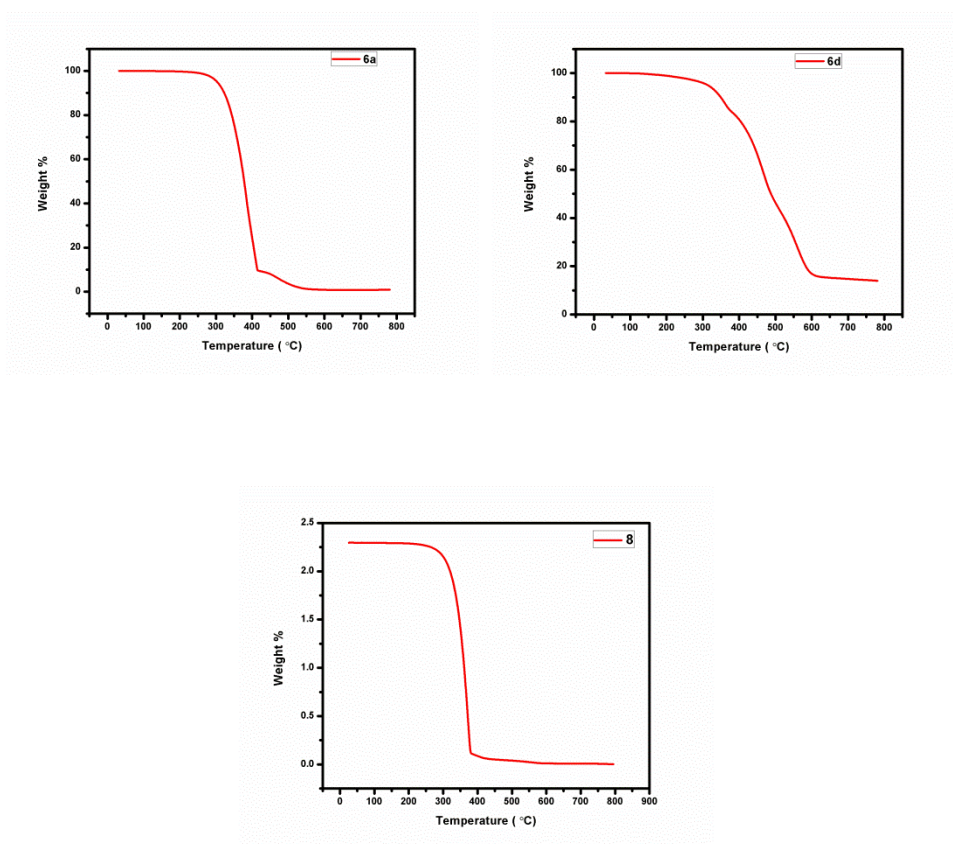


Fig. 4.9. TGA Curves of **6a**, **6d** and **8**

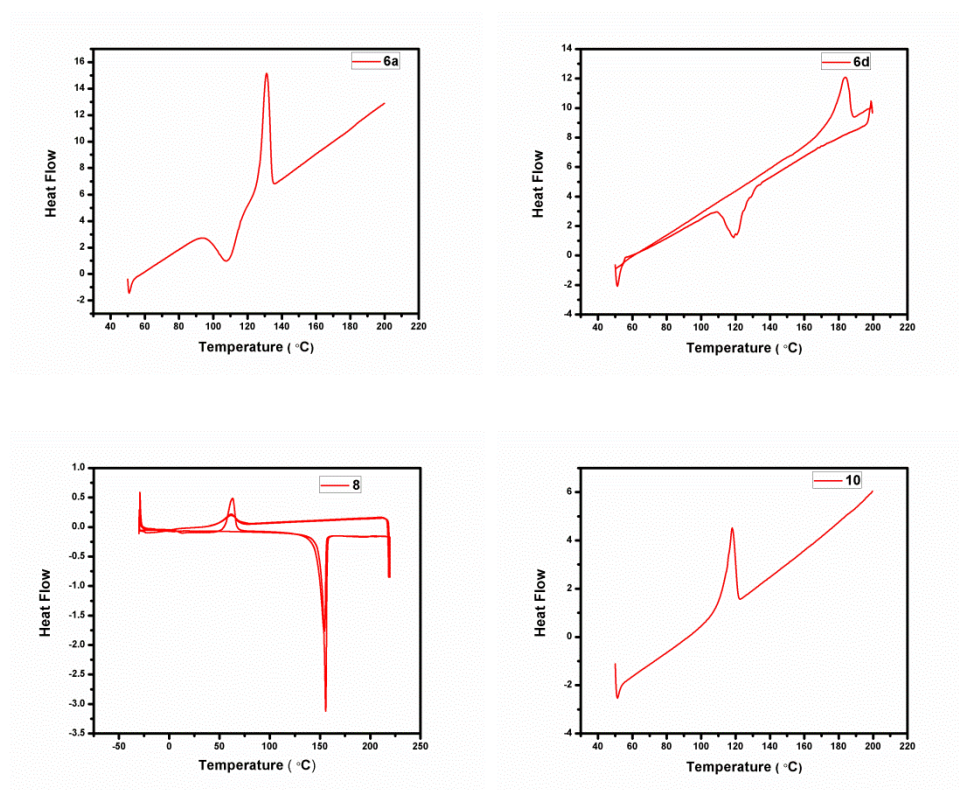


Fig. 4.10. DSC traces of **6a**, **6d**, **8** and **10**

Table 4.7. Thermal properties of selected fluorophores

Compounds	Melting point T_m (°C)	Crystallisation temperature T_c (°C)	Decomposition temperature (°C)
6a	131	108	303.36
6d	119	184	313.71
8	155	63	323.16
10	119	-	-

4.3.7. Nonlinear Optical Properties

The third order nonlinear optical properties of fluorophores were probed using Z-scan technique. Open aperture (OA) Z-scan traces of molecules **6a**, **6d**, **8**, **10**, **12** and **15** in dilute CHCl_3 are shown in Fig.

4.11(a,b,c). The solid curves in the Fig. 4.11(a,b,c) are theoretical fit to the experimental data, similar to 1,3,4-oxadiazole-phenothiazine fluorophores here also two photon absorption (TPA) is the mechanism involved in the nonlinear absorption process.

Using open aperture Z-scan configuration, the NLO absorption coefficients of **6a**, **6d**, **8**, **10**, **12** and **15** were calculated using Equation 4.5.⁴³ All the studied fluorophores showed reverse saturable absorption (RSA) with a positive absorption coefficient.

$$T(z) = \frac{c}{q_0\sqrt{\pi}} \int_{-\infty}^{\infty} \ln(1 + q_0 e^{-t^2}) dt \quad (4.5)$$

Where $q_0(z, r, t) = \beta I_0(t) L_{eff}$ and $L_{eff} = (1 - e^{-\alpha l})/\alpha$ are the effective thickness with the linear absorption coefficient, α and I_0 is the irradiance at focus. The imaginary part of the third-order susceptibility, $\text{Im } \chi^{(3)} = \frac{n_0^2 c^2 \beta}{240 \omega \pi^2}$ where n_0 is the linear refractive index of compounds, c is the velocity of light under vacuum and ω is the angular frequency of radiation used.

The nonlinear absorption coefficient (β) and imaginary part of nonlinear susceptibility ($\text{Im } \chi^{(3)}$) are calculated and summarized in Table 4.8. Results obtained in NLO revealed that fluorophores exhibited good nonlinear characteristics, which indicates the π electron delocalization and polarizability in the molecules. In the series, **15** showed highest nonlinear responses with a β value of 2.63×10^{-10} m/W and $\text{Im } \chi^{(3)}$ is 8.88×10^{-12} . Similar to nonlinear optical properties of phenothiazine attached molecules, here also compound **15** is a highly expanded

molecule with D-A- π -A-D architecture, large electronic delocalisation occurs from the terminal carbazole moiety to oxadiazole.

The optical limiting threshold values of all the fluorophores **6a**, **6d**, **8**, **10**, **12** and **15** are investigated and summarized in Table 4.8.

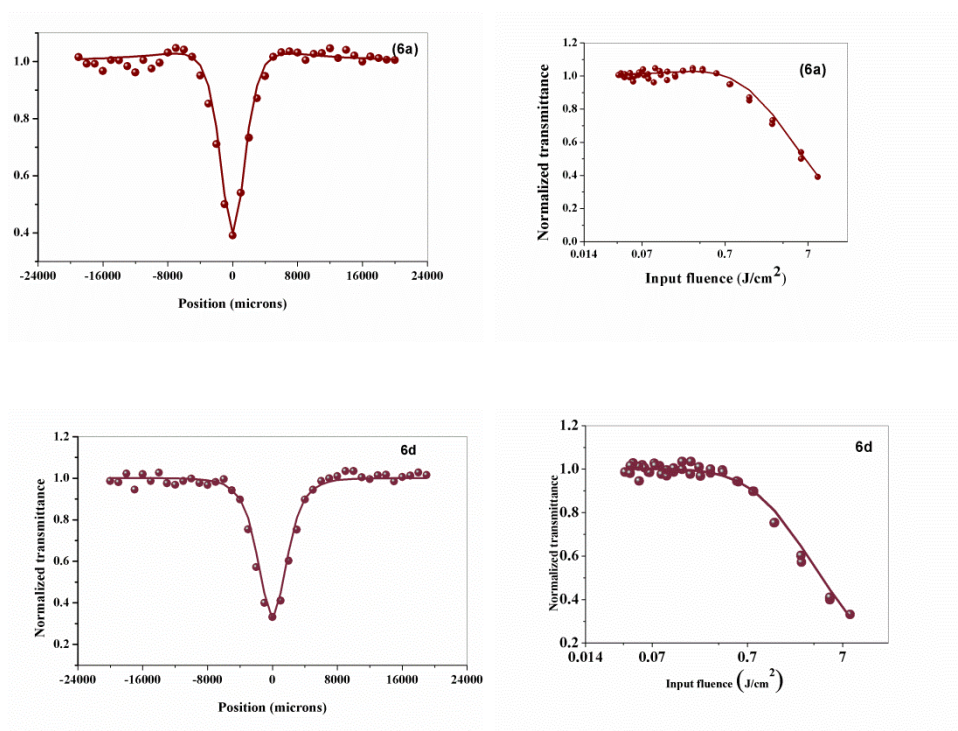


Fig. 4.11a. Normalized open aperture and optical limiting curves of **6a** and **6d**

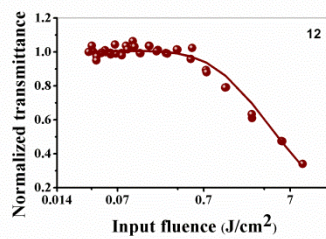
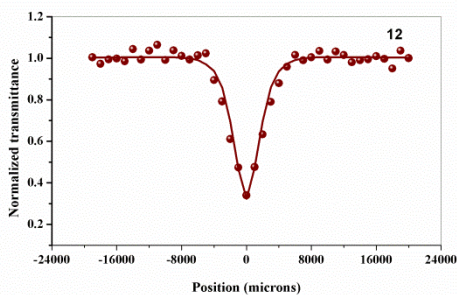
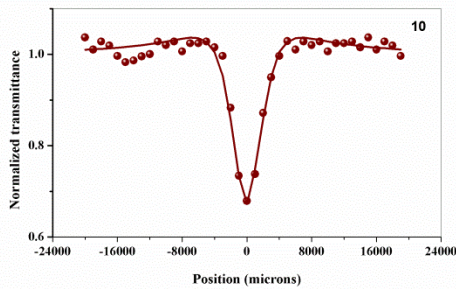
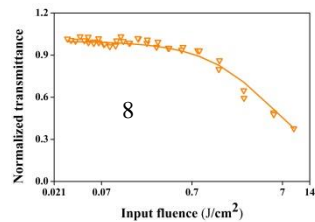
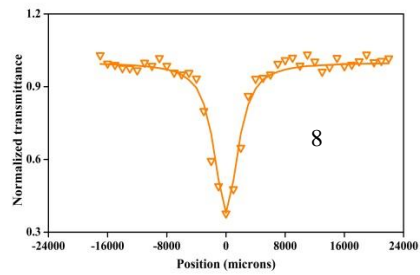


Fig. 4.11b. Normalized open aperture and optical limiting curves of **8**, **10** and **12**

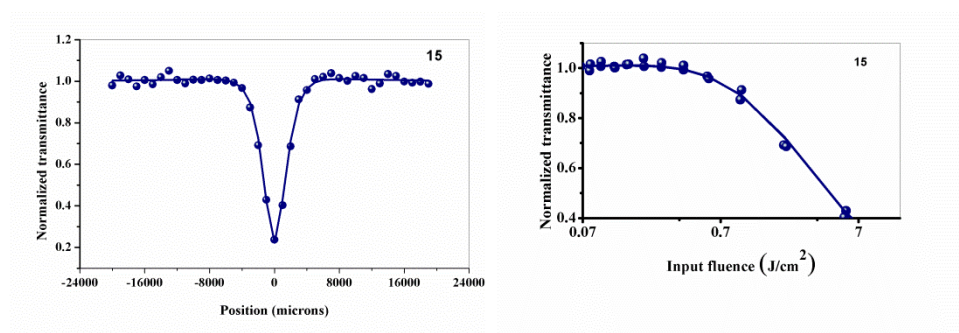


Fig. 4.11c. Normalized open aperture and optical limiting curves of **15**

Table 4.8. NLO properties of the compounds

Compound	Nonlinear absorption coefficient (β , m/W)	Imaginary part of nonlinear susceptibility ($\text{Im } \chi^{(3)}$, esu)	Optical Limiting Threshold (J/cm^2)
6a	1.73×10^{-10}	5.86×10^{-12}	6.34
6d	2.50×10^{-10}	8.46×10^{-12}	4.38
8	1.80×10^{-10}	6.07×10^{-12}	2.37
10	1.28×10^{-10}	4.38×10^{-12}	-
12	2.00×10^{-10}	6.76×10^{-12}	6.34
15	2.63×10^{-10}	8.88×10^{-12}	4.22

4.4. Conclusions

We have successfully designed and synthesized a series of 1,3,4-oxadiazole and carbazole containing push-pull fluorophores by a simple synthetic methodology (iodine mediated oxidative cyclization). Structure of the fluorophores was established on the basis of analytical and spectral data. These fluorophores are found to be highly emissive with moderately high quantum yields. Fluorophores **6a**, **8**, **10** and **15** showed positive solvatochromic behaviour mainly in the emission

spectra which indicates the more polar nature of the excited state compared to the ground state. We performed theoretical calculations to map HOMO and LUMO and to estimate HOMO-LUMO bandgaps, the results of which is well matched with bandgap obtained from absorption threshold and CV measurements. Fluorophore **6d** showed smallest bandgap of 3.33 eV. Due to high electron donating ability of carbazole and electron accepting power of oxadiazoles, we observed strong π electron delocalization which is confirmed by DFT studies. Due to this asymmetric electron distribution, these molecules showed high third order nonlinear property which is confirmed by relatively good nonlinear absorption coefficient (β) value, among the series **15** showed highest β value of 2.63×10^{-10} m/W. These molecules also exhibited potential optical limiting property which is confirmed by optical limiting curves. Hence these fluorophores are promising materials for further photonic applications.

4.5. Experimental Section

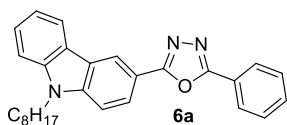
4.5.1. Reagents and instruments

The required starting materials 9-octyl-9*H*-carbazole-3-carbaldehyde (**3**), 9-octyl-9*H*-carbazole-3,6-dicarbaldehyde (**11**) were prepared according to reported procedures.^{44,45} All the details about the instruments are given in chapter 3 (Section **3.5.1**).

4.5.2. Synthesis and Characterization

4.5.2.1. Synthesis of 2-(9-octyl-9H-carbazol-3-yl)-5-phenyl-1,3,4-oxadiazole (6a)

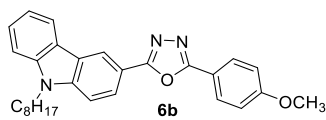
Compound **6a** was prepared by iodine mediated oxidative cyclization reaction which is described in chapter 3 (Procedure **3.5.2.1**)³⁷ by using 9-octyl-9H-carbazole-3-carbaldehyde (310 mg, 1 mmol) and benzohydrazide (138 mg, 1 mmol).



Yield 61%, mp: 128-133 °C; UV-Vis (CHCl₃) (λ_{\max}): 328 nm; IR (KBr): 2900, 1480, 1288, 1045, 690 cm⁻¹; ¹H NMR (500 MHz, CDCl₃): δ (ppm) 8.79-8.78 (m, 2H), 8.19-8.12 (m, 4H), 7.49-7.18 (m, 7H), 4.28-4.24 (m, 2H), 1.84-1.82 (m, 2H), 1.33-1.18 (m, 10H), 0.79-0.77 (m, 3H); ¹³C-NMR (125 MHz, CDCl₃): δ (ppm) 164.8, 163.1, 141.2, 140.0, 130.4, 128.0, 125.8, 125.6, 123.5, 122.1, 119.8, 118.8, 118.7, 113.4, 108.2, 42.3, 30.7, 28.3, 28.1, 27.9, 26.3, 21.6, 13.0; MS: m/z 423 (M^+), 424 ($M+1$); Elemental analysis calculated for C₂₈H₂₉N₃O: C: 79.40, H: 6.90, N: 9.92; Found C: 79.38, H: 6.92, N: 9.91.

4.5.2.2. Synthesis of 2-(4-methoxyphenyl)-5-(9-octyl-9H-carbazol-3-yl)-1,3,4-oxadiazole (6b)

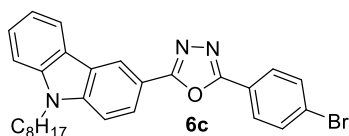
The reaction was performed as described in the procedure **3.5.2.1** with 9-octyl-9H-carbazole-3-carbaldehyde (310 mg, 1 mmol) and 4-methoxybenzohydrazide (170 mg, 1 mmol). White solid.



Yield: 68%, mp: 85-90 °C; IR (KBr): 2818, 1576, 1468, 1037, 686 cm⁻¹; ¹H NMR (500 MHz, CDCl₃): δ (ppm) 8.84-7.31 (m, 11H), 4.33 (t, 2H), 1.92-1.89 (m, 2H), 1.39-1.25 (m, 12H), 0.86 (s, 3H); ¹³C NMR (125 MHz, CDCl₃): δ (ppm) 164.3, 162.9, 161.1, 141.1, 139.9, 127.6, 125.5, 123.5, 122.1, 121.7, 119.7, 118.8, 115.8, 113.4, 108.2, 54.4, 42.3, 30.9, 30.7, 28.7, 28.3, 28.1, 26.3, 21.7, 13.0; MS: m/z 453 (M^+), 454 ($M+1$); Elemental analysis calculated for C₂₉H₃₁N₃O₂: C: 76.79, H: 6.89, N: 9.26; Found C: 76.77, H: 6.88, N: 9.25.

4.5.2.3. Synthesis of 2-(4-bromophenyl)-5-(9-octyl-9H-carbazol-3-yl)-1,3,4-oxadiazole (6c)

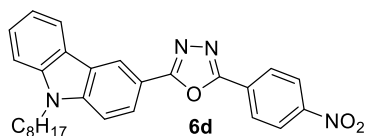
The reaction was performed according to the procedure 3.5.2.1 with 9-octyl-9H-carbazole-3-carbaldehyde (305 mg, 1 mmol) and 4-bromobenzohydrazide (218 mg, 1 mmol). White solid.



Yield: 62%, 123-128 °C; IR (KBr): 2966, 1565, 1428, 1062, 623, 547 cm^{-1} ; ^1H NMR (500 MHz, CDCl_3): δ (ppm) 8.23-6.94 (m, 11H), 3.97 (t, 2H), 1.99-1.18 (m, 15H); ^{13}C NMR (125 MHz, CDCl_3): δ (ppm) 163.4, 161.9, 161.5, 141.5, 139.7, 127.4, 125.3, 123.3, 122.5, 121.4, 119.6, 118.5, 116.8, 115.4, 106.8, 53.4, 44.3, 30.7, 30.5, 28.3, 27.1, 26.3, 13.0; MS: m/z 501 (M^+), 502 ($M+1$); Elemental analysis calculated for $\text{C}_{28}\text{H}_{28}\text{BrN}_3\text{O}$: C: 66.93, H: 5.62, N: 8.36; Found C: 66.91, H: 5.63, N: 8.34.

4.5.2.4. Synthesis of 2-(4-nitrophenyl)-5-(9-octyl-9H-carbazol-3-yl)-1,3,4-oxadiazole (6d)

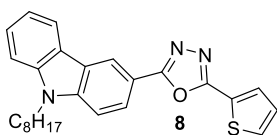
The reaction was performed according to the procedure 3.5.2.1 with 9-octyl-9H-carbazole-3-carbaldehyde (311 mg, 1 mmol) and 4-nitrobenzohydrazide (177 mg, 1 mmol). Orange solid.



Yield 62%, mp 117-122 °C; UV-Vis (CHCl_3): 371 nm (λ_{max}); IR (KBr): 2968, 1532, 1458, 1128, 639, 558 cm^{-1} ; ^1H NMR (500 MHz, CDCl_3): δ (ppm) 8.84-7.31 (m, 11H), 4.31 (t, 2H), 1.89-1.12 (m, 15H); ^{13}C NMR (125 MHz, CDCl_3): δ (ppm) 165.7, 161.3, 148.2, 141.4, 139.9, 128.7, 126.5, 125.7, 123.6, 119.7, 119.0, 118.9, 112.4, 108.3, 42.2, 30.5, 28.7, 28.4, 28.1, 27.9, 26.3, 21.6, 13.1; MS: m/z 468 (M^+), 469 ($M+1$); Elemental analysis calculated for $\text{C}_{28}\text{H}_{28}\text{N}_4\text{O}_3$: C: 71.78, H: 6.02, N: 11.96; Found C: 71.77, H: 6.00, N: 11.94.

4.5.2.5. Synthesis of 2-(9-octyl-9H-carbazol-3-yl)-5-(thiophen-2-yl)-1,3,4-oxadiazole (8)

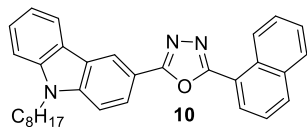
This compound was prepared by a procedure similar to that of **6a** except that thiophene-2-carbohydrazide (140 mg, 1 mmol) was used as the reactant in place of benzohydrazide. White solid.



Yield : 66%, mp: 153-158 °C; UV-Vis (CHCl₃): 331 nm (λ_{\max}); IR (KBr): 2921, 1255, 1056, 930.5, 886 cm⁻¹; ¹H NMR (400 MHz, CDCl₃): δ (ppm) 8.75 (s, 1H), 8.16-8.12 (m, 2H), 7.82-7.80 (m, 1H), 7.51-7.37 (m, 4H), 7.26-7.22 (m, 1H), 7.15-7.13 (m, 1H), 4.27 (t, $J = 7.2$ Hz, 2H), 1.87-0.77 (m, 15H); ¹³C NMR (100 MHz, CDCl₃): δ (ppm) 164.3, 159.4, 141.2, 140.0, 128.7, 128.3, 127.1, 125.6, 124.7, 123.6, 122.2, 121.7, 119.8, 118.9, 118.7, 113.2, 108.2, 108.2, 42.4, 30.7, 28.3, 28.1, 27.9, 26.3, 21.6, 13.0; MS: m/z 429 (M^+), 430 ($M+1$); Elemental analysis calculated for C₂₆H₂₇N₃OS: C: 72.70, H: 6.34, N: 9.78, S: 7.46; Found C: 72.68, H: 6.32, N: 9.77, S: 7.45.

4.5.2.6. Synthesis of 2-(naphthalen-1-yl)-5-(9-octyl-9H-carbazol-3-yl)-1,3,4-oxadiazole (10)

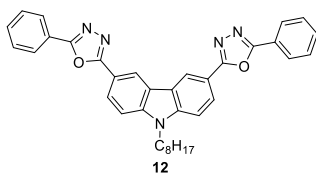
This compound was prepared by a procedure similar to that of **6a** except that 1-naphthohydrazide (163 mg, 1 mmol) was used as the reactant in place of benzohydrazide. White solid.



Yield: 64%, mp: 117-122 °C; UV-Vis (CHCl₃) (λ_{\max}): 340 nm; IR (KBr): 2922, 1459, 1270, 1057, 672 cm⁻¹; ¹H NMR (400 MHz, CDCl₃): δ (ppm) 9.27 (d, $J = 8.4$ Hz, 1H), 8.82 (s, 1H), 8.23-8.21 (m, 2H), 8.13 (d, $J = 7.6$ Hz, 1H), 7.97 (d, $J = 8.4$ Hz, 1H), 7.87 (d, $J = 8$ Hz, 1H), 7.67-7.63 (m, 1H), 7.57-7.43 (m, 4H), 7.37 (d, $J = 8$ Hz, 1H), 7.26-7.23 (m, 1H), 4.26 (t, $J = 7.6$ Hz, 2H), 1.87-1.79 (m, 2H), 1.35-1.17 (m, 10H), 0.80-0.77 (m, 3H); ¹³C NMR (100 MHz, CDCl₃): δ (ppm) 164.3, 163.0, 141.2, 140.0, 132.9, 131.2, 129.2, 127.6, 127.2, 127.0, 125.6, 125.4, 123.9, 123.6, 122.2, 121.7, 119.9, 119.8, 118.8, 118.7, 113.4, 108.2, 42.3, 30.7, 28.3, 28.1, 27.9, 26.3, 21.6, 13.0; MS: m/z 473 (M^+), 474 ($M+1$); Elemental analysis calculated for C₃₂H₃₁N₃O: C: 81.15, H: 6.60, N: 8.87; Found C: 81.13, H: 6.59, N: 8.86.

4.5.2.7. Synthesis of 5,5'-(9-octyl-9H-carbazole-3,6-diyl)bis(2-phenyl-1,3,4-oxadiazole) (12)

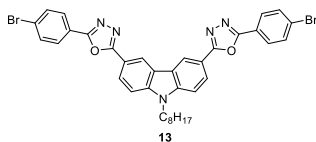
This compound was prepared by a procedure similar to that used for **6a**, except that 9-octyl-9H-carbazole-3,6-dicarbaldehyde (334 mg, 1 mmol) was used as the reactant instead of 9-octyl-9H-carbazole-3-carbaldehyde and two equivalence of benzohydrazide (275 mg, 2 mmol) is added then cyclization occurs on both sides to yield the product as an orange solid.



Yield: 68%, mp: 208-213 °C; UV-Vis (CHCl₃) (λ_{max}): 348 nm; IR (KBr): 2925, 1476, 1276, 1067, 676 cm⁻¹; ¹H NMR (400 MHz, CDCl₃): δ (ppm) 8.29 (s, 1H), 8.11-7.88 (m, 6H), 7.50-7.42 (m, 6H), 7.27-7.25 (m, 1H), 4.03(m, 2H), 1.65-1.16 (m, 13H), 0.79-0.75 (m, 3H); ¹³C NMR (100 MHz, CDCl₃): δ (ppm) 164.4, 163.1, 132.5, 130.9, 130.5, 129.4, 128.1, 127.7, 126.5, 125.8, 124.6, 123.9, 123.1, 121.9, 121.7, 120.5, 120.2, 118.7, 114.5, 108.4, 48.1, 30.6, 28.2, 28.1, 27.9, 26.2, 21.4, 13.2; MS: m/z 567 (M^+), 568 ($M+1$); Elemental analysis calculated for C₃₆H₃₃N₅O₂: C: 76.17, H: 5.86, N: 12.34; Found C: 76.16, H: 6.59, N: 12.32.

4.5.2.8. 5,5'-(9-Octyl-9H-carbazole-3,6-diyl)bis(2-(4-bromophenyl)-1,3,4-oxadiazole) (13)

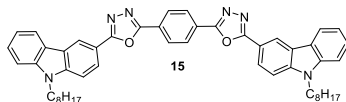
This compound was prepared by a procedure similar to that used for **12**, except that two equivalence of 4-bromobenzohydrazide (430 mg, 2 mmol) is used in place of benzohydrazide. White solid.



Yield: 62%, mp: 207-212 °C; IR (KBr): 2988, 1569, 1436, 1052, 635, 567 cm⁻¹; ¹H NMR (500 MHz, CDCl₃): δ (ppm) 8.76-7.41 (m, 14H), 4.26 (t, $J = 7.5$ Hz, 2H), 1.86-1.83 (m, 3H), 1.34-1.18 (m, 10H), 0.80-0.75 (m, 4H); ¹³C NMR (125 MHz, CDCl₃): δ (ppm) 164.3, 162.4, 141.7, 131.4, 127.2, 125.2, 124.3, 121.9, 121.8, 118.9, 114.3, 108.8, 42.6, 30.7, 28.3, 28.1, 27.9, 21.6, 13.0; MS: m/z 725 (M^+), 726 ($M+1$); Elemental analysis calculated for C₃₆H₃₁Br₂N₅O₂: C: 59.60, H: 4.31, N: 9.65; Found C: 59.58, H: 4.30, N: 9.64.

4.5.2.9. Synthesis of 1,4-bis(5-(9-octyl-9H-carbazol-3-yl)-1,3,4-oxadiazol-2-yl)benzene (15)

This compound was prepared by a procedure similar to that used for **6a**, except that terephthalohydrazide (194 mg, 1 mmol) was used in place of benzohydrazide and two equivalence of 9-octyl-9H-carbazole-3-carbaldehyde (665 mg, 2 mmol) is added. Cyclization occurs in both sides to yield the product as a white solid.



Yield 63%, mp: 117-122 °C; UV-Vis (CHCl₃): 348 nm (λ_{max}); IR (KBr): 2912, 1472, 1265, 1082, 660 cm⁻¹; ¹H NMR (500 MHz, CDCl₃): δ (ppm) 8.83 (s, 2H), 8.32 (s, 4H), 8.21 (d, J = 8.5 Hz, 2H), 8.16 (d, J = 7.5 Hz, 2H), 4.29 (t, J = 7.5 Hz, 4H), 1.87-1.83 (m, 5H), 1.36-1.18 (m, 20H), 0.80 (t, J = 7.5 Hz, 6H); ¹³C NMR (125 MHz, CDCl₃): δ (ppm) 165.2, 141.3, 126.3, 125.6, 123.6, 118.9, 113.0, 112.3, 108.2, 42.4, 30.7, 28.3, 28.1, 27.9, 26.2, 21.6, 13.0; MS: m/z 768 (M^+), 769 ($M+1$); Elemental analysis calculated for C₅₀H₅₂N₆O₂: C: 78.09, H: 6.82, N: 10.93; Found C: 78.07, H: 6.81, N: 10.90.

4.6. References

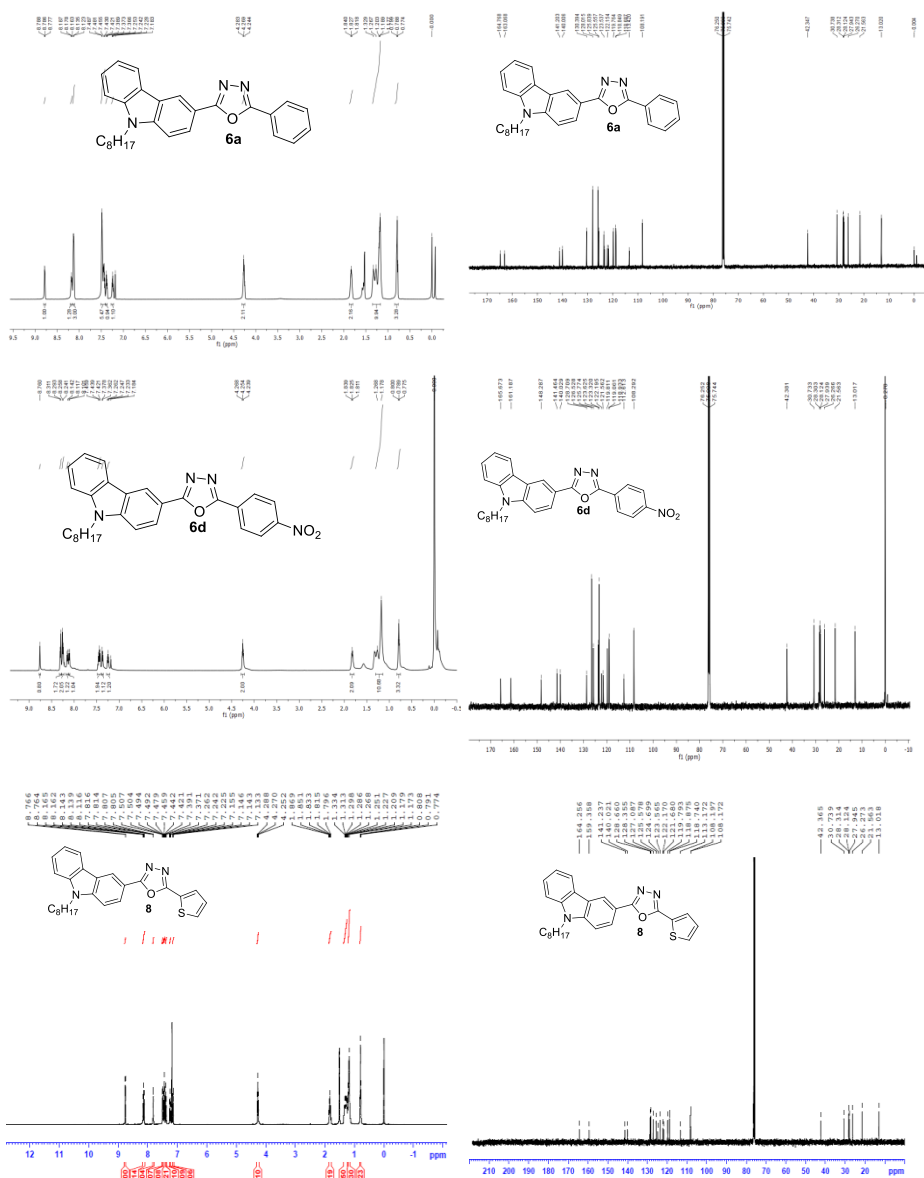
- (1) Garmire, E. *Opt. Express* **2013**, *21*, 30532.
- (2) Tang, C.; Zheng, Q.; Zhu, H.; Wang, L.; Chen, S.-C.; Ma, E.; Chen, X. *J. Mater. Chem. C* **2013**, *1*, 1771.
- (3) Dvornikov, A. S.; Walker, E.P.; Rentzepis, P. M. *J. Phys. Chem. A* **2009**, *113*, 13633.
- (4) Gindre, D.; Iliopoulos, K.; Krupka, O.; Champigny, E.; Morille, Y.; Sallé, M. *Opt. Lett.* **2013**, *38*, 4636.
- (5) Albota, M. *Science* **1998**, *281*, 1653.
- (6) Pawlicki, M.; Collins, H. A.; Denning, R. G.; Anderson, H. L. *Angew. Chem. Int. Ed.* **2009**, *48*, 3244.

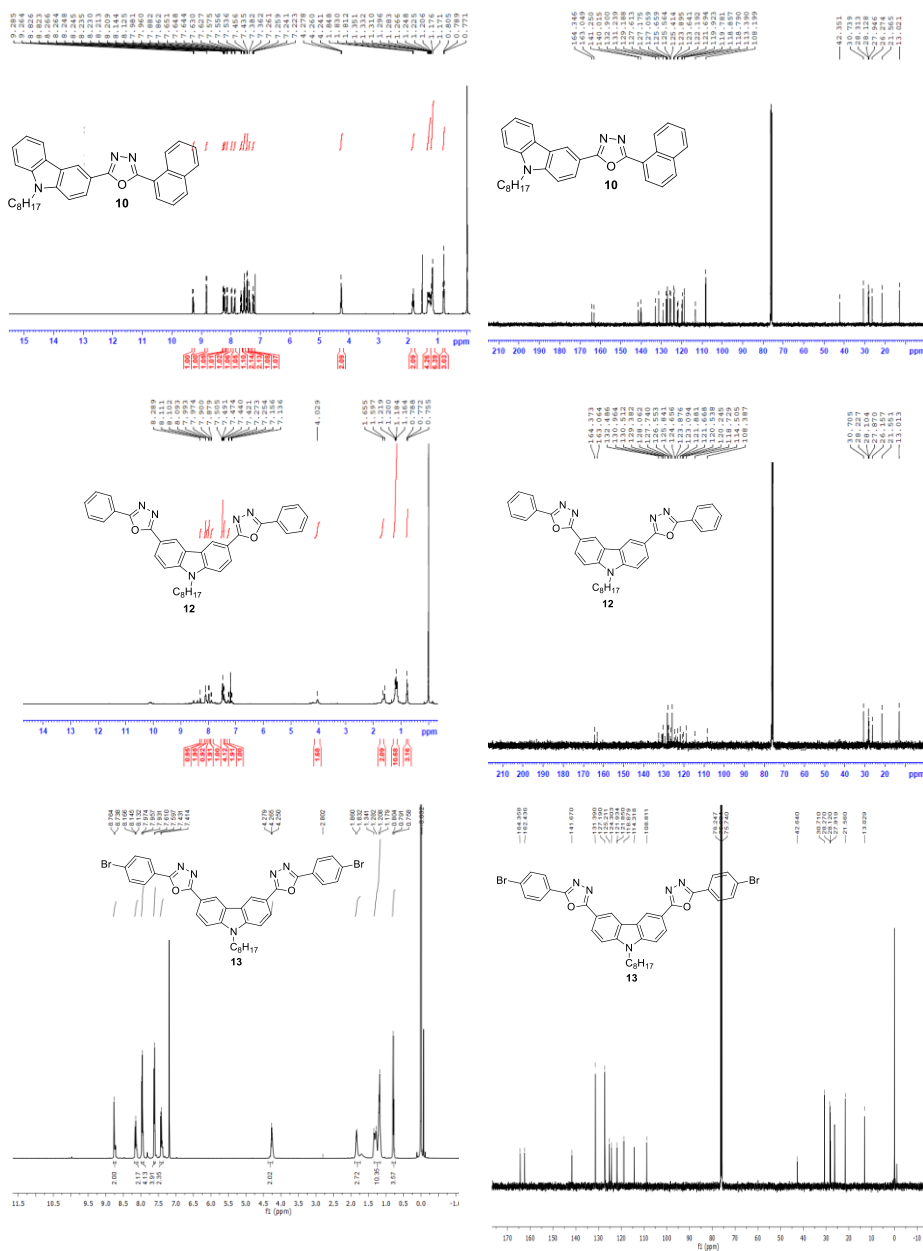
- (7) Yang, C.; Zheng, M.; Li, Y. P.; Zhang, B. L.; Li, J. F.; Bu, L. Y.; Liu, W.; Sun, M. X.; Zhang, H. C.; Tao, Y.; Xue, S. F.; Yang, W. J. *J. Mater. Chem. A* **2013**, *1*, 5172.
- (8) Ando, M.; Kadono, K.; Haruta, M.; Sakaguchi, T. *Nature* **1995**, *374*, 625.
- (9) Fainman, Y.; Ma, J.; Lee, S. H. *Mater. Sci. Reports* **1993**, *9*, 53.
- (10) Hales, J. M.; Cozzuol, M.; Screen, T. E. O.; Anderson, H. L.; Perry, J. W. *Opt. Express* **2009**, *17*, 18478.
- (11) He, G. S.; Tan, L. S.; Zheng, Q.; Prasad, P. N. *Chem. Rev.* **2008**, *108*, 1245.
- (12) Gieseking, R. L.; Mukhopadhyay, S.; Risko, C.; Marder, S. R.; Brédas, J. L. *Adv. Mater.* **2014**, *26*, 68.
- (13) Ohkoshi, S.; Takano, S.; Imoto, K.; Yoshikiyo, M.; Namai, A.; Tokoro, H. *Nat. Photonics* **2013**, *8*, 65.
- (14) Wang, C.; Jung, G.-Y.; Batsanov, A. S.; Bryce, M. R.; Petty, M. C. *J. Mater. Chem.* **2002**, *12*, 173.
- (15) Cha, S. W.; Choi, S. H.; Kim, K.; Jin, J. I. *J. Mater. Chem.* **2003**, *13*, 1900.
- (16) Schulz, B.; Bruma, M.; Brehmer, L. *Adv. Mater.* **1997**, *9*, 601.
- (17) Wong, M. Y.; Leung, L. M. *Dye. Pigment.* **2017**, *145*, 542.
- (18) Wang, H. Y.; Liu, F.; Xie, L. H.; Tang, C.; Peng, B.; Huang, W.; Wei, W. *J. Phys. Chem. C* **2011**, *115*, 6961.
- (19) Huang, H.; Fu, Q.; Pan, B.; Zhuang, S.; Wang, L.; Chen, J.; Ma, D.; Yang, C. *Org. Lett.* **2012**, *14*, 4786.
- (20) Sathiyar, G.; Sivakumar, E. K. T.; Ganesamoorthy, R.; Thangamuthu, R.; Sakthivel, P. *Tetrahedron Lett.* **2016**, *57*, 243.
- (21) Li, J.; Liu, D.; Li, Y.; Lee, C. S.; Kwong, H. L.; Lee, S. *Chem. Mater.* **2005**, *17*, 1208.
- (22) Hudson, Z. M.; Wang, Z.; Helander, M. G.; Lu, Z. H.; Wang, S. *Adv. Mater.* **2012**, *24*, 2922.
- (23) Wong, W. Y.; Ho, C. L.; Gao, Z. Q.; Mi, B. X.; Chen, C. H.; Cheah, K. W.; Lin, Z. *Angew. Chem. Int. Ed.* **2006**, *45*, 7800.
- (24) Qian, Y.; Xiao, G.; Wang, G.; Sun, Y.; Cui, Y.; Yuan, C. *Dye. Pigment.* **2006**, *71*, 109.
- (25) Jiang, D.; Chen, S.; Xue, Z.; Li, Y.; Liu, H.; Yang, W.; Li, Y. *Dye. Pigment.* **2016**, *125*, 100.
- (26) Zhan, X.; Liu, Y.; Zhu, D.; Liu, X.; Xu, G.; Ye, P. *Chem. Phys. Lett.* **2002**, *362*, 165.
- (27) Li, S.; Gao, C.; Liu, F.; Wei, W. *React. Funct. Polym.* **2013**, *73*, 828.

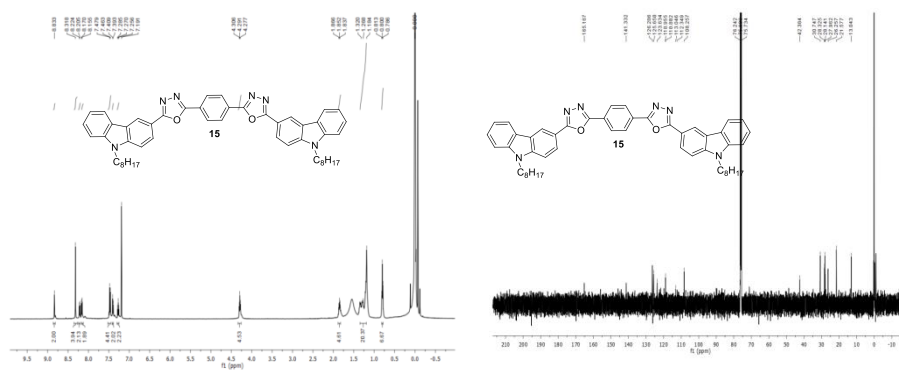
- (28) Venkateswararao, A.; Thomas, K. R. J.; Lee, C. P.; Li, C. T.; Ho, K. C. *ACS Appl. Mater. Interfaces* **2014**, *6*, 2528.
- (29) Feng, L.; Chen, Z. *Spectrochim. Acta - Part A Mol. Biomol. Spectrosc.* **2006**, *63*, 15.
- (30) Tao, Y.; Yang, C.; Qin, J. *Chem. Soc. Rev.* **2011**, *40*, 2943.
- (31) Zhang, K.; Tao, Y.; Yang, C.; You, H.; Zou, Y.; Qin, J.; Ma, D. *Chem. Mater.* **2008**, *20*, 7324.
- (32) Lee, A. R.; Lee, J.; Lee, J.; Han, W. S. *Org. Electron. physics, Mater. Appl.* **2016**, *38*, 222.
- (33) Paun, A.; Hadade, N. D.; Paraschivescu, C. C.; Matache, M. J. *Mater. Chem. C* **2016**, *4*, 8596.
- (34) Shin, M. H.; Wong, F. F.; Lin, C. M.; Chen, W. Y.; Yeh, M. Y. *Heteroat. Chem.* **2006**, *17*, 160.
- (35) Manjunatha, M. G.; Adhikari, A. V.; Hegde, P. K. *J. Electron. Mater.* **2010**, *39*, 2711.
- (36) Uduma, Y. A.; Hizliates, C. G.; Ergün, Y.; Toppare, L. *Thin Solid Films* **2015**, *595*, 61.
- (37) Yu, W.; Huang, G.; Zhang, Y.; Liu, H.; Dong, L.; Yu, X.; Li, Y.; Chang, J. J. *Org. Chem.* **2013**, *78*, 10337.
- (38) Allen, M. W. *Measurement of Fluorescence Quantum Yields*. Technical note 52019, Thermo Fisher Scientific, Madison, WI, USA.
- (39) Deshapande, N.; Pujar, G. H.; Sunagar, M. G.; Khazi, I. A. M. *Chemistryselect* **2017**, *2*, 1793.
- (40) Deshapande, N.; Belavagi, N. S.; Sunagar, M. G.; Khazi, I. A. M. *RSC Adv.* **2015**, *5*, 86685.
- (41) Gaussian 09, Revision D.01, M. J. Frisch, G. W. Trucks, H. B. Schlegel, G. E. Scuseria, M. A. Robb, J. R. Cheeseman, G. Scalmani, V. Barone, B. Mennucci, G. A. Peterson, H. Nakatsuji, M. Caricato, X. Li, H. P. Hratchian, A. F. Izmaylov, J. Bloino, G. Zheng, J. L. Sonnenberg, M. Hada, M. Ehra, K. Toyota, R. Fukuda, J. Hasegawa, M. Ishida, T. Nakajima, Y. Honda, O. Kitao, H. Nakai, T. Vreven, J. A. Montgomery, Jr., J. E. Peralta, F. Ogliaro, M. Bearpark, J. J. Heyd, E. Brothers, K. N. Kudin, V. N. Staroverov, T. Keith, R. Kobayashi, J. Normand, K. Raghavachari, A. Rendell, J. C. Burant, S. S. Iyengar, J. Tomasi, M. Cossi, N. Raga, J. M. Millam, M. Klene, J. E. Knox, J. B. Cross, V. Bakken, C. Adamo, J. Jaramillo, R. Gomperts, R. E. Stratmann, O. Yazyev, A. J. Austin, R. Cammi, C. Pomelli, J. W. Ochterski, R. L. Martin, K. Morokuma, V. G. Zakrzewski, G. A. Voth, P. Salvador, J. J. Dannenberg, S. Dapprich, A. D. Daniels, O. Farkas, J. B. Foresman, J. V. Ortiz, J. Cioslowski, and D. J. Fox, *Gaussian, Inc.*, Wallingford CT, **2013**.

- (42) Fan, L.; Cui, R.; Jiang, L.; Zou, Y.; Li, Y.; Qian, D. *Dye. Pigment.* **2015**, *13*, 458.
- (43) Zhang, C.; Song, Y.; Xu, Y.; Fun, H.; Fang, G.; Wang, Y. *J. Chem. Soc. Dalton Trans.* **2000**, *16*, 2823.
- (44) Sathiyar, G.; Sakthivel, P. *Dye. Pigment.* **2017**, *143*, 444.
- (45) Sathiyar, G.; Thangamuthu, R.; Sakthivel, P. *RSC Adv.* **2016**, *6*, 69196.

4.7. Appendix

 ^1H and ^{13}C NMR spectra of significant compounds





SYNTHESIS AND EVALUATION OF THIRD-ORDER NONLINEAR OPTICAL PROPERTIES OF A FEW 1,3,4-OXADIAZOLE-PYRENE PUSH-PULL FLUOROPHORES

5.1. Abstract

In continuation of our investigations on donor-acceptor systems, we synthesized a few blue light emitting 1,3,4-oxadiazole-pyrene push-pull fluorophores by iodine mediated oxidative cyclization reaction. In these molecules, pyrene act as the electron donor and 1,3,4-oxadiazole as the acceptor part. These fluorophores were characterized using ^1H NMR, ^{13}C NMR and LC-MS analysis. Photophysical properties and electrochemical properties were monitored by using UV-Vis absorption, fluorescence spectroscopy, time resolved fluorescence measurements and CV experiment. Theoretical calculations were carried out using DFT for evaluating structure-nonlinear property relationship; the theoretical values are well matched with the experimental results. Thermal studies revealed that all the molecules are thermally stable. The nonlinear optical properties of the D-A molecules were also studied using Q switched Z scan technique with a 7 ns laser pulses at 532 nm. The molecules exhibited good third-order nonlinear absorption and optical power limiting property at 532 nm.

5.2. Introduction

Nonlinear optical phenomenon of D-A materials have emerged as a promising area of research.¹ The most interesting design approach in the field of organic electronics is synthesis of stable molecules possessing a combination of electron accepting and donating groups connected by a π linker. In this type of push-pull systems intramolecular

charge transfer (ICT) occurs from donor to acceptor which will enhance the photophysical properties. Here electron density in HOMO is mainly located on donor and electron density in LUMO is concentrated on acceptor. Hence there is a definite charge separation in these types of molecules. This type of inherent polarizability is one of the most important criteria for showing NLO activity.

As described in previous chapters, 1,3,4-oxadiazole based D-A type small molecules and polymers are widely employed in organic electronics.²⁻⁷ Pyrene is a typical polyaromatic hydrocarbon which is also widely employed in organic electronics due to its high photoluminescence quantum yield and proficient excimer emission.^{8,9} Inherent planarity and extended π conjugation in pyrene stretched its applications to NLO activity, optical limiting and bioimaging.¹⁰⁻¹⁷ So, we surmised that 1,3,4-oxadiazole and pyrene will make an ideal pair for fabricating a D-A type system for photonic application. Indeed, Rao *et al.* in 2015 synthesized a few pyrene-(1,3,4-oxadiazole) hybrid molecules and employed them for OLED application.¹⁸

To the best of our knowledge, no reports are available on the third-order nonlinear optical properties of 1,3,4-oxadiazole-pyrene push-pull molecules. We have designed and synthesized a few 1,3,4-oxadiazole and pyrene based push-pull fluorophores in which pyrene act as electron donor and 1,3,4-oxadiazole as electron acceptor (Chart 5.1). Structural, photophysical, electrochemical, theoretical and thermal properties of the fluorophores **4a** and **7** were investigated.

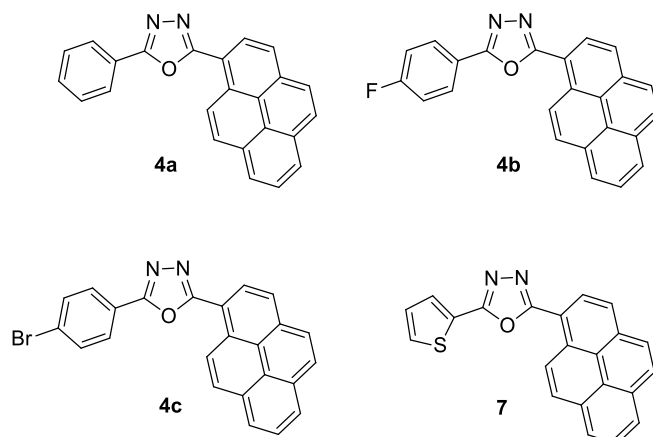
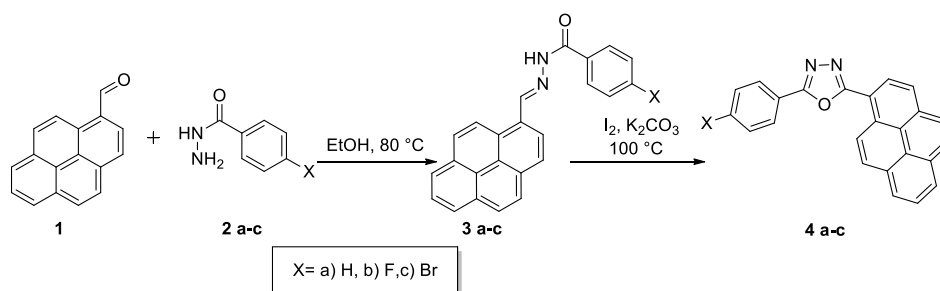


Chart. 5.1. Selected targets

5.3. Results and Discussion

5.3.1. Synthesis of Fluorophores

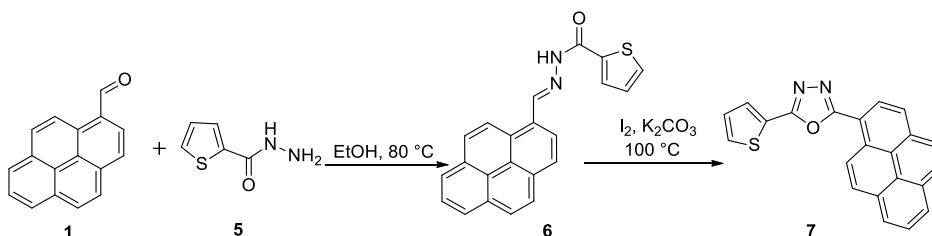
Iodine mediated oxidative cyclization was used for the synthesis of fluorophores (Scheme 5.1).¹⁹ These compounds were characterized by ¹H NMR, ¹³C NMR, IR spectroscopy and mass spectrometry.



Scheme 5.1. Synthesis of 4a-c

Similarly, thiophene-appended compound **7** was synthesized from pyrene-2-carboxaldehyde (**1**) and thiophene-2-carbohydrazide (**5**) by a

two-step reaction protocol (Scheme 5.2).



Scheme 5.2. Synthesis of 7

5.3.2. Photophysical Properties

5.3.2.1. UV-Vis Absorption and Photoluminescence (PL) spectra

Molecules **4a** and **7** are soluble in common organic solvents such as toluene, dichloromethane, dimethylformamide and dimethyl sulfoxide. Both **4a** and **4b** exhibited nearly identical absorption and emission characteristics. Compound **4c**, on the other hand, exhibited muted fluorescence due to heavy atom effect. In the present investigation, we restricted photophysical investigations to **4a** and **7**. Fig. 5.1 shows the normalized UV-Vis absorption spectra of the fluorophores in CHCl₃ (HPLC grade). The maximum absorption wavelengths (λ_{max}) of compounds **4a** and **7** were 369 and 372 nm respectively. Small increment in absorption maximum of **7** is due to the presence of electron rich thiophene moiety.

Fig.5.2 shows the normalized emission spectra of **4a** and **7** in chloroform at room temperature. The emission maxima of **4a** and **7** were 427 and 432 respectively. Stokes shift values for compounds **4a** and **7** are nearly identical at 3681 and 3734 cm⁻¹ respectively (Table 5.1). Both absorption and emission spectra of **4a** and **7** are redshifted with respect to

those for pyrene indicating ground as well as excited state interaction between pyrene and oxadiazole components in these molecules.

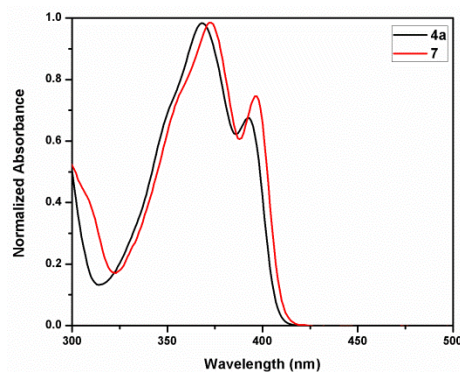


Fig. 5.1. Normalized UV-Vis absorption spectra of **4a** and **7** in CHCl_3 at room temperature

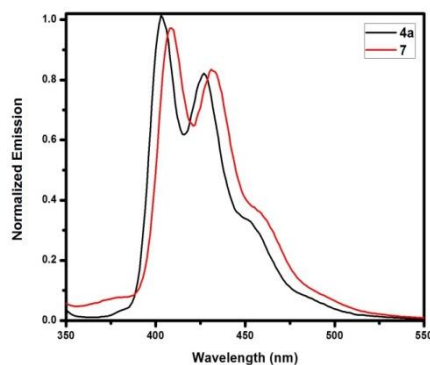


Fig. 5.2. Normalized emission spectra of **4a** and **7** in CHCl_3 at room temperature

5.3.2.2. Quantum Yield (ϕ) Measurements

Fluorescence quantum yield (ϕ) of **4a** and **7** were measured in chloroform at room temperature by comparison with quinine sulfate of known quantum yield (ϕ) using the Equation 5.1.²⁰

$$\phi = \phi_R \frac{I n_{\text{solvent}}^2 \frac{A_R}{I_R}}{A} \quad (5.1)$$

where I is the integrated intensity, A is the optical density, n is the refractive index and R stands for reference dye with known quantum yield. The calculated quantum yields of fluorophores **4a** and **7** are 0.63 and 0.64 respectively (Table 5.1). It may be mentioned here that fluorescence quantum yield for pyrene measured in hexane is lower at 0.32.²¹

Table 5.1. Summary of absorption and emission data for **4a** and **7**

Compounds	Absorption $\lambda_{\max}^{\text{abs}}$ (nm) (log ϵ)	Emission $\lambda_{\max}^{\text{emi}}$ (nm)	Stokes Shift (cm^{-1})	Quantum Yield
4a	369 (4.6)	427	3681	0.63
7	372 (4.3)	432	3734	0.64

5.3.2.3. Optical Bandgap

The optical bandgap (E_g^{opt}) values were approximated from the onset of the low energy side of the absorption spectra (λ_{onset} , solution) to the baseline according to Equation 5.2 and are summarized in Table 5.2. The optical bandgap observed for **4a** and **7** are 3.08 and 3.00 eV respectively.

$$E_g^{\text{opt}} = 1240/\lambda_{\text{onset}} \quad (5.2)$$

Table 5.2. Optical bandgaps of **4a** and **7**

Compound	E_g^{opt} (eV)
4a	3.08 (402)
7	3.00 (413)

5.3.2.4. Solvatochromic Behavior

To shed more light on intramolecular charge transfer (ICT) characteristics of the fluorophores, solvatochromic studies were

performed and the results are summarized in Table 5.3 and 5.4 and Fig 5.3. Solvent effects were checked using general solvents such as toluene, chloroform, dichloromethane, dimethylformamide and dimethyl sulfoxide. Results showed that these fluorophores did not exhibit any change in absorption maximum on moving from relatively nonpolar toluene to highly polar DMSO. However, with increasing solvent polarity, a slight redshift was observed in the emission peak which revealed a slightly higher polar nature of the excited state compared to the ground state.

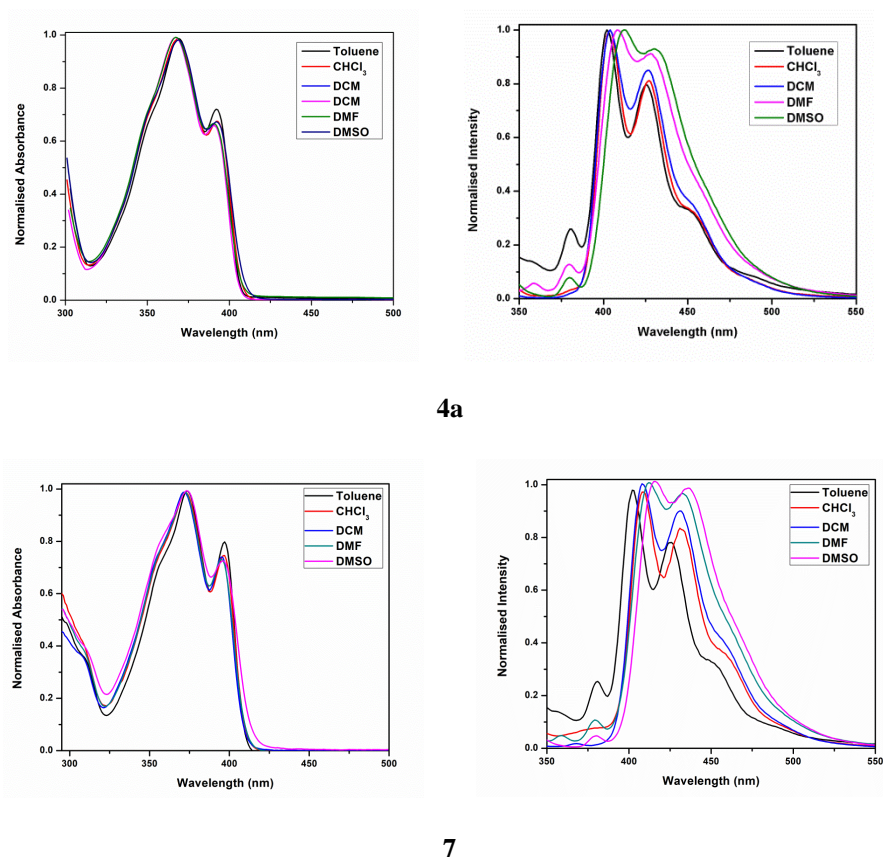


Fig. 5.3. Normalized absorption and emission spectra of **4a** and **7** in different solvents

Table 5.3. Summary of optical properties of **4a** in different solvents

Solvents	Absorption λ_{max}^{abs} (nm)	Emission λ_{max}^{em} (nm)	Stokes Shift (cm ⁻¹)
Toluene	369	425	3571
Chloroform	369	427	3681
DCM	369	427	3681
DMF	367	428	3883
DMSO	369	430	3844

Table 5.4. Summary of optical properties of **7** in different solvents

Solvents	Absorption λ_{max}^{abs} (nm)	Emission λ_{max}^{em} (nm)	Stokes Shift (cm ⁻¹)
Toluene	374	425	3209
Chloroform	372	432	3734
DCM	373	432	3662
DMF	373	433	3715
DMSO	374	436	3802

5.3.2.5. Time Resolved Fluorescence Life-time Measurements

The fluorescence decay character of **4a** and **7** were monitored in toluene and DMF. Individual time resolved fluorescence decay profiles of the compounds are shown in Fig. 5.4. Decay experiments were performed at an excitation wavelength of 340 nm and decays were examined at respective emission maxima. The decays were fitted monoexponentially and the fluorescence lifetime of fluorophores **4a** and **7** are between 1.79 and 2.13 ns (Table 5.5). Fluorescence life times for both compounds are slightly higher in a polar solvent.

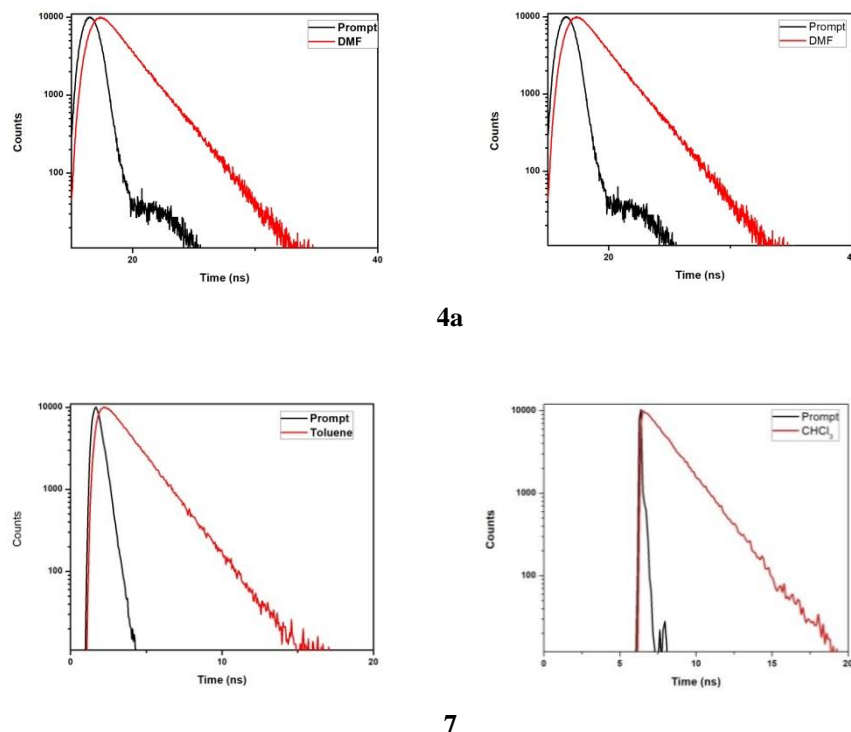


Fig. 5.4. Fluorescence lifetime decay curves of fluorophores in toluene and DMF

Table 5.5. Fluorescence lifetime of **4a** and **7**

Compound	Toluene (ns) τ	DMF (ns) τ
4a	1.92	2.13
7	1.79	1.83

5.3.3. Electrochemical Properties

Electrochemical properties of fluorophores **4a** and **7** were calculated by cyclic voltammetry. CV was done in a three-electrode cell with Pt disc as working electrode, Ag/AgCl as reference electrode and Pt wire as the auxiliary electrode with a scan rate of 100 mV/s using 0.1 M $n\text{Bu}_4\text{NPF}_6$ as supporting electrode and ferrocene as the internal standard in dry dichloromethane. The corrected values are reported against

standard hydrogen electrode (SHE). Using cyclic voltammetry, HOMO-LUMO energy levels of these D-A molecules were calculated. Cyclic voltammograms of the compounds are shown in Fig.5.5. HOMO and LUMO energy levels were calculated using the Equations 5.3 and 5.4 respectively and listed in Table 5.6.²² Electrochemical band gaps are in excellent agreement with optical bandgap.

$$\text{HOMO} = - [E_{ox}^{onset} + 4.44] \text{ (eV)} \quad (5.3)$$

$$\text{LUMO} = - [\text{HOMO} + E_g^{opt}] \text{ (eV)} \quad (5.4)$$

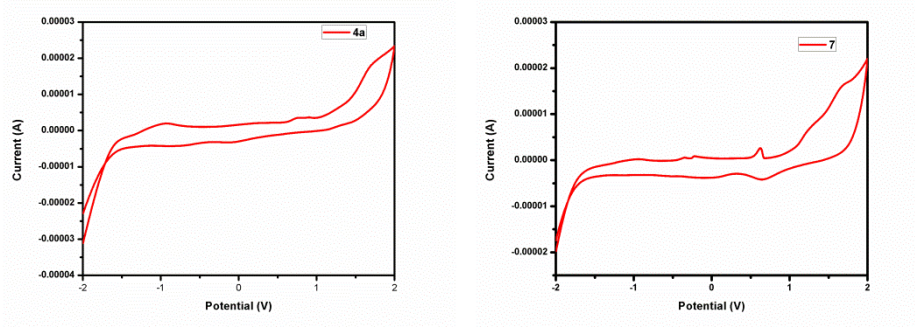


Fig. 5.5. Cyclic voltammogram of compounds in degassed CH_2Cl_2 with 0.1 M $n\text{Bu}_4\text{NPF}_6$ as the supporting electrolyte

Table 5.6. Electrochemical properties of **4a** and **7**

Compound	E_{onset}^{ox} (V)	E_{onset}^{ox} vs E_{FOC}/V	HOMO (eV)	LUMO (eV)	E_g^{EC} (eV)
4a	0.61	0.88	-5.32	-2.24	3.08
7	0.53	0.75	-5.19	-2.19	3.00

$E_{FOC} = 0.22 \text{ V vs Ag/AgCl}$

5.3.4. Theoretical Studies

To assess the geometry and HOMO-LUMO energy levels of the fluorophores, density functional theory (DFT) calculations were performed using GAUSSIAN 09 quantum chemistry package and

B3LYP exchange-correlation functional.²³ The ground state optimized geometry, HOMO and LUMO are shown in Fig. 5.6. From the figure, it is clear that the electron clouds of HOMO and LUMO are spread over the entire framework *i.e.* there is no localization in electron density, which reduces the polarizability of these molecules. Theoretically calculated HOMO energies for **4a** and **7** are found to be identical at -5.76 eV. The LUMO values are -2.30 eV and -2.27 eV for **4a** and **7** respectively. Further the band gaps obtained for **4a** and **7** are 3.46 eV and 3.49 eV respectively (Fig. 5.7).

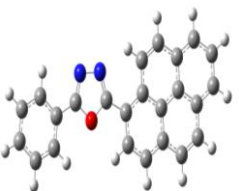
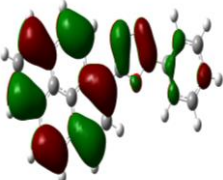
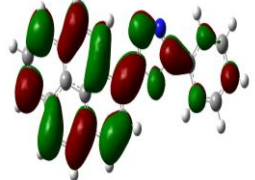
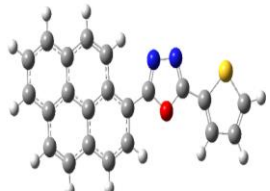
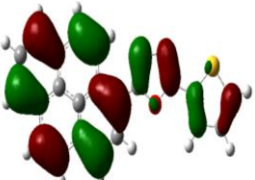
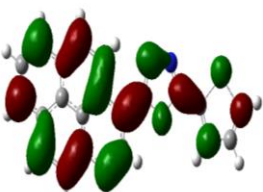
COMPOUNDS	HOMO (eV)	LUMO (eV)
 4a	 -5.76	 -2.30
 7	 -5.76	 -2.27

Fig. 5.6. HOMO and LUMO levels and optimized molecular structures of fluorophores

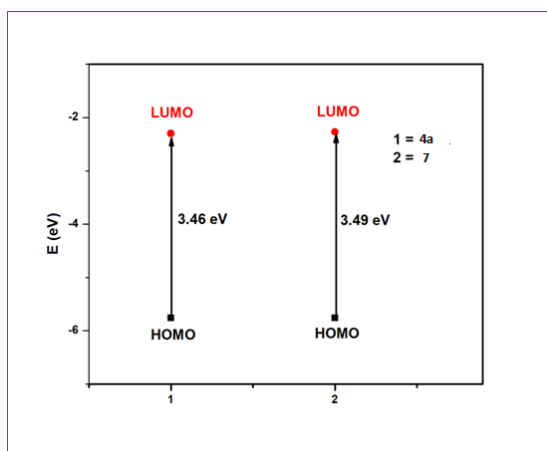
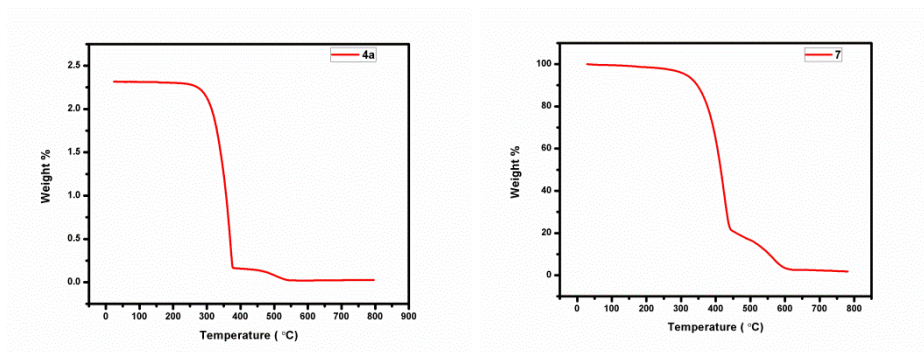
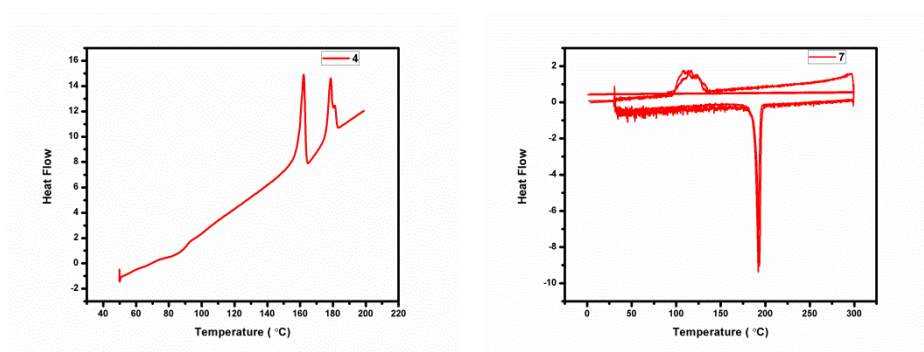


Fig. 5.7. Energy diagram of the frontier orbitals calculated from DFT

5.3.5. Thermal Properties

The thermal and morphological stabilities were examined by differential scanning calorimetry (DSC) and thermal gravimetric analysis (TGA). The results are shown in Fig. 5.8 and 5.9 and are summarized in Table 5.7. The phase transition characteristics of these compounds were investigated using DSC; it revealed that the compounds **4a** and **7** are crystalline. Compound **4a** and **7** showed melting points at 165 °C and 194 °C respectively. Crystallization temperature is observed only for compound **7**, which is 114 °C. The TGA results showed that the molecules are thermally stable with 5% weight loss at 300 °C and 337 °C for **4a** and **7** respectively.

Fig. 5.8. TGA Curves of **4a** and **7**Fig. 5.9. DSC traces of fluorophores **4a** and **7**Table 5.7. Thermal properties of **4a** and **7**

Compounds	Melting point, T_m (°C)	Crystallisation temperature, T_c (°C)	Decomposition temperature. (°C)
4a	165		300.00
7	194	114	337.20

5.3.6. Nonlinear Optical Properties

The third order nonlinear optical properties of fluorophores were explored using Z-scan technique.²⁴ Open aperture (OA) Z-scan traces of molecules in dilute CHCl_3 are shown in Fig. 5.10. The solid line in the figure indicates the theoretical fit to the experimental data. Data fitted well with TPA theory, which point out that TPA is the mechanism

involved in NLO process. The open-aperture profile of both **4a** and **7** showed reverse saturable absorption behavior in CHCl_3 .

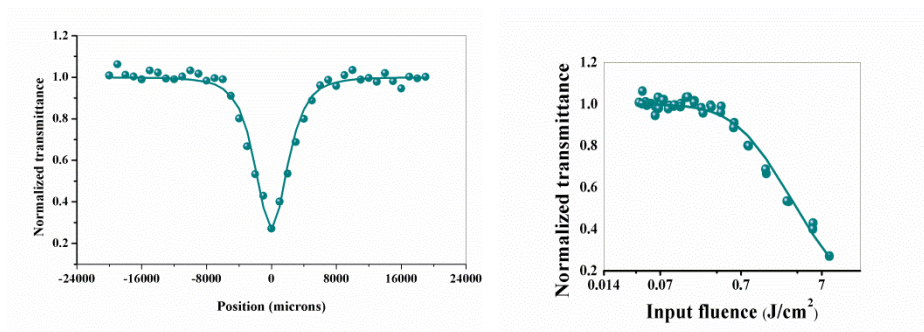
Using open aperture Z-scan experimental setup, the absorption coefficients, β of the targeted fluorophores were calculated using the Equation 5.5.²⁵

$$T(z) = \frac{c}{q_0 \sqrt{\pi}} \int_{-\infty}^{\infty} \ln(1 + q_0 e^{-t^2}) dt \quad (5.5)$$

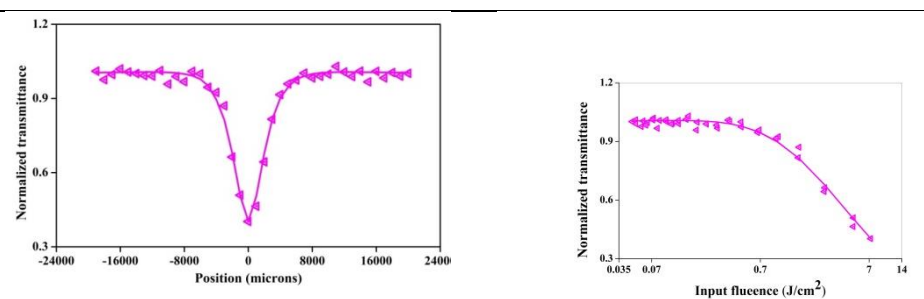
Where $q_0(z, r, t) = \beta I_0(t) L_{\text{eff}}$ and $L_{\text{eff}} = (1 - e^{-\alpha l})/\alpha$ are the effective thickness with the linear absorption coefficient, α and I_0 is the irradiance at focus. The imaginary part of the third-order susceptibility, $\text{Im } \chi^{(3)} = \frac{n_0^2 c^2 \beta}{240 \omega \pi^2}$ where n_0 is the linear refractive index of compounds, c is the velocity of light under vacuum and ω is the angular frequency of radiation used.

The nonlinear absorption coefficient, β and imaginary part of nonlinear susceptibility ($\text{Im } \chi^{(3)}$) are calculated and summarized in Table 5.8. Value for β is obtained to be 2.89×10^{-10} m/W and 1.91×10^{-10} m/W for **4a** and **7** respectively. Furthermore, $\text{Im } \chi^{(3)}$ values are 6.76×10^{-12} for **4a** and 6.45×10^{-12} for **7**.

Using open aperture Z-scan technique optical limiting properties were measured. The input fluence corresponds to half of normalized transmittance, gives the optical limiting threshold and is given in Table 3.8. The optical limiting threshold obtained for **4a** and **7** are 3.84 and 4.78 respectively.



4a



7

Fig. 5.10. Normalized open aperture and optical limiting curves of **4a** and **7**

Table 5.8. NLO properties of **4a** and **7**

Molecule	Nonlinear absorption coefficient (β , m/W)	Imaginary part of nonlinear susceptibility ($\text{Im } \chi^{(3)}$, esu)	Optical Limiting Threshold (J/cm^2)
4a	2.89×10^{-10}	6.76×10^{-12}	3.84
7	1.91×10^{-10}	6.45×10^{-12}	4.78

5.4. Conclusions

We have synthesized a few 1,3,4-oxadiazole and pyrene based donor-acceptor molecules *via* iodine mediated oxidative cyclization of respective acylhydrazones. Structures of the fluorophores were

established on the basis of analytical and spectral data. We have studied the photophysical properties like UV-Vis absorption spectra, emission spectra, quantum yield and time resolved fluorescence measurements. The fluorophores exhibited intense blue fluorescence with relatively good quantum yields. Solvatochromic studies showed that compounds **4a** and **7** exhibited moderate ICT character. We have calculated bandgap experimentally by CV. The bandgap obtained from DFT and optical bandgap calculated from absorption thresholds are well matched with each other. TGA and DSC analysis confirms the thermal stability of the compounds. In addition, we have studied the third-order nonlinear optical properties of the fluorophores **4a** and **7** using Q switched Z-scan technique with a 7 ns laser pulses at 532 nm. Theoretical calculations indicated lower polarizability for these compounds despite which they exhibited good nonlinear responses in CHCl₃ solution as well as good optical limiting property.

5.5. Experimental Sections

5.5.1. Reagents and Instruments

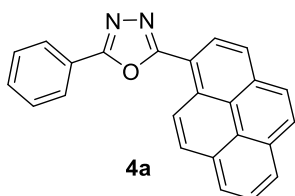
Details of reagents and instruments are given in Chapter 3 (Section 3.5.1).

5.5.2. Synthesis and Characterization

5.5.2.1. Synthesis of 2-phenyl-5-(pyren-1-yl)-1,3,4-oxadiazole (**4a**)

Compound **4a** was prepared by iodine mediated oxidative cyclization reaction which is described in chapter 3 (Procedure 3.5.2.1),

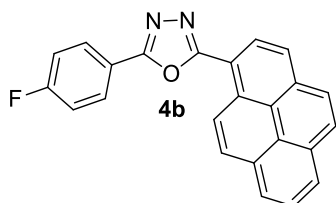
³⁷ by using pyrene-1-carbaldehyde (230 mg, 1 mmol) and benzohydrazide (136 mg, 1 mmol). Light yellow powder.



Yield: 85%, mp: 163-168 °C; UV-Vis (CHCl₃) (λ_{max}): 369 nm; IR (KBr): 2980, 1645, 1568, 1585, 1434, 1412 cm⁻¹; ¹H NMR (CDCl₃, 500 MHz): δ (ppm) 9.56-7.25 (m, 14H); ¹³C NMR (CDCl₃, 125 MHz): δ (ppm) 165.3, 164.2, 133.7, 131.8, 131.2, 130.8, 129.9, 129.7, 129.6, 129.3, 127.2, 126.6, 126.5, 126.4, 125.4, 125.1, 124.7, 124.3, 124.2, 116.9, 96.3; MS: m/z 346 (M^+), 347 ($M+1$); Elemental analysis calculated for C₂₄H₁₄N₂O: C: 83.22, H: 4.07, N: 8.09; Found C: 83.20, H: 4.08, N: 8.08.

5.5.2.2. Synthesis of 2-(4-fluorophenyl)-5-(pyren-1-yl)-1,3,4-oxadiazole (4b)

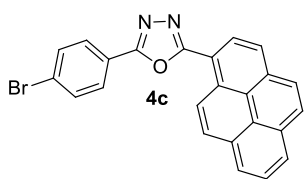
The reaction was performed according to the procedure 3.5.2.1 with pyrene-1-carbaldehyde (230 mg, 1 mmol) and 4-fluorobenzohydrazide (155 mg, 1 mmol). Yellow powder.



Yield: 78%, mp: 193-198 °C; UV-Vis (CHCl₃) (λ_{max}): 370 nm; IR (KBr): 2852, 1814, 1580, 1517, 1430, 1312 cm⁻¹; ¹H NMR (CDCl₃, 500 MHz): δ (ppm) 9.58-7.26 (m, 14H); ¹³C NMR (CDCl₃, 125 MHz): δ (ppm) 166.0, 165.4, 164.0, 163.4, 133.8, 131.3, 130.8, 130.1, 129.8, 129.7, 129.5, 129.4, 127.3, 126.7, 126.6, 126.5, 125.4, 125.2, 124.7, 124.4, 120.6, 116.9, 116.7, 116.6, 96.4; MS: m/z 364 (M^+), 365 ($M+1$); Elemental analysis calculated for C₂₄H₁₃FN₂O: C: 79.11, H: 3.60, N: 7.69; Found C: 79.10, H: 3.58, N: 7.68.

5.5.2.3. Synthesis of 2-(4-bromophenyl)-5-(pyren-1-yl)-1,3,4-oxadiazole (4c)

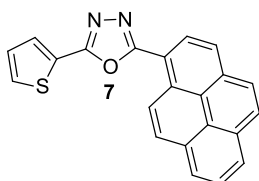
The reaction was performed according to the procedure 3.5.2.1 with pyrene-1-carbaldehyde (235 mg, 1 mmol) and 4-bromobenzohydrazide (154 mg, 1 mmol). Yellow powder.



Yield: 75%, mp: 205 °C; UV-Vis (CHCl₃): 370 nm (λ_{max}); IR (KBr): 2950, 1914, 1560, 1524, 1490, 1380, 580 cm⁻¹; ¹H NMR (CDCl₃, 500 MHz): δ (ppm) 8.68-7.23 (m, 13H); ¹³C NMR (CDCl₃, 125 MHz): δ (ppm) 169.2, 166.3, 166.1, 165.0, 164.1, 163.2, 142.9, 141.3, 131.7, 131.6, 131.2, 129.6, 129.5, 128.9, 128.8, 127.9, 127.0, 126.5, 125.9, 125.3, 120.6, 120.5, 117.4, 116.8, 116.6, 96.3; MS: m/z 424 (M^+), 425 ($M+1$); Elemental analysis calculated for C₂₄H₁₃BrN₂O: C: 67.78, H: 3.08 N: 6.59; Found C: 67.76, H: 3.09, N: 6.60.

5.5.2.4. Synthesis of 2-(pyren-1-yl)-5-(thiophen-2-yl)-1,3,4-oxadiazole (7)

This compound was prepared by a procedure similar to that of **4a** except that thiophene-2-carbohydrazide (140 mg, 1 mmol) was used as the reactant in place of benzohydrazide. Yellow crystals.



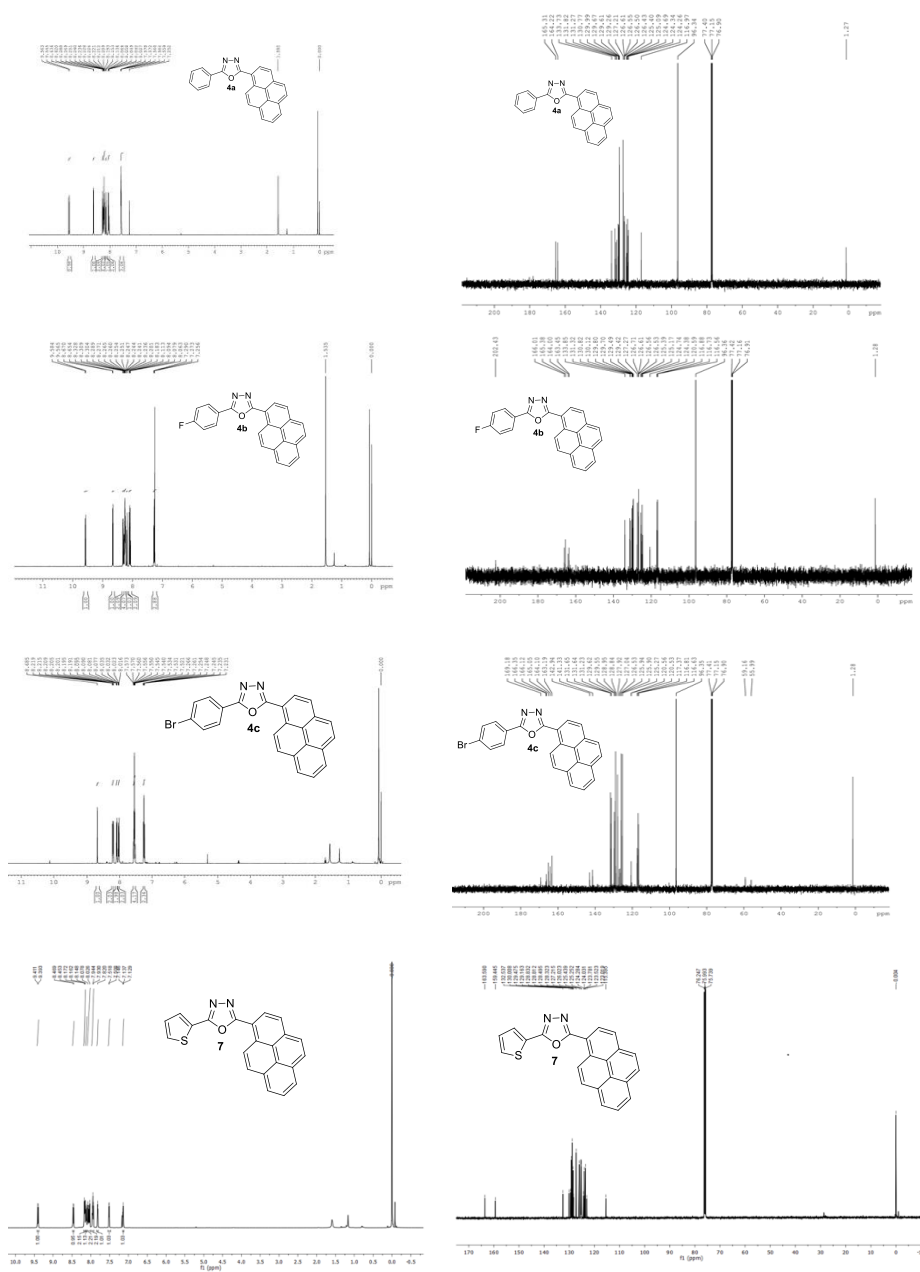
Yield: 72%, mp: 192-197 °C. UV-Vis (CHCl₃): 372 nm (λ_{max}); IR (KBr): 2964, 1635, 1590, 1538, 1494, 1424 cm⁻¹; ¹H NMR (CDCl₃, 500 MHz): δ (ppm) 9.40 (d, J = 9 Hz, 1H), 8.46 (d, J = 8 Hz), 8.17-7.93 (m, 7H), 7.82 (d, J = 3.5 Hz, 1H), 7.51 (d, J = 5 Hz, 1H), 7.14 (t, J = 4.5 Hz, 1H); ¹³C NMR (CDCl₃, 125 MHz): δ (ppm) 163.6, 159.4, 132.5, 130.0, 129.5, 129.2, 128.8, 128.8, 128.5, 128.3, 127.2, 126.0, 125.4, 125.2, 124.3, 124.0, 123.8, 123.5, 123.0, 115.4; MS: m/z 352 (M^+), 353 ($M+1$); Elemental analysis calculated for C₂₂H₁₂N₂OS: C: 74.98, H: 3.43 N: 7.95, S: 9.10; Found C: 74.96, H: 3.44, N: 7.96, S: 9.11.

5.6. References

- (1) Kanis, D. R.; Ratner, M. A.; Marks, T. J. *Chem. Rev.* **1994**, *94*, 195.
- (2) Wang, C.; Jung, G.-Y.; Batsanov, A. S.; Bryce, M. R.; Petty, M. C. *J. Mater. Chem.* **2002**, *12*, 173.
- (3) Cha, S. W.; Choi, S. H.; Kim, K.; Jin, J. I. *J. Mater. Chem.* **2003**, *13*, 1900.
- (4) Tasaganva, R. G.; Kariduraganavar, M. Y.; Inamdar, S. R. *Synth. Met.* **2009**, *159*, 1812.
- (5) Lin, T. C.; Lee, Y. H.; Huang, B. R.; Hu, C. L.; Li, Y. K. *Tetrahedron* **2012**, *68*, 4935.
- (6) Prashanth Kumar, K. R.; Murali, M. G.; Udayakumar, D. *Des. Monomers Polym.* **2014**, *17*, 7.
- (7) Sunitha, M. S.; Adhikari, A. V.; Vishnumurthy, K. A.; Safakath, K.; Philip, R. *Int. J. Polym. Mater. Polym. Biomater.* **2012**, *61*, 483.
- (8) Figueira-Duarte, T. M.; Müllen, K. *Chem. Rev.* **2011**, *111*, 7260.
- (9) Wang, D.; Jin, Z.; Tang, J.; Liang, P.; Mi, Y.; Miao, Z.; Zhang, Y.; Yang, H. *Tetrahedron* **2012**, *68*, 6338.
- (10) Lavanya Devi, C.; Yesudas, K.; Makarov, N. S.; Jayathirtha Rao, V.; Bhanuprakash, K.; Perry, J. W. *J. Mater. Chem. C* **2015**, *3*, 3730.
- (11) Kim, H. M.; Lee, Y. O.; Lim, C. S.; Kim, J. S.; Cho, B. R. *J. Org. Chem.* **2008**, *73*, 5127.
- (12) Jin, Z.; Wang, D.; Wang, X.; Liang, P.; Mi, Y.; Yang, H. *Tetrahedron Lett.* **2013**, *54*, 4859.
- (13) Wan, Y.; Yan, L.; Zhao, Z.; Ma, X.; Guo, Q.; Jia, M.; Lu, P.; Ramos-Ortiz, G.; Maldonado, J. L.; Rodríguez, M.; Xia, A. *J. Phys. Chem. B* **2010**, *114*, 11737.
- (14) Niko, Y.; Moritomo, H.; Sugihara, H.; Suzuki, Y.; Kawamata, J.; Konishi, G. *J. Mater. Chem. B* **2015**, *3*, 184.
- (15) Morales-Espinoza, E. G.; Lijanova, I. V.; Morales-Saavedra, O. G.; Torres-Zuñiga, V.; Hernandez-Ortega, S.; Martínez-García, M. *Molecules* **2011**, *16*, 6950.
- (16) Liang, P.; Li, Z.; Mi, Y.; Yang, Z.; Wang, D.; Cao, H.; He, W.; Yang, H. *J. Electron. Mater.* **2015**, *44*, 2883.
- (17) Hu, Y.; Heo, C. H.; Kim, G.; Jun, E. J.; Yin, J.; Kim, H. M.; Yoon, J. *Anal. Chem.* **2015**, *87*, 3308.
- (18) Paun, A.; Hadade, N. D.; Paraschivescu, C. C.; Matache, M. *J. Mater. Chem. C* **2016**, *4*, 8596.
- (19) Yu, W.; Huang, G.; Zhang, Y.; Liu, H.; Dong, L.; Yu, X.; Li, Y.; Chang, J. *J. Org. Chem.* **2013**, *78*, 10337.

- (20) Allen, M. W. *Measurement of Fluorescence Quantum Yields*. Technical note 52019, Thermo Fisher Scientific, Madison, WI, USA
- (21) Berlman, I. B. *Handbook of fluorescence spectra of aromatic compounds*. 2nd edition, New York Academic Press, 1971.
- (22) Deshapande, N.; Belavagi, N. S.; Sunagar, M. G.; Khazi, I. A. M. *RSC Adv.* **2015**, *5*, 86685.
- (23) Gaussian 09, Revision D.01, M. J. Frisch, G. W. Trucks, H. B. Schlegel, G. E. Scuseria, M. A. Robb, J. R. Cheeseman, G. Scalmani, V. Barone, B. Mennucci, G. A. Peterson, H. Nakatsuji, M. Caricato, X. Li, H. P. Hratchian, A. F. Izmaylov, J. Bloino, G. Zheng, J. L. Sonnenberg, M. Hada, M. Ehra, K. Toyota, R. Fukuda, J. Hasegawa, M. Ishida, T. Nakajima, Y. Honda, O. Kitao, H. Nakai, T. Vreven, J. A. Montgomery, Jr., J. E. Peralta, F. Ogliaro, M. Bearpark, J. J. Heyd, E. Brothers, K. N. Kudin, V. N. Staroverov, T. Keith, R. Kobayashi, J. Normand, K. Raghavachari, A. Rendell, J. C. Burant, S. S. Iyengar, J. Tomasi, M. Cossi, N. Raga, J. M. Millam, M. Klene, J. E. Knox, J. B. Cross, V. Bakken, C. Adamo, J. Jaramillo, R. Gomperts, R. E. Stratmann, O. Yazyev, A. J. Austin, R. Cammi, C. Pomelli, J. W. Ochterski, R. L. Martin, K. Morokuma, V. G. Zakrzewski, G. A. Voth, P. Salvador, J. J. Dannenberg, S. Dapprich, A. D. Daniels, O. Farkas, J. B. Foresman, J. V. Ortiz, J. Cioslowski, and D. J. Fox, *Gaussian, Inc.*, Wallingford CT, **2013**.
- (24) Sheik-Bahae, M.; Said, A. A.; Wei, T. H.; Hagan, D. J.; Stryland, E. W. *IEEE J. Quantum Electron.* **1990**, *26*, 760.
- (25) Zhang, C.; Song, Y.; Xu, Y.; Fun, H.; Fang, G.; Wang, Y. *J. Chem. Soc. Dalton Trans.* **2000**, *16*, 2823.

5.7. Appendix

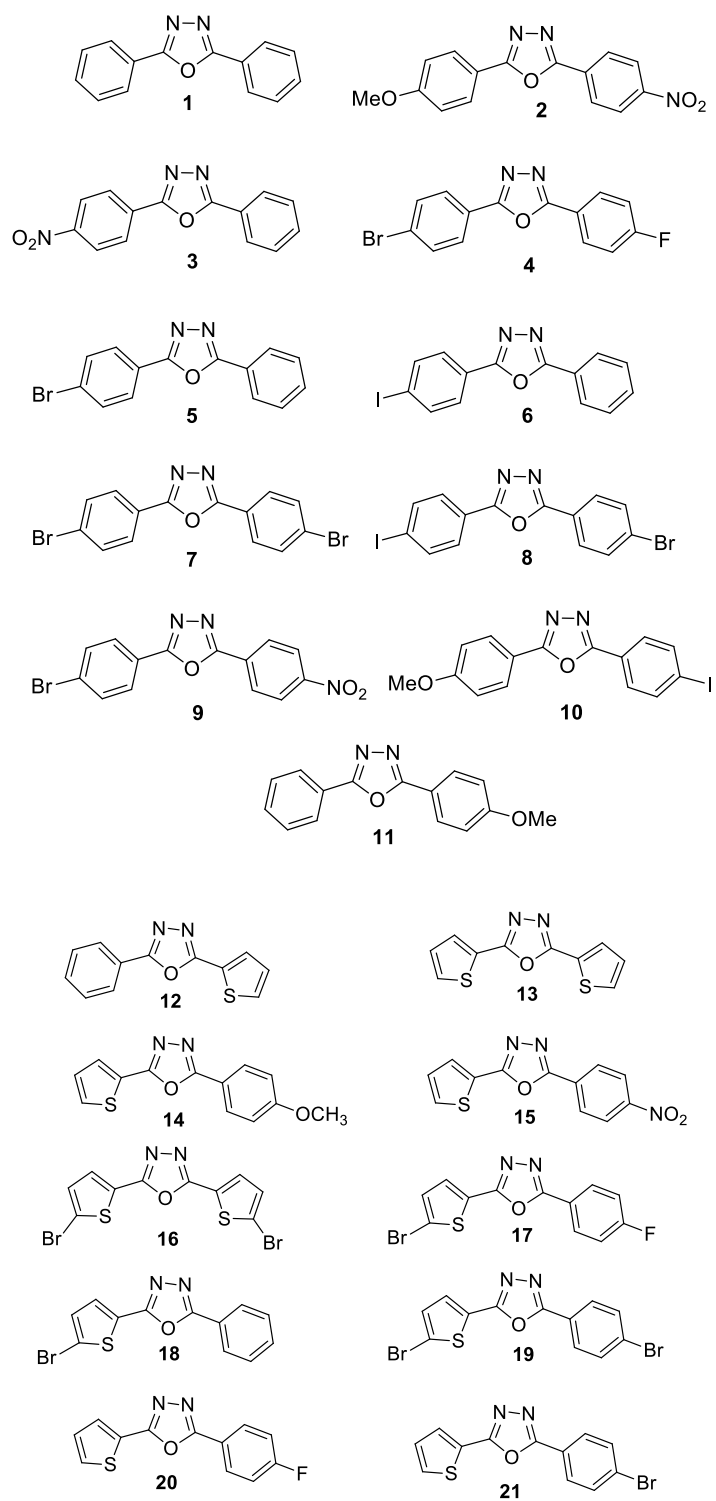
 ^1H NMR and ^{13}C NMR spectra of significant compounds

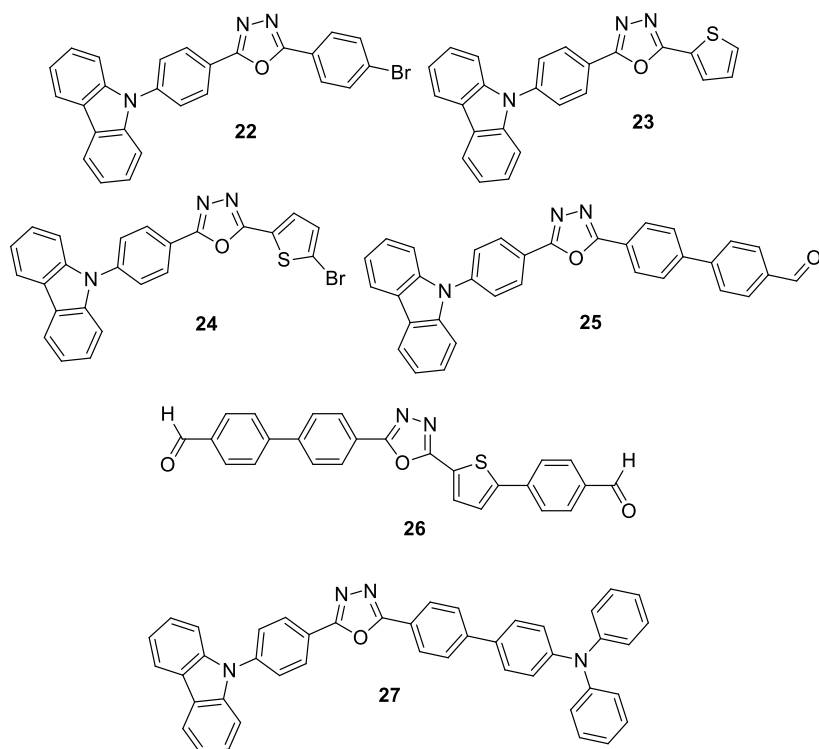
Chapter 6

SUMMARY AND CONCLUSIONS

The thesis entitled “**Synthesis and evaluation of third-order nonlinear optical properties of a few 1,3,4-oxadiazole based push-pull fluorophores**” deals with the design and synthesis of 1,3,4-oxadiazole based push-pull fluorophores and exploring their application in third-order nonlinear optical field. In the design strategy for organic push-pull systems, tuning charge transfer by proper crafting of donor, acceptor or π -bridge is a major objective. In these types of systems, asymmetric polarizability developed by ICT is responsible for their remarkable third-order nonlinear properties.

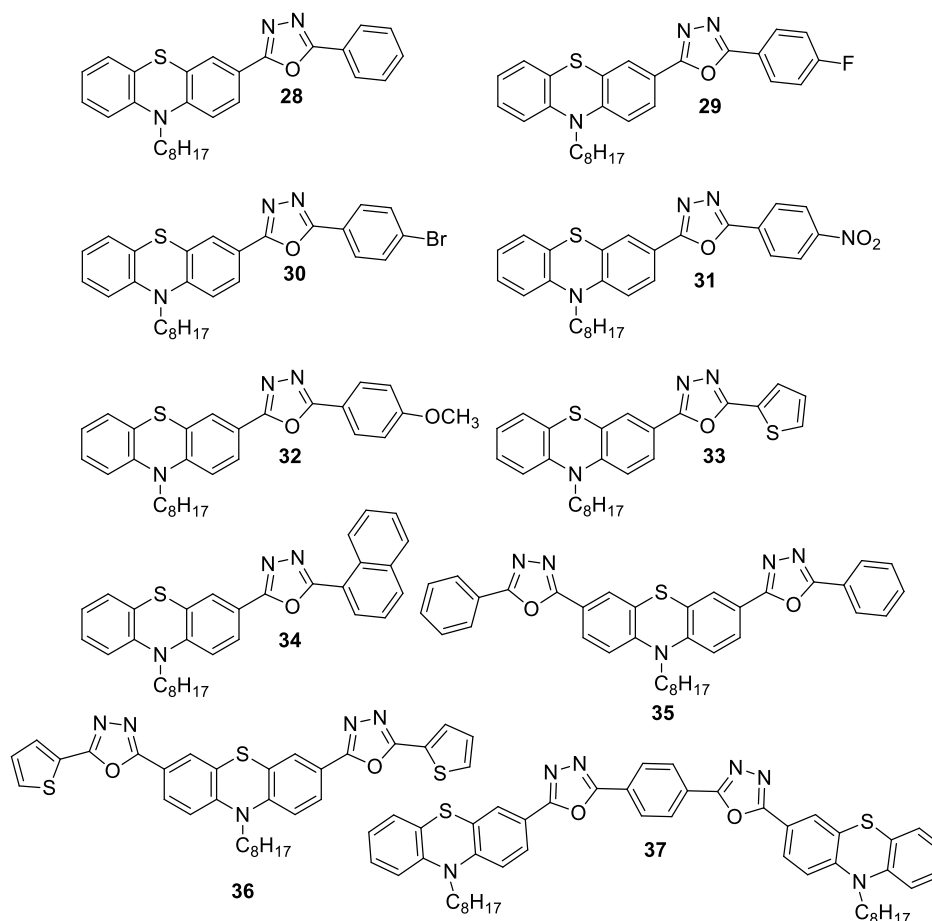
To establish a simple yet robust synthetic strategy and to demonstrate its wide applicability, we synthesized a series of symmetrical and unsymmetrical expandable 2,5-diaryl-1,3,4-oxadiazoles (**1-11**) and oxadiazole-thiophene hybrid molecules (**12-21**). In addition we expanded a few selected molecules to elaborate hybrid materials by postfunctionalization employing nucleophilic aromatic substitution and Suzuki coupling reactions (**22-27**).





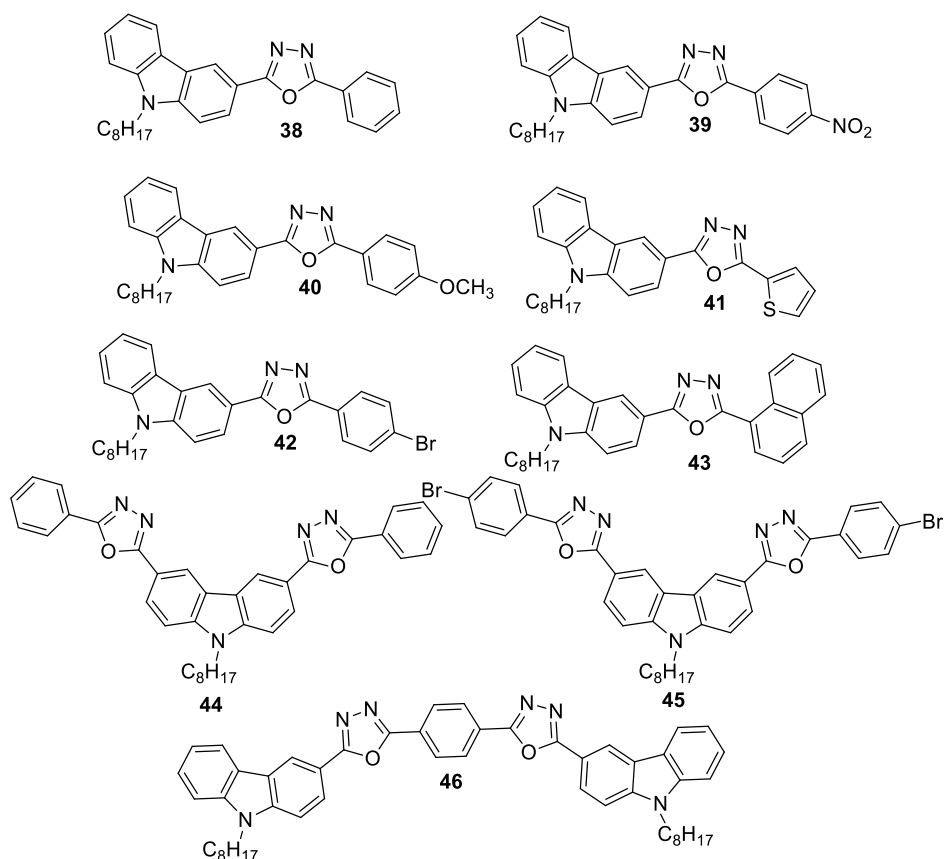
Phenothiazine, carbazole and pyrene coupled with 1,3,4-oxadiazole based push-pull fluorophores were designed and synthesized (**28-50**); in which phenothiazine, carbazole and pyrene act as electron donor and 1,3,4-oxadiazole as acceptor. A relatively simple and efficient transition metal free iodine mediated oxidative cyclization was employed for the synthesis of targeted fluorophores. The synthesized molecules were characterized by ^1H NMR, ^{13}C NMR, IR and LC-MS analysis. The photophysical properties like UV-Vis absorption spectra, emission spectra, quantum yield and time resolved fluorescence measurements were monitored. Majority of the fluorophores exhibited intense fluorescence with moderately high quantum yields. The emission spectra of most of the phenothiazine and carbazole based 1,3,4-oxadiazole fluorophores revealed decent positive solvatochromic behavior, which

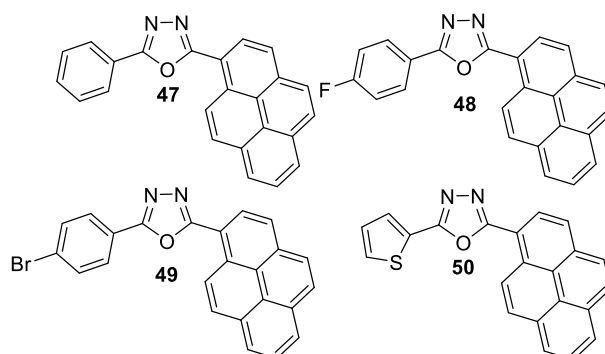
indicates the more polar nature of the excited state compared to the ground state. On the other hand, 1,3,4-oxadiazole-pyrene based molecules showed only a small positive solvatochromism.



To estimate the geometry and HOMO-LUMO energy levels of the fluorophores, DFT calculations were executed using GAUSSIAN 09 quantum chemistry package and B3LYP exchange-correlation functional. Theoretical studies clearly indicated that for phenothiazine and carbazole attached molecules, electron density in HOMO is predominantly located on donor fragment while that of LUMO is concentrated on oxadiazole

(acceptor) framework. This shows the charge separation in the entire molecular systems and also the strong intramolecular charge transfer property. In the case of pyrene attached molecules the electron cloud of HOMO and LUMO are spread in the entire framework which signifies the slighter delocalization in the electron density and hence reducing the polarizability. Not surprisingly, these molecules exhibited negligible solvatochromism as well. The bandgaps obtained from theoretical calculations, electrochemical measurements and absorption thresholds were well matched with each other.





Powder XRD pattern of the fluorophores showed both sharp and broad peaks indicating their semicrystalline nature. The thermal and morphological stabilities were monitored by differential scanning calorimetry (DSC) and thermal gravimetric analysis (TGA). TGA reports confirmed that the fluorophores are thermally stable making them suitable for device fabrication.

To explore the nonlinear optical properties as well as the optical limiting properties of the synthesized fluorophores, we performed open aperture Z-scan technique using a Q switched Nd:YAG laser with a 7 ns laser pulses at 532 nm in CHCl_3 solution. The results suggested that all the compounds displayed a reverse saturable absorption (RSA) with a positive absorption coefficient and also the experimental data are well fitted with the two photon absorption (TPA) theory, which suggests that TPA is involved in the exhibition of NLO property. Optical limiting property was shown by all the fluorophores. Calculated nonlinear absorption coefficient β and imaginary part of nonlinear susceptibility ($\text{Im } \chi^{(3)}$) values are summarized in Table 6.1. Interestingly the tabulated values are found to be comparable or even better than other push-pull molecules reported in literature.

Table 6.1. Nonlinear optical properties of the fluorophores

Molecule	Nonlinear absorption coefficient (β , m/W)	Imaginary part of nonlinear susceptibility ($\text{Im } \chi^{(3)}$, esu)	Optical Limiting Threshold (J/cm ²)
28	2.89×10^{-10}	9.77×10^{-12}	3.84
31	2.80×10^{-10}	9.77×10^{-12}	2.37
33	5.52×10^{-10}	1.86×10^{-11}	2.37
34	7.31×10^{-10}	2.48×10^{-11}	1.70
35	5.15×10^{-10}	1.74×10^{-11}	2.04
36	1.50×10^{-10}	4.95×10^{-12}	7.32
37	9.85×10^{-10}	3.33×10^{-11}	2.04
38	1.73×10^{-10}	5.86×10^{-12}	6.34
39	2.50×10^{-10}	8.46×10^{-12}	4.38
41	1.80×10^{-10}	6.07×10^{-12}	2.37
43	1.28×10^{-10}	4.38×10^{-12}	-
44	2.00×10^{-10}	6.76×10^{-12}	6.34
46	2.63×10^{-10}	8.88×10^{-12}	4.22
47	2.89×10^{-10}	6.76×10^{-12}	3.34
50	1.91×10^{-10}	6.45×10^{-12}	4.78

The results suggested that donor strength and symmetry have marked effect on the nonlinear optical properties of the molecules. Among the synthesized molecules nonlinearity of phenothiazine-1,3,4-oxadiazole hybrids is observed to be superior than carbazole and pyrene based fluorophores due to excellent electron donating ability of phenothiazine. Theoretical calculations also revealed sharper electron density distribution in both HOMO and LUMO for phenothiazine-oxadiazole based systems. Hence these fluorophores are promising candidates for photonic applications.

Even though 1,3,4-oxadiazole based small molecules and polymers have been used for third-order NLO applications, 1,3,4-oxadiazoles based push-pull fluorophores having phenothiazine,

carbazole and pyrene remained unexplored. We were successful in the design and synthesis of 1,3,4-oxadiazole-phenothiazine, 1,3,4-oxadiazole-carbazole and 1,3,4-oxadiazole-pyrene based push-pull fluorophores with remarkable third order NLO activity. Several of the newly synthesized molecules are further expandable by postfunctionalization to more complex architectures.

List of publications

1. Synthesis and characterization of a few 1,3,4-oxadiazole-pyrene hybrid molecules, **Shandev P. P.**, Jyothi C. M., Unnikrishnan P. A., Prathapan, S. *International conference on Materials for the Millenium - MatCon 2016*, Department of Applied Chemistry, Cochin University of Science and Technology. **ISBN 978-93-80095-738.**
2. Synthesis and characterization of covalently-linked 1,3,4-oxadiazole-phenothiazine hybrid molecules, **Shandev P. P.**, Jyothi C. Mary., P. A. Unnikrishnan and S. Prathapan. *International conference on Materials for the Millenium - MatCon 2016*, Department of Applied Chemistry, Cochin University of Science and Technology. **ISBN 978-93-80095-738.**
3. Synthesis, Characterization and Photophysical Investigation of Covalently-linked 1,3,4-Oxadiazole-Carbazole Hybrid Molecules, **Shandev P. P.**, S. Prathapan and P. A. Unnikrishnan, *International Symposium on New Trends in Applied Chemistry, NTAC-2017*, Sacred Heart College (Autonomous), Thevara. **ISBN 978-81-930558-2-3.**

Poster presentations in conferences

1. Synthesis of 1,3,4-Oxadiazole-Thiophene Hybrid Molecules, **P. P. Shandev**, S. Prathapan and P. A. Unnikrishnan, *Current Trends in Chemistry, CTriC-2017*, Cochin University of Science and Technology, 2017.
2. A Convenient Synthesis of Unsymmetrical 2,5-Disubstituted-1,3,4- Oxadiazoles, **P. P. Shandev**, P. A. Unnikrishnan and S. Prathapan, *Current Trends in Chemistry, CTriC-2014*, Cochin University of Science and Technology, 2014.